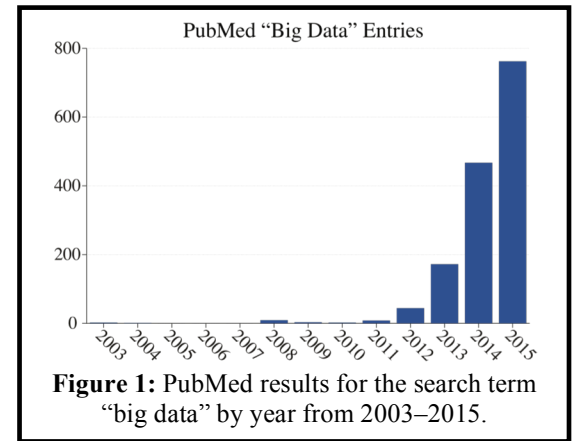


# Big Data Analysis in Medicine

## 1. PROJECT BACKGROUND

The term “Big Data” refers to the amalgamation and processing of huge data sets that are composed of different data types (e.g. clinical, genomic, imaging, pathological, etc.) and have rapidly become more massive and complex, particularly with the advent of new technologies. Big Data within the context of biomedical research is a major problem that needs to be solved due to substantial increases in the amount of medical data routinely generated and collected by healthcare providers over the last two decades [1,2]. A recent PubMed search for the term “big data” yields 1470 entries, with the earliest occurring in 2003. A breakdown by year shows the majority of publications are from 2012 or later (Figure 1). In 2011, the McKinsey Global Institute issued a 156-page report titled “Big data: The next frontier for innovation, competition, and productivity” [3]. This report indicated \$300 billion in potential annual value in Big Data to health care in the U. S., with a shortage of 140,000 to 190,000 individuals with the required deep analytical skills, indicating a need for programs to train the next generation of scientists with the necessary skill set to deal with all aspects of Big Data.

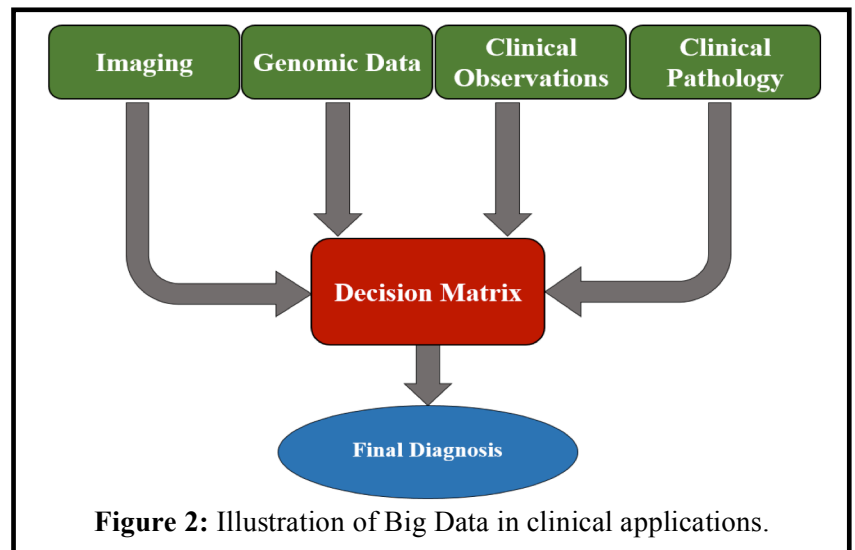


The current main challenge is that our ability to advance medical care and efficiently translate science into modern medicine is bounded by our capacity to process and understand these big data. So, there is an urgent need to develop and integrate new statistical, mathematical, visualization, and computational models with the ability to analyze Big Data in order to retrieve useful information to aid clinicians in accurately diagnosing and treating patients to improve patient outcomes. **Thus, the main objective of this proposal is to develop new computational models and implement new state-of-the-art machine learning approaches to analyze and integrate multiple data types for the creation of a decision matrix that aids clinicians in the early diagnosis and identification of high risk patients for human diseases and disorders (Figure 2).**

## 2. PROJECT SCOPE AND APPROACH

### a. Project Scope:

The primary scope of this project is to develop a new paradigm for integrating Big Data from multiple sources such as anatomical and functional biomarkers from medical images, genomic information consisting of genetic variants, biomarkers and the spatial relation between them, quantitative clinical data (e.g., blood test, urine test, pathology report) together with qualitative clinical data produced through observations by the physicians and nurses. This project strengthens existing partnerships between the Speed School of Engineering and the School of Medicine to create, validate and verify an innovative platform technology for propelling the University of Louisville to the forefront in becoming a nationally recognized leader in Big Data analysis. A strong team of biomedical engineers, computer scientists, and clinicians, with complementary research expertise, in excellent biomedical research environments have been assembled to implement innovative and groundbreaking bioengineering techniques using currently available big data to develop new, innovative clinical paradigms such as medical devices, biomarkers, and predictive and adaptive models for diagnosis and identification of high risk patients for human diseases and disorders to improve patient outcomes. The proposed approach is generic and can be applied to any clinical problem. However, the initial focus of this research proposal will be in three clinical areas that leverage existing collaborations:



### i) Autism:

**Project Goal/Specific Aim:** The main goal of this project is to develop a machine learning computer-assisted diagnosis (CAD) system for the early diagnosis and identification of high-risk patients of autism using imaging, genomics, and behavioral and psychometric reports.

**Personnel:** G. Barnes (M.D., Ph.D.), R. Keynton (Ph.D.), A. El-Baz (Ph.D.), O. Nasraoui (Ph.D.), H. Frigui (Ph.D.), E. Rouchka (Ph.D.), N. Altiparmak (Ph.D.) and N. Cooper (Ph.D.).

**Big Data:** We have access to data obtained from the IBIS database archived by NIH as part of the National Database for Autism Research (NDAR): 3D T1-Weighted MRI, 3D T2-Weighted MRI, 3D DTI, and behavioral and psychometric reports from infant between 3 months to two years of age. Genomic data archived by NDAR includes sequence variants (single nucleotide polymorphisms and copy number variants) from over 10000 individuals; AutismKB [4] archives approximately 4500 copy number variations, 3400 SNPs, and 158 genomic regions putatively involved autism spectrum disorders, which represent a small fraction of known sequence variants. For example, dbSNP, one of several collections made available by the National Center for Biotechnology Information [5], contain over  $10^8$  validated records.

## ii) Heart Failure:

**Project Goal/Specific Aim:** The main goal of this project is to develop and validate a machine learning CAD system for the early diagnosis and identification of high-risk patients for heart failure.

**Personnel:** R. Bolli (M.D.), R. Keynton (Ph.D.), A. El-Baz (Ph.D.), M. Slaughter (M.D.), S. Koenig (Ph.D.), O. Nasraoui (Ph.D.), H. Frigui (Ph.D.), E. Rouchka (Ph.D.), N. Altiparmak (Ph.D.) and N. Cooper (Ph.D.).

**Big Data:** We have access to data from heart failure patients enrolled in the stem cell therapy clinical trial at UofL and implanted with cardiovascular assist devices. The big data comprise 4D cardiac Cine MRI data, 4D Tagged MRI data, 4D dynamic contrast-enhanced MRI data, 3D late contrast MRI data, 3D ultrasound data, clinical reports, and family history. We will also incorporate the wealth of clinico-pathological data from the national STS general thoracic surgery database [6], genetic data from the national coronary artery disease (CADgene) database [7] that have been collected as far back as 1989, and the INTERMACS database [8].

## iii) Retinal Diseases:

**Project Goal/Specific Aim:** The main goal of this project is to develop a machine learning CAD system that has the ability to provide objective information to aid in early diagnosis, identification of high-risk patients and management of retinal diseases.

**Personnel:** H. Kaplan (M.D.), R. Keynton (Ph.D.), A. El-Baz (Ph.D.), O. Nasraoui (Ph.D.), H. Frigui (Ph.D.), E. Rouchka (Ph.D.), N. Altiparmak (Ph.D.) and N. Cooper (Ph.D.).

**Big Data:** We have access to 3D OCT data and clinical reports that have been collected from patients who are regularly examined at the University of Louisville's Kentucky Lions Eye Center. Genotyping will also be performed on this patient population, focusing on genes known to be associated with macular degeneration [9, 10].

## b. Project Approach

We propose to create a data analysis system model that integrates local feature data, which are extracted directly from the raw data, with global feature data, which have anatomical and physiological relevance (Figures 3, 4). The main idea of integrating global features with local features is to enhance the robustness of the proposed Big Data analysis system. The local feature data will be extracted via a conventional deep-learning network and the global feature data (appearance, shape, and spatial interaction models) will be extracted by our novel computational models. Subsequently, a multi-view deep network (MVDN) based on generalized canonical correlation analysis (GCCA) [11, 12] will be utilized on the Big Data (structural images, functional images, genomic data, clinical reports, etc.) to extract the significant discriminatory features

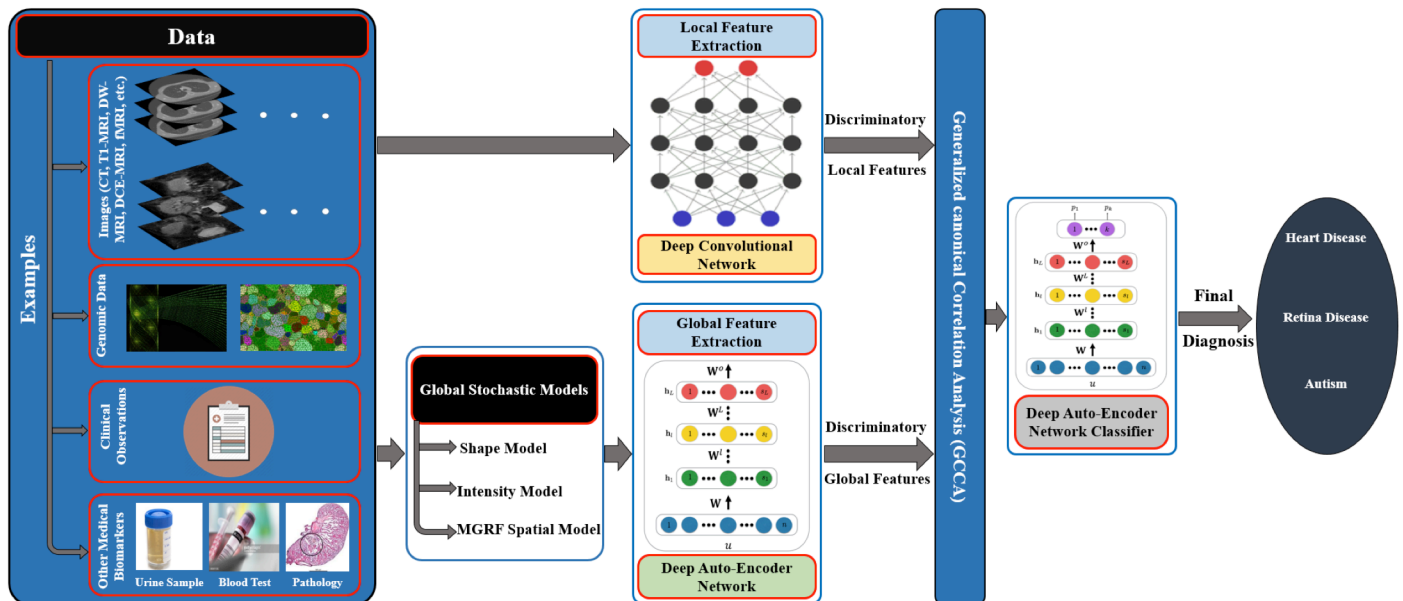


**Figure 3:** The proposed model for Big Data analysis.

which will be used to acquire an accurate diagnostic decision. Specifics of each of the model components are described in detail below.

### i) Extraction of local features using convolutional network:

Convolutional Networks (Convnet) are developed for local-level feature extraction of high-dimensional images in the MVDN framework. The main advantage of using Convnet is that it operates directly on the raw data without any pre-processing, which makes the developed framework completely objective and is not sensitive to any pre-processing artifacts. The Convnet is composed of several layers of convolution and pooling to extract low-dimensional features in hierarchical order. For this project, the Convnet will extract the following information from the big data: i) local anatomical and functional features from the 3D/4D medical images; ii) identification of influential genes from genomic data, iii) extraction of consistently predictive clinical quantitative and observation data.

### ii) Global stochastic models:

Global features will be extracted using the following novel stochastic models developed by our group over the last 15 years:

1) **Models of spatial interaction:** To better account for the large inhomogeneity of the organ-of-interest, we propose adding, to the traditional pairwise spatial interactions between the data voxels, the higher-order interaction families of the triple and quad cliques. This will help to account for large variations of the multidimensional data. The technique has applicability beyond images. Human genotypes also exhibit spatial interactions where sequence variants at nearby loci tend to occur in tandem (haplotypes). **This spatial model will be used in the analysis of big data to model: i) the interaction between the voxels in the 3D/4D**

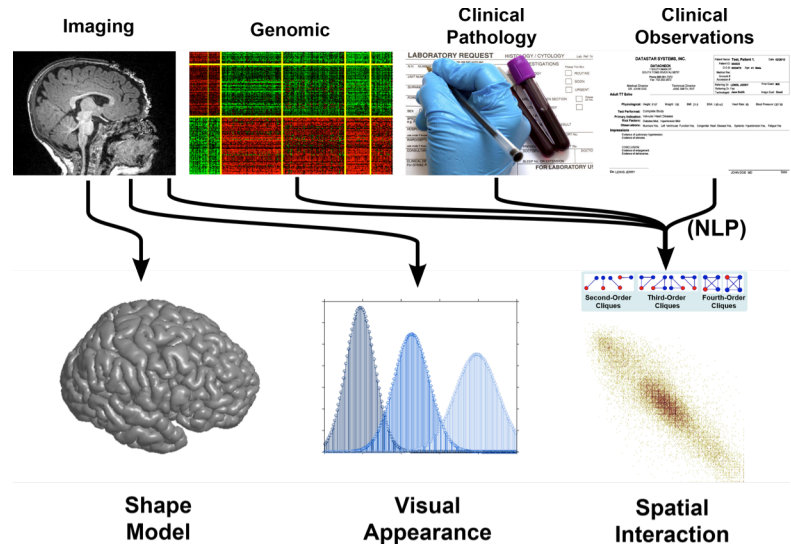


**Figure 4:** Global feature models as they apply to different facets of biomedical information.

**medical images; ii) the spatial relation between the genetic loci from genomic data; iii) the spatial relation between the clinical data extracted from urine tests, blood tests, and pathology reports; and, iv) the spatial relation in the clinical observation data.** See [13, 14] for more mathematical details about the spatial interaction model. Additionally, much of the clinical observations will be in the form of free text that must undergo a different pipeline than the rest of the data. In addition to parsing, indexing, and specialized deep learning for text, we will explore both shallow and deep Natural Language Processing (NLP) techniques to inform feature engineering [15].

2) **Models of Shape priors:** Most of the organs-of-interest in 3D medical images—such as the lung, heart, or liver—or in time series—such as the QRS complex—have well-defined shapes. Therefore, the use of shape constraints—combined, in the case of imaging data, with the visual appearance models—can considerably increase the diagnosis accuracy. To build accurate shape models for different human organs, we propose to model the boundary of any object with the vector of distances from points along the boundary to some central point, e.g. the centroid, then a linear combination of the distance vectors for a set of mutually aligned training boundaries will serve as the shape prior. All the aligned boundaries have the same center, and corresponding points of these boundaries lie on the same rays from the center. **The shape model will be used to specify the anatomy of human organs/structures which is important in the diagnosis of human disorders (e.g., autism, congestive heart failure, and diabetic retinopathy), See [16] for more mathematical details about the shape model.**

**Models of visual appearance:** The visual appearance of both the organ-of-interest and its surrounding tissues in a medical image is modeled by separating a mixed empirical marginal 1D distribution of voxel intensities into two individual components, associated with the dominant object-of-interest and background modes of the mixture, respectively. To model the current organ-of-interest appearance, the empirical distribution is precisely approximated with the linear combination of discrete Gaussians (LCDG) developed by our group, with positive and negative Gaussian components being automatically separated into the distinct object and background LCDG components. In many cases for empirical densities, it is difficult, if not impossible, to accurately approximate the shape using only a single symmetric kernel. The LCDG probabilistic model, on the other hand, is flexible enough to fit any empirical distribution. **This model will be used to describe the distribution of voxel intensity in 3D/4D medical images, which is an important feature that aid in describing the functionality of a human organ/structure.** See [17, 18,

## **19] for more mathematical details about the LCDG model.**

### **iii) Global feature extraction:**

These global features will be extracted from the global models (appearance, spatial, and shape models) described above by using stacked auto-encoder (SAE) networks [20]. Several auto-encoder networks can be separately pre-trained with an unsupervised learning algorithm, a technique known as greedy layer-wise pre-training, to extract the global features from the global models developed above. Then the whole SAE is fine-tuned using supervised learning to diagnose and/or identify the high-risk patients for a particular disease. Low-level features, useful for discriminant analysis, are extracted from the topmost hidden layer.

### **iv) Generalized canonical correlation analysis (GCCA) and multiview auto-encoders**

In order to fuse the extracted local and global features from all the available data that come from different modalities, we propose to use a GCCA model. GCCA is a standard statistical technique for finding linear projections of two random vectors that are maximally correlated. GCCA is used as an unsupervised multi-view learning technique, for learning maximally correlated linear projections of data in more than two data sets. In addition to GCCA, we will explore extending stacked auto-encoders to multiview data in a similar way to the Asymmetric and Mixed matrix factorization models [21]. We can thereby reduce the Big Data to a feature set that is both salient and computationally tractable in the context of a predictive and adaptive model for diagnosis and identification of high-risk patients for human diseases and disorders.

### **c. Relationship to the 2020 Plan and 21st Century University Strategic Mission**

This proposal directly addresses the UoFL 2020 Plan via: 1) enhancing the research, scholarship, creative activity and innovations by creating a nationally recognized program through strong intramural collaborations between the Schools of Medicine and Engineering; 2) advancing community engagement by enhancing excellence in health care delivery; 3) developing a high quality training program in Big Data to attract motivated, prepared and talented students; 4) establishing areas of research excellence in “Engineering Human Health”; 5) translating research innovations into commercial products; 6) increase research opportunities for underrepresented students in engineering; and, 8) enhancing research computing capabilities. Through the interdisciplinary collaborations established by this project, the new technological innovations in Big Data integration, analysis and interpretation will enable physicians to develop new, innovative clinical paradigms, such as predictive and adaptive models, to improve patient outcomes. Moreover, this research proposal will directly train the next generation of post-doctoral fellows, graduate and undergraduate students with the required skill set and technological expertise to manage Big Data in a clinical environment and address a critical global and societal need of the 21<sup>st</sup> Century.

### **d. Financial Commitments**

As indicated in the attached letters of support, the Deans of Speed School of Engineering and School of Medicine commit to providing more than the required one-to-one match (\$357,748/yr) compared to the amount requested from the university (\$250,000/yr). The details on the commitments of each participating department are described in the budget justification.

## **3. PROJECT MANAGEMENT TIMELINE, AND EXPECTED BENEFITS**

The inter-disciplinary team comprises experts in clinical, medical imaging, and computational domains. Dr. El-Baz and Dr. Keynton will serve as the Principal Investigators of the proposed project. Dr. El-Baz is a professor and Interim Chair of Bioengineering. Dr. Keynton is a professor, the Lutz Endowed Chair of Biomechanical Devices of the Department of Bioengineering, and Director of Research Initiatives in the Office of the Executive Vice President for Research and Innovation. The Co-Investigators include Dr. Bolli (Cardiology), Dr. Cooper (Anatomical Sciences & Neurobiology), Dr. Kaplan (Ophthalmology & Visual Sciences [OVS]), Dr. Koenig (Bioengineering; Cardiovascular & Thoracic Surgery [CVTS]), and Dr. Slaughter (CVTS), Dr. Nasraoui (Computer Engineering & Computer Science [CECS], founding director of the Knowledge Discovery & Web Mining Lab), Dr. Frigui (CECS, director of the Multimedia Lab), Dr. Rouchka (CECS, director Bioinformatics Core), and Dr. Altiparmak (CECS) [Note: Please see the personal statements in the individual biosketches for the roles of each PI and co-I for this project]. Drs. El-Baz, Keynton, Nasraoui, Frigui, Rouchka, and Altiparmak will oversee the computational aspects of Big Data analyses in close partnership with the clinical investigators to cross-train post-doctoral fellows and students (graduate, medical and undergraduate) while developing and implementing innovative and ground-breaking bioengineering, deep learning and data mining techniques on currently available Big Data to create new, innovative clinical paradigms, such as predictive and adaptive models, to improve patient outcomes through the diagnosis and identification of high risk patients for autism, heart failure and retinal diseases. Please see schematic (Figure A1) in Appendix I for an overview of the core components and the interactions between each component and team members.

### **a. Expected Outcomes**

The major outcomes of the proposed project are: i) develop novel machine learning tools and models that have the ability to analyze clinical Big Data and provide useful information to the clinician to aid them in making clinical decisions. These



new machine-learning tools will improve the delivery of healthcare in Kentucky, across the country, and worldwide by providing a new early diagnostic and high-risk patient identification tool for autistic, heart failure and retinal disease patients. ii) train a diverse group of next generation scientists and engineers with the technological expertise to analyze “Big Data in Medicine”; and, iii) establish a nationally recognized program in Big Data by strengthening intramural collaboration between School of Medicine and Speed School of Engineering.

#### **b. Project Milestones and Timeline**

Project Milestones		Year 1			Year 2			Year 3		
1.	Developing and implementing local features extraction deep learning networks.									
2.	Developing and implementing global features extraction stochastic models.									
3.	Applying the proposed Big Data developed approach on the proposed clinical studies									
4.	Creating Big Data analysis center by applying on NIH-T32 grant									
5.	Compilation of results, organization of data, and publications.									

#### **c. Assessment Plan**

The following objective metrics will be used to measure the outcomes of the proposed project: 1) number of students and post-docs trained in the program; 2) number of peer-reviewed journal publications published by the teams per year; 3) number of patent applications filed per year by the teams; 3) number of extramural grants on Big Data successfully funded; and, 4) clinicians’ appraisal on the utility of the Big Data methodologies.

### **4. PROJECT IMPACT ON SOCIETY AND UNIVERSITY’S MISSION**

By funding the proposed project, the following impacts on society and University of Louisville are anticipated: i) Improving patient outcomes to enrich the quality of life of patients and reduce healthcare costs. ii) Developing a critical mass of faculty in the area of Big Data to enhance the team’s competitiveness in securing a T32 grant from the NIH and establish a nationally recognized center for Big Data analysis at UofL. iii) Enhancing the reputation of the graduate programs at Speed School and School of Medicine by training the next generation of students with the technological expertise to face the challenges in Big Data analysis and preparing them for successful careers. iv) Increasing research opportunities for graduate, medical and undergraduate students, post-doctoral fellows and faculty by creating novel multidisciplinary research projects between the schools of medicine and engineering, and, v) Elevating the reputation of the University through an increase in research and scholarly productivity for all participating investigators.

### **5. SUSTAINABILITY PLAN**

#### **a. Evidence of national funding program**

In 2012, the Obama Administration announced a “Big Data Research and Development Initiative” with \$200 million in research and development commitments to Big Data for scientific discovery across the National Science Foundation (NSF), the National Institutes of Health (NIH), Department of Defense (DoD), Defense Advanced Projects Agency, Department of Energy (DOE), and the U.S. Geological Survey (USGS). At the same time, the NIH launched a trans-NIH Big Data to Knowledge (BD2K) initiative to address research and training issues related to biomedical Big Data. Specifically, in 2015, the NIH employed U24, R25 (multiple), T15, K01, UH2 and T32 funding mechanisms to support the advancement of Big Data methodologies and training programs to address healthcare needs in Big Data analysis.

#### **b. Engrained structure and plan to grow beyond this investment**

Currently, the structure of the Big Data program at UofL consists of multiple individual research projects. The proposed project will facilitate the formation of a structured program that will evolve into a Big Data Center at the University of Louisville. The proposed program consists of the core research team that has a demonstrated track record of securing extramural funding from the majority of governmental agencies including NIH, NSF, NASA, DoD and VA. After two years of implementation of this project, the members of the research team will submit multiple proposals to secure funding from the NIH T32 Predoctoral Training in Biomedical Big Data Science program, NIH R01 Biomedical Research Partnerships program or NSF Engineering Research Center program. Furthermore, all members of this project team will continue seeking external team funding (both federal and private foundation) for their research. It is anticipated that commercially viable products (e.g. algorithms, software, etc.) will be developed through the proposed efforts, which will lead to additional funding through the intellectual property. Furthermore, upon creation of the center, the team will partner with the university administration to secure philanthropic gifts to help establish the center, in addition to the extramural funding. Over the long-term, an external advisory board consisting of internationally and nationally renowned researchers will be formed to provide guidance and counsel on the progression of the program center.

## REFERENCES

1. C. Snijders, U. Matzat, and U. D. Reips, "Big gaps of knowledge in the field of internet science," *International Journal of Internet Science*, vol. 7, no. 1, pp. 1-5, 2012.
2. G. Ostrouchov, D. Schmidt, W.C. Chen, and P. Patel, "Combining R with scalable libraries to get the best of both for Big Data," *Proceedings of the IASC Satellite Conference for the ISI WSC*, vol. 59, pp. 85–90, 2013.
3. J. Manyika, M. Chui, B. Brown, J. Bughin, R. Dobbs, C. Roxburgh, et al., "Big data: The next frontier for innovation, competition, and productivity," 2011.
4. L.M. Xu, J.R. Li, Y. Huang, M. Zhao, X. Tang, L. Wei, "AutismKB: an evidence-based knowledgebase of autism genetics," *Nucleic Acids Research*, vol. 40, pp. D1016–D1022, 2012.
5. NCBI Resource Coordinators, "Database resources of the National Center for Biotechnology Information," *Nucleic Acids Research*, vol. 43, pp. D6–D17, 2015.
6. Society of Thoracic Surgeons, "2014 STS general thoracic surgery database specifications," Available at [http://www.sts.org/sites/default/files/documents/STSThoracicDataSpecsV2\\_3.pdf](http://www.sts.org/sites/default/files/documents/STSThoracicDataSpecsV2_3.pdf), Accessed 2016 January 11.
7. H. Liu, W. Liu, Y. Liao, L. Chen, Q. Liu, X. Ren, et al., "CADgene: a comprehensive database for coronary artery disease genes," *Nucleic Acids Research*, vol. 39, pp. D991–D996, 2011.
8. J.K. Kirklin, D.C. Naftel, F.D. Pagani, R.L. Kormos, L.W. Stevenson, E.D. Blume, S.L. Myers, M.A. Miller, J.T. Baldwin, J.B. Young, "Seventh INTERMACS annual report: 15,000 patients and counting," *Journal of Heart and Lung Transplantation*, vol. 34, pp. 1495–1504, 2015.
9. Y. Yu, R. Reynolds, B. Rosner, M.J. Daly, and J.M. Seddon, "Prospective assessment of genetic effects on progression to different stages of age-related macular degeneration using multistate Markov models," *IOVS*, vol. 53, pp. 1548–1556, 2012.
10. ArcticDx Inc., "AMD progression and prognosis," Available at <http://www.macularisk.com/amd-prognosis.html>, Accessed 2016 January 11.
11. T. W. Anderson, "An Introduction to Multivariate Statistical Analysis," John Wiley and Sons, 2nd edition, 1984.
12. C. Shen, M. Sun, M. Tang, and C. E. Priebe, "Generalized canonical correlation analysis for classification," *Journal of Multivariate Analysis*, vol. 130, pp. 310-22, 2014.
13. A. Farag, A. El-Baz, and G. Gimel'farb. Precise segmentation of multimodal images. *IEEE Transactions on Image Processing*, vol. 15, no 4, pp. 952–968, 2006.
14. F. Khalifa, G. M. Beache, M. Abou El-Ghar, T. El-Diasty, G. Gimel'farb, M. Kong, and A. El-Baz, "Dynamic contrast-enhanced MRI-based early detection of acute renal transplant rejection," *IEEE Transactions on Medical Imaging*, vol. 32, no. 10, pp. 1910–1927, 2013.
15. M Soliman, O Nasraoui, NGF Cooper, "Building a glaucoma interaction network using a text mining approach", *BioData Mining*, 9(17), 2016.
16. A. El-Baz and G. Gimel'farb, "Image Segmentation with a Parametric Deformable Model using Shape and Appearance Priors," *Proc. of IEEE Conference on Computer Vision and Pattern Recognition (CVPR'08)*, Anchorage, Alaska, USA June 24-26, 2008, pp. 1-8.
17. A. El-Baz, A. A. Farag, and G. Gimel'farb. Iterative approximation of empirical grey-level distributions for precise segmentation of multimodal images. *EURASIP Journal Applied Signal Processing*, pp. 1969–1983, 2005.
18. A. El-Baz and G. Gimel'farb. EM-based approximation of empirical distributions with linear combinations of discrete Gaussians. In *Proc. IEEE Int. Conf. Image Process., (ICIP'07)*, volume 4, pages 373–376, 2007.
19. A. El-Baz, A. Elnakib, F. Khalifa, M. Abou El-Ghar, P. McClure, A. Soliman, and G. Gimel'farb. Precise segmentation of 3-D magnetic resonance angiography. *IEEE Transactions on Biomedical Engineering*, vol. 59, pp. 2019–2029, 2012.
20. E. H. Asl, J. Zurada, O. Nasraoui, "Deep Learning of Part-based Representation of Data Using Sparse Autoencoders with Nonnegativity Constraints," *IEEE Transactions on Neural Networks and Learning Systems*, pp 1-13, Oct. 2015.
21. J.C. Caicedo, J. Ben-Abdallah, F. Gonzalez, O. Nasraoui, "Multimodal Representation, Indexing, Automated Annotation and Retrieval of Image Collections via Non-Negative Matrix Factorization", *Neurocomputing*, 76(1): 50-60, 2012.

## **Appendix I: Project Management Figure**

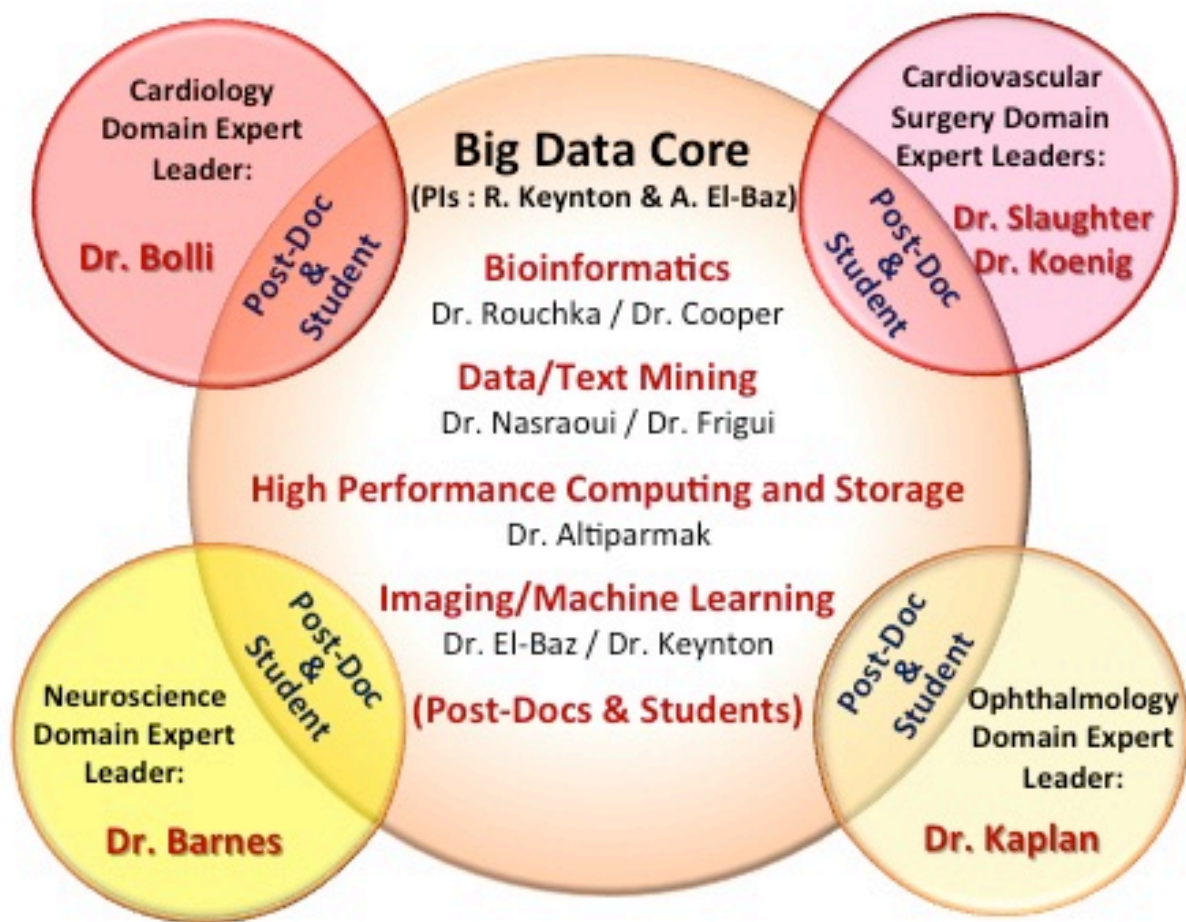


**Figure A1:** An overview of the core components and the roles of each team member on the project.



## **Appendix II: Biosketches**

## BIOGRAPHICAL SKETCH

NAME Robert S. Keynton	POSITION TITLE Professor & Lutz Endowed Chair of Biomech. Devices, Department of Bioengineering, University of Louisville Director of Research Initiatives, Office of EVPRI, UofL
eRA COMMONS USER NAME RSKeynton	

EDUCATION/TRAINING *(Begin with baccalaureate or other initial professional education, such as nursing, include postdoctoral training and residency training if applicable.)*

INSTITUTION AND LOCATION	DEGREE (if applicable)	YY	FIELD OF STUDY
Virginia Tech, Blacksburg, VA	B.S.	1997	Engineering Science and Mechanics
University of Akron, Akron, OH	M.S.	1990	Biomedical Engineering
University of Akron, Akron, OH	Ph.D.	1995	Biomedical Engineering

### A. Personal Statement

The goal of this 21<sup>st</sup> Century Initiative project is to develop a new paradigm for integrating Big Data from multiple sources to create a decision matrix that aids clinicians in the early diagnosis of human diseases and disorders. As the founding Chair of the Department of Bioengineering, I have extensive experience in assembling large teams to accomplish project goals such as developing the current integrated B.S.-M.Eng. degree program curriculum and actively facilitating research collaborations between faculty in Bioengineering and the UofL Health Science and Medical Campus which has lead to the funding of multiple multi-million dollar projects (~\$25M for other BE faculty & ~\$35M for Keynton as PI or co-PI). I have mentored all faculty in the Department of Bioengineering to successfully secure external funding, including four faculty that received the prestigious and highly competitive Wallace H. Coulter Foundation Translational Research Early Career Award, which led to UofL being awarded the \$5M W.H. Coulter Foundation Translation Partnership Award (PI - Keynton), which supports technologies with significant potential for clinical impact and commercialization. In addition, I am PI of the NSF I-Corps Site award at UofL and a member of the Leadership Team and co-Investigator on the UofL ExCITE Hub NIH REACH award. I have co-founded three start-up companies, one of which successfully received Phase I and Phase II NIH-sponsored SBIR funding. To date, I have co-authored 26 patent disclosures, which have resulted in 6 issued patents, 12 patent applications and the issuance of five licenses. I have served as research mentor to a number of post-doctoral fellows, research engineers and Ph.D., Masters and undergraduate students. My research focuses on the creation of data analysis systems; medical devices and systems; micro/nano devices and systems for biological and chemical separation, detection and sensing; tissue engineered scaffolds; drug delivery systems; and, cardiovascular mechanics and fluids. **My role on this project will be as Principal Investigator (Multi-PI) and will be responsible for overall project management, partnering and facilitating interactions between clinical experts with Big Data personnel as well as development of data analysis methodologies and systems, translation of technologies into practice, and mentorship of postdoctoral fellows and students.**

### B. Positions and Honors.

#### Positions and Employment

2016 to Present	Director of Research Initiatives, Office of EVPRI, University of Louisville (UofL)
2016 to Present	Co-founder, CoulSense, LLC, Louisville, KY
2009 to Present	Lutz Endowed Chair of Biomechanical Devices, UofL
2006 to 2009	University Scholar, Bioengineering, UofL
2006 to Present	Co-founder, Ultra-Trace Detection, LLC, Louisville, KY
2006 to Present	Professor, Bioengineering, UofL
2005 to 2016	Chair, Department of Bioengineering, UofL

2005 to 2006	Associate Professor, Bioengineering, UofL
2004 to 2007	Interim Scientific Director & Endowed Chair, Cardiovascular Innovation Institute, UofL
2003 to Present	Co-founder, Assenti, LLC, Louisville, KY
2003 to 2005	Director, Bioengineering Program, UofL
2002 to 2005	Associate Professor, Mechanical Engineering, UofL
1999 to 2002	Assistant Professor, Mechanical Engineering, UofL
1995 to 1998	Assistant Professor, Biomedical Engineering, Louisiana Tech University
1995 to 1998	Faculty Research Associate, Inst. for Micromanufacturing, Louisiana Tech University
1995 to 1998	Adjunct Faculty, Dept. of Phys. & Biophysics, LSU Medical Ctr., Shreveport, LA

### **Other Experience and Professional Memberships**

- Member of the NIBIB Consortium on Addressing Paralysis through Spinal Stimulation Technologies
- Member of 13 professional societies for engineers and scientists.
- Member of American Association for the Advancement of Science, 2008.
- Technology Journal Editorial Board.

### **Honors (selected)**

- American Institute for Medical & Biological Engineering (AIMBE) Board of Directors, 2012-2014.
- Chair of the AIMBE Academic Council, 2012-2014.
- Keynote and Invited speaker at ASAIO Conference, 2010 and 2013, respectively,
- Invited speaker at the 2011 Gordon Research Conference on Assisted Circulation, 2011.
- Elected Secretary of the Bioengineering Council of Chairs, 2010
- Guest panelist on National Public Radio's *State of Affairs* Radio Program on Biotechnology, 2009.
- Fellow – AIMBE, 2007.
- Named University Scholar at the University of Louisville, 2006.
- American Chemical Society: Nano Letters, 2004 article was featured in MIT Technology Review (p. 29, 2004), Chem. and Engineering News (p.24, 2004), MRS Bulletin (pp. 789-790, 2004), High Performance Plastics, Veille strategique Instrumentation pour la biologie, and Micro/Nano Newsletter p.8, 2005.
- Institute of Physics: Journal for Micromechanics and Microengineering, 2002 article was featured in BBC News Online Health, Biophotonics International Magazine, Clinica Magazine, RAD Magazine, Small Times Magazine, The Engineer Magazine, and the radio program "FutureWatch".
- 2001 Outstanding Young Scientist Award, Houston Society of Engineering in Medicine & Biology.
- T.L. James Outstanding Research Award - 1998, Co-recipient, Louisiana Tech University, \$2,500.
- College of Engineering & Science Professional Development Award - 1997, Louisiana Tech Univ., \$1,000.

### **C. Contributions to Science**

1. Related to this application, I have been recently engaged in the development of novel CAD systems for the diagnosis of different human disorders using a variety of imaging modalities for data analysis. This includes, but not limited to, higher-dimensional data from structural magnetic resonance imaging (MRI), Dynamic Contrast-Enhanced Magnetic Resonance Imaging (DCE-MRI), Diffusion-weighted MRI, and Computed Tomography (CT).
  - a. M. Ismail, **R. Keynton**, M. Mostapha, A. ElTanboly, M. Casanova, G. Gimel'farb, and A. El-Baz, "Studying Autism Spectrum Disorder with Structural and Diffusion Magnetic Resonance Imaging: A Survey," *Frontiers in Human Neuroscience*, vol. 10, pp. 211-279, 2016.
  - b. E. Hosseini-Asl, **R. Keynton**, and A. El-Baz, "Alzheimer's Disease Diagnosis by Adaptation of 3D Convolutional Network", ICIP'16, Phoenix, Arizona, USA, September 25–28, 2016 (*In Press*).
  - c. M. Ismail, A. Soliman, A. ElTanboly, A. Switala, M. Mahmoud, F. Khalifa, G. Gimel'farb, M. F. Casanova, **R. Keynton**, and A. El-Baz, "Detection of White Matter Abnormalities in MR Brain Images for Diagnosis of Autism in Children," ISBI'16, Czech Republic, April 13–16, 2016, pp 6-9.
2. Fourteen years ago, my lab established collaborations with an analytical chemist to develop lab-on-a-chip (LOC) devices and data acquisition and analysis systems for electrochemical detection (ED) applications. Our group was the first to successfully fully integrate on a single LOC platform, both the driving and

detection electrodes through the creation of a “shelf” that rapidly decreased the electrical resistance and capillary electrophoresis voltage drop. In recent years, our collaborations have extended to the development of an integrated, ED-based, autonomous, calibration-free, remote sensing LOC platform for monitoring heavy metals with high reproducibility and limits of detection on the order of hundreds of femtomolars. In these projects, my team computationally modeled, designed, developed, fabricated and fluid dynamically characterized the microfluidic platforms and components and also created and constructed the solar powered, microcontroller-based instrumentation, **data analysis and storage systems and system network integration** for remote deployment of the system. These discoveries advanced the field by providing, for the first time, the means by which other investigators could develop fully integrated ED LOC platforms for a variety of micro Total Analytical Systems and Point-of-Care devices.

- a. Baldwin, R., Roussel, T.J., Crain, M.M., Bathlagunda, V., Jackson, D.J., Gullapalli, J., Conklin, J.A., Pai, R., Naber, J.F., Walsh, K.M., and **Keynton, R.S.**, "Fully-Integrated On-Chip Electrochemical Detection for Capillary Electrophoresis in a Microfabricated Device," *Analytical Chemistry*, vol. 74, no. 15, pp. 3690-3697, 2002. DOI: 10.1021/ac011188n.
- b. Jackson, D., Naber, J., Roussel, Jr., T.J., Crain, M.M., Walsh, K.M., **Keynton, R.S.**, and Baldwin, R.P., "Portable High Voltage Power Supply and Electrochemical Detection Circuits for Microchip Capillary Electrophoresis," *Anal. Chem.*, 75(14), 3311-17, 2003. DOI: 10.1021/ac0206622.
- c. **Keynton, R.S.**, Roussel, T.J., Crain, M.M., Jackson, D.J., Franco, D.B., Naber, J.F., Walsh, K.M., and Baldwin, R.P., "Design and development of microfabricated capillary electrophoresis devices with electrochemical detection," *Analytica Chimica Acta*, vol. 507, no. 1, pp. 95-105, April 2004. DOI: 10.1016/j.aca.2003.12.042.
- d. M.M. Marei, T.J. Roussel, R.P. Baldwin and **R.S. Keynton**, "Sequential Multi-Potential Double Potential Step Anodic Stripping Coulometry for Calibration-less Detection of Heavy Metal Mixtures," Provisional Patent Application #62/128,953, filed 3/5/15.
3. In addition to the research mentioned above, my group has been actively involved in the development of a direct-write method for the precise and controllable fabrication of micro- and nano-scale fibers for a variety of applications including the creation of microvasculature, 3-D microfluidic structures, and novel sensors. This innovation has provided engineers and researchers with the ability to produce point-to-point polymer micro- and nano-scale fibers in 3-D with high precision at room temperature for the creation of a wide variety of materials, substrates, complex microfluidic structures and sensing systems.
  - a. S.A. Harfenist, S.D. Cambron, E.W. Nelson, S.M. Berry, A.W. Isham, M.M. Crain, K.M. Walsh, **R.S. Keynton**, and R.W. Cohn, "Direct drawing of suspended filamentary Micro- and Nanostructures from liquid polymers," *NanoLetters*, vol. 4, no. 10, pp. 1931-37, 2004. DOI: 10.1021/nl048919uS.
  - b. Berry, S.A. Harfenist, R.W. Cohn and **R.S. Keynton**, "Characterization of Micromanipulator Controlled Dry Spinning of Micro- and Nanoscale Polymer Fibers," *J. Micromech. Microeng.*, 16 (2006) 1825-1832. DOI: 10.1088/0960-1317/16/9/010
  - c. J.M. Rathfon, Z.M. Al-Badri, R. Shunmugam, S.M. Berry, S. Pabba, **R.S. Keynton**, R.W. Cohn and G.N. Tew, "Fluorimetric Nerve Gas Sensing Based on Pyrene Imines Incorporated into Films and Sub-micron Fibers," *Adv Funct. Mater.*, 2009, vol. 19, pp. 1-7. DOI: 10.1002/adfm.200800947
  - d. S.M. Berry, S.P. Warren, D.A. Hilgart, A.T. Schworer, S. Pabba, A.S. Gobin, R.W. Cohn and **R.S. Keynton**, "Endothelial Cell Scaffolds Generated by 3D Direct Writing of Biodegradable Polymer Microfibers," *Biomaterials*, 2011, vol. 32, issue 7, pp. 1872-79. DOI:10.1016/j.biomaterials.2010.11.023
4. My research program has also been involved in using *in vitro* and *in vivo* models to investigate the role of hemodynamics in the development of intimal hyperplasia in and around distal anastomoses of vascular bypass grafts. At the time, the existing methodologies employed by investigators consisted of indirectly correlating hemodynamic data attained from computational or *in vitro* models, constructed from single casts or averaged images of distal anastomoses within animal models or human subjects, to histological data. My early publications involved the development and characterization of a new pulse ultrasonic Doppler transducer to directly measure *in vivo* wall shear rates and the implementation of this transducer



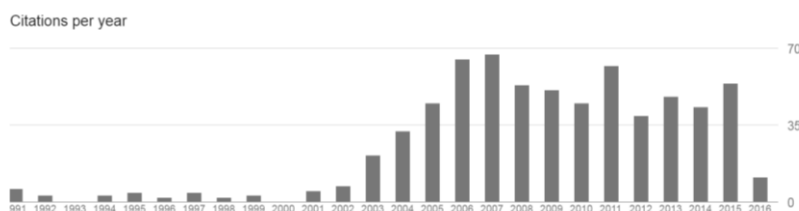
in an *in vivo* model study investigating the effect of graft caliber and wall shear stress on the development of intimal hyperplasia. I designed, fabricated and implemented the pulse ultrasonic Doppler transducer and designed and conducted all the *in vivo* animal studies and corresponding data analysis. This work was able to disprove several hemodynamic parameters that had been theorized to lead to the development of cardiovascular diseases (such as peak wall shear stress and wall shear stress gradient). Furthermore, these results demonstrated that mean and oscillatory shear index best correlated with the development of intimal hyperplasia.

- a. **Keynton, R.S.**, Rodway, N.V., Evancho, M.M., Sims, R.L., Gobin, A.S., and Rittgers, S.E., "Intimal Hyperplasia and Wall Shear in Arterial Bypass Graft Distal Anastomoses: An In Vivo Model Study," J Biomech Engr., 123(5):464-473, 2001. DOI:10.1115/1.1389461
  - b. **Keynton, R.S.**, Evancho, M.M., Sims, R.L., and Rittgers, S.E., "The Effect of Graft Caliber Upon Wall Shear within In Vivo Distal Vascular Anastomoses," J Biomech. Engr., 121(1): 79-88, 1999. DOI:10.1115/1.2798047.
  - c. **Keynton, R.S.**, Nemer, R.E., Neifert, Q.Y., Fatemi, R.S. and Rittgers, S.E., "Design, Fabrication and In Vitro Evaluation of an In Vivo Ultrasonic Doppler Wall Shear Rate Measuring Device," IEEE Trans. Biomed. Eng., 42(5):433-441, 1995. DOI:10.1109/10.376147.
5. Long-term space exploration has created the need to understand the biological effects of hypergravity and radiation exposure on astronauts on a cellular level to enable the development of mitigation strategies. In these publications, my role was to develop and implement an in vitro cell culture system to investigate the effect of hypergravity on endothelial cell (EC) permeability as well as explore potential therapeutic agents to mitigate increases in EC permeability. In recent years, my team has been involved in the identification and delivery of naturally occurring pharmaceutical agents to minimize the effects of radiation in astronauts. These discoveries have advanced the field by identifying specific therapeutic agents and new drug delivery vehicles to mitigate adverse events experienced by astronauts.
- a. C.M. Klinge, K.A. Blankenship, K.E. Risinger, S. Bhatnagar, E.L. Noisin, D.M. Brey, and **R.S. Keynton**, "Resveratrol and estradiol rapidly activate MAPK signaling through estrogen receptors alpha and beta in bovine aortic endothelial cells," J. Biol. Chem. 2005; 280(9): pp. 7460-7468. DOI: 10.1074/jbc.M411565200
  - b. W. Sumanasekera, G. Sumanasekera, **R.S. Keynton** and C.M. Klinge, "Estradiol and dihydrotestosterone regulate endothelial cell barrier function following hypergravity-induced alterations in MAPK activity," Am J Physiol Cell Physiol, 2007, Aug; 293 (2): C566-73. DOI: 10.1152/ajpcell.00418.2006
  - c. W.K. Sumanasekera, L. Zhao, M. Ivanova, D.D. Morgan, E.L. Noisin, **R.S. Keynton**, and C.M. Klinge, "Effect of estradiol and dihydrotestosterone on hypergravity-induced MAPK signaling and occludin expression in human umbilical vein endothelial cells," Cell and Tissue Res., (2006) 324:243-253. DOI: 10.1007/s00441-005-0113-0

#### Complete List of Published Work:

<https://scholar.google.com/citations?user=jlzw2C0AAAAJ&hl=en&oi=ao>

	Google Scholar	
	All	2011-2016
Citations	1553	682
h-index	20	14
i10-index	25	20



## D. Research Support

### Ongoing Research Support

1. **NSF 1450370** **Keynton (PI)** **3/1/15 – 2/28/18**  
University of Louisville Innovation Corps Site (I-Corps Site)  
The goal of the University of Louisville Innovation Corps Site program is to integrate and leverage existing commercialization infrastructure and to establish a sustainable program for the discovery and commercialization of STEM innovations and stimulate regional economic development.  
Role: **PI**
2. **U01 HL127518-01** **Bates (PI)** **3/20/15 – 2/28/18**  
ExCITE – Expediting Commercialization, Innovation, Translation, and Entrepreneurship  
The overarching goal of this project is to create a commercialization program at the University of Louisville to increase the success rate and speed with which the results of basic biomedical research are translated into products that have a positive impact on human health.  
Role: **co-I**
3. **TP2 Program** **Keynton (PI)** **7/1/11 – 6/30/17**  
Wallace H. Coulter Foundation Translational Partnership Award  
The goal of this project is to promote translational research via establishing partnerships between engineers and clinicians for the creation of new innovations to save and improve patient quality of life.  
Role: **PI**
4. **NASA NNX13AD33** **Soucy (PI)** **1/1/13 – 12/31/16**  
A Paradigm-Shifting Therapy for Mitigating Cellular and Tissue Damage in Humans Exposed to Radiation  
The goal of this project is to create curcumin-filled nanoparticles to activate the mediators responsible for cellular self-repair from radiation-induced DNA damage in astronauts.  
Role: **co-I**

### COMPLETED Research Support

1. **NASA NNX10AJ36G** **Keynton (PI)** **9/1/10 – 8/31/12**  
Diagnosing and Mitigating Human Exposure to Radiation Using Micro/Nanotechnology  
The goal of this project was to create a diagnostic tool and countermeasures to assess and mitigate human exposure to radiation.  
Role: **PI**
2. **NSF PFI 090754** **Shaver (PI)** **1/1/10 – 12/31/12**  
Lowcountry Partnership for Biomedical Innovation  
This project will enhance the innovation enterprise by expanding on the medical research capability of the Medical University of South Carolina with the entrepreneurial expertise available at the College of Charleston.  
Role: **Mentor to PI and PI subaward to UofL**
3. **NSF EPSCoR 070678** **Gobin (PI)** **7/1/08 – 5/31/13**  
Engineering Platforms for Exploring Cellular and Molecular Signaling Processes  
The goal was to develop a regionally and nationally recognized center in which we develop new technology to further elucidate cellular and molecular signaling processes with real-time spatial and temporal resolution.  
Role: **co-PI**
4. **NSF EPSCoR 070679** **Walsh (PI)** **7/1/08 – 5/31/13**  
A Statewide Micro/Nano Network for Collaborative Research, Education, and Outreach  
The goal of this project was to develop a physical and virtual network throughout Kentucky for the specific advancement of micro/nanotechnology and the many fields of research /education that utilize this pervasive technology.  
Role: **co-PI**

## BIOGRAPHICAL SKETCH

NAME Ayman S. El-Baz	POSITION TITLE Professor and Interim Chair, Dept. of Bioengineering Director, Bioimaging Laboratory Speed School of Engineering, University of Louisville.
eRA COMMONS USER NAME ASELBA01	

EDUCATION/TRAINING *(Begin with baccalaureate or other initial professional education, such as nursing, include postdoctoral training and residency training if applicable.)*

INSTITUTION AND LOCATION	DEGREE <i>(if applicable)</i>	YY	FIELD OF STUDY
Mansoura University, Egypt	B.S.	1997	Electrical and Computer Engineering
Mansoura University, Egypt	M.S.	2000	Electrical and Computer Engineering
University of Louisville	Ph.D.	2006	Electrical and Computer Engineering

### A. Personal Statement

Ayman El-Baz, Ph.D., Professor and Interim Chair of Bioengineering at the University of Louisville and has 15-years of hands-on experience in the fields of biosignal, bioimaging modeling, machine learning and computer assisted functional diagnostic systems, including those using CT, MRI, EMG, ECG, EEG and other physiological signals. His main research contributions include: 1) Development of a new image-based technology for the early diagnosis of lung cancer, 2) Development of techniques for the early diagnosis of Autism, based on using magnetic resonance images to analysis various brain structures, 3) Development of a new technology for the early detection of acute renal rejection, based on use of dynamic magnetic resonance images, 4) Development of a new technology for the early diagnosis of prostate cancer using non-invasive diffusion magnetic resonance images, and 5) Development of image based systems for the early detection of heart failure using tagged, cine, and late contrast magnetic resonance images. He has also developed new techniques for accurate identification of probability mixtures for segmenting multi-modal images, new probability models and model-based algorithms for recognizing lung nodules and blood vessels in magnetic resonance and computer tomography imaging systems, and new registration techniques based on multiple second-order signal statistics, all of which have been reported in premiere international conference proceedings and archived journals. Dr. El-Baz and the investigators of this proposal have collaborated together on several projects over the last ten years. The current proposal is a natural continuation of their collaborative efforts. **He will serve as a Principal Investigator (Multi-PI) on the proposed project and will be responsible for medical imaging analysis, developing novel algorithms for image processing and facilitating the interactions between bioinformatics, data/text mining, high performance computing and storage, imaging and machine learning methodologies.**

### B. Positions and Honors

#### Positions and Employment

- 2016 – Present Interim Chair, Bioengineering Department, University of Louisville (UofL).
- 2016 – Present Professor – Tenured (Promoted for Early Professorship), Bioengineering Department, Speed School of Engineering, UofL.
- 2013 – 2014 Interim Chair, Bioengineering Department, University of Louisville (UofL).
- 2011 – 2015 Associate Professor, Bioengineering Department, Speed School of Engineering, University of Louisville (UofL).
- 2014 – 2015 Associate Faculty, Computer Engineering and Computer Science Department, Speed School of Engineering, University of Louisville (UofL).

- 2007 – 2015 Associate Faculty – Assistant Professor, Department of Psychiatry & Behavioral Sciences, School of Medicine, University of Louisville (UofL).
- 2007 – 2015 Associate Faculty – Assistant Professor, Department of Electrical and Computer Engineering, Speed School of Engineering, UofL.
- 2006 – 2011 Assistant Professor – **Tenure Track**, Bioengineering Department, Speed School of Engineering, University of Louisville (UofL).
- 2001 – 2006 Research Assistant, Computer Vision & Image Processing laboratory, UofL.

### **Other Experience and Professional Memberships**

- Institute of Electrical and Electronics Engineers (IEEE) – *Member*
- Medical Imaging, Computing and Computer-Assisted Interventions (MICCAI) – *Member*
- International Association of Pattern Recognition (IAPR) – *Member*
- Sigma Xi and Eta Kappa - *Member*

### **Honors**

- University Scholar (University of Louisville), 2013-present.
- Recipient of the Provost's Award for Exemplary Advising Award, 2012-2013.
- Faculty Favorite, an outstanding professor nominated by students, 2012-2013.
- Researchers recognized for work that can lead to commercialization for his new image-based technology for early diagnosis of lung cancer, September 2012.
- Speed School nominee for Outstanding Scholarship in Basic and Applied Sciences, 2011-2012.
- Citation Paper Award from the Society for Neurofeedback & research Conference, 2012.
- 2011-2012 "Top 4" Faculty Favorite.
- The Provost's Award for Exemplary Advising Award Nominee, 2011.
- Coulter Fellow since August 9th, 2011.
- Citation Paper Award from the Society of UroRadiology (SUR), 2011.
- Nominated for early promotion and tenure, 2011.
- Named by Kauffman Foundation among 50 most promising startups worldwide for developing a new technology for early diagnosis of lung cancer, 2010.
- Citation Paper Award from the Association for Applied Psychology and Biofeedback, 2010.
- Wallace H. Coulter Foundation, Early Career Translational Research Award in Biomedical Engineering, Phase I and Phase II.
- EUREKA RO1 award NIMH on autism, 2009- 2013.
- Researchers recognized for work that can lead to commercialization, November 2009.
- PAMI Travel Award to attend IEEE Computer Society Conference on Computer Vision and Pattern Recognition (CVPR'08), 2008.
- The Louisville University's single nominee for Pew Scholars Award, 2007.
- The John M. Houchens Prize for Outstanding Dissertation for summer and fall 2006.
- Best Paper Award, International Conference on Graphics, Vision and Image Processing, 2005.
- First place winner annual Research! Louisville Meeting, 2002, 2005, 2006, 2007, 2008-2011.

### **C. Contribution to Science**

1. Related to this project, my group has been actively engaged in the development of a novel CAD system for the early diagnosis of autism using Magnetic Resonance (MR) images. This CAD system is based on distinguishing autistic brains from normally developed brains based on our new findings that the thickness of the cerebral white matter gyrifications of autistic subjects are thinner than the thickness of CWM matter gyrifications of normal brains. The innovation in this study is based on using Spherical Harmonics (SHs)



decomposition to quantify shape discrepancies in the brain cortex in an effort to extract features that distinguish autistic patients from controls.

- a. M. Ismail, A. Soliman, A. ElTanboly, A. Switala, M. Mahmoud, F. Khalifa, G. Gimel'farb, M. F. Casanova, R. Keynton, and **A. El-Baz**, "Detection of white matter abnormalities in MR brain images for diagnosis of Autism in children," *In: Proceedings of International Symposium on Biomedical Imaging: From Nano to Macro (ISBI'16), Prague, Czech Republic, April 13–16, 2016*, (in press).
- b. M. Ismail, R. Keynton, M. Mostapha, A. ElTanboly, M. Casanova, G. Gimel'farb, and **A. El-Baz**, "Studying Autism Spectrum Disorder with Structural and Diffusion Magnetic Resonance Imaging: A Survey," *Frontiers in Human Neuroscience*, vol. 10, pp. 211-279, 2016.
- c. M. Casanova, **A. El-Baz**, and J. Suri, Editors, *Imaging the Brain in Autism*, Springer-Verlag, New York, May 2013, ISBN-13: 9781461468424, ISBN-10: 1461468426.
- d. M. Casanova, **A. El-Baz**, S. Kamat, B. Dombroski, F. Khalifa, A. Elnakib, A. Soliman, A. Allison-McNutt, and A. Switala, "Focal cortical Dysplasias in Autism Spectrum Disorders," *Acta Neuropathologica Communications* 2013, vol. 1, issue 1, pp. 1-11, October, 2013.
2. Development of a new MRI-based non-invasive CAD system for early detection of Dyslexia.
  - a. M. Nitzken, M. Casanova, G. Gimel'farb, T. Inanc, J. Zurada, and **A. El-Baz**, "Shape Analysis of Human Brain: A Brief Survey," *IEEE Journal of Biomedical and Health Informatics*, vol. 18, pp. 1337-1354, 2014.
  - b. A. Elnakib, A. Soliman, M. Nitzken, M. F. Casanova, G. Gimel'farb, and **A. El-Baz**, "Magnetic Resonance Imaging Findings for Dyslexia: A Review," *Journal of Biomedical Nanotechnology*, vol. 10, pp. 2778-2805, 2014.
  - c. A. Elnakib, M. Casanova, G. Gimel'farb, A. Switala, and **A. El-Baz**, "Dyslexia Diagnostics by 3D Shape Analysis of the Corpus Callosum," *IEEE Transactions on Information Technology in Biomedicine*, vol. 16, no. 4, pp. 700-708, July 2012.
  - d. E. Williams, **A. El-Baz**, M. Nitzken, A. Switala, and M. Casanova, "Spherical Harmonic Analysis of Cortical Complexity in Autism and Dyslexia," *Translational Neuroscience*, vol. 3, no. 1, pp. 36-40, March 2012.
3. Development of a new non-invasive CAD system for the automatic detection of acute renal rejection after kidney transplantation, using Dynamic Contrast-Enhanced Magnetic Resonance Images (DCE-MRI) and Diffusion Weighted MRI (DW-MRI). The innovation in this work is a comprehensive noninvasive CAD system that optimally characterizes the status of the transplanted kidney based on the fusion of stochastic approaches using new MGRF energy models and geometric approaches.
  - a. F. Khalifa, G. Beache, M. Abou El-Ghar, T. El-Diasty, G. Gimel'farb, M. Kong, and **A. El-Baz**, "Dynamic Contrast-Enhanced MRI-Based Early Detection of Acute Renal Transplant Rejection," *IEEE Transactions on Medical Imaging*, vol. 32, no. 10, pp. 1910–1927, 2013.
  - b. F. Khalifa, M. Abou El-Ghar, B. Abdollahi, H. Frieboes, T. El-Diasty, and **A. El-Baz**, "A Comprehensive Non-Invasive Framework for Automated Evaluation of Acute Renal Transplant Rejection using DCE-MRI," *NMR in Biomedicine*, vol. 26, no. 11, pp. 1460–1470, 2013.
  - c. F. Khalifa, **A. El-Baz**, G. Gimel'farb, and M. Abo El-Gahr, "**Non-Invasive Image-Based Approach for Early Detection of Acute Renal Rejection**," *Proc. of International Conference on Medical Image Computing and Computer-Assisted Intervention (MICCAI'10)*, Beijing, China, September 20 - 24, 2010, vol. 1, pp. 10-18.
  - d. M. Shehata, F. Khalifa, A. Soliman, A. Takieldeem, M. Abou El-Ghar, A. C. Dewyer, R. Ouseph, **A. El-Baz**, and R. Keynton, "3D diffusion MRI-based CAD system for early diagnosis of acute renal rejection," *In: Proceedings of International Symposium on Biomedical Imaging: From Nano to Macro (ISBI'16), Prague, Czech Republic, April 13–16, 2016*, (in press).
4. Development of a software system to eliminate the ECG artifacts from EMG recordings. The developed approach has the ability to remove the ECG artifacts without altering the amplitude and frequency components of the EMG signal by using an externally recorded ECG signal as a mask to locate areas of the ECG spikes within EMG data. **These segments containing ECG spikes were decomposed into**

**128 sub-wavelets by a custom-scaled Morlet Wavelet Transform.** The ECG-related sub-wavelets at the ECG spike location were removed and a de-noised EMG signal was reconstructed. Validity of the proposed method was proven using mathematical simulated synthetic signals and EMG obtained from SCI patients. We compare the Root-mean Square Error and the Relative Change in Variance between this method, global, notch and adaptive filters. The results show that the localized wavelet-based filtering has the benefit of not introducing error in the native EMG signal and accurately removing ECG artifacts from EMG signals.

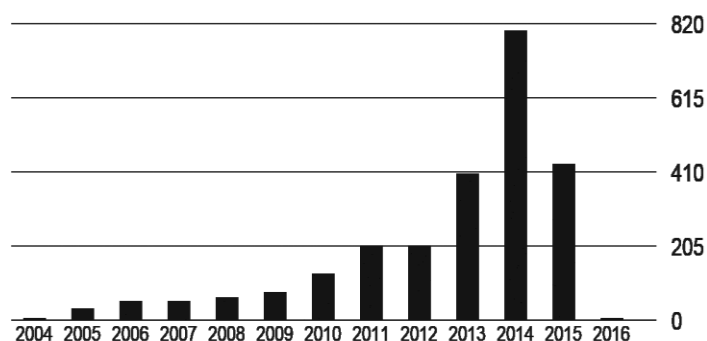
- a. M. Nitzken, N. Bajaj\*, S Aslan, G Gimel'farb, **A. El-Baz**, A. Ovechkin, "Local Wavelet-Based Filtering of Electromyographic Signals to Eliminate the Electrocardiographic-Induced Artifacts in Patients with Spinal Cord Injury," *Journal of Biomedical Science and Engineering*, vol. 6, pp. 1-13, July, 2013.
5. Development of a novel automatic CAD system for the early detection and diagnosis of lung cancer based on estimating new indices (e.g., a shape index, an appearance index, and a growth rate index) from spiral low dose computed tomography images. This system is able to quickly diagnose small, malignant lung nodules at an early stage as well as large nodules located more than 4 cm away from large diameter airways, cases which the current technology, i.e. needle biopsy and bronchoscopy, fail to diagnose.
  - a. **A. El-Baz** and J. Suri, Editors, *Lung Imaging and Computer Aided Diagnosis*, Taylor & Francis, October 2011, ISBN: 9781439845578, ISBN 10:1439845573.
  - b. **A. El-Baz**, A. Elnakib, M. Abou El-Ghar, G. Gimel'farb, R. Falk, and A. Farag, "Automatic Detection of 2D and 3D Lung Nodules in Chest Spiral CT Scans," *International Journal of Biomedical Imaging*, vol. 2013, pp. 1-11, 2013.
  - c. **A. El-Baz**, G. Beache, G. Gimel'farb, K. Suzuki, K. Okada, A. Elnakib, A. Soliman, and B. Abdollahi, "Computer Aided Diagnosis Systems for Lung Cancer: Challenges and Methodologies," *International Journal of Biomedical Imaging*, vol. 2013, pp. 1-46, 2013.
  - d. **A. El-Baz**, P. Sethu, G. Gimel'farb, F. Khalifa, A. Elnakib, R. Falk, and M. Abo El-Ghar, "Elastic Phantoms Generated by Microfluidics Technology: Validation of an Imaged-Based Approach for Accurate Measurement of the Growth Rate of Lung Nodules," *Biotechnology Journal*, vol.6, no.2, pp.195-203, February 2011.

#### Complete List of Published Work:

- <http://scholar.google.com/citations?user=RkQNgg4AAAAJ&hl=en>,
- [https://www.researchgate.net/profile/Ayman\\_El-Baz](https://www.researchgate.net/profile/Ayman_El-Baz)

Google Scholar		
	All	2011-2016
Citations	2730	2282
h-index	27	22
i10-index	85	69
Research Gate		
Research Gate Score	36.81	
Impact Points	189.31	
Read	6576	

Citations per year



## **D. Research Support**

### **Ongoing Research Support**

#### **1. American Cancer Society (Research Scholar Grant)**

"A Novel Image-Based Diagnostic System for Early Diagnosis of Lung Cancer: Shape and Appearance Analysis"

**PI: Dr. El-Baz; \$600,000.00**

08/01/2011-07/30/2016

**Award ID: 120556-RSG-11-266-01-CCE**

#### **2. Kentucky Commercialization Fund Program**

"A Novel Image-Based Diagnostic System for Early Diagnosis of Autism"

**PI: Dr. El-Baz; \$100K**

Grant Number: COMMFUND-1384-RFP-014

01/01/2013-01/31/2015

The major goal is to study is to develop a Computer Aided Diagnosis (CAD) for early diagnosis of autism from DTI-MRI data.

#### **3. Expediting Commercialization, Innovation, Translational & Entrepreneurship (ExCITE an NIH Hub)**

"SpheraHance, a Cancer-Targeted Contrast Agent for MRI and CT Imaging"

PIs: Dr. Malik, and Dr. O'Toole; \$200K

**Co-I: Dr. El-Baz**

10/01/2015-09/30/2017

#### **4. Wallace H. Coulter Foundation: Translational Research Award in Biomedical Engineering, Phase II**

"A Noninvasive CAD System for Early Detection of Acute Renal Rejection"

**PI: Dr. El-Baz; \$123K**

07/01/2015-06/30/2016

### **Completed Research Support**

#### **1. Wallace H. Coulter Foundation: Early Career Translational Research Award in Biomedical Engineering, Phase II**

"Novel Image Analysis Framework for Early Diagnosis of Lung Cancer: Shape Analysis"

**PI: Dr. El-Baz; \$260K**

08/01/2009-07/30/2013

The major goal is to study is to develop a Computer Aided Diagnosis (CAD) for early diagnosis of lung cancer from CT images.

#### **2. Wallace H. Coulter Foundation: Translational Research Award in Biomedical Engineering, Phase I**

"A Novel Image-Based Diagnostic System for Accurate Diagnosis of Autism"

**PI: Dr. El-Baz; \$120K**

08/01/2012-07/30/2013

The major goal is to study is to develop a Computer Aided Diagnosis (CAD) for early diagnosis of autism from structure MRI data.

#### **3. National Institute of Health, Eureka R01 award (R01 MH086784)**

"Building selective cortical inhibition in autism: an rTMS study"

**PI: Dr. Casanova; \$1,332,000.00**

**Co-PI: El-Baz (10% effort)**

Grant Number: R01 MH086784

RO1 Application: 06/30/2009 - 05/31/2013.

The major goal is to study is to develop a Computer Aided Diagnosis (CAD) for early diagnosis of autism based on the analysis of EEG data.

BIOGRAPHICAL SKETCH			
NAME Nihat Altiparmak		POSITION TITLE Assistant Professor,	
eRA COMMONS USER NAME N0ALTIO1		Computer Engineering and Computer Science, Speed School of Engineering, University of Louisville.	
EDUCATION/TRAINING <i>(Begin with baccalaureate or other initial professional education, such as nursing, include postdoctoral training and residency training if applicable.)</i>			
INSTITUTION AND LOCATION	DEGREE <i>(if applicable)</i>	YY	FIELD OF STUDY
Bilkent University, Ankara, Turkey	B.S.	2007	Computer Engineering
The University of Texas at San Antonio	M.S.	2012	Computer Science
The University of Texas at San Antonio	Ph.D.	2013	Computer Science

### A. Personal Statement

Dr. Altiparmak has the expertise, leadership, training, and motivation necessary to successfully carry out the proposed research project. Dr. Altiparmak has a broad background in Big Data processing, storage, and retrieval. He made fundamental contributions to the area of high performance computing, including parallel retrieval techniques through dynamic Big Data reorganization and efficient replica selection, as well as novel parallel processing strategies. His approaches are theoretically motivated and are based on graph coloring, bin packing, set covering, network flows, linear programming, number theory, and design theory. As well as his theoretical background in the field, he also has extensive hands-on experience in Big Data processing environments. Previously, he focused on decreasing the I/O bottlenecks of a large scale (100+ machines) Hadoop cluster by experimenting with various storage and retrieval strategies, and achieved 60% performance improvement. Dr. Altiparmak is also interested in biomedical research. He previously investigated efficient storage and retrieval techniques for disk based suffix tree structures, and experienced with tools and novel storage architectures including solid-state storage technologies for storing and retrieving biomedical datasets. Dr. Altiparmak's commitment to integrating his Big Data research with educational activities will allow several graduate students to gain theoretical and practical knowledge in Big Data science. Dr. Altiparmak is currently teaching Operating Systems and Distributed Systems courses, and assigns projects related to Big Data processing environments including Hadoop and Spark. Dr. Altiparmak believes that efficient storage and retrieval of biomedical datasets in distributed processing environments is crucial to speed-up the innovation process in biomedical sciences that can benefit from big data discovery, and he is well qualified to do the research and provide mentorship for graduate trainees. **Dr. Altiparmak will serve as a Co-I on this project and will be responsible for integrating system-level high performance and distributed real-time data storage and retrieval methodologies and technologies.**

### B. Positions and Honors

#### Positions and Employment

- 2013- Pres. Assistant Professor, Department of Computer Engineering and Computer Science, J.B. Speed School of Engineering, University of Louisville
- 2007-2013 Research and Teaching Assistant, Department of Computer Science, The University of Texas at San Antonio

#### Other Experience and Professional Memberships

- 2010-Pres. Institute of Electrical and Electronics Engineers (IEEE)
- 2011-Pres. Reviewer for IEEE Transactions on Cloud Computing (TCC), Computers and Electrical Engineering - An International Journal, Elsevier, Journal of Computing and Information Technology, IEEE International Symposium on Modeling, Analysis, and Simulation of



Computer and Telecommunication Systems (MASCOTS 2014) - TPC Member, European Symposium on Algorithms (ESA 2012), IEEE Global Communications Conference (GLOBECOM 2011)

### Honors

2013 College of Science Outstanding Research Award, The University of Texas at San Antonio, \$5,000.

### C. Contribution to Science

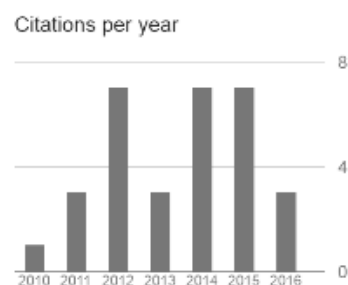
1. Dr. Altiparmak's recent publications mainly focus on the challenges of Big Data. More specifically, they propose novel processing, storage, and retrieval strategies for distributed Big Data processing environments. Previous researchers focused on homogeneous and centralized storage systems, which do not represent the current platforms used to store and analyze large biomedical datasets. Dr. Altiparmak's work was the first to propose retrieval algorithms for replicated data guaranteeing the optimal response time retrieval in current heterogeneous and distributed environments, including flash storage and solid-state storage architectures. By providing low latency access to large datasets, this body of work has changed the standards of Big Data management and accelerated the innovation process in a variety of subject areas of science dealing with large datasets including biomedical science. Dr. Altiparmak has several publications in these topics appeared in respected journals and conferences including:
  - a. **Nihat Altiparmak** and Ali Saman Tosun. *Multithreaded Maximum Flow Based Optimal Replica Selection Algorithm for Heterogeneous Storage Architectures*. IEEE Transactions on Computers (TC 2016), 65(5):1543–1557, May 2016.
  - b. **Nihat Altiparmak** and Ali Saman Tosun. *Continuous Retrieval of Replicated Data from Heterogeneous Storage Arrays*. In 22nd IEEE International Symposium on Modeling, Analysis, and Simulation of Computer and Telecommunication Systems (MASCOTS 2014), Paris, France, September 2014. Acceptance rate: 20.3% (39/192).
  - c. **Nihat Altiparmak** and Ali Saman Tosun. *Generalized Optimal Response Time Retrieval of Replicated Data from Storage Arrays*. ACM Transactions on Storage (TOS 2013), 9(2):5:1–5:36, July 2013.
  - d. **Nihat Altiparmak** and Ali Saman Tosun. *Equivalent Disk Allocations*. IEEE Transactions on Parallel and Distributed Systems (TPDS 2012), 23(3):538–546, March 2012.
2. In addition to the contributions described above, Dr. Altiparmak made significant contributions to networking and network security areas. Some topics he investigated include Denial of Service~(DoS) attacks on streaming servers, techniques to count the number of active users behind a Network Address Translation~(NAT) device, and management of mobile element in wireless sensor networks. Dr. Altiparmak has several publications in these topics appeared in respected journals and conferences including:
  - a. Baris Tas, **Nihat Altiparmak**, and Ali Saman Tosun. *Low-Cost Indoor Location Management for Robots Using IR Leds and an IR Camera*. ACM Transactions on Sensor Networks (TOSN 2014), 10(4):63:1–63:41, June 2014.
  - b. Ali Tekeoglu, **Nihat Altiparmak**, and Ali Saman Tosun. *Approximating the Number of Active Nodes behind a NAT Device*. In 20th IEEE International Conference on Computer Communications and Networks (ICCCN 2011), Maui, Hawaii, August 2011. Acceptance rate: 28.9% (130/450).
  - c. **Nihat Altiparmak**, Ali Tekeoglu, and Ali Saman Tosun. *DoS Resilience of Real Time Streaming Protocol*. In 30th IEEE International Performance Computing and Communications Conference (IPCCC 2011), Orlando, Florida, November 2011. Acceptance rate: 27.9% (36/129).
  - d. Baris Tas, **Nihat Altiparmak**, and Ali Saman Tosun. *Low Cost Indoor Location Management System using Infrared Leds and Wii Remote Controller*. In 28th IEEE International Performance

Computing and Communications Conference (IPCCC 2009), Phoenix, Arizona, December 2009.  
Acceptance rate: 29.7% (43/145).

### Complete List of Published Work in DBLP Computer Science Library

<http://dblp.uni-trier.de/pers/hd/a/Altiparmak:Nihat>

	Google Scholar	
	All	2011-2016
Citations	31	30
h-index	4	4
i10-index	1	1



### D. Research Support

#### Ongoing Research Support

1. **Nihat Altiparmak (PI)**, “*Dynamic Big Data Reorganization in Multi-Disk Storage Systems*”, The Executive Vice President for Research and Innovation (EVPRI), University of Louisville, Research-II Grant Program, \$10,000  
**1/1/2016 - 12/31/2016**
2. **Nihat Altiparmak (PI)**, “*Optimizing Virtual Machine Scheduling in the Cloud*”, The Executive Vice President for Research and Innovation (EVPRI), University of Louisville, Research-I Grant Program, \$3,000  
**1/1/2016 - 12/31/2016**
3. **Nihat Altiparmak (PI)**, “*Exploiting Replication for Energy Efficiency of Large Scale Heterogeneous Storage Systems*”, The Executive Vice President for Research and Innovation (EVPRI), University of Louisville, \$3,000  
**1/1/2016 - 12/31/2016**

---

**BIOGRAPHICAL SKETCH**

---

**NAME**

Gregory Neal Barnes

**eRA COMMONS USER NAME**

BARNESGN

**POSITION TITLE**Associate Professor of Neurology and Pediatrics,  
Director, University of Louisville Autism Center  
School of Medicine, University of Louisville.

*EDUCATION/TRAINING (Begin with baccalaureate or other initial professional education, such as nursing, include postdoctoral training and residency training if applicable.)*

INSTITUTION AND LOCATION	DEGREE (if applicable)	YY	FIELD OF STUDY
Vanderbilt University, TN	B.S.	1981-85	Molecular Biology
University of Kentucky, KY	Ph.D.	1987-90	Biochemistry
University of Kentucky College of Medicine, KY	MD	1985-92	Medicine
Duke University Medical Center, NC		1997-2000	Epilepsy research Fellow

**A. Personal Statement:**

For the last 10 years, our laboratory's main interest was the genetics of guidance cues and other neurodevelopmental genes which influence interneuron circuitry development and as a result impact neurological symptoms in children with developmental disorders including autism spectrum disorders (ASD) and epilepsy. From a functional stand point, the relationship of interictal epileptiform activity (IEDs) and epilepsy to sleep, behavior, and cognition is also poorly understood. The genomic variations responsible for neuronal excitability add a layer of complexity to the expression of the clinical phenotypes. Clinical research studies are directed towards more fully define the extent to which epileptiform activity during development sculpts neuronal circuitry to produce epilepsy, behavioral, and cognitive deficits in humans with neurodevelopmental disorders. Special emphasis is placed on the understanding of the contribution of GABAergic signaling in sleep to epileptogenesis, thereby producing altered daytime function. The delineation of the developmental pathophysiology will identify potential therapeutic targets to ease the suffering and facilitate the learning of those with ASD.

As a PI- or Investigator on several research foundations (Autism Speaks, Simons Foundation, and Epilepsy Foundation of America), Industry (GW Pharma), and federal (NIH-funded) grants, I laid the groundwork for the proposed research by developing effective measures of molecular, cellular, histopathological, electrophysiological, and functional/behavioral changes in several human and animal models of autism and epilepsy. I have built a strong clinical and research consortium of 4 state universities called KAITTR-Kentucky Autism Initiative for Treatment, Training, and Research to establish strong ties with community providers and families that will make it possible to recruit and track participants over time at 7 regional autism centers in Kentucky. I have successfully collaborated on a number of translational neuroscience projects in which I was either the PI or co-PI as a mentor/collaborator and trained more than 30 research associates, postdoctoral or predoctoral students, undergraduate and graduate students, medical students, and residents/clinical neurophysiology fellows. As an ABPN board certified child neurologist and pediatric epileptologist, I have a very broad background in clinical and basic neuroscience of epilepsy, sleep, and neurodevelopmental disorders. As a result of these experiences and in particular leadership in the field of autism, I am keenly aware that continuous input among project members will lead to a realistic research plan/execution which is on time and within the budget. The current application builds on my prior work and interests. **In the proposed project, I will serve as a co-I and will be responsible for overseeing and facilitating the integration of the ASD clinical research, autism/epilepsy genetics, and systems biology to yield success in the ASD precision medicine goals in this project. I strongly support this project, which will likely contribute to new hypotheses and therapeutic targets in the developmental etiology and pathophysiology in neurodevelopmental disorders and epilepsy.**

## **B. Positions and Honors**

### **Positions and Employment**

- 2014-present Associate Professor of Neurology and Pediatrics, Pediatric Neurology and Epilepsy Attending, Associate Director, Pediatric Epilepsy Monitoring Unit, and Director, Autism and Epilepsy Laboratory, Epilepsy Division, University of Louisville School of Medicine.
- 2014-present Spafford Ackerly Chair in Child and Adolescent Psychiatry and Director, University of Louisville Autism Center, University of Louisville/Kosair Children's Hospital, Louisville, KY.
- 2005-2013 Assistant Professor of Neurology and Pediatrics, Pediatric Neurology and Epilepsy Attending, Founder and Director, Pediatric Epilepsy Monitoring Unit, and Director, Developmental Epilepsy Laboratory, Epilepsy Division, Vanderbilt University School of Medicine.
- 2001-2004 Assistant Professor of Neurology, Molecular & Cellular Biochemistry, & Pediatrics, University of Kentucky College of Medicine.
- 1997-2000 Epilepsy Research Fellow, Dr. James McNamara-advisor, Duke University Medical Center.
- 1994-1997 Clinical Fellow in Pediatric Neurology/Epilepsy, Children's Hospital, Boston, MA.
- 1992-1994 Intern and Resident in Pediatrics, St. Louis Children's Hospital, St. Louis, MO

### **Other Experience and Professional Memberships**

**Membership:** American Academy of Neurology, American Neurological Association, American Epilepsy Society, Society for Neuroscience, Child Neurology Society, International Society for Autism Research.

#### **Grant Reviews**

- 2013-2015 Reviewer, Autism Speaks Meixner Translational Postdoctoral Fellowship Grant Program, Autism Speaks Weatherstone Predoctoral Fellowship Grant Program, Autism Speaks DELSIA Innovation Grant Program Washington DC.
- 2004-present Grant Reviewer, Target Research Initiative in Cognition, Partnership for Pediatric Epilepsy Research, Health Sciences Student Fellowship program, American Epilepsy Society and Epilepsy Foundation of America, Epilepsy grants, Tuberous Sclerosis Alliance Research Grants Program, Tuberous Sclerosis Alliance, CURE Foundation, New York City, NY.

#### **Reviewer for Journals**

Hippocampus, Journal of Biological Chemistry, University of Kentucky Press, Experimental Neurology, European Journal of Neuroscience, Journal of Neuroscience, Journal of Bone Marrow Transplantation, Epilepsy Research, Journal of the Neurological Sciences, Neuroscience, Journal of Autism and Developmental Disorders, Journal of Comparative Neurology, Synapse, Epilepsia, Epilepsy and Behavior, Pharmacology/Biochemistry and Behavior, Journal of Chemical Neuroanatomy, Journal of International Pediatrics, Neuroimage, Journal of Biomedical Materials Research, Behavioral Neuroscience, Children's Healthcare, European Journal of Child and Adolescent Psychiatry.

#### **Research Leadership**

- 2014-present Founder and Director, KAITTR- Kentucky Autism Initiative for Treatment, Training, and Research- 4 state university clinical and research consortium with now 7 regional autism centers state wide.
- 2012-present Appointment to the **External Scientific Advisory Committee for the Preclinical Autism Consortium for Therapeutics (PACT)**, Autism Speaks, New York City, NY.
- 2008-2013 Principal Investigator and National Neurology Co-Leader, Autism Treatment Network (ATN), Autism Speaks Foundation.
- 2002-present Scientific Advisory Board, Transverse Myelitis Working Group Consortium (Pediatric Section), National Transverse Myelitis Association.

## Honors

- Spafford Ackerly Endowed Chair in Child and Adolescent Psychiatry and Director, University of Louisville Autism Center, University of Louisville/Kosair Children's Hospital, Louisville, KY, 2014.
- Invited lecturer, NIH Workshop on Autism and Epilepsy, title of talk: "**The Effect of EEG on Sleep, Behavior, and Cognition; Implication for Autism Treatment Studies**", Washington, DC. May 29-30, 2012.
- Invited lecturer and organizer, 2011 ATN Fall Annual Meeting, title of talk: "**Genomics and Cluster Analyses in Children with Autism Spectrum Disorders**", Washington, DC. 2011.
- Invited Lecturer, 2011 University of Missouri Autism Research Summit, title of talk: "**Genotype Phenotype Interactions in Epilepsy and Autism Spectrum Disorders**", Columbia, Missouri, 2011.
- Award, Excellence of Leadership of the ATN Neurology-Genetics-Metabolism Committee, 2011.
- Invited Lecturer, 2010 American Epilepsy Society Investigators Workshop, Interneuronopathies-Diversity in the phenotypes of genetic mutations that alter forebrain GABAergic interneuron ontogeny, title of talk: "**The Role of Semaphorin Signaling in GABAergic Development and Epileptogenesis**" San Antonio, Tx, 2010.
- American Epilepsy Society Young Investigator Travel Award, 2003.
- MSCDA/K08 award, NIH/NINDS, 1997-2002.
- Dean Scholar, MD/PhD Graduation with high honors, Alpha Omega Alpha, University of Kentucky College of Medicine, Lexington, KY, 1985-1992.
- Magna cum laude, Phi Beta Kappa, Vanderbilt University, Nashville, TN, 1981-1985.

## **C. Contributions to Science**

1. My early publications directly addressed how genetics influence the overall formation of circuits in the developing brain. The axon guidance cue signaling system of semaphorin 3F and neuropilin 2 has been found to heavily influence the migrations of interneurons, synapse formation, and pruning of synapses relevant to developmental disorders such as autism spectrum disorders (ASD). We were the first to publish an animal model of autism and epilepsy (Gant et al, 2009). The laboratory is focused on mechanisms of Semaphorin 3F- Neuropilin 2 signaling that plays a key role in interneuron migration, interneuron neurite outgrowth, cell survival, GABAergic synaptogenesis, and neurologic dysfunction in mouse models. Downstream signaling systems of NRP2-Sema 3F such as the PTEN-PI3 kinase heavily influence these morphological and clinical endophenotypes. The current special emphasis is placed on the understanding of the contribution of GABAergic signaling in sleep to epileptogenesis, thereby producing altered daytime function. The work in the field of autism genetics has found both neuropilin 2 (receptor) and semaphorin 3F (ligand) to be a genetic risk factor for autism and epilepsy. We also have experience with a number of toxicants which impact neurodevelopmental disorders including in utero exposure and pesticide exposure. This work demonstrates the lab's expertise in basic neuroscience, neurogenesis, synaptic connectivity and white matter injury, animal models of autism and epilepsy, and environmental exposures.
  - a. **Barnes, G.N.**, Puranam, R., Luo, Y.L., & McNamara, J.O. (2003) Anatomical and Temporal Specific Patterns of Semaphorin Gene Expression in Rat Brain after Kainic Acid Induced Status Epilepticus, *Hippocampus*, 13:1-20.
  - b. **Barnes, G.N.** and Slevin, J.T. (2005) "Effect of Genetic Background on Ionotropic Glutamate Receptor and Neurotrophin Biology: Synaptic Connectivity and Function in Neurological Disease", *Frontiers in Medicinal Chemistry* (Volume 1), editors Drs. Allen B. Reitz, Cheryl P. Kordik, M. Iqbal Choudhary, & Atta-ur-Rahman, Bentham Science Publishers.
  - c. J.C. Gant, O. Thibault, E.M. Blalock, J. Yang, A. Bachstetter, J. Kotick, P.E. Schauwecker, K.F. Hauser, G.M. Smith, R. Mervis, Y.F. Li, and **G. N. Barnes** (2009) Decreased Number of Interneurons and Increased Seizures in Neuropilin 2 Deficient Mice: Implications for Autism and Epilepsy, *Epilepsia*, 50(4):629-45.
  - d. Perdigoto, A.L., Chaudry, N., Filbin, M.T., **Barnes, G.N.**, and Carter, B.D. (2011) A Novel Role for PTEN in the Inhibition of Neurite Outgrowth by Myelin-associated Glycoprotein in Cortical Neurons, *Molecular and Cellular Neuroscience*, 46(1):235-44.

2. Our translational neuroscience focus emphasizes the direct links between genomic factors, particularly those involved in GABAergic interneuron development and function, sleep, EEG, and clinical endophenotypes in developmental disorders such as Angelman syndrome and autism spectrum disorders. This body of work has and will significantly change our clinical approach between genetic testing, treatment of seizures and epileptiform EEGs, sleep, and clinical improvement of challenging behaviors and cognition in developmental disorders. This work has led to our current grant support looking at these mechanisms in human biology and contributed towards the development of our ASD precision medicine initiative. This work demonstrates the lab's expertise in autism/epilepsy genetics, effect of genetics on epileptiform discharges and phenotypes, systems biology, GABA<sub>A</sub> receptors, and in ASD clinical research.
  - a. **G.N Barnes** (2009) Postnatal Influences on Seizure Susceptibility: Does My Mother Really Matter? *Epilepsy Currents* Nov/Dec 2009, 9(6):176-8.
  - b. Vendrame, M., Loddenkemper, T., Zarowski, M., Gregas, M., Sarco, D.P., Morales, A., Nespeca, M., Sharpe, C., Haas, K., **Barnes, G.N.**, Glaze, D., Kothare S.J. (2012) EEG patterns in Angelman Syndrome: correlation with genotype, *Epilepsy and Behavior*, 23(3):261-5.
  - c. Kang, Q. and **Barnes, G.N.** (2013) A common susceptibility factor for autism and epilepsy: functional deficiency of GABA<sub>A</sub> receptors, *J. Autism Develop. Disorders*, 43(1):68-79
  - d. Beversdorf, D, **Barnes, G.N.**, et al for Missouri Autism Summit Consortium (2016) Phenotyping, Etiological Factors, and Biomarkers: Towards Precision Medicine in Autism Spectrum Disorders, *J. Dev. Behavioral Pediatrics*, *in press*

#### Complete List of Published Work:

- <http://www.ncbi.nlm.nih.gov/pubmed/?term=Barnes+GN>

#### **D. Research Support:**

##### Ongoing Research Support

1. **Treatment of Children with ASD and Epileptiform EEGs with Divalproex Sodium**  
**Simons Foundation grant** (Co-PI, Sarah Spence MD is the PI)  
 Funding Period 01/01/15-12/31/17 1.8 calendar months  
 A phase II randomized double blind placebo controlled cross over trial design to answer the question in children without ASD but no seizures whether the mechanism of divalproex sodium in amelioration of behavioral and cognitive deficits is dependent or independent of spike suppression or sleep.
2. **The Role of Cannabinoid Signaling in Autism and Epilepsy: A Pilot Study**  
**GW Pharma- funding agency (Principal Investigator)**  
 Funding Period 07/1/16-6/30/18. 1.2 calendar months  
 A phase I open label trial design to elucidate the relationships between epileptiform discharges, seizures, and sleep to behavior and cognition in 30 children and adolescents with autism and epilepsy who have pathogenic copy number variants. The hypothesis is that enhanced cannabinoid signaling (cannabidiol) will improve clinical endophenotypes associated with GABAergic neurotransmission.
3. **Cognitive Anti-Epileptic Drugs Outcomes in Pediatric Localization Related Epilepsy (Site Investigator) PCORI/NIH**  
 Funding Period 1/1/15-4/30/17 0.6 calendar months  
 This is a prospective multicenter, randomized, open-label, central assessor, parallel-group study of children ages 6 to less than 13 years with newly diagnosed LRE to establish whether 3 common AEDs used as first line LRE treatment (lamotrigine (LTG), levetiracetam (LEV), or oxcarbazepine (OXC) are associated with differential cognitive side effects. The two primary objectives are to: 1) determine which, if any, of 3 monotherapy antiepileptic drugs (AEDs) maximally preserves cognitive function in children with newly diagnosed localization related epilepsy (LRE), and 2) to determine which, if any, of 3 monotherapy AEDs

has the greatest negative impact on behavior.

**4. Dravet Syndrome clinical trial with Epidiolex. GW Pharma- funding agency (Site Investigator)**

Funding Period

1/1/16-6/30/17.

1.2 calendar months

A Phase III randomized double blind trial design to elucidate whether enhanced cannabinoid signaling with cannabidiol (Epidiolex) will improve seizure control in children and adolescents with a severe intractable epilepsy and developmental disorder which has deficit GABAergic signaling as part of its pathogenic mechanism (Dravet Syndrome).

**Completed Research Support**

**Principal Investigator**

**10/01/10-08/30/13**

Agency: 1UA3MC11054-02/Mass General HRSA/Maternal Child Health Bureau ATN Multi Center Grant

Title: "The Relationship of Epileptiform Discharges to Behavior and Cognition in Children with Autism Spectrum Disorders"

Type: U project grant

This grant will test a single hypothesis: Characteristics of interictal epileptiform discharges (IEDs) are associated in patterns of cognition and behavior in children with ASD alone (age 3-7 yrs).

**Principal Investigator**

**07/01/10-09/30/13**

Agency: Epilepsy Foundation

Target Initiatives in Youth

Title: "Epileptiform Discharges and its Relation to Cognition and Behavior in Autism and Epilepsy"

Type: Target Initiatives in Youth Research Grant Program

This grant will test a single hypothesis: Characteristics of interictal epileptiform discharges (IEDs) are associated with patterns of cognition and behavior in children with ASD and epilepsy compared to children with ASD alone (ages 8-17 yrs).

**Principal Investigator**

**1/1/09-2/28/13**

Agency: Autism Speaks

Title: "Relation of Sleep Epileptiform Activity to Insomnia and Daytime Behaviors in Children with Autism Spectrum Disorder"

Type: Pilot Grant

This grant seeks to test two hypotheses: 1) Sleep IEDs and related EEG abnormalities will serve as a reliable biomarker of sleep disturbances; and 2) children with ASD exhibiting sleep IEDs and related abnormalities form a unique group which have more challenging daytime behaviors (specifically in the areas of attention and mood) with normal IQs.

---

**BIOGRAPHICAL SKETCH**

---

NAME Bolli, Roberto	POSITION TITLE Professor of Medicine, Physiology, and Biophysics, Director, Institute of Molecular Cardiology, Scientific Director, Cardiovascular Innovation Institute
eRA COMMONS USER NAME r0boll01	

EDUCATION/TRAINING *(Begin with baccalaureate or other initial professional education, such as nursing, include postdoctoral training and residency training if applicable.)*

INSTITUTION AND LOCATION	DEGREE <i>(if applicable)</i>	YY	FIELD OF STUDY
University of Perugia	M.D.	1976	Medicine
Cardiology Branch, NHLBI, NIH, Bethesda, MD	Res. Fellow	1978-80	Cardiovascular Pathophysiology
Cardiology, Baylor College of Medicine, Houston, TX	Clinical Fellow	1981-83	Cardiology

**A. Personal Statement:**

Cell-based therapies aimed at reconstituting damaged myocardium have the potential to transform the treatment and prognosis of heart failure. Over the last decade, c-kit+ cardiac stem cells (CSCs) have emerged as one of the most promising cell types. Recently, we have spearheaded studies of c-kit+ CSCs for cardiac regeneration. Using both small and large animal models of ischemia-reperfusion cardiac injury, we have demonstrated that intracoronary administration of CSCs results in regeneration of infarcted myocardium, associated with structural and functional improvement. Moreover, we also demonstrated that the therapeutic effects of c-kit+ CSCs are mainly mediated via paracrine mechanisms. These encouraging preclinical results culminated in the first clinical trial of c-kit+ CSCs, the Cardiac Stem Cell Infusion in Patients with Ischemic Cardiomyopathy (SCIPIO) study. SCIPIO, the first clinical trial of c-kit+ CSCs, has produced promising results. In this trial, administration of autologous CSCs to patients with ischemic heart failure was found to be safe and feasible; in addition, CSC-treated patients exhibited a significant improvement in cardiac function, as well as a reduction in scar size and an improvement in quality of life. This groundbreaking work provided a strong rationale for conducting larger clinical studies to determine whether this therapy is efficacious in patients with ischemic cardiomyopathy. As such, my expertise in stem cell therapy for treatment of heart failure as well as in translational and clinical cardiovascular research will undoubtedly contribute to the overall goal of the proposed training grant, as one of its research emphases is on stem cell research. I will be able to provide critical resources and expertise on how to perform cutting-edge basic and clinical research in the cardiovascular field, which is essential for developing innovative and integrated approaches to train pre-doctoral students. **Dr. Bolli will serve as a Co-I in the proposed project. He will be responsible for overseeing and facilitating the integration of cardiology-based clinical trial research with the proposed Big Data Analysis systems as well as partner with the Big Data Core to interpret and validate all medical findings related to cardiomyopathy.**

**B. Positions and Honors****Positions and Employment**

- 2013- Scientific Director, Cardiovascular Innovation Institute, University of Louisville and Jewish Hospital
- 2005- Vice Chairman for Research, Department of Medicine, University of Louisville, Louisville, KY
- 2002-present Director, Institute of Molecular Cardiology, University of Louisville, Louisville, KY
- 1994-present Chief, Division of Cardiovascular Medicine, University of Louisville, Louisville, KY
- 1994 Professor of Medicine, Baylor College of Medicine, Houston, TX
- 1989-94 Associate Professor of Medicine, Baylor College of Medicine, Houston, TX



- 1984-89 Assistant Professor of Medicine, Baylor College of Medicine, Houston, TX

## **Other Experience and Professional Memberships**

2014	Member, NHLBI Think Tank on Research Needs for Cell Therapy in Areas of Heart, Lung and Blood
2009-	Editor-in-Chief, Circulation Research
2008-	Senior Guest Editor, Circulation
2007-10	President, International Society for Heart Research
2006-08	Member, Board of Directors of the AHA
2005-present	Member, Louis and Artur Lucian Award Selection Committee
2004-06	Chairman, Council Operations Committee of the AHA
2003-08	Member, Science Advisory and Coordinating Committee of the AHA
2003-07	Member, NHLBI Advisory Council
2003-05	Chairman, Distinguished Scientist Selection Committee of the AHA
2003	Chairman, NHLBI Working Group on the Translation of Therapies for Protecting the Heart from Ischemia
2003-06	Chairman, Council on Basic Cardiovascular Sciences of the AHA
2003	Chairman, Reynolds Foundation and AHA Peer Review Committee
2002-05	Member, Committee on Scientific Sessions Program of the AHA
2002	Chairman, Distinguished Scientist Task Force for the Scientific Councils of the AHA
2000-03	Program Project Parent Review Committee of the National Heart, Lung, and Blood Institute
1999-2009	Associate Editor, Circulation Research and Journal of Molecular and Cellular Cardiology
1998-2004	Secretary General and Treasurer of the International Society for Heart Research
1998-2000	Chairman, Cardiovascular Pathophysiology National Peer Review Committee of the AHA
1998-2000	National Research Committee of the American Heart Association (AHA)
1992-96	Cardiovascular and Renal Study Section, NIH

## **Honors**

American Society for Clinical Investigation (1991), Association of American Physicians (1999), Basic Research Prize of the AHA (2001), NIH MERIT Award (2001), Keith Reimer Distinguished Lecture of the ISHR (2002), Research Achievement Award of the International Society for Heart Research (ISHR) (2004), Louis and Artur Lucian Award for Research in Circulatory Diseases, McGill University (2004), Robert Berne Distinguished Lecture of the American Physiological Society (2005), Howard Morgan Award, International Academy of Cardiovascular Sciences (2005), Foreign Fellow of the Academy of Sciences of the Royal Society of Canada (2006), Distinguished Achievement Award of the AHA (2006), George E. Brown Memorial Lecture of the AHA (2007), Distinguished Scientist Award of the AHA (2008), Award of Meritorious Achievement of the AHA (2010), Carl J. Wiggers Award of the American Physiological Society (2011), Walter B. Cannon Award of the American Physiological Society (2011), Distinguished Scientist Lecture of the AHA (2011), Rocovich Gold Medal for Excellence in Science, Edward Via College of Osteopathic Medicine (2012), Mikamo Lecture of the Japanese Circulation Society (2013), R.L.J. van Ruyen Award, University of Utrecht (2013), Medal of Merit, International Academy of Cardiovascular Sciences (2013), Research Achievement Award of the AHA (2013), Peter Harris Distinguished Scientist Award of the ISHR (2015).

## **C. Contributions to Science**

- 1. Reversible postischemic dysfunction or myocardial "stunning".** One of our major contributions to science involves unraveling the pathophysiology and pathogenesis of this common form of contractile dysfunction. In a series of studies spanning a decade, we first proposed, and then tested and validated, the concept that myocardial stunning is a manifestation of reactive oxygen species (ROS)-mediated reperfusion injury, a concept that is now widely regarded as a proven hypothesis. This seminal work has laid the groundwork for developing antioxidant therapies to prevent myocardial stunning.

- a. Bolli R, Patel BS, Jeroudi MO, Lai EK, McCay PB.** Demonstration of free radical generation in "stunned" myocardium of intact dogs with the use of the spin trap alpha-phenyl *N*-tert-butyl nitron. *J Clin Invest* 82:476-485, 1988. **Citations: 578**

- b. **Bolli R**, Jeroudi MO, Patel BS, DuBose CM, Lai EK, Roberts R, McCay PB. Direct evidence that oxygen-derived free radicals contribute to postischemic myocardial dysfunction in the intact dog. *Proc Natl Acad Sci USA* 86:4695-4699, 1989. **Citations: 302**
- c. Li XY, McCay PB, ZUghaib M, Jeroudi MO, Triana JF, **Bolli R**. Demonstration of free radical generation in the "stunned" myocardium in the conscious dog and identification of major differences between conscious and open-chest dogs. *J Clin Invest* 92: 1025-1041, 1993.

**2. Late phase (second window) of ischemic preconditioning.** Our work has also significantly advanced understanding of the pathophysiology and pathogenesis of the delayed adaptation of the heart to stress (late phase of preconditioning). Our discovery that late preconditioning is triggered by the generation of ROS has produced a paradigm shift, since postischemic formation of ROS was generally viewed as a deleterious process. We then discovered, for the first time, the molecular mechanisms responsible for late preconditioning, including the signal transduction pathways and the cardioprotective genes. Our discovery that late preconditioning is mediated by iNOS and COX-2 was a major breakthrough, because the mediator of late preconditioning had previously remained elusive. These findings have provided a rationale for a novel therapeutic strategy (prophylactic cardioprotection) based upon chronic upregulation of protective proteins via gene therapy.

- a. Sun JZ, Tang XL, Knowlton AA, Park SW, Qiu Y, **Bolli R**. Late preconditioning against myocardial stunning: An endogenous protective mechanism that confers resistance to postischemic dysfunction 24 hours after brief ischemia in conscious pigs. *J Clin Invest* 95:388-403, 1995. **Citations: 166**
- b. **Bolli R**, Manchikanti S, Tang XL, Takano H, Qiu Y, Guo Y, Zhang Q, Jadoon AK. The protective effects of late preconditioning against myocardial stunning in conscious rabbits are mediated by nitric oxide synthase: Evidence that nitric oxide acts both as a trigger and as a mediator of the late phase of ischemic preconditioning. *Circ Res* 81: 1094-1107, 1997. **Citations: 200**
- c. Guo Y, Jones WK, Xuan Y-T, Tang X-L, Bao W, Wu W-J, Han H, Laubach VE, Ping P, Yang Z, Qiu Y, **Bolli R**. The late phase of ischemic preconditioning is abrogated by targeted disruption of the iNOS gene. *Proc Natl Acad Sci USA* 96:11507-11512, 1999. **Citations: 198**
- d. Shinmura K, Xuan YT, Tang XL, Kodani E, Han H, Zhu Y, **Bolli R**. Inducible nitric oxide synthase modulates cyclooxygenase-2 activity in the heart of conscious rabbits during the late phase of ischemic preconditioning. *Circ Res* 90:602-608, 2002.

**3. Use of stem cells for cardiac regeneration.** Recently, we have spearheaded studies of c-kit<sup>+</sup> cardiac stem cells for cardiac regeneration. Using both small and large animal models of ischemia-reperfusion cardiac injury, we have demonstrated that intracoronary administration of cardiac stem cells results in regeneration of infarcted myocardium, associated with structural and functional improvement. Moreover, we also demonstrated that the therapeutic effects of c-kit<sup>+</sup> cardiac stem cells are mainly mediated via paracrine mechanisms. These encouraging preclinical results culminated in the first clinical trial of c-kit<sup>+</sup> cardiac stem cells, the Cardiac Stem Cell Infusion in Patients with Ischemic Cardiomyopathy (SCIPIO) study.

- a. Li Q, Guo Y, Ou Q, Chen N, Wu WJ, Yuan F, O'Brien E, Wang T, Luo L, Hunt GN, Zhu X, **Bolli R**. Intracoronary administration of cardiac stem cells in mice: a new, improved technique for cell therapy in murine models. *Basic Res Cardiol*. 106(5):849-64. 2011.
- b. Tang XL, Rokosh G, Sanganalath SK, Yuan F, Sato H, Mu J, Dai S, Li C, Chen N, Peng Y, Dawn B, Hunt G, Leri A, Kajstura J, Tiwari S, Shirk G, Anversa P, **Bolli R**. Intracoronary administration of cardiac progenitor cells alleviates left ventricular dysfunction in rats with a 30-day-old infarction. *Circulation*. 121(2):293-305. 2010.
- c. **Bolli R**, Tang XL, Sanganalath SK, Rimoldi O, Mosna F, Abdel-Latif A, Jneid H, Rota M, Leri A, Kajstura J. Intracoronary delivery of autologous cardiac stem cells improves cardiac function in a porcine model of chronic ischemic cardiomyopathy. *Circulation*. 128(2):122-31. 2013.
- d. Hong KU, Guo Y, Li QH, Cao P, Al-Maqtari T, Vajravelu BN, Du J, Book MJ, Zhu X, Nong Y, Bhatnagar A, **Bolli R**. c-kit<sup>+</sup> Cardiac stem cells alleviate post-myocardial infarction left ventricular

dysfunction despite poor engraftment and negligible retention in the recipient heart. *PLoS One*. 9(5):e96725. 2014.

**4. Cardiac Stem Cell Infusion in Patients With Ischemic Cardiomyopathy (SCIPIO) trial.** Recently, we have conducted SCIPIO, the first clinical trial of c-kit+ cardiac stem cells, which has produced promising results. In this trial, administration of autologous cardiac stem cells to patients with ischemic heart failure was found to be safe and feasible; in addition, cardiac stem cell-treated patients exhibited a significant improvement in cardiac function, as well as a reduction in scar size and an improvement in quality of life. This groundbreaking work provided a strong rationale for conducting larger clinical studies to determine whether this therapy is efficacious in patients with ischemic cardiomyopathy.

- a. **Bolli R**, Chugh AR, D'Amario D, Loughran JH, Stoddard MF, Ikram S, Beache GM, Wagner SG, Leri A, Hosoda T, Sanada F, Elmore JB, Goichberg P, Cappetta D, Solankhi NK, Fahsah I, Rokosh DG, Slaughter MS, Kajstura J, Anversa P. Cardiac stem cells in patients with ischaemic cardiomyopathy (SCIPIO): initial results of a randomised phase 1 trial. *Lancet*. 378(9806):1847-57. 2011.
- b. Chugh AR, Beache GM, Loughran JH, Mewton N, Elmore JB, Kajstura J, Pappas P, Tatroles A, Stoddard MF, Lima JA, Slaughter MS, Anversa P, **Bolli R**. Administration of cardiac stem cells in patients with ischemic cardiomyopathy: the SCIPIO trial: surgical aspects and interim analysis of myocardial function and viability by magnetic resonance. *Circulation*. 126(11 Suppl 1):S54-64. 2012.

#### **D. Research Support:**

##### **Ongoing Research Support**

**P01 HL078825 (Bolli, PI)**

**07/11/11 - 05/30/16**

NIH/NHLBI

Protection of the Ischemic Myocardium

The overall objective of this Program Project is to advance our understanding of the use mechanism of action of cardiac stem cells in the treatment of post-infarction LV remodeling and failure.

**U24 HL094373 (Bolli, PI)**

**08/01/10 - 07/31/15**

NIH/NHLBI

“CAESAR (Consortium for Preclinical AssESsment of CARdioprotective Therapies)”

The objective of this consortium is to provide a public infrastructure (available at no cost to all NIH-funded investigators) for rigorous preclinical evaluation of the infarct-sparing ability of potential cardioprotective therapies. Therapies are evaluated by four independent labs in three animal models (mice, conscious rabbits, and conscious pigs) in a blind, randomized fashion using standardized protocols designed by a statistician and data analysis by independent Cores.

**P20 GM103492 (Bhatnagar, PI)**

**08/1/13 - 06/30/18**

NIH/NIGM

Center for Excellence in Diabetes Research (COBRE)

The central focus of the Center is to enable, promote and support research on the cardiovascular causes and consequences of diabetes and obesity. The second major aim of the program is to continue to provide mentoring and guidance to junior investigators in the Center.

Role: Co-Director

**UM1 HL113530 (Bolli, PI)**

**04/01/12 - 03/31/19**

NIH/NHLBI

Regional Clinical Center for the Cardiovascular Cell Therapy Research Network

The overall goal is to contribute to the studies of stem cells within the CCTR network.

## BIOGRAPHICAL SKETCH

NAME Nigel G. F. Cooper	POSITION TITLE Professor, Department of Anatomical Sciences and Neurobiology, University of Louisville.		
eRA COMMONS USER NAME NGCOOP01			
EDUCATION/TRAINING <i>(Begin with baccalaureate or other initial professional education, such as nursing, include postdoctoral training and residency training if applicable.)</i>			
INSTITUTION AND LOCATION	DEGREE <i>(if applicable)</i>	YY	FIELD OF STUDY
The Open University	BA	1974	Biology
The University of Tennessee	Ph.D.	1980	Anatomical Sciences & Neurobiology

### A. Personal Statement

I have a wide range of experiences in independent and collaborative research, as well as, in program management. I served as a Vice Chair for Research for my department for several years. I was the inaugural Graduate Program Director for the University of Louisville's Interdisciplinary Program in Biomedical Sciences (IPIBS) for the 5 basic sciences departments at the School of Medicine for several years. In addition, I have experience in the building of research infrastructure, research programs, and research training programs. I have managed large NIH and NSF funded research infrastructure and network building projects. These experiences provide a suitable background to serve as Director of this INBRE. Of particular relevance, as the PI/Director for the INBRE program in Kentucky, I can report that the rate of new and competing R15 awards in Kentucky has doubled over the last decade of INBRE support compared to a ten year period prior to the instigation of this IDeA-program. This doubling in success rates in Kentucky has occurred in the same period that R15 success rates nationally have decreased to below 15%. The increased number of R15 awards, in particular, provides more spaces for the training of undergraduate students in biomedical and health-related research. As Director of the INBRE program I support 2 scientific cores, in genomics and bioinformatics, which would be of particular relevance to this proposal. My research focus is related to disorders and diseases of the eye with a particular focus on network analysis of genes associated with ischemia-reperfusion and other cns-related injuries. **I will serve as co-I in the proposed project and will oversee, in collaboration with Dr. Rouchka and my clinical domain expert colleagues, the analysis and interpretation of all the genomic data to identify and elucidate the appropriate biomarkers associated with respective diseases to achieve a precision diagnosis.**

### B. Positions and Honors

#### Positions and Employment

1980-1983 Postdoctoral Fellow, University of Tennessee Center for the Health Sciences.  
1983-1988 Assistant Professor, Department of Anatomy and Neurobiology, University of Tennessee (UT).  
1988-1991 Associate Professor, Department of Anatomy and Neurobiology, UT Ctr for the Health Sciences.  
1991-1995 Associate Professor, Department of Anatomical Sciences and Neurobiology, University of Louisville and joint appointment in Ophthalmology and Visual Sciences.  
1995-present Professor, Department of Anatomical Sciences and Neurobiology, University of Louisville and joint appointment in Ophthalmology and Visual Sciences

#### Honors

Distinguished University Scientist Award from the Kentucky Academy of Science 2003.  
Editorial Board, Ophthalmology and Eye Diseases 2009-present  
Editorial Board, Dataset Papers in Science, (Ophthalmology sub-division) 2012-present  
Member of the PubMed Central National Advisory Committee 2015-2018

#### Other Experience and Professional Memberships

- Member, Society for Neuroscience
- Member, Louisville Chapter of the Society for Neuroscience
- Member, Association for Research in Vision and Ophthalmology

- Member, International Society for Eye Research
- Member, Kentucky Academy of Science
- Member, American Association for the Advancement of Science
- Inaugural Graduate Program Director, Integrated Programs in Biomedical Sciences for all Basic Science Departments, University of Louisville School of Medicine 2001-2007
- Vice Chair (Research), Anatomical Sciences and Neurobiology 2003-2013.
- President, Louisville Chapter, Society of Neuroscience, 1996/97.
- Chair, statewide INBRE Steering Committee 2001-present
- President, Kentucky Academy of Science, 2007.
- Member, National Association IDeA Principal Investigators (NAIPI), 2008-present.
- Member Kentucky Academy of Science research grant review committee, 2013-2014

### C. Contribution to Science

Most significant contributions to science:

1. I am trained in the interdisciplinary field of neuroscience. In the 1980s much of my research activity related to the use of plant lectins and antibodies to demarcate patterns of glycosylated molecules in the developing rodent brain. For example, my lab demonstrated the presence of “boundaries” associated with developing barrel fields in the cerebral cortex, highly suggestive of the involvement of glycoconjugates in the development of the early brain. The initial study, a collaboration between my laboratory and Dr. Dennis Steindler’s laboratory, was published: **“Lectins demarcate the barrel subfield in the somatosensory cortex of the early postnatal mouse”**. (1986) *J Comp Neurol.* **249:157-69**. Subsequently, this led to a considerable body of related literature. One of the follow-up studies to identify specific molecules in boundaries was a collaboration with the Melitta Schachner laboratory, and resulted in a publication which currently has 230 citations (according to ResearchGate) **“Boundaries defined by adhesion molecules during development of the cerebral cortex: the JL/tenascin glycoprotein in the mouse somatosensory cortical barrel field”**. (1989) *Developmental Biology* **131:243-60**. Several of our collaborative studies, along with those from other laboratories, demonstrated the plasticity of these boundaries in response to denervation in the periphery indicating an interaction between the periphery and eventually the matrix of the brain as an important substrate for the development of nervous system structures. This eventually gave rise to a series of other such studies in our and many other laboratories culminating with the intriguing suggestion that chondroitin sulphate proteoglycan is a barrier to axonal regeneration in the injured spinal cord: **“Increased chondroitin sulfate proteoglycan expression in denervated brainstem targets following spinal cord injury creates a barrier to axonal regeneration overcome by chondroitinase ABC and neurotrophin-3”** (2008) *Exp. Neurol.* **209:426-45**. This research is now clearly leading down the path to translational and clinically relevant research.
2. I have had a long term involvement in, and commitment to, retinal research which started while in graduate school. One goal of my NIH-funded research program has been to define a molecular characterization and the signal transduction events in animal models of eye diseases and disorders (eg, ischemia-reperfusion related injuries). My lab was the first to demonstrate the involvement of CamKIIa in the signal transduction pathway for excitotoxicity in the retina, and the first to show an up-regulation of a novel nuclear isoform, CamKIIaB, in response to NMDA stimulation of the neural retina. My laboratory was the first to show neuroprotection of glutamate/aspartate mediated, caspase 3 dependent cell death in the retina, with the aid of specific inhibitor of CamKIIa. One of the initial studies in this area is: **“Neuroprotective effect of AIP on N-methyl-D-aspartate-induced cell death in retinal neurons”**, (2000), *Brain Res. Mol Brain Res.* It is now becoming clearer that NMDA receptors and the CamKII signal transduction pathway are implicated in a number of neurodegenerative disorders.
3. My laboratory has used microarray and next generation sequencing technologies to investigate patterns of mRNA and miRNA expression in the retinas of rat and mice looking for prospective molecular biomarkers and signatures for disorders of the retina. Our group has described, in detail, the relationship of transcriptional and post-transcriptional regulators to gene expression during ischemia

reperfusion injury, providing an array of potential therapeutic targets for prospective pharma investigations. Our recent studies were published in the “highly accessed” *BMC Genetics* publication: (“**Regulatory networks in retinal ischemia-reperfusion injury**”, 2015 *BMC Genet.*16:43). Current research seeks to complement such studies with a deep sequencing approach, and we are presently studying the potential role of miRNAs ( **MicroRNAs in the Neural Retina**, *Int J Genomics.* 2014;2014) and circular RNAs (**Circular RNAs: New Players in Gene Regulation**, *Advances in Bioscience and Biotechnology*, 2015, 6, 433-441) in the complex regulatory events in model systems of eye disorders. In addition, in collaboration with computer science faculty, we are developing a data mining approach to network analyses of eye diseases including glaucoma (**Building a Glaucoma Interaction Network using a Text Mining Approach**, *BioData Mining.* 2016 May 5;9:17).

4. Since 2000, I have held a growing interest in bioinformatics, have been able to build some capability and capacity for informatics endeavors at the University of Louisville and throughout Kentucky. My interest in this field has led to a few publications from my own laboratory as well as a number of collaborative publications with other laboratories. From my own laboratory, I have looked at a family of RNA binding proteins, and demonstrated with informatics approaches, the presence of multiple, alternative splicing variants for each member of the family. We predicted the prospective functional consequences for expression of each of the variants. See for example: “**Comparative in silico analyses of cpeb1-4 with functional predictions**”, *Bioinformatics and Biology Insights*: 4:61-83. I see the building of multi-disciplinary and integrative and interdisciplinary approaches to science as an important activity and I have made contributions to this field through many collaborative publications. For example “**Sequence and In Silico Characterization of the Tomato Polygalacturonase (PG) Promoter and Terminator Regions**” *Plant Molecular Biology Reporter* 27: 250-256 (2009) was a collaboration with a professor, Dr. Robinson at a local teaching college. In addition, PI/Director of the KY-INBRE program, I have been able to develop the bioinformatics infrastructure at the University of Louisville. Currently, we have a bioinformatics core with 2 tenure track faculty and several postdoctoral and masters level research associates who are capable of handling large numbers of data analyses for next generation sequencing and microarray projects.

#### **Complete List of Published Work:**

URL to a full list of published work as found in a publicly available digital database such as My NCBI Bibliography, Research Gate, and Scopus.

- [https://www.researchgate.net/profile/Nigel\\_Cooper2](https://www.researchgate.net/profile/Nigel_Cooper2)
- <http://www.scopus.com/authid/detail.url?authorId=7202179876>
- <http://www.ncbi.nlm.nih.gov/sites/myncbi/129qpk8qvPp/bibliography/43276940/public/?sort=date&direction=descending>

#### **D. Research Support**

##### **Ongoing Research Support**

**P20 GM103436**

**Cooper (PI)**

**5/1/14 - 4/30/19**

Kentucky IDeA Network of Biomedical Research Excellence

The goals are to (1) develop competitive biomedical research programs in state-supported universities to enable undergraduate students and enhance their chances of entrance to graduate and professional degree programs in the biomedical sciences; (2) aid the development bioinformatics and genomics infrastructure and capacity at the University of Louisville and the University of Kentucky. My role as Program Director is to lead this statewide effort.

Role: Program Director

##### **Completed Research Support**

**P20 RR016481**

**Cooper (PI)**

**5/1/09 - 4/30/14**

Kentucky IDeA Network of Biomedical Research Excellence

The goals are to (1) develop competitive biomedical research programs in state-supported universities to enable undergraduate students and enhance their chances of entrance to graduate and professional degree programs in the biomedical sciences; (2) aid the development bioinformatics infrastructure and capacity at the

University of Louisville and the University of Kentucky. My role as Program Director is to lead this statewide effort.

Role: Program Director

**P20 RR016481-S1**

**Cooper (PI)**

**9/17/09 - 9/16/11**

Kentucky IDeA Network of Biomedical Research Excellence, ARRA supplement  
Development of System Biology Team

The goal of this award is to recruit and train postdoctoral level investigators in bioinformatics and systems biology at the University of Louisville. My role as Program Director is to develop and grow this program.

Role: Program Director

**P20 RR016481**

**Cooper (PI)**

**5/1/04 - 4/30/09**

Kentucky IDeA Network of Biomedical Research Excellence

The goals are to (1) develop competitive biomedical research programs in state-supported universities to enable undergraduate students and enhance their chances of entrance to graduate and professional degree programs in the biomedical sciences; (2) aid the development bioinformatics infrastructure and capacity at the University of Louisville and the University of Kentucky. My role as Program Director is to lead this statewide effort.

Role: Program Director

**P20 RR016481-02S1**

**Cooper (PI)**

**9/30/02 – 8/31/04**

Supplemental Kentucky Bioinformatics Research Infrastructure Network

The principal goal of this supplement to the NIH-BRIN proposal is to develop a statewide science research core (SRC). The SRC will provide the impetus to build capacity for research activities within the framework of the existing KBRIN. The SRC will consist of a set of research projects. This will entail an expansion of KBRIN to include new faculty and student participation.

Role: Program Director

**P20 RR016481**

**Cooper (PI)**

**9/30/01 - 9/29/04**

Kentucky Biomedical Research Infrastructure Network

The goal of this grant application is to establish the KBRIN, which will consist of a collaborative network of statewide institutions of higher education. The purpose of the network is to enhance the infrastructure, capacity and training in areas relevant to the mission of NIH so that Kentucky institutions can more fully participate in the competition for NIH awards. UL and the University of Kentucky (UK) will lead the consortium of 13 Kentucky universities and colleges in the KBRIN activities.

Role: Program Director

**P30 ES009106**

**Ken Ramos (PI)**

**6/4/07 - 3/31/11**

Center for Environmental Genomics and Integrative Biology

The main goal of the Center for Environmental Genomics and Integrative Biology (CEGIB) is to support outstanding basic and translational investigations into the etiology of environmental disease and the development of new approaches to manage these conditions. My role is Director of Bioinformatics, Biostatistics and Computational Biology Core

Role: Collaborator

**University of Louisville SOM Intramural Research Award**

**Nolan Boyd (PI)**

**10/09 – 10/2010**

The goal of this research project was the bioinformatics analysis of human embryonic stem cell preferential induction to mesodermal germ layer lineage. My role is to aid the bioinformatics analysis of expression arrays.

Role: Collaborator

**R01 EY017954**

**Cooper (PI)**

**6/1/08 - 5/31/13**

The Role of CamKII in Cell Death and Survival Pathways in Retinal Ganglion Cells

The goal of this award is to develop a description of the signature events in retinal ischemia and glaucoma in animal models of these debilitating eye diseases.

Role: PI

## BIOGRAPHICAL SKETCH

NAME Hichem Frigui	POSITION TITLE Professor, Computer Engineering & Computer Science Director, Multimedia Research Lab Speed School of Engineering, University of Louisville.
eRA COMMONS USER NAME hfrigui	

EDUCATION/TRAINING (*Begin with baccalaureate or other initial professional education, such as nursing, include postdoctoral training and residency training if applicable.*)

INSTITUTION AND LOCATION	DEGREE (if applicable)	YY	FIELD OF STUDY
University of Missouri, Columbia	B.S.	1990	Computer Engineering
University of Missouri, Columbia	B.S.	1990	Electrical Engineering
University of Missouri, Columbia	M.S.	1992	Electrical Engineering
University of Missouri, Columbia	Ph.D.	1997	Computer Engineering and Computer Science

### A. Personal Statement

Hichem Frigui, Ph.D., Professor of Computer Engineering and Computer Science at the University of Louisville and has over 25 years of experience in the areas of pattern recognition, machine learning, multimedia data processing and mining. His research focuses on all major steps of the learning process including feature extraction and selection, learning algorithms, information fusion, and decision making. He has contributed to the theoretical and practical aspects of these areas. He has supervised 3 post-doc researchers and 14 PhD students in the above areas. Currently, he is supervising 10 Ph.D. students and 5 M.S. students. He has been working on various applications that include detection of landmines and improvised explosive devices (IED), computational methods to analyze video recordings simulating medical care during crises, computational methods to analyze stable isotope assisted metabolomics to facilitate the identification of metabolites in biochemical pathways, and computational methods for material informatics. Most of his projects include the integration and fusion of data from multiple modalities including text, image, audio, video, hyperspectral, and radar data. Dr. Frigui main contributions include: 1) development of autonomous algorithms for detecting buried explosive devices such as landmines and improvised explosive devices (IED) using Ground Penetrating Radar (GPR) and Wideband Electro-Magnetic Induction (WEMI) sensors, 2) development of a new dynamic information fusion approach that learns different contexts and adapts the fusion to each context, 3) development of several unsupervised learning algorithms. Some of these algorithms have focused on identifying clusters of various shapes. Others have focused on algorithms that are robust to noise and outliers. More recently, we focused on developing algorithms that can learn cluster-dependent dissimilarity measures, 4) identification, indexing, and retrieval of cardio-pulmonary resuscitation (CPR) video scenes of simulated medical crisis, and 5) speech data analysis for semantic indexing of video of simulated medical crisis. **Dr. Frigui is a co-I on this project and will be responsible for developing and implementing new algorithms for image and text pattern recognition and indexing, content-based multimodal image retrieval and multi-domain mining and analytics.**

### B. Positions and Honors

#### Positions and Employment

- 2010 – Present Professor, Department of Computer Engineering and Computer Science, University of Louisville, KY.
- 2006 – 2010 Associate Professor, Department of Computer Engineering and Computer Science, University of Louisville, KY
- 2004 – 2006 Assistant Professor, Department of Computer Engineering and Computer Science, University of Louisville, KY
- 2004 – present Director, Multimedia Research Lab, Department of Computer Engineering and Computer Science, University of Louisville, KY
- 1998 – 2004 Assistant Professor, Department of Electrical and Computer Engineering, University of Memphis, TN



- 2006 Consultant, University of Missouri Columbia, MO
- 2001 Consultant, University of Florida, Gainesville, FL
- 1998 Consultant, University of Missouri Columbia, MO
- 1992 – 1994 Software Engineer, “Informatique Development et Etude (I.D.E.E), Tunis, Tunisia.

### **Other Experience and Professional Memberships**

- 2004-2008 Associate Editor, IEEE Transactions on Fuzzy Systems
- 2004-2010 Associate Editor, International Journal on Fuzzy Sets and Systems
- 2012 -present Editorial Advisory Board, Chiang Mai University Journal of Natural Sciences
- 2014 -2015 Advisory Board, SmartLanes Inc.
- 1998-present Member, Institute of Electrical and Electronics Engineering (IEEE)
- 1998-present Member, IEEE Computer Society
- 2010-present Member, IEEE Computational Intelligence Society
- 2003-2010 NSF Peer Review Committee: Information and Intelligent Systems (IIS)
- 2004-present Army Research Office (ARO) Peer Review Committee.

### **Honors**

- National Science Foundation’s CAREER Award (2002)

### **C. Contribution to Science**

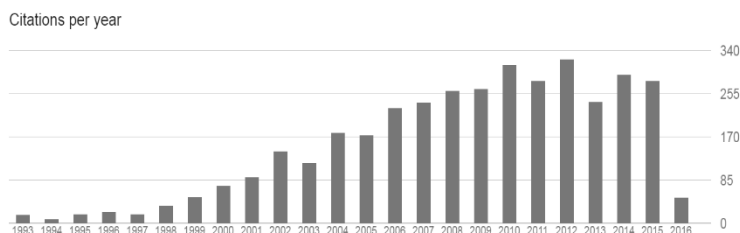
1. Development of a machine learning based approach to detect and classify scenes, from video data simulating medical crisis that involve CPR scenes. It provides answers to queries that are of interest to the physician supervising the training sessions such as: show me all the scenes that have a CPR action from a given video simulation training, or”retrieve time specific data about such critical events as elapsed time between failure of circulation and the initiation of CPR”, a measure clearly association with patient outcome.
  - a. M. S. Anju Panicker, **H. Frigui**, Aaron W. Calhoun, “Identification of cardio-pulmonary resuscitation (CPR) scenes in medical simulation videos using spatio-temporal gradient orientations. Image Processing Theory, Tools and Applications (IPTA Nov. 2015): 365-369
  - b. **H. Frigui**, S. Rawungyot, and A. Hamdi, “Identification of Cardio-Pulmonary Resuscitation (CPR) Scenes in Video Simulating Medical Crises”, International Conference on Advanced Technologies for Signal and Image Processing, March 2014, Tunisia.
2. Development of a machine learning approach that can analyze, segment, and classify speech data extracted from video data simulating medical crisis. The system was designed to provide users the capability to browse the video and retrieve shots that identify "who spoke, when, and the speaker's emotion" for further analysis.
  - a. S. Jiang, **H. Frigui**, Aaron Calhoun, “Text-independent Speaker Identification Using Soft Bag-of-Words Feature Representation”, International Journal of Fuzzy Logic and Intelligent Systems, Vol. 14, No. 4, Jan. 2015
  - b. J. Shuangshuang, **H. Frigui** and A. Calhoun, “Semantic Indexing of Video Simulations for Enhancing Medical Care During Crises”, 11th International Conference on Machine Learning and Applications ICMLA 2012, December 12-15, Boca Raton, Florida, USA
  - c. S. Jiang, **H. Frigui**, Aaron W. Calhoun, “Speaker Identification In Medical Simulation Data Using Fisher Vector Representation”, The 14th International Conference on Machine Learning and Applications (IEEE ICMLA'15) Florida, December 9-11, 2015
3. One of my main contributions to science is the development of autonomous algorithms for detecting buried explosive devices such as landmines and improvised explosive devices (IED) using Ground Penetrating Radar (GPR) and Wideband Electro-Magnetic Induction (WEMI) sensors mounted on a robotic platform and on a vehicle. I have developed several algorithms that have been field tested. In particular, two algorithms have performed extremely well in extensive testing by the US Army. Consequently, these algorithms were implemented in real-time versions in systems that the US Army has deployed for use against terrorist threats, and it has been a great success.

- a. **H. Frigui**, L. Zhang, P. Gader, J. Wilson, K.C. Ho, and A. Mendez-Vasquez, "An Evaluation of Several Fusion Algorithms for Anti-tank Landmine Detection and Discrimination", International Journal on Information Fusion, Vol. 13, No. 2, April 2012, Pages 161–174
- b. W. Missaoui, **H. Frigui**, and P. Gader, "Landmine Detection with Ground Penetrating Radar using Multi-Stream Discrete Hidden Markov Models", IEEE Transactions on Geoscience and Remote Sensing, Issue Date: Vol. 49, No. 6, page(s): 2080 – 2099, June 2011
- c. **H. Frigui** and P. Gader, "Detection and discrimination of land mines in ground-penetrating radar based on edge histogram descriptors and a Possibilistic K-Nearest Neighbor Classifier", IEEE Trans. Fuzzy Systems, Vol. 17, No. 1, pages 185-199, Feb 2009.
- d. **H. Frigui** , K.C. Ho, and Gader P. "Real-time Land Mine Detection with Ground Penetrating Radar using Discriminative and Adaptive Hidden Markov Models", EURASIP Journal on Applied Signal Processing, Vol. 12, 1867-1885, 2005
4. Development of a new dynamic information fusion approach that learns different contexts and adapts the fusion to each context. This approach was applied successfully to semantic multimedia indexing and retrieval and to multi-sensor multi-algorithm fusion for landmine detection.
  - a. C. Ben Abdallah, **H. Frigui**, and P. Gader, "Adaptive Local Fusion with Fuzzy Integrals", IEEE Transactions on Fuzzy Systems, Vol. 20, No. 5, pp 849-864, Oct. 2012.
  - b. **H. Frigui**, L. Zhang, and P. D. Gader, "Context Dependent Multi-Sensor Fusion and its application to Land Mine Detection", IEEE Transactions on Geoscience and Remote Sensing, Vol.48, No. 6, June 2010, pp. 2528-2543.
  - c. D. Kim, **H. Frigui** , and A. Fadeev, "A Generic Approach to Semantic Video Indexing using Adaptive Fusion of Multi-Modal Classifiers", International Journal of Imaging Systems and Technology (IJIST), special issue on Multimedia Information Retrieval, Vol. 18, No. 2-3, pages 124-136, August 2008.
5. Development of several data clustering algorithms. Some of these algorithms have focused on identifying clusters of various shapes. Others have focused on algorithms that are robust to noise and outliers. More recently, we focused on developing algorithms that can learn cluster-dependent dissimilarity measures.
  - a. M. Ben Ismail and **H. Frigui**., "Image Database Categorization using Robust Modeling of Finite Generalized Dirichlet Mixture", International Journal of Signal and Imaging Systems Engineering, Vol. 5, No. 2, pp. 143-153, 2012
  - b. **H. Frigui** and C. Hwang, "Fuzzy Clustering and Aggregation of Relational Data With Instance-Level Constraints", IEEE Trans. Fuzzy Systems, Vol. 16, No. 6, pages 1565-1581, Dec. 2008.
  - c. **H. Frigui**, C. Hwang, and F. Rhee, "Clustering and Aggregation of Relational Data with Applications to Image Database Categorization", International Journal on Pattern Recognition, Vol. 40, 3053—3068, 2007
  - d. **H. Frigui**, "Unsupervised Learning of Arbitrarily Shaped Clusters using Ensembles of Gaussian Models", International Journal of Pattern Analysis and Applications, Vol. 8, No. 1, 32-49, 2005.

### Complete List of Published Work:

- <https://scholar.google.com/citations?user=kj8gkFAAAAAJ&hl=en>

	Google Scholar	
	All	2011-2016
Citations	3764	1464
h-index	26	18
i10-index	54	29



## D. Research Support

### Ongoing Research Support

1. ARO W911NF-13-1-0066      Frigui (PI)      \$1,003,862      **03/27/2013-03/26/2017**  
**Multiple Instance Learning for Detecting Buried Objects**  
This proposed research focuses on developing robust algorithms for detecting buried objects using multi-sensor systems to deal with the inherent ambiguity. The main focus will be on systems that use GPR and EMI sensors. The goal of the proposed research is to develop a Multiple Instance Learning (MIL) framework that can learn from ambiguous examples. The proposed techniques aim to (1) investigate, and analyze various feature representation techniques; (2) develop statistical optimization algorithms that can identify multiple target concepts simultaneously; (3) investigate strategies to project data on the target concept space; and (4) investigate various algorithms that can classify the high-dimensional projected data.
2. ARO W911NF-14-1-0589      Frigui (PI)      \$338,468      **09/01/2014-08/31/16**  
**Multisensor Handheld Explosive Hazard Detection using Bag of Words and Fuzzy Inference**  
The proposed research has two main objectives. First, we propose developing discrimination algorithms for GPR sensor data using a bag-of-words approach. We will develop methods to identify regions of interest within each alarm, extract salient features, and represent them by a bag-of-words. Then, we will develop classification algorithms that learn the discriminative instances within the bags and identify the characteristics of the different targets. The second goal of the proposed research is to devise, analyze, and demonstrate methods based on adaptive fuzzy inference for building multi-sensor and multi-algorithm systems for detecting buried objects.
3. The LoKator Pitching Academy      Frigui (PI)      \$56,455      **01/01/2016-12/31/16**  
**Developing Computer Vision Technology to Automate and Extend the Functionalities of the LoKator System**  
The purpose of this research project is to investigate and develop computer vision algorithms to automate and extend the functionalities of the Lokator System. Lokator is a baseball and softball training system designed to document pitch location data while teaching pitch command, selection, and sequencing. Using video data recorded at 200 frames per sec, we will develop algorithms to detect the ball, track it, and identify the target zone it hits.

### Completed Research Support

1. "Multi-Sensor Detection of Obscured and Buried Objects", (PI, 100%), US Army Research Office (Subcontract through Univ. Florida), \$914,623      **10/01/08--9/30/13**
2. "Ensemble Hidden Markov Model Classifiers for Detecting Explosive Devices", (PI, 100%), Kentucky Science & Engineering Foundation, \$80,000,      **09/01/10--08/31/12**
3. "Context-Dependent Fusion of Multi Algorithm Systems for Detecting Explosive Objects", DEPSCoR (through US Army Research Office), \$697,990,      **07/15/08 07/14/11**
4. "Collaborative Research: Optimized Multi-Algorithm Systems for Detecting Explosive Objects Using Robust Clustering and Choquet Integration", (PI, 100%) National Science Foundation (NSF), \$429,881,      **09/01/07--08/31/10**

5. "Development, Integration, and Testing of Algorithms for Countermine Mine Detection Systems", (PI, 100%), Army Research Office (Subcontract through Univ. Florida), \$223,990, **06/15/07--06/14/10**
6. "Developing Robust Clustering and HMM Parameter Estimation Algorithms with Application to Land Mine Detection", (PI, 100%), ONR-DEPSCoR, \$557,668, **06/01/2005—05/01/2008**
7. "Developing Robust and Adaptive HMM Parameter Estimation Algorithms with Applications", (PI, 100%), Kentucky Science & Engineering Foundation, \$104,040, **11/01/05 10/31/07**
8. "Development, Integration, and Testing of algorithms for Countermine Mine Detection Systems", (PI, 100%), US Army (Subcontract through Univ. Missouri), \$54,000, **06/23/2005—12/31/2005.**
9. "A New Approach to Clustering Based on Synchronization of Oscillators with Application to Content-Based Image Retrieval", (PI, 100%), NSF-CAREER, \$300,100, **08/31/04—06/30/07** (no-cost extension until 08/31/09).
10. "US-France (INRIA) Cooperative Research: Robust Semi-Supervised Clustering with Application to Multi-Modal Database Categorization", NSF, **08/31/04 – 07/31/07** (no-cost extension until 07/31/09), \$30,000.

## BIOGRAPHICAL SKETCH

NAME Henry J Kaplan	POSITION TITLE
eRA COMMONS USER NAME hjkapl01	Evans Professor of Ophthalmology & Visual Sciences.

EDUCATION/TRAINING *(Begin with baccalaureate or other initial professional education, such as nursing, include postdoctoral training and residency training if applicable.)*

INSTITUTION AND LOCATION	DEGREE (if applicable)	YY	FIELD OF STUDY
Columbia University , New York, NY	AB	1964	Pre-Medicine
Cornell Medical School, New York, NY	MD	1968	Medicine
University of Texas Medical School, Dallas, TX	Fellowship	1974	Immunology
University of Iowa Hospitals & Clinics, Iowa City, IA	Residency	1978	Ophthalmology
Medical College of Wisconsin, Milwaukee, WI	Fellowship	1979	Retina

### A. Personal Statement

I have a novel background as a clinician scientist with scientific expertise in immunology and clinical expertise in vitreo-retinal diseases. My postdoctoral training at the University of Texas at Southwestern Medical School under the mentorship of J Wayne Streilein and Ruppert Billingham launched my interest in autoimmune diseases of the eye and led to the discovery of anterior chamber-associated immune deviation (ACAID). My clinical interest in uveitis has led to my research in ocular immunology and autoimmune diseases which has been funded by the NEI for past 30 years. Subsequently, my clinical training in retinal diseases was obtained under the tutelage of Thomas M Aaberg at the Medical College of Wisconsin. My interest in retinal diseases has involved the study of the pathogenesis and treatment of both age-related macular degeneration and hereditary retinal diseases. Many novel observations and insights were made in collaboration with many different colleagues, including the first successful submacular surgery to recover central vision in the presumed ocular histoplasmosis syndrome (POHS); the development of techniques to harvest and transplant sheets of RPE cells into the subretinal space of man and other species; the first clinical trial of human allogenic RPE cell transplantation in patients with exudative age-related macular degeneration (AMD) in the United States; the role of senescent Bruch's membrane in RPE attachment and differentiation; the study of RPE cell differentiation and dedifferentiation in vitro. We are now involved in identifying novel therapies for Retinitis Pigmentosa (RP) using a mini swine model of the most common form of autosomal dominant RP, a Pro23His mutation in RHO, investigating stem cell therapy, gene therapy and neuroprotection. **I will serve as a co-Investigator on this project. I will be primarily responsible for overseeing and facilitating the post-doctoral fellow and graduate student in acquiring the clinical data related to retinal diseases and collaborate with the Big Data Core to interpret and validate of all medical findings related to retinal disease.**

### B. Positions and Honors

#### Positions and Employment

- 2000 – Present Evans Professor of Ophthalmology, University of Louisville School of Medicine; Chairman, Department of Ophthalmology and Visuals Sciences, University of Louisville School of Medicine; Director, Kentucky Lions Eye Center, Louisville, KY.
- 1988 – 1998 Chairman, Department of Ophthalmology and Visual Sciences, Washington University School of Medicine, St. Louis, MO.
- 1988 – 2000 Professor of Ophthalmology and Visual Sciences, Washington University School of Medicine, St. Louis, MO.
- 1984 – 1988 Professor & Director of Research, Department of Ophthalmology, Emory University School of Medicine, Atlanta, GA.

- 1979 – 1984 Associate Professor, Department of Ophthalmology, Emory University School of Medicine, Atlanta, GA.
- 1974 – 1975 Assistant Professor, Department of Cell Biology, University Texas (Southwestern) Medical School, Dallas, TX.

### **Other Experience and Professional Memberships**

- 1982- American Uveitis Society  
**President, 1997-1999**
- 1985-1989 Visual Disorders Study Section A-1 (Member)  
National Eye Institute, National Institutes of Health  
1987-1989, **Chairman**, Visual Disorders Study Section A-1
- 1992- Ocular Immunology and Inflammation  
1992-1998, Co-editor  
1998- 2008, **Editor-in-Chief**
- 2011 **Consultant:** California Institute of Regenerative Medicine
- 2011 **Consultant:** FDA Cellular, Tissue and Gene Therapies Advisory Committee  
Washington, DC – June 29, 2011
- 2011- Translational Vision Science and Technology, Associate Editor, Association for Research in Vision and Ophthalmology
- 2015 **Consultant:** FDA Cellular, Tissue and Gene Therapies Advisory Committee

### **Honors**

- 1984 Designated the Olga Keith Weiss Scholar; Research to Prevent Blindness, Inc.
- 1987 Recipient of the Alcon Research Institute's Scientific Award
- 2010 Gold Fellow ARVO

## **C. Contribution to Science**

### **1. Immune privilege within the Anterior Chamber of the Eye**

My research career in immunology was launched by my identification of a phenomenon subsequently known as anterior chamber-associated immune deviation (ACAID) with J. Wayne Streilein. The presence of immune privilege in the eye was then studied by us, as well as many other scientists and laboratories, and resulted in the recognition that it existed not because of sequestration from the host immune system but rather from distinctive immune regulatory mechanisms. The primary purpose of this phenomenon appears to be protection of the sensitive structures of the eye from infection without the potential destructive effects of cell-mediated immunity. Some of the novel mechanisms identified by my collaborators and me concerning immune privilege are:

- Kaplan, H.J.**, Streilein, J.W.: Immune response to immunization via the anterior chamber of the eye. II. An analysis of F<sub>1</sub> lymphocyte-induced immune deviation. J. Immunol. 120:689-693, 1978. PMID: 632581,
- Waldrep, J.C., **Kaplan, H.J.**: Anterior chamber associated immune deviation induced by TNP-splenocytes (TNP-ACAID). II. Suppressor T cell networks. Invest. Ophthalmol. Vis. Sci. 24:1339-1345, 1983. PMID: 6225745.
- Ferguson, T.A., Waldrep, J.C., **Kaplan, H.J.**: The immune response and the eye. II. The nature of T suppressor cell induction in anterior chamber-associated immune deviation (ACAID). J. Immunol. 139:352-357, 1987. PMID: 2955039.
- Ferguson, T.A., Mahendra, S.L., Hooper, P., **Kaplan, H.J.**: The wavelength of light governing intraocular immune reactions. Invest. Ophthalmol. Vis. Sci. 33:1788-1795, 1992. PMID: 1550779.

## 2. Role of complement in the Eye

Although complement components were recognized to be present in the normal murine eye, as well as in induced intraocular inflammation (i.e. experimental autoimmune uveitis – EAU), their role and regulation was unknown. We were the first to show the expression of complement regulatory proteins (CRPs) in the normal murine eye, as well as the importance of these proteins in preventing autoimmune uveitis and in the induction of tolerance. Our studies also demonstrated experimentally that the alternate pathway of complement was important in the generation of laser-induced choroidal neovascularization, just prior to identification of the genetic importance of Factors H and B and other CRPs.

- a. Sohn, J.-H., **Kaplan, H.J.**, Suk, H.-J., Bora, P.S., Bora, N.S.: Complement regulatory activity of normal human intraocular fluid is mediated by MCP, DAF and CD49. *Invest. Ophthalmol. Vis. Sci.* 41:4195-4202, 2000. PMID: PMC 1821086.
- b. Sohn, J.-H., Bora, P.S., Suk, H.-J., Molina, H., **Kaplan, H.J.**, Bora, N.S.: Tolerance is dependent on complement C3 fragment iC3b binding to antigen-presenting cells. *Nat. Med.* 9(2):206-212, 2003. PMID: PMC 1821085.
- c. Jha, P., Sohn, J.H., Xu, Q., Nishihori, H., Wang, Y., Nishihori, S., Manickam, B., **Kaplan, H.J.**, Bora, P.S., Bora, N.S.: The complement system plays a critical role in the development of experimental autoimmune uveitis. *Invest Ophthalmol Vis Sci.* 47(3):1030-8, 2006. PMID: PMC 1975680.
- d. Bora, N.S., Kaliappan, S., Jha, P., Xu, Q., Sohn, J.H., Dhaulakhandi, D.B., **Kaplan, H.J.**, Bora, P.S.: Complement activation via alternative pathway is critical in the development of laser-induced choroidal neovascularization: role of factor B and factor H. *J. Immunol.* 177(3):1872-8, 2006. PMID: 1985467.

## 3. Development of submacular surgery

Prior to the development of pharmacologic agents in the treatment of choroidal neovascularization (CNV) the mainstay of treatment was laser photocoagulation. Even subfoveal CNV membranes were treated with Argon laser despite even though loss of central vision would occur immediately with treatment. As a consequence of this suboptimal treatment we identified the first successful use of submacular surgery for the treatment of subfoveal CNV in the presumed ocular histoplasmosis syndrome (POHS). This surgical approach was very helpful for this subset of patients with CNV and allowed us, and others, to gain many new important insights into CNV in AMD.

- a. Thomas, M.A., **Kaplan, H.J.**: Surgical removal of subfoveal neovascularization in the presumed ocular histoplasmosis syndrome. *Am. J. Ophthalmol.* 111:1-7, 1991. PMID: 1985467.
- b. Desai, V.N., Del Priore, L.V., **Kaplan, H.J.**: Choriocapillaris atrophy after submacular surgery in the presumed ocular histoplasmosis syndrome. *Arch. Ophthalmol.* 113:408-09, 1995. PMID: 7710384.
- c. Reddy, V., Zamora, R., **Kaplan, H.J.**: Distribution of growth factors in subfoveal neovascular membranes in age related macular degeneration and presumed ocular histoplasmosis syndrome. *Am. J. Ophthalmol.* 120:291-301, 1995. PMID: 7661200.
- d. Berger, A.S., Conway, M., Del Priore, L.V., Walker, R.S., Pollack, J.S., **Kaplan, H.J.**: Submacular surgery for subfoveal choroidal neovascular membranes in patients with presumed ocular histoplasmosis. *Arch. Ophthalmol.* 115:991-996, 1997. PMID: 9258220.

## 4. Immune regulation in experimental autoimmune uveitis (EAU)

My interest in autoimmune uveitis stemmed from my initial identification of ACAID with J Wayne Streilein. My collaboration with many colleagues allowed us to generate a model of acute anterior uveitis to a collagen peptide bound to melanin within the eye, the study of T regulatory (i.e. suppressor) cells and many other features of immune regulation in EAU.

- a. Cui Y, Shao H, Sun D, **Kaplan HJ**: Regulation of interphotoreceptor retinoid-binding protein (IRBP)-specific Th1 and Th17 cells in anterior chamber-associated immune deviation (ACAID). *Invest Ophthalmol Vis Sci.* 2009, Dec;50(12):5811-7. PMID: PMC 3275438.
- b. Jiang G, Sun D, Yang H, Lu Q, **Kaplan HJ**, Shao H: HMGB1 is an early and critical mediator in an animal model of uveitis induced by IRBP-specific T cells. *J Leukoc Biol.* 2014;95(4): 599-607. PMID: PMC 3958740.

- c. Liang D, Zuo A, Shao H, Chen M, **Kaplan HJ**, Sun D: Anti-inflammatory or proinflammatory effect of an adenosine receptor agonist on the Th17 autoimmune response is inflammatory environment-dependent. *J Immuno*. 2014;193(11):5498-505. PMID: PMC 4299924.
- d. Ke Y, Sun D, Jiang G, **Kaplan HJ**, Shao H. IL-22-induced regulatory CD11b+ APCs suppress experimental autoimmune uveitis. *J Immunol*. 2011 Sep 1;187(5):2130-9. Epub 2011 Jul 27. PMID: PMC 3197698.

## 5. Retinal transplantation in retinal degeneration

As a vitreoretinal surgeon and scientist I have had a career long interest in retinal regeneration as a therapeutic tool in hereditary retinal degeneration (i.e. Retinitis Pigmentosa – RP) and age-related macular degeneration (AMD). We have pursued RPE and photoreceptor transplantation in patients, as well as developed a pig model of autosomal dominant Pro23His RP, the most common form of RP in North America. We have most recently conducted studies using transplantation of rod-derived pig iPSCs, as well as pig fetal retinal progenitors cells, to rescue cone photoreceptors in our pig model.

- a. Zhou L, Wang W, Liu Y, de Castro JF, Ezashi T, Telugu BP, Roberts RM, **Kaplan HJ**, Dean DC: Differentiation of induced pluripotent stem cells of swine into rod photoreceptors and their integration into the retina. *Stem Cells*. 2011 June;29(6):972-80. PMID: PMC 4263955.
- b. Ross JW, Fernandez de Castro JP, Zhao J, Samuel M, Walters E, Rios C, Bray-Ward P, Jones BW, Marc RE, Wang W, Zhou L, Noel JM, McCall MA, Demarco PJ, Prather RS, **Kaplan HJ**. Generation of an inbred miniature pig model of retinitis pigmentosa. *Invest Ophthalmol Vis Sci*. 2012 Jan 31;53(1):501-7. PMID: PMC 3292381.
- c. Wang W, Zhou L, Lee SJ, Liu Y, Fernandez de Castro J, Emery D, Vukmanic E, **Kaplan HJ**, Dean DC: Swine cone and rod precursors arise sequentially and display sequential and transient integration and differentiation potential following transplantation. *Invest Ophthalmol Vis Sci*. 2014;55(1):301-9. PMID: PMC 3894797.
- d. Fernandez de Castro JP, Scott PA, Fransen JW, Demas J, DeMarco PJ, **Kaplan HJ**, McCall MA. Cone photoreceptors develop normally in the absence of functional rod photoreceptors in a transgenic swine model of retinitis pigmentosa. *Invest Ophthalmol Vis Sci*. 2014 Apr 17;55(4):2460-8. PMID: 24618325

## D. Research Support

### Ongoing Research Support

**1RP1EY024051** (Shao, PI; Kaplan, PI)

**12/1/2014 – 11/30/2018**

The Danger Signals in Autoimmune Uveitis

The role of danger signals (DAMPs), like HMGB1, in the induction of autoimmune uveitis is not well defined. The goal of this grant is to study the signaling pathways triggered by DAMPs to identify novel therapeutic targets for the treatment of autoimmune uveitis.

**1R21EY025408** (Shao, PI; Kaplan, PI)

**4/1/2015 - 3/31/2017**

Exosomes Derived From Retinal Astrocytes in the Regulation of Retinal Vasculature

A major cause of blindness in children born prematurely is retinopathy of prematurity (ROP). Retinal angiogenesis is aberrant in ROP and the role of retinal astrocytes in development of the normal retinal vasculature is important. The contribution of retinal astrocytes to the aberrant angiogenesis in ROP is being studied.

**W81XWH-14-2-0163** (Dean, PI; Kaplan, PI)

**9/22/2014 – 9/21/2017**

DOD - Vision Restoration with Granulocyte Colony-Stimulating Factor (GCSF)

Retinal damage from blast injuries to soldiers in combat has become a significant cause of visual disability. The goal of this project is to study the ability of GCSF to stimulate retinal photoreceptor degeneration following blast injuries in a rodent model.



**Completed Research Support**

**R21EY020647-01A1** (Kaplan, PI)

**12/1/2010-11/30/2013**

Expansion of the Pro23His rhodopsin transgenic mini swine model of Retinitis Pigmentosa.

Following the clinical characterization of this model, the colony was expanded to allow collaborative studies with swine induced pluripotent stem cells (iPSC), swine embryonic retinal cells, as well as human ESC to rescue cone photoreceptors.

## BIOGRAPHICAL SKETCH

NAME Koenig, Steven C	POSITION TITLE Professor of Bioengineering and Cardiothoracic Surgery, Endowed Chair of Cardiac Implant Science.
eRA COMMONS USER NAME sckoen01	

EDUCATION/TRAINING (*Begin with baccalaureate or other initial professional education, such as nursing, include postdoctoral training and residency training if applicable.*)

INSTITUTION AND LOCATION	DEGREE (if applicable)	YY	FIELD OF STUDY
University of New Hampshire	B.S.	1989	Electrical Engineering
University of New Hampshire	M.S.	1990	Electrical Engineering
University of Texas	Ph.D.	1996	Biomedical Engineering

### A. Personal Statement

I have twenty-four years' experience as a biomedical engineer whose broad research focus is to understand the effect of mechanical circulatory support (MCS) devices on the heart and vasculature for the treatment of cardiac dysfunction and how it may lead to pathologic remodeling. My areas of research expertise are biomedical instrumentation (sensors, signal conditioning, and data acquisition and analysis), MCS device development (efficacy, safety, reliability, hemocompatibility, and biocompatibility) in compliance with Good Laboratory Practices (GLP), and developing effective physiologic control strategies for MCS device-based therapy for Advanced Heart Failure. Our UofL research laboratory has extensive experience using computer simulation, mock circulation, acute and chronic large animal models (ischemic heart failure, pulmonary hypertension), and human cadavers to comprehensively simulate and analyze the performance of medical devices and to study their impact on cardiovascular function as evidenced by many of these devices in clinical use today. We have extensive experience and expertise developing medical devices from initial concept through pre-clinical testing (GLP study) and translation into clinical practice. I also understand the importance of productive collaboration between industry and research institutions, effective communication among project members, and timely dissemination of significant discoveries, findings, and outcomes. I have experience developing and executing realistic research plans, timelines, and budgets as evidenced by service in leadership roles, including PI of 11 NIH SBIR grants (current and completed) in collaboration with research partners (Abiomed, APK, HeartWare, SCR), which have been successfully translated into clinical practice.

The goal of this proposal is to develop new computational models and implement new state-of-the-art machine learning approaches to analyze and integrate multiple data types for the creation of a decision matrix that aids clinicians in the early diagnosis of human diseases and disorders. **For this study, I will serve as a co-I sharing my expertise in the diagnosis and treatment of advanced heart failure, including data collection, analysis, and documentation; identifying key model parameters and providing model data; liaison with clinical collaborators (Dr. Slaughter); and presenting results at scientific meetings, in peer-reviewed journals, and in future grant applications.**

### B. Positions and Honors

#### Positions and Employment

- 2014 – Present Co-Founder and Chief Scientific Officer (CSO), Cor Habere, Louisville, KY
- 2014 – Present Co-Founder and Chief Scientific Officer (CSO), MAST, Louisville, KY
- 2010 – Present Professor, Departments of Bioengineering & Surgery, Univ. of Louisville, Louisville, KY
- 2005 – 2010 Associate Professor, Department of Bioengineering, Univ. of Louisville, Louisville, KY
- 2002 – 2010 Associate Professor, Department of Surgery, Univ. of Louisville, Louisville, KY
- 1997 – 2002 Assistant Professor, Department of Surgery, University of Louisville, Louisville, KY
- 1996 – 1997 Instructor, Department of Surgery, University of Louisville, Louisville, KY

- 1994 – 1996           USAF (CAPT), Chief of Engineering, Physiology Research Branch, Brooks AFB, TX
- 1991 – 1994           USAF (LT), Bioengineer, Laboratory Aerospace and Cardiovascular Research, Brooks AFB, TX

### **Other Experience and Professional Memberships**

- 2012-present   Association for the Advancement of Medical Instrumentation (AAMI)
- 2009-present   American Institute for Medical and Biological Engineering (AIMBE)
- 1997-present   American Society for Artificial Internal Organs (ASAIO)

### **Honors**

- 2014            Presidents Distinguished Faculty Award in Research for Basic & Applied Sciences (UofL)
- 2013-present   Endowed Chair Cardiac Implant Science (University of Louisville)
- 2009-2013     University Scholar (University of Louisville)
- 2011-2012     Faculty Favorite (University of Louisville)
- 2009-present   Fellow, American Institute for Medical and Biological Engineering (AIMBE),
- 2007            Kolff Young Investigator Fellowship Award (ASAIO)
- 2005            1st Place Innovation in Biotechnology, Research!Louisville
- 2005            Most Outstanding Management & Technology Paper (AAMI)
- 1999            2nd Place-National Instruments LabVIEW Biomedical Application of the Year (Austin, TX)
- 1998            Most Productive Researcher, Research!Louisville

### **C. Contribution to Science**

1. Early in my research career, I collaborated with cardiac surgeons (Dr. Paul Spence and Dr. Robert Dowling) to improve and develop novel techniques for quantifying and improving anastomotic quality during coronary artery bypass graft (CABG) and partial left ventriculectomy (PLV) procedures. In the late 1990s, there was tremendous interest in developing surgical tools and techniques for performing minimally-invasive 'off pump' (no CPB) CABG procedures. Our research addressed the clinical need to eliminate any potential risk of suboptimal anastomoses by quantifying coronary graft blood flow intraoperatively using transit-time flow probes. In a series of publications, we presented our work in the canine model with key finding that even small errors in anastomotic quality may lead to significantly reduced graft flows. The new knowledge generated from our work led, in part, to clinical adaptation of the intraoperative use of transit-time flow probes by cardiac surgeons to validate graft flow (Europe, Asia).
  - a) **Koenig SC**, DJ VanHimbergen, SF Jaber, DL Ewert, P Cerrito, and PA Spence. Spectral analysis of graft flow for anastomotic error detection in off-pump CABG. *European Journal of Cardiothoracic Surgery*, 16:S83-S87, 1999.
  - b) Cerrito P, **SC Koenig**, DJ Van Himbergen, S Jaber, DL Ewert, B BhaskerRao, and PA Spence. Neural Network Pattern Recognition Analysis of Graft Flow Characteristics Improves Intra-operative Anastomotic Error Detection in Minimally Invasive CABG. *European Journal of Cardiothoracic Surgery*, 16:88-93, 1999.
  - c) BhaskerRao B, DJ VanHimbergen, HL Edmunds, S Jaber, A Ali, S Pagni, **SC Koenig**, and PA Spence. Evidence for Improved Cerebral Function after Minimally Invasive Bypass Surgery. *Journal of Cardiac Surgery*, 13:27-31, 1999.
  - d) **Koenig SC**, M Shafie, A Pearson, MA Laureano, P Cerrito, DL Ewert, MJ Schroeder, and RD Dowling. Intraoperative assessment of acute hemodynamic changes after partial left ventriculectomy. *Journal of Cardiac Surgery*, 14:152-56, 2000.

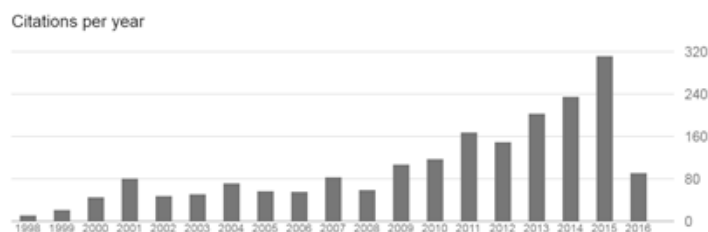
2. Heart failure (HF) is increasing worldwide and represents a major burden in terms of health care resources and costs. Despite advances in medical care, prognosis with HF remains poor, especially in advanced stages. The use of left ventricular assist devices (LVAD), though increasing, has also been limited due to the need for major operative intervention, use of cardio-pulmonary bypass (CPB), and high cost. To address these limitations, we developed a partial support counterpulsation device (Symphony) in collaboration with industry partners (SCR, Louisville KY and Abiomed, Danvers MA). Specifically, our laboratory completed research demonstrating the physiologic benefits of chronic counterpulsation (reduced afterload, increased coronary perfusion, eliminate reverse flow) and pre-clinical performance testing (efficacy, biocompatibility) of the Symphony system (pump, portable driver, and subcutaneous EKG leads). With R&D funding provided, in part, by six NIH SBIR and five matching KSTC grants (\$6.8 million), we successfully completed prototype development and feasibility testing and pre-clinical GLP study, which led to clinical use in HF patients (Montreal Canada). I served as subcontract PI on all of our grants, study director for all experiments including GLP pre-clinical study, and senior author for twelve publications.
  - a) **Koenig SC**, KN Litwak, GA Giridharan, GM Pantalos, RD Dowling, SD Prabhu, MS Slaughter, MA Sobieski, and PA Spence. Chronic Counterpulsation for Heart Failure: Hemodynamic Performance and Hemocompatibility of a 30-ml Subcutaneous Counterpulsation Device. *ASAIO J* 54:578-584, 2008.
  - b) Bartoli CR, PA Spence, T Siess, DH Raess, **SC Koenig**, and RD Dowling. Nonphysiologic blood flow triggers endothelial and arterial remodeling in vivo: implications for novel LVAD with a peripheral anastomosis. *Journal of Thoracic and Cardiovascular Surgery*, 148:311-21, 2014.
  - c) Giridharan GA, C Lederer, A Berthe, L Goubergrits, J Hutzenlaub, MS Slaughter, PA Spence, and **SC Koenig**. Flow dynamics of a novel counterpulsation device characterized by CFD and PIV modeling. *Medical Engineering and Physics*, 33(10):1193-1202, 2011.
  - d) Warren S, GA Giridharan, RD Dowling, PA Spence, L Tompkins, E Gratz, LC Sherwood, MA Sobieski, CR Bartoli, MS Slaughter, RS Keynton, and **SC Koenig**. Feasibility of Subcutaneous ECG leads for synchronized timing of a counterpulsation device. *Cardiovascular Engineering and Technology*, 3(1):17-25, 2012.
3. The technical advantages and improved outcomes with continuous flow (CF) left ventricular assist devices (LVAD) have led to their nearly exclusive use as mechanical circulatory support in heart failure (HF) patients. We demonstrated in clinical LVAD that rotary blood pumps operate at a constant pump speed (rpm) that reduces variation and end-systolic and end-diastolic volumes and diminishes vascular pulsatility. We developed innovative physiologic control algorithms that enable CF LVAD to phasically unload ventricular volume and restore pulsatility. Using computer simulation, mock circulation, and bovine ischemic HF models, we demonstrated the potential clinical benefits of this technology with key findings that low frequency asynchronous pump speed modulation generated the largest pulse pressures, volume variation, and improvements in hemodynamic efficacy and regional blood flows while also offering the technological benefit of not requiring any sensors for feedback control. The clinical need for vascular pulsatility has been highly controversial for decades, but has generated great interest in the LVAD industry due to adverse clinical events reported with CF LVAD, including AI, AVM, GI bleeding, and right HF.
  - a) Travis AR, GA Giridharan, GM Pantalos, RD Dowling, SD Prabhu, MS Slaughter, MA Sobieski, A Undar, and **SC Koenig**. Vascular pulsatility in patients with a pulsatile or continuous flow ventricular assist device. *Journal of Thoracic and Cardiovascular Surgery*, 133:517-24, 2007.
  - b) Ising MS, Warren S, Sobieski MA, Slaughter MS, **Koenig SC**, Giridharan GA. Flow modulation algorithms for a continuous flow ventricular assist device to increase vascular pulsatility: computer simulation study. *Cardiovascular Engineering & Technology*. 2(2):90-100, 2011.
  - c) Soucy KG, **SC Koenig**, GA Giridharan, MA Sobieski, and MS Slaughter. Defining pulsatility during continuous flow ventricular assist device support. *Journal of Heart & Lung Transplant*, 32(6):581-87, 2013.
  - d) Soucy KG, GA Giridharan, Y Choi, MA Sobieski, G Monreal, A Cheng, E Schumer, MS Slaughter, and **SC Koenig**. Rotary pump speed modulation for generating pulsatile flow and phasic left ventricular volume unloading in bovine model of chronic ischemic heart failure. *Journal of Heart and Lung Transplantation*, 34(1):122-31, 2015.

4. Cardiac surgery often requires major surgical interventions (open heart) and cardiopulmonary bypass (CPB) due to the large size of medical devices and implant tools, which can result in significant adverse events (bleeding, infection, thrombus), long recovery times, and substantial expenses (post-operative management). To address the clinical need for less invasive surgery, we are developing smaller devices (pumps, cannula, connectors) and surgical tools. Currently, we are funded by three separate NIH SBIR grants to develop LVAD transapical cannulation (HeartWare, Miami Lakes FL), LVAD inflow connector (Thoratec, Burlington MA), and LVAD transeptal cannulation (SCR, Louisville KY). Each of these technologies will enable LVAD to be implanted using less invasive surgical approach (mini-thoracotomy) and off-pump (no CPB), which should be introduced clinically within the next 12-18 months following successfully pre-clinical GLP testing by our research program.
  - a) Slaughter MS, Giridharan GA, Tamez D, LaRose J, Sobieski MA, Sherwood L, and **Koenig SC**. Transapical miniaturized ventricular assist device: Design and initial testing. *Journal of Thoracic and Cardiovascular Surgery*, 142(3):668-74, 2011.
  - b) Soucy KG, JD Graham, CJ Benzinger, MK Sharp, GA Giridharan, MA Sobieski, MS Slaughter, and **SC Koenig**. Feasibility of ventricular-arterial cannula for aortic valve bypass. *Cardiovascular Engineering and Technology*, 44(2):161-70, 2013.
  - c) Tamez D, J LaRose, MA Sobieski, LC Sherwood, GA Giridharan, **SC Koenig**, and MS Slaughter. Development of a transapical miniaturized ventricular assist device. *ASAIO J*, 60(2):170-177, 2014.
  - d) **Koenig SC**, JH Jimenez, MA Sobieski, Y Choi, G Monreal, GA Giridharan, KG Soucy, and MS Slaughter. Early feasibility testing and engineering development of a universal sutureless beating heart (SBH) connector for left ventricular assist devices (LVAD). *ASAIO J*, 60(6):617-25, 2014.
5. I led the development and application of medical instrumentation, mock circulation flow loop, and large animal ischemic heart failure models in support of our research and development (R&D) of mechanical circulatory support (MCS) devices. Specifically, we published techniques for hemodynamic data acquisition and analysis and blood trauma testing in compliance with Good Laboratory Practices (GLP) as well as development and post-operative management of chronic ischemic heart failure (IFH) bovine model. GLP studies using these instrumentation and models led to clinical use and/or approval of medical devices in use today, including AbioCor, Impella, and Symphony (Abiomed, Danvers MA), HVAD (HeartWare, Miami Lakes FL), and TAH (SynCardia, Tucson AZ).
  - a) **Koenig SC**, GA Giridharan, DL Ewert, MJ Schroeder, C Ionan, MS Slaughter, MA Sobieski, GM Pantalos, RD Dowling, and SD Prabhu. Human, bovine and porcine systemic vascular input impedance are not equivalent: Implications for device testing in heart failure. *J Heart Lung Transplant*, 27:1340-47, 2008.
  - b) Giridharan GA, Sobieski MA, Ising MS, Slaughter MD, and **Koenig SC**. Blood trauma testing for mechanical circulatory support devices. *Biomedical Instrumentation & Technology*, 45(4):334-39, 2011.
  - c) Bartoli CR, LS Sherwood, GA Giridharan, MS Slaughter, WB Wead, SD Prabhu, and **SC Koenig**. Bovine model of chronic ischemic cardiomyopathy: implications for ventricular assist device testing. *Artificial Organs*, 37(12):E202-E214, 2013.
  - d) Sherwood LC, MA Sobieski, **SC Koenig**, GA Giridharan, and MS Slaughter. Benefits of aggressive medical management in a bovine model of chronic ischemic heart failure. *ASAIO J*, 59:221-29, 2013.

#### Complete List of Published Work:

<http://scholar.google.com/citations?user=dG4MZsAAAAJ&hl=en>

	Google Scholar	
	All	2011-2016
Citations	1993	1155
h-index	24	18
i10-index	53	36



## D. Research Support

### Ongoing Research Support

1. **NIH/NHLBI 1R01 HL124170-01A1 (PI: Wu/Griffith)** **04/15/2015-03/31/2019**  
Shear-Induced Hemostatic Dysfunction and Bleeding in CF-VAD recipients  
The goals of this project are to advance the understanding of device-induced hemostatic dysfunction and bleeding in heart failure patients supported with continuous flow ventricular assist device (CF-VAD) and to use this knowledge to guide the design ventricular assist devices and the clinical practice of device-based therapy.  
Role: Co-Investigator
2. **R44HL123120-01 (PI: Spence, Koenig, Slaughter)** **6/1/2014 –5/31/2017**  
NIH SBIR phase I-II: *Development of SVAD for HF Therapy*  
The major goal of this project is to complete pre-clinical testing of SVAD system (SCR, Louisville KY) to provide partial cardiac assist in patients with less advanced stage heart failure.  
Role: subcontract PI
3. **1R44HL117426-01 (PI: Jimenez, Koenig, Slaughter)** **3/1/2013 –2/28/2016**  
NIH SBIR phase I-II: *Apical access system with universal connector for beating heart LVAD implantation*  
The major goal of this project is to test a novel Apical Access System (AAS) device (APK Medical, Atlanta, GA) to facilitate less invasive LVAD implant-explant surgical procedures by enabling suture-less, valved inflow connector without need for CPB to treat earlier stage HF patients.  
Role: subcontract PI
4. **R44 HL103014-01 (PI: Tamez, Koenig, Slaughter)** **8/1/2013 –7/31/2016**  
NIH SBIR phase II: *Development of transapical MVAD for HF therapy*  
The major goal of this project is to completed development of the tMVAD (HeartWare, Miami Lakes, FL) and pre-clinical testing in large animal model to demonstrate safety, reliability, and efficacy.  
Role: subcontract PI

### Completed Research Support

1. **2R43HL102981-02A (PI: Spence, Koenig, Slaughter)** **4/1/2012 –3/31/2015**  
NIH SBIR phase II: *Subcutaneous ECG sensing*  
The major goal of this project is to complete development of novel subcutaneous EKG integrated with Symphony device and portable driver.  
Role: subcontract PI
2. **KSTC-17-OICS-189 (PI: Spence, Koenig, Slaughter)** **1/1/2013 –12/31/2015**  
Kentucky Science and Technology Corporation (KSTC): *Counterpulsation device with integrated EKG sensing*  
The major goal is this project is to complete development Symphony system by integrating a subcutaneous lead system for EKG detection, signal conditioning, and control.  
Role: subcontract PI
3. **R43 HL103014-01A1 (PI: Tamez, Slaughter, Koenig)** **4/1/2011 –9/30/2012**  
NIH SBIR phase I: *Feasibility Testing of Longhorn MVAD*  
The major goal of this project is to test re-designed Longhorn MVAD (HeartWare, Miami Lakes, FL) in an acute animal model to demonstrate feasibility.  
Role: PI subcontract
4. **2R44HL088760-02 (Spence, Koenig)** **5/15/2009 –4/14/2011**  
NIH-SBIR phase II: *Portable pneumatic driver for counterpulsation therapy*  
The major goals of this project are to (1) complete engineering development, (2) demonstrate reliability and hemocompatibility, and (3) demonstrate safety and biocompatibility of a portable pneumatic driver for a novel counterpulsation device (CPD) to treat early stage heart failure.  
Role: PI subcontract

## BIOGRAPHICAL SKETCH

NAME Olfa Nasraoui	POSITION TITLE Professor, Computer Engineering and Computer Science, Speed School of Engineering, University of Louisville.
eRA COMMONS USER NAME O0NASR01	

EDUCATION/TRAINING (*Begin with baccalaureate or other initial professional education, such as nursing, include postdoctoral training and residency training if applicable.*)

INSTITUTION AND LOCATION	DEGREE (if applicable)	YY	FIELD OF STUDY
University of Missouri, Columbia, MO	B.S.	1990	Electrical Engineering
University of Missouri, Columbia, MO	B.S.	1990	Computer Engineering
University of Missouri, Columbia, MO	M.S.	1992	Computer Engineering
University of Missouri, Columbia, MO	Ph.D.	1999	Computer Engineering & Computer Science

### A. Personal Statement

My general research interest is in the foundations of data mining and machine learning (Big Data) with a special emphasis on mining Web data (text, clickstream sessions and event data, annotations, social networks/graphs, social media streams, semantic web and ontologies) and in-depth practical mastery of Data Science. Some of the Web domain problems that I worked on are both shallow and deep Text Mining, Web usage mining and personalization, intelligent information retrieval, and multimodal and heterogeneous multiple domain data-driven discovery, search, annotation, and predictive modeling. Over the years, my research has targeted challenging problems with applications mainly in the Web domain, but also in other domains, such as standard structured databases, multiple domain biological data (comprised of text, microarray gene expression and ontologies), astronomy, and network event data. Funding was acquired at a level slightly below \$3 Million, mainly as a PI, from NSF, but also from NASA, Kentucky Science & Engineering Foundation and industry. Over the years, my research contributions, in collaboration with many researchers, have been in the areas of bio-inspired and physics-inspired clustering algorithms; robust clustering algorithms; clustering for web usage mining and application to web personalization; single-pass stream clustering for scaling up to evolving data streams; mining heterogeneous (text, image, annotations, and ratings) data; and recommender systems. I will serve as the lead on mining medical record data, which comprise a heterogeneous mix of text, patient demographic, and event data and will also contribute to the liaison between the different data domains such as text and other modalities. My expertise in web mining, in particular, text analytics and semantic web (ontologies), developing clustering algorithms, handling streaming data, and practical real-life Data Science and Data Mining experience that span the entire data science pipeline from project scoping and data acquisition and preparation to feature engineering, modeling, visualization and interpretation, are geared towards Big Data applications and will contribute to achieving the goals of this 21st Century iRFP proposal on Big Data in Medicine. **I will serve as co-I in the proposed project. I will oversee, in collaboration with Dr. Frigui, image indexing and retrieval and, in collaboration with Dr. Altiparmak, implement the Big Data CAD-based system through high performance, cloud-based distributed systems. Additionally, I will mentor a postdoctoral fellow in developing methodologies for real-life data science and data mining in medical applications.**

### B. Positions and Honors

#### Positions and Employment

2014-pres.	University of Louisville: Professor and Endowed Chair of E-Commerce, Computer Engineering and Computer Science (CECS)
5/15-8/15.	University of Chicago: Technical mentor and Project Lead, Data Science for Social Good Fellowship, Harris School of Public Policy.
2007-2014	University of Louisville: Associate Professor and Endowed Chair of E-Commerce, CECS

2004-2007	University of Louisville: Assistant Professor and Endowed Chair of E-Commerce, CECS
2000-2004	The University of Memphis: Assistant Professor in Electrical & Computer Engineering.
1999-2000	The University of Memphis: Instructor in Electrical & Computer Engineering Dept.
1998-1999	Colorado School of Mines: Research Assistant in Mathematics and Computer Science Dept.
8/97-12/97	Colorado School of Mines: Visiting Scholar, Mathematics and Computer Science Dept.
1994-1997	University of Missouri-Columbia: Research Assistant and Instructor.
1992-1994	Informatique, Développement, Et Etudes, Tunis, Tunisia: Software Engineer.
1990-1992	University of Missouri-Columbia: Research and Teaching Assistant.

## **Honors**

### ***Program and Conference Committees***

- **Vice Chair or Senior Program Committee in several conferences:** ACM KDD, IEEE ICDM, SIAM Data Mining (SDM).
- **Awards Chair:** DSSA 2016- IEEE International Conference on Data Science and Advanced Analysis, Montreal, Canada, 2016
- **General Co-Chair:** ICEDc 2016 International Conference on Digital economy, Carthage, Tunisia, 2016.
- **Publicity Co-Chair:** ICDM 2011- IEEE International Conference on Data Mining, Vancouver, Canada, 2011.
- **Program Committee member (Selected recent service):**
  - ACM KDD: Knowledge Discovery in Data: 2007-present
  - IEEE International Conference on Data Mining (ICDM), 2004-present
  - SIAM International Conference on Data Mining (SDM), Senior PC/Vice Program Chair: 2004-2014
  - International World Wide Web Conference – Web Mining track 2009-present
  - AAAI (AI & the Web track), 2011-present

### ***Professional Offices***

- Associate Editor, IEEE Access Journal.
- Member, Task Force on 'Data Visualization and Data Analysis' of the IEEE CIS Technical Committee on Data Mining

### ***Professional Memberships***

- Member, **ACM** (Association of Computing Machinery)
- Member, **ACM Special Interest Group on Knowledge Discovery in Databases** (ACM-SIGKDD)
- Member, **IEEE** (Institute of Electrical and Electronics Engineers)
- Member, **IEEE Computer Society**
- Member, **IEEE Computer Society Technical Committee on Computational Intelligence**
- Member, **IEEE Women In Engineering (WIE)**
- Member, **ACM Computer Science Teacher Association (CSTA)**

### ***Awards***

- Elevated to status of IEEE Senior member, 2015
- **National Science Foundation CAREER Award, 2002**
- *Best Paper Award* for theoretical developments in computational intelligence in the Artificial Neural Networks In Engineering (ANNIE 2001) conference, St. Louis, MO, 2001
- Nominated for Outstanding Faculty Mentor of Doctoral Student Award, University of Louisville, 2011, 2013
- Nominated for the Committee on the Status of Women, University of Louisville, 2013
- *Nomination for Best Paper Award* for “A Semi-supervised Learning Framework to Cluster Mixed Data Types”, in the *International Conference on Knowledge Discovery and Information Retrieval (KDIR)*, Barcelona, 2012
- Top 9 Faculty Favorites Award, University of Louisville, 2010

## **C. Contribution to Science**

**1. Robust clustering algorithms:** One distinguishing characteristic of these algorithms, which are derived from robust statistical estimation, is that they incorporate an automated estimation of an adaptive robust scale for each cluster and use the scale in formulating the cost function. As a result, the cost function takes into



account not only cluster compactness but also density, which makes it resistant to outliers in the data. Furthermore the parameter estimation was shown to be equivalent to robust statistical estimation and the robustness properties can therefore be proven.

- González F., D. Bermeo, L. Ramos, and **O. Nasraoui**, "On the Robustness of Kernel-Based Clustering", 17th Ibero-American Congress on Pattern Recognition CIARP 2012. Buenos Aires, Argentina, Sep. 2012.
- **Nasraoui O.**, and Krishnapuram R., "Clustering Using a Genetic Fuzzy Least Median of Squares Algorithm," Proceedings of the North American Fuzzy Information Processing Society Conference, Syracuse, NY, September 1997.
- **Nasraoui O.**, and Krishnapuram R., "An Improved Possibilistic C Means Algorithm with Finite Rejection and Robust Scale Estimation," Proceedings of the North American Fuzzy Information Processing Society Conference, Berkeley, CA, June 1996, pp. 395-399.
- **Nasraoui O.**, Krishnapuram R., "A Robust Estimator Based on Density and Scale Optimization, and its Application to Clustering," Proc. of IEEE International Conf. on Fuzzy Systems, New Orleans, Sep'96, pp. 1031-1035.

**2. Clustering for Web usage mining and application to Web personalization:** Some of the earliest robust clustering algorithms for clustering noisy, sparse, high dimensional Web session data, have been developed. These include evolutionary clustering algorithms that can optimize arbitrarily complex cost functions using specialized Web session similarity measures, and that can furthermore be formulated to be robust to outliers in the data. New similarity measures were proposed to take advantage of the semantics within a Web usage domain, for example by incorporating the site structure, and later an ontology of concepts, when computing the similarity between user sessions. Using these clustering algorithms, automatically detected user session profiles can be mined from anonymous web server access log data. This research has later been extended to further enrich the profiles with the semantics of dynamic websites and additional data such as search queries.

- a. **Nasraoui O.**, M. Soliman, E. Saka, A. Badia, R. Germain, "A Web Usage Mining Framework for Mining Evolving User Profiles in Dynamic Websites", IEEE Transactions on Knowledge and Data Engineering (TKDE), 20(2), Feb. 2008, pp. 202-215. (selected as the featured article of the Feb. 2008 issue).
- b. **Nasraoui O.**, Rojas C., and Cardona C., "A Framework for Mining Evolving Trends in Web Data Streams using Dynamic Learning and Retrospective Validation", *Computer Networks- Special Issue on Web Dynamics*, 50(10), 1425-1652, July 2006.
- c. Krishnapuram R., Joshi A., **Nasraoui O.**, and Yi L. "Low Complexity Fuzzy Relational Clustering Algorithms for Web Mining," *IEEE Transactions on Fuzzy Systems, Special Issue on Fuzzy Logic at the Turn of the Millennium*, Vol. 9, No. 4 (2001) pp. 595-607.
- d. **Nasraoui O.**, Frigui H., Joshi A., and Krishnapuram R., "*Mining Web Access Logs Using a Fuzzy Relational Clustering Algorithm based on a Robust Estimator*", Proc. of 8th International World Wide Web Conference (WWW), Toronto, May 1999. (**Acceptance rate: 15.8%**)

**3. Single-pass stream clustering for scaling up to evolving data streams:** Research resulted in some of the earliest algorithms for clustering noisy evolving data streams, including high dimensional data sets. More recent algorithms were developed to automatically validate and track evolution of clusters over the length of a data stream. The first stream clustering algorithms were based on the immune system metaphor for optimization via cloning and hyper-mutation. The second family contains stream clustering algorithms that are formulated based on robust statistical estimation concepts. Chebyshev Bounds are used in order to formulate an automated test for outlier detection. This test makes the outlier identification grounded in a rigorous foundation and less sensitive to thresholds and assumptions about probability distributions. Recent work (Stream-Dashboard) has focused on the development of a comprehensive and generic framework for tracking, validation, summarization, and visualization of the cluster evolution using any online data stream clustering algorithm. The most significant contribution in this latest approach, is that the data need not be stored, thus adhering to the strict demands of stream data mining. Evolution trends include internal transitions (that affect a single cluster), external transitions (that affect the relationship between two or more clusters) and milestones (times of significant change), all of which are detected automatically.

- a. B. Hawwash and **O. Nasraoui**, "Stream-Dashboard: A Framework for Mining, Tracking and Validating Clusters in a Data Stream", International Workshop on Big Data, Streams and

Heterogeneous Source Mining: Algorithms, Systems, Programming Models and Applications. Big-Mine 2012, part of ACM KDD: Knowledge Discovery and Data Mining Conference, Beijing, China, Aug. 2012, 109-117.

- b. Hawwash B, **Nasraoui O**, “Robust Clustering of Data Streams using Incremental Optimization”, *The IVth Alberto Mendelzon International Workshop on Foundations of Data Management. AMW 2010*, Buenos Aires, Argentina, May 2010.
- c. **Nasraoui O**, Cardona C, Rojas C. “Using Retrieval Measures to Assess Similarity in Mining Dynamic Web Clickstreams”. Proceedings of ACM KDD: Knowledge Discovery and Data Mining Conference, Chicago, IL, 2005, 439-448. **(acceptance rate: 11.2%)**
- d. **Nasraoui O.**, C. Cardona, C. Rojas, F. González, “TECNO-STREAMS: Tracking Evolving Clusters in Noisy Data Streams with a Scalable Immune System Learning Model”, in Proc. of Third IEEE International Conference on Data Mining (ICDM'03), Melbourne, FL, November 2003, pp. 235-242.

**4. Mining heterogeneous data:** Recent research includes proposing a new Inter-Domain Supervision (IDS) clustering framework for clustering data with attributes that come from different domains or different sources (such as categorical, text, numerical, visual features, etc). The main originality of this approach is the use of semi-supervised learning without any external labels. Instead of requiring some of the data to be labeled in any given domain, these labels are automatically inferred from the high confidence clustering results in the other domain. As a result, the two data domains exchange supervision knowledge with each other, in the form of confident seeds or constraints, in order to improve the clustering in their own domains.

Another area of recent research activity consists of exploiting new formulations of Non-negative Matrix Factorization (NMF) for improved machine learning in incomplete and heterogeneous data sets with different modalities, such as textual, categorical, numerical, transactional, ratings, etc. The recent algorithms based on mixed NMF and Asymmetric NMF have been successfully applied to multimodal data clustering, indexing and retrieval, as well as automated annotation and recommendation. Other work targeted focused crawling in social media-sharing websites with multimodal data, thus exploiting the synergy between the visual and text/tag domain.

- a. J.C. Caicedo, J. Ben-Abdallah, F. Gonzalez, **O. Nasraoui**, “Multimodal Representation, Indexing, Automated Annotation and Retrieval of Image Collections via Non-Negative Matrix Factorization”, *Neurocomputing*, 76(1): 50-60, 2012.
- b. A. Abdullin and **O. Nasraoui**, “A Semi-supervised Learning Framework to Cluster Mixed Data Types”, *International Conference on Knowledge Discovery and Information Retrieval (KDIR)*, Barcelona, Spain, Oct. 2012. **(acceptance rate: 12.68%), nominated for Best Paper Award.**
- c. Ben Abdallah, J. C. Caicedo, F. A. Gonzalez, **O. Nasraoui**, “Multimodal Image Annotation Using Non-negative Matrix Factorization,” *IEEE/WIC/ACM International Conference on Web Intelligence and Intelligent Agent Technology (WI)*, Vol. 1, 128-135, 2010. **(acceptance rate: 16%)**
- d. Z. Zhang and **O. Nasraoui**, “Profile-based focused Crawling for Social Media-Sharing Websites”, *EURASIP Journal on Image and Video Processing*, *EURASIP Journal on Image and Video Processing*, Volume 2009, Article ID 856037, 2009.

**5. Recommender systems:** Some of the early algorithms for automated recommendations were developed using computational intelligence methods. I have also developed an open source search engine-based hybrid recommender system for multiple websites (<http://webmining.spd.louisville.edu/open-source-recommender/>). This approach was extended in 2 different directions as part of 2 dissertations I supervised, and implemented in a real life setting on two e-learning systems. Based on Search Query Log Mining, one of the earliest query recommendation systems was proposed, based on a novel consecutive query graph model that captures reformulation patterns in search engine queries. Recent work has turned toward developing algorithms for generating recommendations that can be explained and automated explanation generation.

- a. B. Abdollahi and **O. Nasraoui**. Explainable Matrix Factorization for Collaborative Filtering. In Proceedings of the 25th International Conference Companion on World Wide Web (WWW '16 Companion), 2016. **(acceptance rate: 16%)**
- b. B. Abdollahi and **O. Nasraoui**. A cross-modal warm-up solution for the cold-start problem in collaborative filtering recommender systems. In *Proceedings of the 2014 ACM conference on Web science (WebSci '14)*. ACM, New York, NY, USA, 257-258, 2014. **(acceptance rate: 20%)**

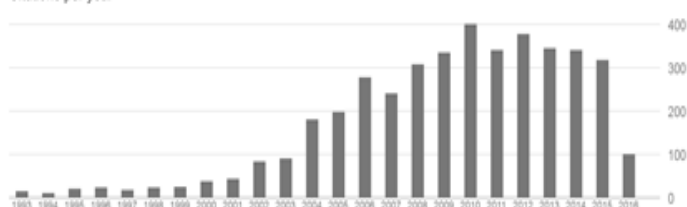
- c. Z. Zhang and **O. Nasraoui**, "Mining Search Engine Query Logs for Social Filtering-based Query Recommendation", *Applied Soft Computing – Special Issue on Dynamic Data Mining*, 8(4), Sep. 2008, 1326-1334.
- d. **O. Nasraoui**, Cerwinski J., Rojas C., and Gonzalez F., "Performance of Recommendation Systems in Dynamic Streaming Environments", in *Proc. of SDM 2007 – SIAM International Conference on Data Mining*, Minneapolis MI, Apr. 2007. (**acceptance rate: 12%**)

#### Complete List of Published Work on Google Scholar:

<https://scholar.google.com/citations?user=SGscZDgAAAAJ&hl=en>

	Google Scholar	
	All	Since 2011
Citations	4250	1826
h-index	35	22
i10-index	69	45

Citations per year



#### D. Research Support Ongoing Research Support

**NSF-IIS-1549981**

**10/01/15-09/30/18**

INSPIRE: Not Unbiased: The Implications of Human-Algorithm Interaction on Training Data and Algorithm Performance

**National Science Foundation**

**PI: O. Nasraoui; \$813,222.00**

The deep research into how the human decision process affects machine learning, and how machine learning impacts the human decision process, can provide significant advances in the accuracy and utility of systems using machine learning. The project builds on analysis of machine learning algorithms based on Hidden Markov Models (HMMs). The formal analysis initially looks at "blind spots" - the impact of bias from users not getting complete (or a random sample) of data. Further analysis will be based on the outcome of human experiments. The results will be used to develop improved machine learning approaches based on antidotes (altering learned models to reduce bias) and reactive learning (active learning that takes into account the human and machine biases).

#### Selected Completed Research Support

**KSEF-3113-RDE-017**

**07/01/14-06/30/15**

Humanizing Black Box Big Data Predictors with the Power of Explanations

**Kentucky Science and Engineering Foundation**

**PI: O. Nasraoui; \$29,776.**

**NSF IIS 0916489**

**09/01/09-08/31/13**

Stream Clustering Algorithms in Mixed Domains with Soft Two-way Semi-Supervision

**National Science Foundation**

**PI: O. Nasraoui; \$450,000**

"Architecture Analysis of Peer-to-Peer Data Exchanges", **PI, Kentucky Science and Engineering Foundation**, \$99,413, 2008-2010.

"Solar Loop Mining for the Coronal Heating Problem", **PI, NASA - Applied Information Systems Research Program (AISRP)**, \$385,000, **2004-2009**

"Mining Solar Images to Support Astrophysics Research", **PI, National Science Foundation – IIS: Science and Engineering Information Integration and Informatics**, \$200,000, **2004-2009**

"CAREER: New Clustering Algorithms Based on Robust Estimation and Genetic Niches with Applications to Web Usage Mining", **PI, National Science Foundation – Intelligent Information Systems (IIS) - Information and Data Management**, \$300,080, **2002-2009**

## BIOGRAPHICAL SKETCH

NAME Eric Christian Rouchka	POSITION TITLE Assistant Professor, Computer Engineering and Computer Science, Speed School of Engineering, University of Louisville.		
eRA COMMONS USER NAME ECROUC01			
EDUCATION/TRAINING <i>(Begin with baccalaureate or other initial professional education, such as nursing, include postdoctoral training and residency training if applicable.)</i>			
INSTITUTION AND LOCATION	DEGREE <i>(if applicable)</i>	YY	FIELD OF STUDY
Rockhurst College, Kansas City, MO	B.S.	1994	Computer Science, Mathematics and Biology
Rensselaer Polytechnic Institute, Troy, NY	M.S.	1996	Computer Science
Washington University in St. Louis, St. Louis, MO	D.Sc.	2002	Computer Science

### A. Personal Statement

Our lab has a current focus on implementing meta-analysis techniques for comparing gene expression data across platforms, developing methodologies for integrating data from various slices of the -omics stack at a common conceptual level, and developing algorithmic approaches for understanding transcriptional and translational control mechanisms using high-throughput sequencing technologies. The University of Louisville Bioinformatics Laboratory which I direct has a wide range of bioinformatics interests, particularly in the areas of transcriptional and translational regulation. As director of the Kentucky Bioinformatics Research Infrastructure Network's (KBRIN) Bioinformatics Core, I have led groups on the analysis of over 50 projects, the overwhelming majority of which involved either microarray or next-generation sequencing, including variant detection, whole genome sequencing, small RNA and transcriptome analysis. We currently have a number of lab members focusing on systems biology aspects, including understanding the intricate relationship between mRNA expression and miRNA expression, in particular as it relates to transcription factors. **I will serve as co-I in the proposed project and will collaborate with Dr. Cooper to analyze and interpret all the genomic data to identify and elucidate the appropriate biomarkers associated with the respective diseases as well as mentor postdoctoral fellows and students in this process.**

1. Harrison BJ, Venkat G, Lamb J, Drury C, Hutson T, Hill C, **Rouchka EC**, Moon LDF, Petruska JC. (2016) **the adaptor protein CD2AP is a Coordinator of Neurotrophin Signaling-Mediated Axon Arbour Plasticity.** *Journal of Neuroscience* 36(15):4259-4275. (doi: 10.1523/JNEUROSCI.2423-15.2016; PMID: 27076424; PMCID: Forthcoming).
2. Harrison BJ, Venkat G, Hutson T, Rau KK, Bartlett Bunge M, Mendell LM, Gage FH, Johnson RD, Hill C, **Rouchka EC**, Moon L, Petruska JC. (2015) **Transcriptional changes in sensory ganglion associated with primary afferent axon collateral sprouting in spared dermatome model.** *Genomics Data* 6(2015):249-252. (doi: 10.1016/j.gdata.2015.10.005; PMID: 26693787; PMCID: PMC4664766)
3. **Rouchka EC**, Flight RM, Fasciotto BH, Estrada R, Eaton JW, Patibandla PK, Waigel SJ, Li D, Kirtley JK, Sethu P, Keynton RS. (2016) **Transcriptional Profile of Immediate Response to Ionizing Radiation Exposure.** *Genomics Data* 7(2015):82-85. (doi: 10.1016/j.gdata.2015.11.027; PMID: 26981369; PMCID: PMC4778620)
4. Hougland MT, Harrison BJ, Magnuson DSK, **Rouchka EC**, Petruska JC. (2013) **The transcriptional response of neurotrophins and their tyrosine kinase receptors in lumbar sensorimotor circuits to spinal cord contusion is affected by injury severity and survival time.** *Frontiers in Integrative Physiology*, 3:478. (doi:10.3389/fphys.2012.00478; PMID: 23316162; PMCID: PMC3540763)

### B. Positions and Honors

#### **Positions and Employment**

1994-2001 Teaching Assistant, St. Louis University, Washington University, RPI  
1996 Senior Computer Programmer, Health Research Incorporated, Albany, NY

1997-2002 Graduate Research Assistant, Department of Computer Science, Washington University  
 2002-2003 Visiting Instructor, Department of Computer Engineering and Computer Science, University of Louisville  
 2003-2004 Visiting Assistant Professor, Department of Computer Engineering and Computer Science, University of Louisville  
 2002-present Director, University of Louisville Bioinformatics Research Laboratory  
 2005-2010 Assistant Professor, Department of Computer Engineering and Computer Science, University of Louisville  
 2010-present Associate Professor, Department of Computer Engineering and Computer Science, University of Louisville

## **Professional Honors and Activities**

### ***Program and Conference Committees***

2013-present Program Committee, BIOINFORMATICS Conference  
 2010 Technical Program Committee Chair, International Conference on Trends in Information Technology and Applications 2010 (ICTITA 2010)  
 2009 Program Committee, 2009 ICMLA Special Session on Machine Learning Applications in Bioinformatics and Computational Biology  
 2008 co-Chair, ISSPIT 2008 Special Session on Bioinformatics and Computational Biology  
 2007 Local organization committee, Kentucky Academy of Sciences  
 2004-present Organization committee, UT-ORNL-KBRIN Bioinformatics Summit

### ***Professional Offices***

2006-present External Advisor, Western Kentucky University Bioinformatics and Information Science Center  
 2004-2006,  
 2007-2011 Secretary for Computer and Information Sciences, Kentucky Academy of Sciences  
 2006-2007 Chair for Computer and Information Sciences, Kentucky Academy of Sciences

### ***Professional Memberships***

2006-present Member, Institute of Electrical and Electronics Engineers (IEEE)  
 2004-present Member, Association of Computing Machinery  
 2004-present Member, Kentucky Academy of Sciences  
 2004-present Upsilon Pi Epsilon International Honor Society in the Computing and Information Disciplines  
 2002-present Member, International Society for Computational Biology (ISCB)  
 2002-present Member, University of Louisville Bioinformatics Research Group (BRG)

## **C. Contribution to Science**

1. One of the constant themes throughout my research has focused on understanding alternative splicing events throughout an individual's transcriptome. Before the availability of whole genome assemblies, I worked closely with Zhengyan Kan to develop methodologies for assembling individual sequencing clones into larger contigs which were then used as reference sequences for mapping ESTs. This allowed, for the first time, for researchers to get a feel for the number of isoform variants present for each gene, which was much higher than previously thought. With the advent of next-generation sequencing technologies, the understanding of these events has become much greater, thanks to the improved depth of sequencing coverage. More recently, I have been collaborating with Dr. Yvonne Fondufe-Mittendorf of the University of Kentucky for understanding the role arsenite exposure and differential expression of the PARP-1 protein play in alternative splicing.
  - a. Kan Z, **Rouchka EC**, Gish WR, States DJ. (2001) **Gene structure prediction and alternative splicing analysis using genomically aligned ESTs**. *Genome Research*, 11(5):889-900. (PMID: 11337482; PMCID: PMC311065)
  - b. **Rouchka EC**, Gish W, States DJ. (2002) **Comparison of Whole Genome Assemblies of the Human Genome**. *Nucleic Acids Research*, 30(22):5004-5014. (PMID: 12434005; PMCID: PMC137179)
  - c. Riedmann C, Ma M, Melikishvili M, Godfrey SG, Zhang Z, **Rouchka E**, Chen KC, Fondufe-Mittendorf YN. (2015) **Inorganic Arsenic-induced cellular transformation is coupled with genome wide changes in chromatin structure, transcriptome and splicing patterns**. *BMC Genomics*, 16:212 (doi: 10.1186/s12864-015-1295-9; PMID: 25879800; PMCID: PMC4371809).

- d. Matveeva E, Maiorano J, Zhang Q, Eteleeb AM, Convertini P, **Rouchka EC**, Wang J, Fondufe-Mittendorf Y. (2016) **Involvement of PARP1 in the regulation of alternative splicing**. *Cell Discovery* 2:15046. (doi: 10.1038/celldisc.2015.46; PMID: forthcoming; PMCID: forthcoming)
2. Building upon the work with the above contribution, we had specific interests upon how the untranslated regions (UTRs) of a gene could be differentially expressed, even in the absence of differential expression within the coding region. My first venture into this area was in looking at the EST mapping, which allowed us to more accurately reconstruct the UTR regions, which continue to this day to be poorly annotated. Our research interests have led us to apply techniques to discover alternative splicing in the UTR regions of genes including PHKG1, and CamKIV. The latter is of specific interest, since the isoform with the alternatively spliced UTR localizes within axons in a manner that was previously unreported. We have developed unpublished techniques for performing differential expression analysis in UTR regions of microarrays, as well as within next-generation sequencing datasets.
  - a. Kan Z, Gish W, **Rouchka E**, Glasscock J, States D. (2000) **UTR Reconstruction and Analysis Using Genomically Aligned EST Sequences**. *ISMB*, 8:218-227. (PMID: 10977083)
  - b. Winchester JS, **Rouchka EC**, Rowland NS, Rice NA (2007) **In silico characterization of Phosphorylase kinase: evidence for an alternative intronic polyadenylation site in PHKG1**. *Molecular Genetics and Metabolism*. 92(2007): 234-242. (PMID: 17692548; PMCID: 2706538)
  - c. Harrison BJ, Flight RM, Gomes C, Venkat G, Ellis SR, Sankar U, Twiss JL, **Rouchka EC**, Petruska JC. (2014) **IB4-binding sensory neurons in the adult rat express a novel 3' UTR-extended isoform of CAMK4 that is associated with its localization to axons**. *The Journal of Comparative Neurology*, 522(2):308-336. (doi:10.1002/cne.23398; PMID: 23817991; PMCID: PMC3855981)
  - d. Eteleeb AM, Flight RM, Harrison BJ, Petruska JC, **Rouchka EC**. (2013) **An Island-Based Approach for Differential Expression Analysis**. *Proceedings of the International Conference on Bioinformatics, Computational Biology and Biomedical Informatics (ACM-BCB 2013)*, pp. 419-429. September 22-25, 2013, Washington, D.C. (doi:10.1145/2506583.2506589; PMID: 25632406; PMCID: 4306332) [Peer-reviewed conference proceeding]
3. Beginning in the early 2000's, the use of both custom and commercial microarray technologies became more widespread in order to understand the underlying transcriptome for a given set of conditions. One of the most important issues early on was understanding the effect of probe design for microarrays. Our group developed an approach, MPrime, which allowed for the development of unique probes with consistent thermodynamic properties for the purpose of custom array design. In addition, we further interrogated the role that SNPs play in probe design, showing that a number of SNPs are located within probes. We also illustrated that often the probes located within SNP regions are discarded due to inconsistent expression levels. However, we showed how these probes could actually be used in analysis as part of a combined transcriptomic and variant analysis.
  - a. **Rouchka EC**, Khalyfa A, Cooper NGF. (2005) **MPrime: efficient large scale multiple primer and oligonucleotide design**. *BMC Bioinformatics*, 6:175. (PMID: 16014168; PMCID: PMC1187872)
  - b. **Rouchka EC**, Phatak AW, Singh AV. (2008) **Effect of single nucleotide polymorphisms on Affymetrix® match-mismatch probe pairs**. *Bioinformation*, 2(9):405-411. (PMID: 18795114; PMCID: PMC2533060)
  - c. Flight RM, Eteleeb AM, **Rouchka EC**. (2012) **Affymetrix® Mismatch(MM) Probes: Useful After All**. *Proceedings of the 2012 ASE International Conference on BioMedical Computing (BioMedCom 2012)*, pp. 561-568. December 14-16, 2012, Washington, D.C. (doi:10.1109/BioMedCom.2012.8 DOI 10.1109/SocialInformatics.2012.36)
  - d. **Rouchka E**, Montoya D, Stribinskis V, Ramos K, Kalbfleisch, T. (2010) **Assessment of genetic variation for the LINE-1 retrotransposon from next generation sequence data**. *BMC Bioinformatics* 11(Suppl 9):S12. (doi:10.1186/1471-2105-11-S9-S12; PMID: 21044359; PMCID: PMC2967742).
4. The advent of next-generation sequencing technologies brought with it the need to develop better algorithms for analysis and mining of biological data. We therefore developed machine learning based methodologies for optimal mining using radial basis functions, and integration of multiple sources of data using a Bayesian co-clustering methodology.



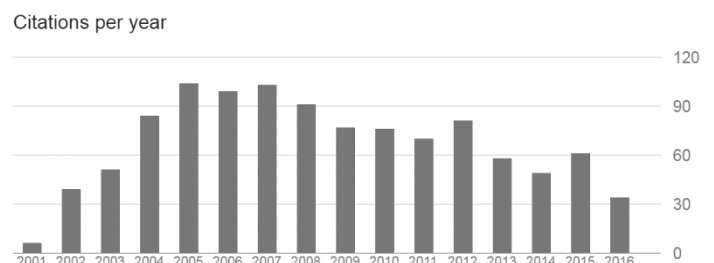
- a. Li D, **Rouchka EC**, Shafto P. (2010) **Phylogenomic analysis using Bayesian congruence measuring**. Proceedings of the Second International Conference on Bioinformatics and Computational Biology (BICoB-2010). pp. 30-37. March 24-26, 2010, Honolulu, HI.
  - b. Li D, Mohammad F, **Rouchka EC**. (2010) **A Bayesian Nonparametric Model for Joint Relation Integration and Domain Clustering**. Proceedings of the Ninth International Conference on Machine Learning and Applications (ICMLA 2010), pp. 969-974. December 12-14 2010, Washington, D.C. (doi: 10.1109/ICMLA.2010.168)
  - c. Mahdi RN, **Rouchka EC**. (2011) **Reduced HyperBF Networks: Regularization by Explicit Complexity Reduction and Scaled Rprop Based Training**. Neural Networks, IEEE Transactions on, 22(5):673-686. (PMID: 21421438)
  - d. Mahdi R, **Rouchka EC**. (2008) **Model based unsupervised learning guided by abundant background samples.** Proceedings of the Seventh International Conference on Machine Learning and Applications (ICMLA 2008), pp 203-210. December 11-13, 2008, San Diego, CA. (PMID: 20436793; PMCID: PMC2861841).
5. The final region deals with understanding and annotating information on a global perspective. In our work, we saw that many genetic identifiers wind up being misclassified, due to how the annotations are handled in an indirect fashion. We therefore developed AbsIDconvert as a methodology for using the common sequence information as a starting point. Along similar lines, we observed that often researchers would look at results of gene expression studies, find a set of common genes, and then find the common annotations between those genes. However, this leaves out the reality that different genes within the same process may be present at different timings. We therefore developed categoryCompare as a methodology to visualize the enriched annotations in a more encompassing fashion. Many genes also share common features in terms of how they are transcribed. Working with Chip Lawrence and Bill Thompson, I developed a Recursive Gibbs Sampler for detecting transcription factor binding sites, and approach that was widely cited. In order to understand transcription start sites more completely, I also worked with a graduate student, Rami Mahdi, to develop a radial basis function approach to identify transcriptional start sites based on sequence information.
- a. Mohammad F, Flight RM, Harrison BJ, Petruska JC, **Rouchka EC**. (2012) **AbsIDconvert: An Absolute Approach for Converting Genetic Identifiers at Different Granularities.** *BMC Bioinformatics* 2012, 13:229. (doi: 10.1186/1471-2105-13-229; PMID: 22967011; PMCID: PMC3554462)
  - b. Flight RM, Harrison BJ, Mohammad F, Bunge MB, Moon LDF, Petruska JC, **Rouchka EC**. (2014) **categoryCompare, an analytical tool based on feature annotations.** *Frontiers in Genetics*, 5:98. (doi: 10.3389/fgene.2014.00098; PMID: 24808906; PMCID: PMC4010757)
  - c. Thompson, W., Rouchka, E.C., Lawrence, C.E. (2003) **Gibbs Recursive Sampler: finding transcription factor binding sites.** *Nucleic Acids Research*, 31(13):3580-3585. (PMID: 12824370; PMCID: PMC169014)
  - d. Mahdi RN, **Rouchka EC**. (2009) **RBF-TSS: Identification of transcription start site in human using radial basis functions network and oligonucleotide positional frequencies.** *PLoS One*, 4(3):e4878. (PMID: 19287502; PMCID: PMC2654504)

#### Complete List of Published Work in Google Scholar and NIH MyBibliography

<http://scholar.google.com/citations?user=0RPDeS8AAAAJ&hl=en>

<http://www.ncbi.nlm.nih.gov/myncbi/collections/bibliography/43275692/>

	Google Scholar	
	All	2011-2016
Citations	1122	356
h-index	10	8
i10-index	11	5



## **D. Research Support**

### **Ongoing Research Support**

**P20 GM103436**

**Cooper (PI)**

**9/30/2001 – 4/30/2019**

National Institutes of Health (NIH), National Center for Research Resources (NCRR)

KY-IDeA Networks of Biomedical Research Excellence.

This grant is building the necessary research infrastructure to increase statewide competitiveness for extramural funding. My role is to serve many of the bioinformatics needs and education within Kentucky.

Role: co-I : Bioinformatics Core Director (40%)

(Formerly P20 RR016481)

### **Completed Research Support**

**NNX10AJ36G**

**Keynton (PI)**

**9/1/2010-8/31/2012**

National Aeronautical and Space Administration (NASA)

Diagnosing & Mitigating Human Exposure to Radiation Using Micro-Nanotechnology

This project sets the framework for creating diagnostic tools and countermeasures to assess and mitigate human exposure to radiation. The diagnostic system will consist of a “lab-on-a-chip,” LOC, platform for biochemical reactions which will allow low blood volume analysis similar to those used in diabetic patient monitoring. The envisioned applications for the diagnostic tool will be to identify when individuals have been exposed to sufficient levels of radiation leading to cellular damage which will: 1) compromise the health of astronauts while in space; 2) determine the extent of accidental radiation exposure of operators at nuclear facilities; and, 3) enable first responders to identify the potential threat of radiation exposure via terrorist attacks and/or on the battlefield, especially in remote areas with little infrastructure.

Role: co-PI

**DE-EM0000197**

**Rouchka, Kalbfleisch (PI)**

**1/1/2010-3/1/2012**

Department of Energy (DOE)

Extension of Informatics Infrastructure to Support Translational and Basic Research

The goal of this project is to enhance the bioinformatics and computational biology research presence at UofL in order to complement existing bioinformatics-related service cores found within a number of entities including KBRIN, CTSI, and CEGIB. A direct result will be to bring to the forefront of the University the prominent interdisciplinary role that bioinformatics research plays across schools within UofL. By establishing bioinformatics as a University-recognized resource of excellence, we hope to forge a nationally-recognized bioinformatics research agenda. This presence in bioinformatics research will be achieved by directly supporting research projects for seven bioinformatics junior faculty located across the School of Medicine (SOM), Speed School of Engineering (SSoE), School of Public Health and Information Sciences (SPHIS), and the School of Arts and Sciences (A&S). In addition, a bioinformatics seminar series will be established to bring in nationally recognized speakers to help promote the bioinformatics presence across the University.

Role: PI

**P20 RR016481S1**

**Cooper (PI)**

**9/17/2009-9/16/2011**

National Institutes of Health, National Center for Research Resources

Development of a Systems Biology Team

The goal of this grant is to create a core of excellence in systems biology and bioinformatics at the university through a bioinformatics research core, including three additional postdocs; one bioinformatics staff; two bioinformatics graduate students; and creation of a Kentucky Online Bioinformatics Seminar Series.

Role: co-Investigator

**P30 ES014443**

**Ramos (PI)**

**6/4/2007-3/31/2011**

National Institutes of Health (NIH), National Institute of Environmental Health Science (NIEHS)

Center for Environmental Genomics and Integrative Biology (CEGIB)

This is an NIEHS Environmental Health Sciences Core Center Grant application. The goal of the Center is to support outstanding basic and translational investigations into the etiology of environmental disease and the development of new approaches to manage these conditions.

Role: co-Investigator



## BIOGRAPHICAL SKETCH

NAME Mark S. Slaughter	POSITION TITLE Professor and Chair, Cardiovascular and Thoracic Surgery; Director, Mechanical Assist Device and Heart Transplant Program, University of Louisville, KY
eRA COMMONS USER NAME MSLAU01	

EDUCATION/TRAINING (Begin with baccalaureate or other initial professional education, such as nursing, include postdoctoral training and residency training if applicable.)

INSTITUTION AND LOCATION	DEGREE (if applicable)	YY	FIELD OF STUDY
Purdue University	B.S.	1982	Civil Engineering
Indiana University School of Medicine	M.D.	1986	M.D.
McGaw Medical Center of Northwestern University	Residency	1991	General Surgery
University of Minnesota	Fellowship	1994	Cardiovascular and Thoracic Surgery

### A. Personal Statement

As a clinician-scientist, my broad research focus is to understand the mechanisms of cardiac dysfunction, pathology associated with advanced heart failure, and the development and clinical translation of innovative therapies to improve patient outcomes and restore quality of life. Specifically, I have particular interest in device-based therapy for cardiac disease, including mechanical circulatory support (MCS) devices, ventricular assist devices (VAD), total artificial hearts (TAH), and left atrial occluder devices. In clinical practice, I have performed over 600 MCS device implants with over 100 patients currently supported at home on pulsatile and continuous flow device systems.

Our clinical program participates in numerous clinical trials directly related to heart failure, including pharmacology, stem cells, and mechanical circulatory support devices, and actively contributes to many national clinical data registries (i.e. STS, INTERMACS). Our laboratory uses an integrative approach for developing medical devices and surgical procedures (using human cadavers and several large animal models), evaluating anatomical fit (in human cadavers), and careful physiological assessments of cardiac function (large animal models and clinical patients) with the use of medical instrumentation (hemodynamic instrumentation), echocardiography (Phillips 3D, GE 3D), and fluoroscopy (GE Innova 3100 All-Digital Cardiovascular Imaging System). These resources enable us to quantify hemodynamic efficacy, hemocompatibility, and MCS device safety and reliability, including pre-clinical testing (GLP). Our laboratory is particularly well suited for contributing our wealth of information, expertise, and experiences developing surgical procedures and post-operative management required for the development of 'Big Data' clinical tools. The goal of this proposal is to develop new computational models and implement new state-of-the-art machine learning approaches to analyze and integrate multiple data types for the creation of a decision matrix that aids clinicians in the early diagnosis of human diseases and disorders. **In support of this proposal, I will serve as co-I and I will share my clinical expertise as a practicing cardiovascular surgeon and research expertise in advanced heart failure with the engineering development team in developing model parameters (i.e. patient demographics, biomarkers, adverse event data, etc.), diagnostic and therapeutic decision trees, and clinical assessment paradigms.**

### B. Positions and Honors

#### Positions and Employment

2008 – Present	Professor of Surgery, Chair of Department of Cardiovascular and Thoracic Surgery, University of Louisville, Louisville, KY
2008 – Present	Director, Heart Transplant and Mechanical Assist Device University of Louisville/Jewish Hospital and St. Mary's Healthcare System, Louisville, KY
2008 – Present	Associate Medical Director, Cardiovascular Innovation Institute (CII), Louisville, KY

2011 – Present    Oversight Committee, W.H. Coulter Foundation, Translational Research Partners Program Grant, Bioengineering Department, University of Louisville, Louisville, KY.

### **Other Experience and Professional Memberships**

- FDA –Consultant to the Circulatory System (Devices Panel); SBIR/STTR National Science Foundation (Grant Reviewer).
- Health and Human Services (Medicare Coverage Advisory Committee).
- International Scientific Committee (World Artificial-Organ, Immunology and Transplantation Society (WAITS), Ottawa, Canada).
- UNOS – Region 7 / Thoracic Review Board.
- Society of Thoracic Surgeons (co-chair STS University course on VADs).
- Gift of Hope Organ & Tissue Donor Network - CV Member Advisory Council.
- Association for the Advancement of Medical Instrumentation (AAMI Medical Device Particulates Committee, AAMI Mechanical Circ. Support Device Committee).
- American Society for Artificial Internal Organs (Board of Directors, Abstract Review Committee - ASAIO Annual Meeting, Cardiac Track Annual Meeting Chairman, Website Editor - Artificial Heart/Cardiac Support Section).
- International Society of Heart and Lung Transplantation (Editorial Board).
- American Association of Thoracic Surgeons.
- American College of Chest Physicians.
- American College of Surgeons.
- American Heart Association.
- American Medical Association.
- American Society for Artificial Internal Organs (Board of Trustees, Journal Editor, President, Program Chair).
- American Society of Transplant Physicians.
- American Society of Transplant Surgeons.
- International Society of Heart and Lung Transplantation.
- International Society of Rotary Blood Pumps (President, Program Chair).
- Society of Thoracic Surgeons.
- Society of University Surgeons.
- Southern Thoracic Surgical Association.
- Southern Surgical Association.

### **Honors**

2010    Medical News Physician of the Year.  
2007    Science Diplomat, Louisville Science Center 2009, Outstanding Physician Leader ACMC.  
1991    Alley-Sheridan Scholar.  
1991    Northwestern University Medical School Outstanding Resident Teacher.  
1990    Northwestern University Harold L Method, MD Award Outstanding Surgical Resident.  
1990    Northwestern University Outstanding Surgical Resident – Teacher of the Year.

### **C. Contribution to Science**

1. **Heart failure (HF)** is increasing in prevalence, with nearly 30 million people in some stage of failure. Despite the increased use of left ventricular assist devices (LVAD) as destination therapy or bridge to transplantation, new clinical technologies are in demand to counter the HF epidemic. I am involved with the development and testing of novel clinical technologies for this patient population. I was the PI of a multi-center clinical trial examining the safety and efficacy of using the novel, miniaturized HeartWare HVAD as bridge to transplant in end-stage HF patients. Patients with devices that have blood-contacting

surfaces require careful clinical management to minimize thrombus formation. We developed and tested novel biocompatible surfaces (Forcefield) that minimize platelet adhesion for future clinical devices.

- a. **Slaughter MS**, Pagani FD, McGee EC, Birks EJ, Cotts WG, Gregoric I, Howard Frazier O, Icenogle T, Najjar SS, Boyce SW, Acker MA, John R, Hathaway DR, Najarian KB, Aaronson KD; HeartWare Bridge to Transplant ADVANCE Trial Investigators. HeartWare ventricular assist system for bridge to transplant: combined results of the bridge to transplant and continued access protocol trial. *J Heart Lung Transplant*. 2013 Jul;32(7):675-83.
  - b. **Slaughter MS**, Pagani FD, Rogers JG, Miller LW, Sun B, Russell SD, Starling RC, Chen L, Boyle AJ, Chillcott S, Adamson RM, Blood MS, Camacho MT, Idrissi KA, Petty M, Sobieski M, Wright S, Myers TJ, Farrar DJ; HeartMate II Clinical Investigators. Clinical management of continuous-flow left ventricular assist devices in advanced heart failure. *J Heart Lung Transplant*. 2010 Apr;29:S1-39.
  - c. **Slaughter MS**, Pederson B, Graham JD, Sobieski MA, Koenig SC. Evaluation of new Forcefield technology: reducing platelet adhesion and cell coverage of pyrolytic carbon surfaces. *J Thorac Cardiovasc Surg*. 2011 Oct;142(4):921-5.
2. Surgical treatment of HF often requires major surgical interventions (open heart) and cardiopulmonary bypass (CPB) due to current LVAD designs, which can result in significant adverse events (bleeding, infection, thrombus), long recovery times, and substantial expenses (post-operative management). To address the clinical need for less invasive and cost effective surgical approaches, our lab participates in pre-clinical development of smaller devices (pumps, cannula, and connectors), implantation techniques and surgical tools. Currently, we are funded by three separate NIH SBIR grants to develop LVAD transapical cannulation (HeartWare, Miami Lakes FL), LVAD inflow connector (Thoratec, Burlington MA), and LVAD transeptal cannulation (SCR, Louisville KY). Each of these technologies will enable LVADs to be implanted using less invasive surgical approach (mini-thoracotomy) and off-pump (no CPB), which should be introduced clinically within the next 18-24 months following successfully pre-clinical GLP testing by our research program. This area of research is directed toward improved patient outcomes while reducing overall cost per quality-adjusted life year (QALY).
- a. **Slaughter MS**, Rogers JG, Milano CA, Russell SD, Conte JV, Feldman D, Sun B, Tatroles AJ, Delgado RM 3rd, Long JW, Wozniak TC, Ghumman W, Farrar DJ, Frazier OH; HeartMate II Investigators. Advanced **heart failure** treated with continuous-flow left ventricular assist device. *N Engl J Med*. 2009 Dec 3;361(23):2241-51.
  - b. Park SJ, Milano CA, Tatroles AJ, Rogers JG, Adamson RM, Steadley DE, Ewald GA, Sundareswaran KS, Farrar DJ, **Slaughter MS**. Outcomes in Advanced **Heart Failure** Patients with Left Ventricular Assist Devices for Destination Therapy. *Circulation*. Heart failure, 2012 Mar 1; 5(2): 241-8.
  - c. **Slaughter MS**, Pagani FD, McGee EC, Birks EJ, Cotts WG, Gregoric I, Frazier OH, Icenogle T, Najjar SS, Boyce SW, Acker MA, John R, Hathaway DR, Najarian KB, Aaronson KD. HeartWare Ventricular Assist System for Bridge to Transplant: Combined Results of the Bridge to Transplant and Continued Access Protocol Trial. *J Heart Lung Transplant*. 32.7 (2013): 675-683.
  - d. Rogers JG, Bostic RR, Tong KB, Adamson R, Russo M, **Slaughter MS**. Cost-effectiveness analysis of continuous-flow left ventricular assist devices as destination therapy. *Circ Heart Fail*. 2012 Jan;5:10-6.
3. As a clinician-scientist, I believe that the best outcome for left ventricular assist device (LVAD) patients would be myocardial recovery followed by LVAD removal without relapse of **heart failure (HF)** symptoms. To advance the goal of patient recovery and LVAD removal, I have served as the PI on multiple studies to develop new therapeutic strategies that may potentially rehabilitate the diseased heart. Early on, I lead a study to optimize a device weaning protocol for pulsatile flow LVAD (PVAD, Thoratec). Currently, I have established a collaboration with CorMatrix Cardiovascular Inc. (Roswell, GA) to develop a synergistic **heart failure** therapy involving CorMatrix injectable extracellular matrix (ECM) product with LVAD support. My laboratory completed a large-animal pilot study that demonstrated the combination therapy of ECM + LVAD induced the greatest improvements in heart function and cellular proliferation markers after 60- and 90-day treatment periods. I also provided my clinical expertise and conducted testing (cadaver and in vivo animal experiments) to assist in development of a custom injection tool to accurately deliver the material to ischemic regions.
- a. **Slaughter MS**, Sobieski MA, Koenig SC, Pappas PS, Tatroles AJ, Silver MA. Left ventricular assist device weaning: Hemodynamic response and relationship to stroke volume and rate reduction protocols. *ASAIO J*. 2006; 52:228-23.

- b. Cowger J, Sundareswaran K, Rogers JG, Park SJ, Pagani FD, Bhat G, Jaski B, Farrar DJ, **Slaughter MS**. Predicting survival in patients receiving continuous flow left ventricular assist devices: the HeartMate II risk score. *J Am Coll Cardiol*. 2013 Jan 22;61(3):313-21.
  - c. Soucy KG, Koenig SC, Giridharan GA, Sobieski MA, **Slaughter MS**. Rotary pumps and diminished pulsatility: do we need a pulse? *ASAIO J*. 2013 Jul-Aug;59(4):355-66.
  - d. **Slaughter MS**, Soucy KG, Matheny RG, Lewis BC, Hennick MF, Choi Y, Monreal G, Sobieski MA, Giridharan GA, Koenig SC. Development of an Extracellular Matrix (ECM) Delivery System for Effective Intramyocardial Injection in Ischemic Tissue. *ASAIO J*. 2014; 60(6):730-6.
4. Blood flow patterns and blood responses to biomaterials are critical considerations during LVAD design and development. Despite advances in device technologies, thrombi and bleeding remain clinical concerns and often limit long-term LVAD use. As one of the lead investigators of the ADVANCE Trial, we examined the incidence of pump thrombus in the HeartWare HVAD in bridge to transplant patients and studied characteristics that predispose patients to thrombus formation. We have also examined the role of platelet activation in HeartMate II patients, specifically to elucidate the roles of the adhesion markers P-selectin and CD40 ligand. In conjunction with clinical investigations, our laboratory has also developed a standardized hemolysis testing protocol to facilitate blood trauma characterization towards demonstrating device safety for FDA 510(k) approval of cardiac devices.
- a. Najjar SS, **Slaughter MS**, Pagani FD, Starling RC, McGee EC, Eckman P, Tatroles AJ, Moazami N, Kormos RL, Hathaway DR, Najarian KB, Bhat G, Aaronson KD, Boyce SW; HVAD Bridge to Transplant ADVANCE Trial Investigators. An analysis of pump thrombus events in patients in the HeartWare ADVANCE bridge to transplant and continued access protocol trial. *J Heart Lung Transplant*. 2014 Jan;33(1):23-34.
  - b. Giridharan GA, Sobieski MA, Ising M, **Slaughter MS**, Koenig SC. Blood trauma testing for mechanical circulatory support devices. *Biomed Instrum Technol*. 2011 Jul-Aug;45(4):334-9.
  - c. **Slaughter MS**, Sobieski MA 2nd, Graham JD, Pappas PS, Tatroles AJ, Koenig SC. Platelet activation in **heart failure** patients supported by the HeartMate II ventricular assist device. *Int J Artif Organs*. 2011 Jun;34(6):461-8.
  - d. **Slaughter MS**. Hematologic effects of continuous flow left ventricular assist devices. *J Cardiovasc Transl Res*. 2010 Dec;3(6):618-24.
5. I have also been involved in the development and testing of technology to improve LVAD implantation procedures. These technologies incorporate significant changes in standard LVAD implantation protocols, and ultimately aim to increase operation safety via less invasive and reduced surgery duration. I was one of the lead investigators for the HeartWare transapical MVAD (tMVAD), which is an innovative device that is implanted intra-ventricular and extends across the aortic valve. By removing the need for aortic anastomosis, I helped to develop a modified implantation protocol with a smaller surgical window, off-pump, and reduced implant time. In addition, I also serve as a co-Principal Investigator for an NIH SBIR subcontract to test an apical access system (AAS) (APK, Inc.) that quickly attaches LVAD inflow cannula for implantation. AAS is sutureless and is meant to replace conventional, yet time-consuming, suture rings. Data demonstrated that LVAD implant time can be reduced to less than 2 minutes (vs. nearly 20 minutes with existing methods) and this technology has recently been licensed to a major U.S. LVAD company.
- a. **Slaughter MS**, Giridharan GA, Tamez D, LaRose J, Sobieski MA, Sherwood L, Koenig SC. Transapical miniaturized ventricular assist device: design and initial testing. *J Thorac Cardiovasc Surg*. 2011; 142(3):668-74.
  - b. Tamez D, Larose JA, Shambaugh C, Chorpenning K, Soucy KG, Sobieski MA, Sherwood L, Giridharan GA, Monreal G, Koenig SC, **Slaughter MS**. Early Feasibility Testing and Engineering Development of the Transapical Approach for the HeartWare MVAD Ventricular Assist System. *ASAIO J*. 2014; 60(2):170-7.
  - c. Koenig SC, Jimenez JH, Sobieski MA, Choi Y, Monreal G, Giridharan GA, Soucy KG, **Slaughter MS**. Early Feasibility Testing and Engineering Development of a Universal Sutureless Beating Heart (SBH) Connector for Left Ventricular Assist Devices (LVAD). *ASAIO J*. 2014; 60(6):617-25.

#### Complete List of Published Work:

- <http://www.ncbi.nlm.nih.gov/pubmed/?term=Slaughter+MS%5BAuthor%5D>

## D. Research Support

### Ongoing Research Support:

**NIH/NHLBI 1R01 HL124170-01A1**

**(PI: Wu/Griffith)**

**04/15/2015-03/31/2019**

Shear-Induced Hemostatic Dysfunction and Bleeding in CF-VAD recipients

The goals of this project are to advance the understanding of device-induced hemostatic dysfunction and bleeding in **heart failure** patients supported with continuous flow ventricular assist device (CF-VAD) and to use this knowledge to guide the clinical practice of device-based therapy and the design improvement of ventricular assist devices.

Role: Co-Investigator

**1UM1HL-113530**

**(PI: Bolli & Slaughter)**

**3/1/2012 –3/31/2019**

National Institutes of Health

Regional Clinical Center for NHLBI Cardiovascular Cell Therapy Research

The major goal of this project is to complete clinical trials of cell therapy for **heart failure** patients.

Role: co-investigator

**OICN111220**

**(PI: Birks & Slaughter)**

**3/1/2013 - 1/1/2017**

REVIVE-IT Trial: Randomized Evaluation of VAD Intervention before Inotropic Therapy

The major goal of this project is Randomising patients with an earlier stage of **heart failure** (Class III) to LVAD vs. medical therapy.

Role: co-PI

**Coulter Foundation**

**(PI: Keynton & Slaughter)**

**1/1/2012 –12/31/2016**

Clinical Translational Research Program

The major goal of this project is to fund and develop clinical translational therapies from bench to bedside.

Role: PI

**R44HL123120-01**

**(PI: Spence, Koenig, Slaughter)**

**6/1/2014 –5/31/2017**

NIH SBIR phase I-II: Development of SVAD for HF Therapy

The major goal of this project is to complete pre-clinical testing of SVAD system (SCR, Louisville KY) to provide partial cardiac assist in patients with less advanced stage heart failure.

Role: subcontract co-PI

**1R44HL117426-01**

**(PI: Jimenez, Koenig, Slaughter)**

**3/1/2013 –2/28/2016**

NIH SBIR phase I-II: Apical access system with universal connector for beating heart LVAD implantation

The major goal of this project is to test a novel Apical Access System (AAS) device (APK Medical, Atlanta, GA) to facilitate less invasive LVAD implant-explant surgical procedures by enabling suture-less, valved inflow connector without need for CPB to treat earlier stage HF patients.

Role: subcontract co-PI

**R44 HL103014-01**

**(PI: Tamez, Koenig, Slaughter)**

**8/1/2013 –7/31/2016**

NIH SBIR phase II: Development of transapical MVAD for HF therapy

The major goal of this project is to completed development of the tMVAD (HeartWare, Miami Lakes, FL) and pre-clinical testing in large animal model to demonstrate safety, reliability, and efficacy.

Role: subcontract co-PI

**KSTC-17-OICS-189**

**(PI: Spence, Koenig, Slaughter)**

**1/1/2013 –12/31/2015**

Kentucky Science and Technology Corporation (KSTC): Counterpulsation device with integrated EKG sensing

The major goal is this project is to complete development Symphony system by integrating a subcutaneous lead system for EKG detection, signal conditioning, and control.

Role: subcontract co-PI

### Completed Research Support:

**R43 HL103014-01A1**

**(PI: Tamez, Slaughter, Koenig)**

**4/1/2011 –9/30/2012**

NIH SBIR phase I: Feasibility Testing of Longhorn MVAD

The major goal of this project is to test re-designed Longhorn MVAD (HeartWare, Miami Lakes, FL) in an acute animal model to demonstrate feasibility.

Role: subcontract co-PI

## **Appendix III: Budget**

## Proposal Grant Budget Sheet

GRA insurance	\$2,642
---------------	---------

Requested Funds TOTAL	Cost Share Amount	GRAND TOTAL	Cost Share Speedtype
\$ -	\$ -	\$ -	
\$ -	\$ -	\$ -	
\$ -	\$ -	\$ -	
\$ -	\$ -	\$ -	
\$ -	\$ -	\$ -	

\$	-	\$	-	\$	-	
\$	-	\$	-	\$	-	
\$	-	\$	-	\$	-	
\$	-	\$	-	\$	-	
\$	-	\$	-	\$	-	

\$ 66,000	\$ -	\$ 66,000	
\$ -	\$ 44,000	\$ 44,000	01385/01138
\$ 66,000	\$ 44,000	\$ 110,000	

\$	7,926	\$	-	\$	7,926	
\$	-	\$	5,284	\$	5,284	01385/01138
\$	7,926	\$	5,284	\$	13,210	

\$ 15,000	\$ -	\$ 15,000	
\$ -	\$ -	\$ -	
\$ 15,000	\$ -	\$ 15,000	

\$	1,148	\$	-	\$	1,148	
\$	-	\$	-	\$	-	
\$	1,148	\$	-	\$	1,148	

\$ 20,000	\$ 20,000	\$ 40,000	P0030
\$ 20,000	\$ 20,000	\$ 40,000	HA02A
\$ 20,000	\$ 20,000	\$ 40,000	E0658
\$ 20,000	\$ 20,000	\$ 40,000	E0331
\$ 20,000	\$ 20,000	\$ 40,000	GB131493A
\$ 20,000	\$ 20,000	\$ 40,000	GB131493A
<b>\$ 120,000</b>	<b>\$ 120,000</b>	<b>\$ 240,000</b>	

\$	5,700	\$	5,700	\$	11,400	P0030
\$	5,700	\$	5,700	\$	11,400	HA02A
\$	5,700	\$	5,700	\$	11,400	E0658
\$	5,700	\$	5,700	\$	11,400	E0331
\$	5,700	\$	5,700	\$	11,400	GB131493A
\$	5,700	\$	5,700	\$	11,400	GB131493A
\$	34,200	\$	34,200	\$	68,400	

<b>TOTAL</b>			
\$ 1,665	\$ -	\$ 1,665	
\$ 4,061	\$ 21,439	\$ 25,500	01383
\$ -	\$ -	\$ -	
\$ 5,726	\$ 21,439	\$ 27,165	

TOTAL				
\$	-	\$	17,496	\$ 17,496 01385
\$	-	\$	17,496	\$ 17,496 E1323
\$	-	\$	36,411	\$ 36,411 01385
\$	-	\$	36,411	\$ 36,411 01138
\$	-	\$	36,411	\$ 36,411 E0331
\$	-	\$	144,225	\$ 144,225

TOTAL					
\$	201,000	\$	164,000	\$	365,000
\$	43,274	\$	39,484	\$	82,758
\$	5,726	\$	21,439	\$	27,165
\$	-	\$	144,225	\$	144,225
\$	250,000	\$	369,148	\$	619,148
\$	750,000	\$	1,107,444	\$	1,857,444

Keynton/Nasraoui Bioengineering/CECS

Slaughter	CVT Surgery
Bolli	Cardiology
Kaplan	Ophthalmology
Barnes	Austism Center
Cooper	KBRIN
Cooper	KBRIN

Keynton	Bioengineering
SSoE Dean	SSoE
Keynton	Bioengineering
Nasraoui	CECS
Barnes	Autism

## BUDGET JUSTIFICATION

### 21<sup>ST</sup> CENTURY INITIATIVE: BIG DATA IN MEDICINE

The total cost of this three-year project is \$1,857,444 (\$619,148/yr). The Big Data team, Speed School of Engineering and School of Medicine recognize the importance and potential impact that this project will have on research, educational and economic development activities and is committed to ensure its success by providing a cost share of \$369,148/yr. Details of the project costs appear below.

**Senior Personnel.** No salary is requested for senior personnel.

**Other Personnel.** 50% salary support is requested for six new post-doctoral associate positions (\$120,000), 100% stipend support is requested for three new Ph.D. students (\$66,000) and salary is requested for three undergraduate summer interns (\$15,000) per year. These post-doctoral fellows and students will be involved in the creation of the computational models, collection and organization of the clinical data into the appropriate form, integration of the different data types from the multiple sources, perform the data analysis and interface between the clinicians and engineers in the development of the diagnosis matrix.

**Fringe Benefits.** A fringe benefit rate of 28.5% is used for the post-doctoral associates, 7.65% fringe benefit rate is used for the undergraduate interns and health insurance for the graduate students is \$2,642 per year per student. The total fringe benefits costs are \$43,274.

**Equipment.** No funds are requested for capital equipment.

**Travel.** No funds are requested for travel.

**Participant Support Costs.** No funds are requested for participant costs.

**Other Direct Costs.** Funds are requested for the purchase of 9 three terabyte external hard drives for data storage (\$1,665) and to purchase computers (\$4,061 + Speed School of Engineering Match, see details below) for each clinical partner to perform Big Data analysis in their respective laboratories. Total other direct costs are \$5,726.

**Indirect Costs.** No indirect costs are requested.

**Matching or Cost Share.** As a match, the Deans of the Speed School of Engineering and School of Medicine commit to providing more than the required one-to-one match (\$369,148/yr) compared to the amount requested from the university (\$250,000/yr). As a match, the Department of Bioengineering will commit support for one full-time, graduate teaching assistantship (stipend, out-of-state tuition & health insurance = \$60,671/yr); and, in-state tuition for a graduate student (\$17,496/yr). The Department of Computer Science and Engineering will commit support for one full-time, graduate fellowship (stipend, out-of-state tuition & health insurance = \$60,671/yr). The Speed School of Engineering Dean's Office (please see attached letter of support) will provide in-state tuition for one graduate student (\$17,496/yr) and support for the purchase of Big Data Analysis Computers (\$21,439). The Autism Center (please see attached letter of support) will be providing 50% salary and fringe support (\$25,700/yr) for a new post-doctoral fellow and out-of-state tuition for one PhD student per year. While the Departments of Cardiology, Cardiovascular Thoracic Surgery, and Ophthalmology and Visual Sciences will each provide 50% salary and fringe (\$25,700/yr) support for a new post-doctoral fellow and KY INBRE, in the Department of Anatomical Sciences & Neurobiology, will provide 50% salary and fringe support for two new post-doctoral fellows (\$51,400/yr).



## **Appendix IV: Letters of Support**

January 7, 2016

Dr. Neville Pinto  
Executive Vice President and University Provost  
University of Louisville  
Louisville, KY 40292

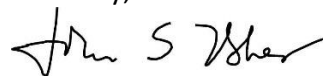
Dear Dr. Pinto,

I am writing in strong support of the enclosed proposal for the UofL 21<sup>st</sup> Century Initiative entitled: **Big Data Analysis in Medicine**. This request for funding is being submitted as a multidisciplinary collaboration between the J.B. Speed School of Engineering, and the School of Medicine to develop new computational models and implement new state-of-the-art machine learning approaches to analyze and integrate multiple data types for the creation of a decision matrix that aids clinicians in the early diagnosis of human diseases and disorders. The PIs on the grant (Drs. Keynton and El-Baz) and Co-PIs (Dr. Bolli, Dr. Cooper, Dr. Kaplan, Dr. Schaal, and Dr. Slaughter) form an extremely strong team of proven researchers. This group of biomedical engineers and clinicians have complimentary expertise and tremendous experience working in excellent biomedical research environments to ensure that this project is successful.

This project will serve to strengthen the existing partnerships between the Speed School of Engineering and the School of Medicine to create, validate and verify an innovative platform technology for propelling the University of Louisville to the forefront in becoming a nationally recognized leader in Big Data analysis. I feel strongly that this project can also lead to the development of a Big Data Center here at the University of Louisville, which is something I know will be needed for us to remain competitive in the future. And finally, because the core research team has such a distinguished and demonstrated track record of securing extramural funding from key governmental sponsors (NIH, NSF, NASA, DoD and VA), I feel strongly that this work will lead to the creation of multiple proposals for follow-on that will generate additional significant funding, (e.g., NIH T32 Pre-doctoral Training in Biomedical Big Data Science program, NIH R01 Biomedical Research Partnerships program or NSF Engineering Research Center programs.

In conclusion, I have tremendous confidence in this team's ability to get the work done and generate an outstanding return on the university's investment. Both Dean Ganzel and I are demonstrating our confidence through the cost sharing as outlined in the budget. I heartily endorse this proposal and will be happy to provide you with any additional information that you might need. Thank you.

Sincerely,



John Usher  
Acting Dean

January 13, 2016

Neville Pinto, Ph.D.  
Executive Vice President and University Provost  
University of Louisville  
Louisville, KY 40292

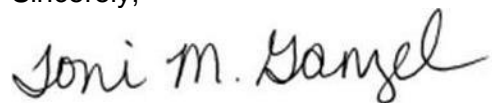
Dear Dr. Pinto:

On behalf of the School of Medicine, I offer my support for the University of Louisville 21<sup>st</sup> Century Initiative proposal "Big Data in Medicine". This proposed project represents a multidisciplinary approach to solving a major challenge in the field of medicine. Specifically, the data generated in the healthcare field continues to grow at an exponential rate, but our ability as clinicians to interpret and analyze the vast amounts of data remains a challenge. Development of new approaches for analyzing and integrating data collected from multiple sources and technologies will greatly aid our ability to more effectively and efficiently diagnose disease within patients. As a result, the proposed project not only addresses a global and societal need, it also directly relates to our 2020 Strategic Plan by helping with community engagement to enhance excellence in health care delivery and enhancing research computing capabilities.

This project creates a partnership between some of our strongest programs in the School of Medicine and the Speed School of Engineering with the demonstrated ability to translate research from the "bench-top to the bedside." The investigative team (Drs. Barnes, Bolli, Cooper, El-Baz, Kaplan, Keynton, Koenig, Schaal and Slaughter) consists of a select group of nationally and internationally recognized faculty with impressive track records for securing significant extramural funding, publishing in high quality impact factor journals and mentoring students at all levels. This project will train four new post-doctoral research associates, five Ph.D. level graduate students and 9 undergraduate students, which will lay the foundation for a highly competitive program in Big Data analysis. Thus, I am highly confident that this team will be successful in securing the necessary resources to sustain the program through extramural funding.

To demonstrate our support, the School of Medicine has committed 50% salary and fringe support for four new post-doctoral fellows, out-of-state tuition support for one Ph.D. student, and additional resources in our Bioinformatics core facility as committed by the Autism Center, KBRIN and the Departments of Cardiology, Cardiovascular & Thoracic Surgery and Ophthalmology & Visual Sciences. We fully endorse this application and feel that it will have a significant positive impact on the delivery of healthcare, our community and society. If you need any additional information, please do not hesitate to contact me.

Sincerely,



Toni M. Ganzel, M.D., M.B.A.

January 14<sup>th</sup>, 2016

Dear Drs. Robert Keynton and Ayman El-Baz,

I am delighted to write this letter in support of your University of Louisville 21<sup>st</sup> Century application entitled "Big Data Analyses in Medicine." The University of Louisville Autism Center is the single largest diagnostic and treatment center for Autism Spectrum Disorders in the State of Kentucky. Last year, we impacted some 4000 autism families. The ULAC is also the lead center for KAITTR (Kentucky Autism Initiative for Treatment, Training, and Research)- a consortium of 4 state universities (UL, UK, EKU, and WKU) dedicated to diagnostic and treatment services, training, and research of autism spectrum disorders in our state. The interest of your neurodevelopmental group is to **develop new computational models and implement new state-of-the-art machine learning approaches to analyze and integrate multiple data types for the creation of a decision matrix that aids clinicians in the early diagnosis of human diseases and disorders**. These interests precisely mirror our initial goals in the ASD precision medicine initiative to understand how genetic factors and other factors ultimately impact response to treatment.

The IRB entitled "***The University of Louisville Autism Center Precision Medicine Initiative***" holds as its central hypothesis that a personalized approach to treatment can be more effective than uncoordinated standard neurodevelopmental treatment. Autism spectrum disorder (ASD) is a neurobiologic disease characterized by communication, sensory and social deficits plus repetitive behaviors. Most geneticists agree that the etiology of ASD is 50% genetic and 50% environmental. Polymorphic allele variation in the ASD populations may cause the key variation in behavioral and neurological symptoms such as epilepsy and sleep disorders observed in these children and youth. For example, multiple candidate genes and genomic loci have been identified in ASD, suggesting the presence of complex inheritance patterns. A genetic mechanism to explain this complexity is the inheritance of multiple alleles in the heterozygous state within a given gene pathway. The impact on transcriptional regulation of autism gene networks, relationship to aberrant synaptogenesis and circuit formation, and clinical expression of ASD is not well characterized.

As a set of developmental disconnection syndromes, the local histogenetic events of axon guidance, dendritic development, synapse formation, and axon pruning in ASD have implicated autism candidate genes including the GABA<sub>A</sub> receptor  $\beta 3$  (GABRB3), UBE3A, TSC1/2, neuroligins, and MECP2. In fact, gene network regulatory connections have been suggested among UBE3A, GABRB3, and MECP2 and at least validated in the prefrontal cortex of the genetic human reference populations. Using systems biology, doctors can map actual genetically deleted pathways of a subject to multiple brain regions in order to understand how a set of genetically defined lesions may impact both the clinical endophenotypes observed, the defined developmental trajectories, and importantly the impact on a subject's response to treatment. As an example, our laboratory has mapped (using systems biology) the deleted genes from multiple ASD copy number variants in the TGF-beta signaling pathway. This pathway is expressed in multiple developing brain regions including the prefrontal cortex, orbital frontal cortex, hippocampus, mediodorsal thalamic nucleus, striatum, primary motor cortex, primary auditory cortex, and the amygdala. A subject with multiple deletions in this pathway may have deficits in social interactions, visual processing, attention to emotional stimuli, executive function, reward circuit difficulties, fear/anxiety, and eye contact. Thus, an individual with one pathway primarily affected may present with a set of distinct clinical phenotypes and response to treatments.

The IRB will recruit diverse state wide ASD and epilepsy populations of multiple locations and ages. Blood and urine samples plus other biospecimens, medical and developmental histories, electrophysiology (sleep and epilepsy), and clinical phenotyping (IQ, sensory, social scales, core autism symptoms, sleep, motor, adaptive scales, language) will be performed. Response to treatment modalities will also be characterized. The preliminary plan was to investigate the role of neurotrophin signaling in immune function by systems biology experiments using exome sequencing. As other biological factors clearly impact this and other signaling pathways, the additional collaboration of your neurodevelopmental group would provide great synergy and provide a very unique look at interactions of different factors which are likely among the key etiologies of autism spectrum disorders. An iterative process between the animal models and humans will be applied to identify factor responsive signaling pathways associated with clinical endophenotypes, define the mechanistic relationship among these genes, exposures and phenotypes, and identify new target genes in the models to be assessed in humans. Ultimately, this approach can be used to identify small molecule therapeutics/biomarkers to ameliorate clinical symptoms.

In terms of resources for this project, the ULAC will support this endeavor with resources of \$500,000 dollars over the timeline of the grant if it is funded. We would commit \$315K in funding to support the actual project itself including human, animal, and genomic research expenses of the project. The ULAC will also support with \$185K the following personnel: Out of state tuition- \$36K for one graduate PhD student per year; and ½ of a post-doctoral scholar salary and benefits at \$25,700.

We look forward to the successful funding of this proposal in the 21<sup>st</sup> Century Initiative. Additionally, the ULAC is truly excited about developing a collaborative research program in genetics, engineering, and ASD.

Please let me know if there are any questions related to our initiatives or this letter.

Best Regards,

A handwritten signature in cursive script that reads "Greg Barnes MD/PhD".

Greg Barnes MD/PhD

Spafford Ackerly Chair and Director, UL Autism Center

Associate Professor of Neurology and Pediatrics

Director, UL Autism Center

## **Appendix V: Samples for Accepted Publications**



# Studying Autism Spectrum Disorder with Structural and Diffusion Magnetic Resonance Imaging: A Survey

Marwa M. T. Ismail<sup>1</sup>, Robert S. Keynton<sup>1</sup>, Mahmoud M. M. O. Mostapha<sup>1</sup>, Ahmed H. ElTanboly<sup>1</sup>, Manuel F. Casanova<sup>2</sup>, Georgy L. Gimel'farb<sup>3</sup> and Ayman El-Baz<sup>1\*</sup>

<sup>1</sup> Biolmaging Laboratory, Department of Bioengineering, University of Louisville, Louisville, KY, USA, <sup>2</sup> Departments of Pediatrics and Biomedical Sciences, University of South Carolina, Columbia, SC, USA, <sup>3</sup> Department of Computer Science, University of Auckland, Auckland, New Zealand

## OPEN ACCESS

### Edited by:

Yong He,  
Beijing Normal University, China

### Reviewed by:

Dong-Hoon Lee,  
Johns Hopkins University School of  
Medicine, USA

Miao Cao,  
Beijing Normal University, China

### \*Correspondence:

Ayman El-Baz  
aselba01@louisville.edu

**Received:** 05 January 2016

**Accepted:** 25 April 2016

**Published:** 11 May 2016

### Citation:

Ismail MMT, Keynton RS, Mostapha MMO, ElTanboly AH, Casanova MF, Gimel'farb GL and El-Baz A (2016) Studying Autism Spectrum Disorder with Structural and Diffusion Magnetic Resonance Imaging: A Survey. *Front. Hum. Neurosci.* 10:211. doi: 10.3389/fnhum.2016.00211

Magnetic resonance imaging (MRI) modalities have emerged as powerful means that facilitate non-invasive clinical diagnostics of various diseases and abnormalities since their inception in the 1980s. Multiple MRI modalities, such as different types of the sMRI and DTI, have been employed to investigate facets of ASD in order to better understand this complex syndrome. This paper reviews recent applications of structural magnetic resonance imaging (sMRI) and diffusion tensor imaging (DTI), to study autism spectrum disorder (ASD). Main reported findings are sometimes contradictory due to different age ranges, hardware protocols, population types, numbers of participants, and image analysis parameters. The primary anatomical structures, such as amygdalae, cerebrum, and cerebellum, associated with clinical-pathological correlates of ASD are highlighted through successive life stages, from infancy to adulthood. This survey demonstrates the absence of consistent pathology in the brains of autistic children and lack of research investigations in patients under 2 years of age in the literature. The known publications also emphasize advances in data acquisition and analysis, as well as significance of multimodal approaches that combine resting-state, task-evoked, and sMRI measures. Initial results obtained with the sMRI and DTI show good promise toward the early and non-invasive ASD diagnostics.

**Keywords:** autism, structural MRI, diffusion tensor MRI, multi-modal approaches, life stages

## 1. INTRODUCTION

The term “autism spectrum disorder” (ASD) refers to a collection of neuro-developmental disorders that affect linguistic, behavioral, and social skills. Autism has many symptoms, most prominently, social impairment and repetitive behaviors. The most severe form of the ASDs is autistic disorder (AD), while milder forms include Asperger syndrome (ASP), childhood disintegrative disorder, and not-otherwise-specified pervasive developmental disorder (NPDD). By some estimates, the ASD affects 1 out of 68 eight years of age, with males being four times more likely to develop it than females. About 30% of children with ASD have epilepsy at later stages NIMH (2015). Autism is typically diagnosed at the age of 3; however, some characteristics can sometimes be observed at around 12 months of age. What causes autism is yet unknown;

however, it is mainly believed that genetic and environmental factors in complex combinations are responsible NIMH (2015).

After the advent in the nineteen eighties, MRI soon became one of the most promising non-invasive modalities for visualization and diagnostics of ASD-related abnormalities. Along with its main advantage of no exposure to radiation, high contrast and spatial resolution, the recent advances to MRI modalities have notably increased diagnostic certainty. The modalities, being most helpful for studying ASD, include structural MRI (sMRI; Damasio and Maurer, 1978; Bauman and Kemper, 1985; Gaffney et al., 1987a,b; Courchesne et al., 1988; Gaffney et al., 1988; Horwitz et al., 1988; Minshew and Payton, 1988; Ritvo and Garber, 1988; Gaffney et al., 1989; Garber et al., 1989; Murakami et al., 1989), and diffusion tensor imaging (DTI; Gropman et al., 2010; Mori and Tournier, 2013).

In applications to ASD, sMRI helps in investigating structural brain changes in autistic subjects. Many scan sequences of the sMRI are volumetric, i.e., allow for measuring specific brain structures to calculate tissue volumes. In spite of diagnostic abilities found for the sMRI, the earlier published results obtained for a limited number of subjects were often contradictory. Specific pulse sequences employed in the sMRI help to reveal different properties of normal and abnormal brain tissues. Modifying the pulse sequence parameters, such as repetition time (TR) and echo time (TE), may emphasize the contrast between gray matter (GM) and white matter (WM), e.g., in the T1-weighted sMRI with short TR and TE, or brain tissue and cerebrospinal fluid (CSF), e.g., in the T2-weighted sMRI with long TR and TE.

The recent DTI characterizes three-dimensional (3D) diffusion of water molecules in a biological tissue Basser et al. (1994a,b). The DTI has a wide range of clinical applications. In particular, it is used to examine normative white matter (WM) development, neurodevelopmental disorders, and neurodegenerative disorders, e.g., autism, and amyotrophic lateral sclerosis Dong et al. (2004).

In neurological studies, where each patient's status can be assessed, the chosen imaging modality should be able to clearly demonstrate the abnormalities. The conventional MRI lacks sensitivity in distinguishing the abnormalities on an individual-subject basis Mori and Tournier (2013), whereas the DTI has the potential to reveal such abnormalities. This new information comes from better image contrast, more detailed WM morphology, refined anatomical locations, and more accurate connectivity analysis Mori and Tournier (2013). Additional DTI offers many contrast-related measurements, including the widely used fractional anisotropy (FA) and estimates of shapes and sizes of specific WM tracts, i.e., WM morphology Mori and Tournier (2013). Moreover, DTI provides superior anatomical information for clearer identification of areas with WM abnormalities Gropman et al. (2010). It also provides unique brain connectivity measurements via 3D fiber reconstruction, e.g., tractography, Basser et al. (2000).

This survey presents applications of the sMRI and DTI to study the ASD (mostly, for the last two decades) in order to outline the most important findings with these modalities across all life stages. This provides a comprehensive study unlike the

recent surveys that either focus on one modality, Palmen and van Engeland (2004); Blackmon (2015); Conti et al. (2015); Rane et al. (2015), or address a specific life stage, Conti et al. (2015); Zeglam et al. (2015). Moreover, this survey highlights the methodologies conducted in each study and categorizes them with respect to the approach (e.g., whether they are volumetric-based, or surface-based in sMRI), and user's intervention (manual, automated, semi-automated).

The survey is structured as follows: Sections 2, 3 below address the use of the sMRI and DTI, respectively. Findings in the reviewed publications emphasize benefits for studies of the ASD, as well as other medical abnormalities, by acquiring and analyzing complementary multi-modality data.

## 2. STUDYING ASD WITH SMRI

The earlier findings of the 1980s–1990s Damasio and Maurer (1978); Bauman and Kemper (1985); Gaffney et al. (1987a,b); Courchesne et al. (1988); Gaffney et al. (1988); Horwitz et al. (1988); Minshew and Payton (1988); Ritvo and Garber (1988); Gaffney et al. (1989); Garber et al. (1989); Murakami et al. (1989); Nowell et al. (1990); Hsu et al. (1991); Zola-Morgan et al. (1991); Garber and Ritvo (1992); George et al. (1992); Hashimoto et al. (1992, 1993); Holtum et al. (1992); Kleiman et al. (1992); Piven et al. (1992); Bailey et al. (1993); Courchesne et al. (1993, 1994a,b); Adolphs et al. (1994); Bachevalier (1994); Bauman and Kemper (1994); Minshew and Dombrowski (1994); Egaas et al. (1995); Hashimoto et al. (1995); Piven et al. (1995); Saitoh et al. (1995); Zilbovicius et al. (1995); Schaefer et al. (1996); Giedd et al. (1996); Piven et al. (1996); Siegel et al. (1996); Ciesielski et al. (1997); Elia et al. (1997); Lainhart et al. (1997); Piven et al. (1997); Bailey et al. (1998); Dawson et al. (1998); Piven et al. (1998); Abell et al. (1999); Aylward et al. (1999); Courchesne et al. (1999); Fombonne et al. (1999); Gillberg (1999); Levitt et al. (1999); Manes et al. (1999); Sears et al. (1999); Townsend et al. (1999) have many contradictions. However, the much better spatial resolution and contrast of the recent advanced MRI technology made the recent findings of the 2000s–2010s more consistent Brambilla et al. (2003); Stanfield et al. (2008); Chen et al. (2011). This survey focuses on the latter studies and attempts to classify the reported abnormalities at different life stages for each of the autism-related anatomical structures.

Cross-sectional or longitudinal sMRI scans, collected at different time instants for the same individual, are studied by either region-of-interest (ROI) based volumetry, or surface-based morphometry (abbreviated as RBV, and SBM respectively). The **RBV** usually focuses on the total volume or area measures for a chosen region, but requires manual intervention by experts to delineate it. This age-sensitive and time consuming process depends on level of automation, yet is powerful in a statistical sense. A method that is correlated to RBV and is known as voxel-based morphometry, **VBM**, targets tissue density, e.g., relative GM concentration, or volume, e.g., regional volume differences of a certain tissue. The **SBM** addresses topological shape features, like surface curvature and folding degree, that cannot be obtained directly using the RBV on a brain sMRI. The SBM is applied



mostly to the cerebral cortex, along with its lobes and gyrification patterns.

The ASD studies with the sMRI, including data processing tools and main abnormalities found in brain structures are considered below. Abnormalities found in the cerebral cortex; posterior fossa (vermis, brain stem, and cerebellum); corpus callosum; amygdalae; hippocampus, and thalamus, are addressed at four main life stages: infancy (0–2 years); childhood (3–11 years); adolescence (12–18 years), and adulthood (above 18 years). The measurements include also the total brain volume and head circumference.

## 2.1. Studying ASD Impacts on Anatomical Structures with sMRI

### 2.1.1. Cerebral Cortex

This uppermost brain layer that plays a leading role in human intelligence and perception has been the focus of plenty of sMRI studies on ASD. Changes of cortical thickness and gyrification patterns were analyzed with the SBM, whereas the RBV and VBM measured regional differences in volumes and densities of the cerebral GM and WM.

#### 2.1.1.1. Infancy

According to the longitudinal VBM Hazlett et al. (2005) on 51 autistic children and 25 controls (aged 18–35 months), both the cerebral GM and WM volumes increase in autistic brains. The longitudinal RBV on children aged 1.5 to 5 years Schumann et al. (2010) revealed no changes in the occipital lobe. On the other hand, the cerebral GM volumes were significantly enlarged in the frontal, temporal, and parietal lobes, and in the cingulate gyrus (located in the limbic lobe) of autistic toddlers (aged about 2.5 years). Additionally, there were more abnormal growth profiles for females. The RBV in Hazlett et al. (2012) monitored the total brain volume changes for children aged 6 months to compare high risk infants to low risk ones with no autistic family members. The fact that cerebrum or lateral ventricle volumes had no significant difference for both groups confirmed earlier findings that the brain enlargement is a postnatal event, occurring around 12 months of age. Another extended longitudinal study Shen et al. (2013) pursued the goal of identifying 6–9-month-old infants who might later develop the ASD. It was revealed that the ASD causes an extra-axial fluid and is characterized by excessive CSF over the frontal lobes at 6–9 months of age, which persists at 12–15 and 18–24 months. This leads to large total cerebral volumes that tend to increase with age at a higher rate in males, than females. This finding contradicts the earlier one Schumann et al. (2010), which showed more enlargement in females. This inconsistency might be caused by manual segmentation, along with the younger ages and the 20% smaller number of participants in Shen et al. (2013).

#### 2.1.1.2. Childhood

Volumetric, voxel-wise, and thickness changes in the cerebral cortex in children with autism have been extensively studied in the literature. In particular, the autistic children aged 2–3 years had 18% and 12% larger cerebral cortical WM and GM volumes, respectively, than the control ones, while the older children did

not demonstrate such enlargement Courchesne et al. (2001). The increased frontal and temporal GM and frontal and parietal WM volumes at such a young age (2–4 years) was confirmed in Carper et al. (2002). The increased cerebral volumes in autistic children aged around 4 years and 6 years were found also in Sparks et al. (2002) and Akshoomoff et al. (2004), respectively. The latter study reported the increased total cerebral volume, as well as the increased WM and GM volumes for children with both low-functioning autism (LFA) and high-functioning autism (HFA), the total cerebral volume being significantly larger in the LFA group.

The VBM of the GM and WM densities on autistic children around 9 years of age Boddaert et al. (2004) has found a significant decrease in the GM density in the superior temporal sulcus and a decrease in the WM density in the right temporal pole. This finding was supported by McAlonan et al. (2005) where the GM density was found to significantly decrease in the frontostriatal and parietal networks, as well as in the ventral and superior temporal gyrus in autistic children aged around 12 years. The RBV revealed the decreased GM volume in the right lateral orbitofrontal cortex in 10-year-old boys in Girgis et al. (2007) and the decreased GM volumes in the parietal, left temporal, and left occipital lobes bilaterally in Brun et al. (2009). The left and right frontal lobes of the autistic boys had enlarged 3.6 and 5.1%, respectively, while all the other lobes grew more significantly.

The cerebral cortices of children with autism were often studied with the SBM as well. The atlas-based SBM in Hardan et al. (2006b) monitored the cortical thickness changes in autistic brains of children aged 10 years. The frontal or occipital lobes did not change, whereas the temporal and parietal lobes had most prominent increases of the total cerebral sulcal and gyral thicknesses. According to the subsequent longitudinal SBM Hardan et al. (2009) on 10-year old autistic children, with a follow-up scan 2 years later, the cortical thickness in autistic subjects has decreased in the frontal, temporal, and occipital lobes, comparing to controls. Also, the SBM Jiao et al. (2010) on 9-year-old children with autism showed the decreased thickness in the right entorhinal, right lateral orbitofrontal, left lateral orbitofrontal, right medial orbitofrontal, left medial orbitofrontal cortex, and right pars triangularis. However, the thickness also increased in the left caudal anterior cingulate cortex and left frontal pole. Significant bilateral differences in sulcal depth in restricted portions of the anterior-insula, frontal-operculum, and in tempoparietal junction, were found in Dierker et al. (2015). The study by Gori et al. (2015) on 4-year-old males was based on extracting features from GM, WM, and CSF to classify autistic and control brains. Only GM features in different subregions showed a classification performance that reached up to 80%.

#### 2.1.1.3. Adolescence

Volumetric and voxel-wise cerebral changes have been investigated in a number of publications. The VBM in Waiter et al. (2004), for example, revealed the increased GM volume in the cortical lobes of 15-year-old autistic males, namely, in the right fusiform gyrus, right temporal and occipital region, and left frontal pole. This work was extended in Waiter et al. (2005) to investigate changes of the WM volume in 15-year-old autistic

males and found that the WM volume decreases at the left middle temporal, right middle frontal, and left superior frontal gyri. The VBM in Kwon et al. (2004) conducted on subjects with the HFA and ASP showed the lower cortical GM density in the right inferior temporal gyrus, entorhinal cortex, and right rostral tip of fusiform gyrus. The RBV in Lotspeich et al. (2004) reported a growth of the cerebral GM in both the HFA and LFA subjects, compared to the controls, but only non-significant changes for people with the ASP. The VBM in Chung et al. (2004) on 16-year-old males revealed the lesser WM concentration in the genu, rostrum, and splenium regions in autistic brains, whereas the RBV in Hazlett et al. (2006) on a group of young adolescents has found a larger total cerebral volume of the autistic brains. The lobe volume growth due to the GM volume enlargement was also noticed in the frontal and temporal, but not parietal or occipital lobes. The VBM on autistic and control males around the age of 13 in Bonilha et al. (2008) has found an increase in the GM volume in the parietal lobes, medial and dorsolateral frontal areas, and lateral and medial parts of temporal lobes, as well as a decrease in the WM volume in the frontal, parietal, temporal, and occipital lobes. The longitudinal RBV on 13-year-old adolescents in Hua et al. (2013) has found a decelerated WM growth in the frontal, temporal, parietal, and occipital lobes, together with an abnormally accelerated GM expansion in the putamen and anterior cingulate cortex.

To monitor cortical changes in the adolescent groups due to autism, the SBM on a group of 12-year-old autistic and control adolescents was used in Hardan et al. (2004) to measure changes in the cerebral folding and better investigate the gyrification patterns. As was found, the adolescents had the higher left frontal gyrification index, than the adults, as well as the cortical folding had decreased bilaterally with age in all the autistic subjects, but not in the controls. The SBM on a wide variety of patients including the LFA, HFA, and ASP subjects aged 11–13 years in Nordahl et al. (2007) has found for the LFA subjects prominent shape abnormalities centered on pars opercularis of the inferior frontal gyrus, associated with sulcal depth differences in the anterior insula and frontal operculum. The bilateral shape abnormalities in the HFA group were similar to those of the LFA group, but smaller in size and centered more posteriorly in and near the parietal operculum and ventral postcentral gyrus. The ASP group had the correlated with age bilateral abnormalities in the intraparietal sulcus. All these cortical shape abnormalities were more pronounced in the children than in the adolescents. Two successive longitudinal studies on the same group of subjects when their mean age was 17.4 and 19 years, respectively, in Wallace et al. (2015) demonstrated an accelerated cortical thinning in the autistic brains with respect to the controls in two areas in the left hemisphere, namely, in the posterior portion of the ventral temporal cortex and the superior parietal cortex. This acceleration has happened only for the older adolescents and young adults of the second study.

#### 2.1.1.4. Adulthood

The RBV on 16 autistic males of the average age of 22 years in Hardan et al. (2001b) revealed the larger mean cerebral and third ventricle volumes in the autistic subjects rather than in the

controls. The VBM in Rojas et al. (2006) gave the larger GM volume in the medial frontal gyri, left precentral gyrus, right postcentral gyrus, and right fusiform gyrus. The more recent VBM Toal et al. (2010) showed the decreased GM volume in the medial, temporal, and fusiform regions. The SBM in Hardan et al. (2004) explored changes of the cerebral folding in 27-year-old males. While the left frontal gyrification index had no changes, the cortical folding decreased in autistic adults, compared to children and adolescents. The SBM in Hadjikhani et al. (2006) on the autistic, ASP, and NPDD subjects aged around 33 years has shown the decreased thickness in the inferior frontal gyrus, pars opercularis, inferior parietal lobule, superior temporal sulcus, precentral and postcentral gyrus, inferior occipital gyrus, prefrontal cortex, anterior cingulate, medial parietal cortex, supramarginal gyrus, and middle and inferior temporal cortex. The SBM in Hyde et al. (2010) on 15 autistic 22.7-year-old (on average) males has shown that the thickness increases in the frontal, temporal, occipital, cingulate, and parietal gyrus, as well as in the fusiform gyri, but decreases in the pre- and post-central gyri and para-central gyrus.

### Conclusions

According to the above studies, the cerebral cortex starts changing in the autistic brains at the age of around 12 months, and no significant differences could be monitored earlier, except of the recent findings in Shen et al. (2013). The cerebrum changes of an autistic brain at such an early age include the age-proportional enlargements of the lobes and increases of the cortical WM and GM. The growing cerebral volume, including the GM and WM, in early childhood indicates simultaneously the decreasing GM and WM density. Also, children with autism demonstrate significant changes in the cortical thickness. These volumetric and thickness differences continue to increase at the later stages of life.

#### 2.1.2. Posterior Cranial Fossa (Cerebellum, Vermis, and Brain Stem)

Posterior cranial fossa has also been investigated in the literature for any correlates with ASD at different life stages.

##### 2.1.2.1. Childhood

Area measurements on 22 autistic children in Elia et al. (2000) showed no abnormalities in the total vermis, vermis lobules VI–VII, pons, and midbrain, which could be related to autism. However, the decreased WM density in the cerebellum of children with autism was reported in McAlonan et al. (2005) and Boddaert et al. (2004), and the larger by 39% cerebellar WM volume was found in Courchesne et al. (2001) for 2–3-year-old children with autism compared to controls. Autistic boys had the lesser GM and smaller GM-to-WM ratios and vermian lobules than the normal ones. The reduced cross-sectional areas of the vermis lobules VI–VII in autistic children were also reported in Courchesne et al. (2001), Kaufmann et al. (2003), and Carper and Courchesne (2000). The larger cerebellar WM and GM volumes and increased area of the anterior and posterior cerebellar vermis were found in the 6-year-old children with the LFA, HFA, and NPDD in Akshoomoff et al. (2004).

Multiple brain stem volume studies gave contradicting conclusions. The early areal measurements in Gaffney et al. (1988) and Ciesielski et al. (1997) claimed reduced brain stem size, whereas the subsequent works, such as Garber and Ritvo (1992), Piven et al. (1992), Kleiman et al. (1992), Hsu et al. (1991), and Elia et al. (2000) found no significant differences between the autistic and control groups. No differences in the brain stem volumes for these groups were found also in Hardan et al. (2001a) and Herbert et al. (2003). However, the recent study Jou et al. (2013) of 10-year-old children, with a follow-up after 2 years, came up with different findings: the brain stem volume was stable in the controls over the 2-year period, but the increased GM volume of an autistic brain implied the larger entire brain stem volume, so that the autistic brain volumes eventually became comparable to those of the 15-year old controls.

### 2.1.2.2. Adolescence and adulthood

An increase in the GM volume in the cerebellum in Bonilha et al. (2008) is consistent with the studies of children. The cerebellar volumes of autistic children and adolescents are also consistent with those of adults. As shown in Hardan et al. (2001a) on 22-year-old subjects, the total cerebellar volume and cerebellar hemispheres are larger in the autistic group both with and without correction by the total brain volume. But the volumetric and area measurements of the vermis and brain stem did not differ significantly between the autistic and control groups. Also, the lower GM density in the frontostriatal and cerebellar regions, along with the widespread WM differences, had been reported in McAlonan et al. (2002) and the lower brain stem and total brain stem GM volumes in the autistic adults have been found in Jou et al. (2009).

### Conclusions

The posterior fossa structures are significantly affected with the ASD from an early age of 2 years and during all the subsequent life stages. Some inconsistencies in the brain stem abnormalities found might be caused by wide age and gender differences of the participants.

### 2.1.3. Amygdalae

Amygdalae have also been investigated in efforts to find any correlates with the ASD.

#### 2.1.3.1. Infancy

To our knowledge, the amygdalar changes in the infancy period are not studied yet, and the youngest subjects in such studies are around 3 years old.

#### 2.1.3.2. Childhood

The RBV on 29 autistic and 26 control subjects (the average age of 3.9 years) in Sparks et al. (2002) has shown that in the autistic subjects the amygdalae are enlarged proportionally to the overall increase of the entire cerebral volume. The more recent volumetry Munson et al. (2006) on a larger group of the 45 autistic subjects suggested the enlargement of only the right amygdalar volume at the ages of 3–4 years. The longitudinal RBV in Nordahl et al. (2012), which was performed in order to precisely define the age at which the amygdalae begin to enlarge,

started with the 85 autistic subjects aged 37 months on average, and had the follow-up scan 1 year later on 45 of these autistic subjects. That enlarging the amygdalar volume was found in both the cases, although with a higher rate for the latter group, confirms that this enlargement is present at such an early age of around 3 years. The volumetry on an older population (7.5–12.5 years) in Schumann et al. (2004) demonstrated that both the right and left amygdalae volumes were enlarged. However, the longitudinal RBV in Barnea-Goraly et al. (2014), which involved 15 autistic subjects aged 10.6 years on average and their follow-up scan after reaching adolescence, has found no significant difference between the left, right, or total amygdalar volumes for the autistic and control subjects. This contradiction to all other studies might be caused by the relatively small population used.

#### 2.1.3.3. Adolescence

No significant difference in left, right, or total amygdalae volumes in the adolescents was found in various studies, e.g., Schumann et al. (2004) and Barnea-Goraly et al. (2014).

#### 2.1.3.4. Adulthood

The RBV in Rojas et al. (2004) explored the hypothesis that parents of autistic children would show similar structural changes. This study was conducted in part on the amygdalar volumes of 15 autistic subjects (the average age of 30.3 years), 17 controls (the average age of 43.6 years), and 17 parents of autistic children. The amygdalae were smaller in the autistic group than in the other two groups.

### Conclusions

The amygdalar volumes generally increase in autistic brains at early stage of life, with the rate of increase being proportional to the age (the known studies started from the 3-year-old subjects). By adolescence, no significant differences in this structure could be found. However, at the subsequent life stages its volume decreases in autistic brains.

### 2.1.4. Hippocampus

Hippocampus also proved to have some correlates with the ASD from a young age.

#### 2.1.4.1. Infancy

Similarly to Section 2.1.3 above, no hippocampal changes have been explored at this period, with the youngest subjects age having been around 2.5–3 years.

#### 2.1.4.2. Childhood

The enlarged hippocampus was found in autistic children at the ages of both 3–4 Sparks et al. (2002) and 7.5–12.5 years Schumann et al. (2004), especially at the HFA group in the latter study. The enlargement only in the right hippocampus in children aged around 10 years was reported in Barnea-Goraly et al. (2014). The earlier study Saitoh et al. (2001) suggested that the area dentata in autistic subjects was significantly smaller than in the normal ones, with the largest deviation at the ages from 29 months to 4 years.

#### 2.1.4.3. Adolescence

The hippocampus was found enlarged in autistic subjects in Schumann et al. (2004); however, this finding differs from the more recent results in Barnea-Goraly et al. (2014), where the right hippocampal volume has increased in the autistic children, but not in the adolescents. In the latter case, it was found that differences between hippocampal volumes in autistic and control brains became insignificant with time.

#### 2.1.4.4. Adulthood

The hippocampus of autistic adults was confirmed to be significantly enlarged Rojas et al. (2004), compared to controls and also to parents of autistic children. The left hippocampus was larger in both the parents of autistic children and the adults with autism, compared to the controls. The VBM in Rojas et al. (2006) has shown an increase in the GM volume of the left hippocampus.

#### Conclusion

In autism, the hippocampus is enlarged at all ages.

#### 2.1.5. Corpus Callosum

Corpus callosum is found to be correlated with the ASD. In particular, the two successive longitudinal RBV studies Frazier et al. (2012) on 19 subjects with autism and 4 subjects with NPDD (first, at the age of 10.6 years and then 13.1 years on average) have found persistent reductions in the total corpus callosum volumes in the autistic subjects compared to the healthy controls. Only the size of rostral body subdivision has normalized over time. The centerline length of the corpus callosum was significantly reduced in young adults with autism compared to controls Elnakib et al. (2011).

##### 2.1.5.1. Conclusion

The corpus callosum is reduced in size in the ASD.

#### 2.1.6. Thalamus, Caudate, and Putamen

The GM volume decreases in the right thalamus of adolescent males with autism and the thalamic volume decreases in adults with autism compared to controls, as was found, respectively, in Waiter et al. (2004) and Tsatsanis et al. (2003). However, no volume differences of the basal ganglia, caudate, or putamen at all ages have been found in Hardan et al. (2003). The more recent RBV by the same research group Hardan et al. (2006a) found no differences in both the right and left thalamic nuclei between the 19-year-old, on average, control and autistic groups. Studying the older adults (aged 28 years on average) showed that the right caudate nucleus has a larger volume in the autistic brain Haznedar et al. (2006).

#### 2.1.7. Total Brain Volume and Head Circumference

Changes in the total brain volume and head circumference have been associated with the ASD in several publications.

##### 2.1.7.1. Infancy

As shown in Hazlett et al. (2005) for 18–35 month-old infants, the total brain volume increases in the group with autism and their normal at birth head circumference becomes significantly larger around 12 months of age compared to the healthy group.

This finding was confirmed in Hazlett et al. (2012), showing no significant difference in the head circumference at 6 months of age in infants with high risk of autism.

##### 2.1.7.2. Childhood

The head circumference grows also in children with autism. The increased brain volume and head circumference in a large group of 10-year-old children with autism have been confirmed in Aylward et al. (2002) and supported in other studies, e.g., in Herbert et al. (2003) on 9-year-old autistic males and in Carper et al. (2002). However, a more recent publication Hardan et al. (2006b) reported insignificant increases in the total brain volumes for children with autism (this contradiction to the above findings might be due to a small number of participants). The later stages of life show no difference between the autistic and neurotypical groups in the total brain volumes, probably because the growth rate of the normal brains increases at these stages.

### 2.2. Summary

Tables 1–4 summarize, in accordance with the life stage, basic current results of studying the ASD with the sMRI.

## 3. STUDYING ASD WITH DTI

DTI characterizes 3D diffusion of water molecules in a biological tissue with DT Basser et al. (1994a,b). The DTI is widely used in clinical applications, e.g., to examine a normative WM development, neurodevelopmental disorders, like ASD, and neurodegenerative disorders, such as amyotrophic lateral sclerosis Dong et al. (2004). For completeness, basic principles of the DTI are reviewed first below.

### 3.1. DTI: Basic Concepts

An unconstrained medium, such as the CSF, ensures the isotropic diffusion where the water molecules move in a similar manner in all directions. The isotropic diffusion is typical, e.g., for the brain ventricles, whereas the molecular diffusion in the WM is constrained by spatial orientations of the WM tracts. The molecules can diffuse along a fiber track more freely than across it, so that the diffusion becomes anisotropic with a privileged direction. As a result, water diffusion patterns for the brain tissues provide information about the underlying anatomical structures Mori and Tournier (2013).

Generally, a fiber is oriented arbitrarily and has different diffusion coefficients along different directions.

DT is usually specified with certain parameters at each voxel, that are usually converted into maps of scalar diffusion measurements to facilitate interpreting the voxel-wise DTI data. The most common anisotropy and microstructural measurements include fractional (FA) and relative (RA) anisotropy together with mean (MD), axial ( $\lambda_{\parallel}$ ), and radial ( $\lambda_{\perp}$ ) diffusivity.

The orientation-independent **mean diffusivity**, also called the *trace*, measures an overall diffusion in a voxel or region. A slightly different MD definition has been used to measure the diffusion descent in brain ischemia van Gelderen et al. (1994). Since the MD values in the CSF are higher than it is in other types of



TABLE 1 | sMRI-based studying of the ASD at infancy.

Rf	Autistic group			Control group			sMRI	Brain regions	Data analysis	Findings
	Age, mo	IQ	Size	Age, mo	IQ	Size				
Hazlett et al., 2005	18–35	45–63	46 m; 5 f	18–35	89–127 TD; 49–68 DD	10 m, 4 f TD; 6 m, 5 f DD	1.5T; 1.5 mm	Cerebral GM, WM; cerebellar GM, WM	RBV; NLMM; BRAINS2 + EMS to segment tissues	Increase in cerebral and no change in cerebellar GM and WM volumes at 24 mo of age
Schumann et al., 2010	22–67 m; 26–58 f	FSIQ: 39–75 m; 34–80 f	32 m; 9 f	12–63 m; 12–61 f	FSIQ: 95–127 m; 101–131 f	32 m; 12 f	1.5 T; 1.5 mm	Cerebral GM, WM	RBV; SPSS14.0; SPSS16.0; ANCOVA + semi-automatic GWseg segmentation	Significant enlargement in cerebral WM and GM; notably, in frontal, temporal, and cingulate cortices by 30 mo of age (more abnormal growth of f than m)
Hazlett et al., 2012	6–7	–	61 m; 37 f	6–7	–	21 m; 15 f	3 T; 1 mm	Cerebrum, cerebellum	RBV; ITK-SNAP; GLM + AutoSeg, ANOVA; HeadCirc	No significant difference for HC; cerebral cortex, cerebellum, or lateral ventricle volumes; unchanged TBV
Shen et al., 2013	6–9 t1; 13–14 t2; 19–21 t3	–	22 m; 11 f	6–10 t1; 14–15 t2; 21–22 t3	–	15 m; 7 f	3 T; 1 mm	Cerebrum	RBV; LMM; manual segmentation + LS	Excessive CSF over frontal lobes at ages 6–9 mo; large total cerebral volumes at 12–15 mo, 18–24 mo, with higher rate of enlargement in m than f

Additional abbreviations: f, females; m, males; mo, month; Rf, reference;  
T, MRI magnetic field strength (tesla); GLM, general linear models; HC, head circumference;  
ANOVA, analysis of variances; ANCOVA, analysis of covariances; DD, developmental delay;  
LMM, linear mixed models; LS, longitudinal segmentation; t1, t2, t3, time periods during longitudinal studies;  
NLMM, non-linear mixed models; TBV, total brain volume; TD, typical development;  
AutoSeg, BRAINS2, EMS, GWseg, ITK-SNAP, HeadCirc, SPSS14.0, SPSS16.0, data processing packages.

TABLE 2 | sMRI-based studying of the ASD at childhood.

Rf	Autistic group			Control group			sMRI	Brain regions	Data analysis	Findings
	Age, y	IQ	Size	Age, y	IQ	Size				
Elia et al., 2000	5–17	<70	22 m	5–15	VIQ: 86–132	11 m	0.5 T; 5 mm	Midsagittal area of cerebrum corpus callosum, midbrain cerebellar vermis and vermis lobules	Area measurements; t-test; regression analysis	Negative correlation between midsagittal cerebrum area and age in patients with AD; no abnormalities in total vermis, vermis lobules VI–VII, pons, midbrain, and cerebrum areas; no anatomical abnormalities in brain stem
Carper and Courchesne, 2000	4–7	57–102	42 m	4–8	102–126	29 m	1.5 T; 3–4 mm	Vermis lobules, cerebellum frontal lobes	Area measurements; RBV; SEGMENT	Reduced vermis lobules VI–VII areas; no abnormalities in frontal lobe volumes; inverse correlation between lobules areas and frontal cortex volumes
Courchesne et al., 2001	2–16	36–122	60 m	2–16	90–140	52 m	1.5 T; 3–4 mm	Vermis, cerebellum	Area measurements; RBV; SPSS	Larger cerebellar WM and brain volumes in 2–4-y-old autistic patients; reduced vermis lobules VI–VII cross-sectional areas
Saitoh et al., 2001	2–42	VIQ: 41–135	52 m; 7 f	2–43	VIQ: 88–150	40 m; 11 f	1.5 T; 5 mm	Hippocampus area dentata and combined area of subiculum	Area measurements; ANOVA; tracing anatomical landmarks	Significantly smaller than normal area dentata in AD subjects; the largest deviation from normal in 29 mo–4 y
Carper et al., 2002	4–8	>70 in 26 m	38 m	2–12	>80	39 m	1.5 T; 3 mm	WM and GM volumes	RBV; SPSS	Increased frontal and parietal WM and frontal and temporal GM volumes in 2–4 y-old AD subjects
Aylward et al., 2002	9–29	87–118	58 m; 9 f	9–29	95–120	76 m; 7 f	1.5 T; 1.5 mm	TBV; HC	RBV; MEASURE	Increased TBV and HC in 8–12 y-old AD subjects
Sparks et al., 2002	AD: 3–5; NPDD: 4–5	<80	AD: 26 m; 3 f, NPDD: 12 m; 4 f	TD: 3–6, DD: 3–6	Normal	TD: 18 m; 8 f, DD: 6 m; 8 f	1.5 T; 1.5–2 mm	Cerebrum, cerebellum, amygdala, hippocampus	RBV; SPSS; ANCOVA	Increased TBV and enlarged amygdala, cerebellar volume, and hippocampus in AD subjects
Kaufmann et al., 2003	5–9	52–81	10 m	6–10	112–130	22 m	1.5 T; 3 mm	Cerebellar vermis: anterior vermis lobules I–V, posterior superior vermis VI–VII, posterior inferior vermis VIII–X	Area measurements; manual segmentation; BrainImage	Reduced in volume vermis lobules VI–VII

(Continued)

TABLE 2 | Continued

Rf	Autistic group			Control group			sMRI	Brain regions	Data analysis	Findings
	Age, y	IQ	Size	Age, y	IQ	Size				
Boddaert et al., 2004	7–15	21–64	16 m; 5 f	7–15	–	7 m; 5 f	1.5 T; 1.2 mm	GM, WM regional density	VBA; ANCOVA; SPM99	Significantly decreased GM concentration in temporal sulcus; decreased WM concentration in right temporal pole and cerebellum
Schumann et al., 2004	LFA: 56, 9–16, HFA: 91, ASP: 106 LFA: 56, 9–16, HFA: 91, ASP: 106	LFA: 56, HFA: 91, ASP: 106	LFA: 19 m, HFA: 27 m, ASP: 25 m	10–16	104–126	27 m	1.5 T; 1.5 mm	Amygdala, hippocampus	RBV; SPSS; ANOVA; BrainImage5.x	7.5–12.5 y: larger right and left amygdala volumes, enlarged hippocampus, no change in cerebral volume; 12.75–18.5 y: no change in amygdala
Hardan et al., 2004	13–15	89–121	12 m	11–15	97–123	13 m	1.5 T; 1.5 mm	Cerebral folding (gyrification patterns)	SBM; BRAINS2	Higher left frontal gyrification index in children and adolescents, but not adults; decreased bilaterally with age cortical folding in all AD subjects, but not in controls
Akshoomoff et al., 2004	LFA: 5–8, HFA: 4–10, NPDD: 5–8	LFA: 26–63, HFA: 73–85, NPDD: 72–101	LFA: 30 m, HFA: 12 m, NPDD: 10 m	2–5	86–132	15 m	1.5 T; 3 mm	TBV; GM, WM volumes of cerebrum, cerebellum, and cerebellar vermis	RBV; ANOVA; SEGMENT	LFA: significantly larger brain and cerebral volumes than in controls; all AD groups: higher overall cerebral volume, cerebral GM and WM, cerebellar volume, cerebellar GM and WM, and anterior and posterior cerebellar vermis area
McAlonan et al., 2005	10–14	91–111	16 m; 1 f	10–13	100–128	16 m; 1 f	1.5 T; 3 mm	Regional GM and WM density	VBV; MANCOVA; BAMB for measuring brain volumes	Decreased GM density in frontostriatal and parietal networks and in ventral and superior temporal gyrus; decreased WM density in cerebellum and left internal capsule and fornices; in general, severe reduction in GM and significant increase in CSF in autistic brains
Munson et al., 2006	ASD: 4, NPDD: 4–5	–	ASD: 26 m; 3 f, NPDD: 12 m; 4 f	–	–	–	1.5 T; 1.55 mm	Amygdala, hippocampus	RBV; MEASURE	Larger right amygdalar volumes at ages 3–4, but not left amygdalar, hippocampal, or total cerebral volumes
Hardan et al., 2006b	8–13	64–128	17 m	9–13	91–130	14 m	1.5 T; 1.5 mm	Cortical thickness	SBM; BRAINS	Most prominent changes in temporal and parietal lobes: increased total cerebral sulcal and gyral thicknesses; no changes in frontal and occipital lobes

(Continued)

TABLE 2 | Continued

Rf	Autistic group			Control group			sMRI	Brain regions	Data analysis	Findings
	Age, y	IQ	Size	Age, y	IQ	Size				
Girgis et al., 2007	8–13	77–109	11 m	9–12	91–131	18 m	1.5 T; 1.5 mm	TBV	RBV; BRAINS2	Decreased GM in right lateral orbitofrontal cortex
Nordahl et al., 2007	LFA: 10–16; HFA: 8–14; ASP: 9–16	LFA: 46–66; HFA: 73–105; ASP: 80–114	LFA: 17 m, HFA: 14 m, ASP: 15 m	9–14	103–127	29 m	1.5 T; 1.5 mm	Cortex	SBM; Caret5.4; Caret5.5	LFA: prominent shape abnormalities centered on pars opercularis of inferior frontal gyrus, associated with sulcal depth differences in anterior insula and frontal operculum; HFA: bilateral shape abnormalities similar to LFA, but smaller in size and centered more posteriorly in and near parietal operculum and ventral postcentral gyrus; ASP: bilateral abnormalities in intraparietal sulcus correlated with age; all cortical shape abnormalities – more pronounced in children
Brun et al., 2009	6–13	FSIQ: 84–107	24 m	8–13	FSIQ: 94–117	26 m	3 T; 1.2 mm	Cortex	RBV; BAMB	Bilaterally decreased GM volumes in parietal, left temporal, and left occipital lobes; enlarged by 3.6% left, and 5.1% right frontal lobes in AD boys; significantly enlarged all other lobes
Hardan et al., 2009	10–12	FSIQ: 77–111	18 m	10–12	100–126	16 m	1.5 T; 1.5 mm	Cortex, TBV	RBV; longitudinal SBM; MANOVA; BRAINS; BRAINS2	Decreased total GM volume over time, decreased cortical thickness in AD subjects in frontal, temporal, and occipital lobes compared to controls
Jiao et al., 2010	7–11	80–124	19 m; 3 f	8–12	87–129	13 m; 3 f	1.5 T; 2 mm	Cortex	SBM; t-test; WEKA; FreeSurfer	Decreased thickness in right entorhinal, right lateral orbitofrontal, left lateral orbitofrontal, right medial orbitofrontal, left medial orbitofrontal cortex, and right pars triangularis; increased thickness in left caudal anterior cingulate cortex and left frontal pole
Nordahl et al., 2012	2–4	DQ: 41–85 ASD: 79 m, NPD: 6 m	ASD: 79 m, NPD: 6 m	2–4	92–116	47 m	3 T; 1 mm	Amygdala	RBV; longitudinal; ANCOVA; ANALYZE 10.0; BET	Amygdala enlargement at two time points with a higher rate at the second point; total cerebral volume enlargement with the same rate at both the points

(Continued)



TABLE 2 | Continued

Rf	Autistic group			Control group			sMRI	Brain regions	Data analysis	Findings
	Age, y	IQ	Size	Age, y	IQ	Size				
Frazier et al., 2012	7–13 t1, 9–16 t2	FSIQ: 75–115	ASD: 19 m, NPDD: 4 m	7–13 t1, 9–16 t2	FSIQ: 103–129	23 m	1.5 T; 1.5 mm	Corpus callosum	RBV; longitudinal; MERM; BRAINS2	Persistent reductions in corpus callosum volume in AD subjects compared to healthy controls; size normalization over time of only rostral body subdivision
Jou et al., 2013	7–17	75–115	23 m	7–17	103–129	23 m	1.5 T; 1.5 mm	Brainstem	RBV; longitudinal; ANOVA; BRAINS2	Stable brain stem volume in controls over the 2-y period; increased GM volume of autistic brains resulting in the increased whole brainstem volume, comparable to volumes of 15 y-old controls
Dierker et al., 2015	9–12	FSIQ: 99–124	28 m; 6 f	10–12	FSIQ: 104–126	23 m; 9 f	3 T; 1 mm	Cortex sulci	SBM; t-test; ANOVA; Freesurfer5.1	Bilateral significant differences in sulcal depth in restricted portions of anterior-insula and frontal operculum and in tempoparietal junctions
Barnea-Goraly et al., 2014	8–12 t1, 11–15 t2	78–118	15 m	7–13 t1, 9–16 t2	105–129	22 m	1.5 T; 1.5 mm	Amygdala, hippocampus	RBV; longitudinal; SPSS; BrainImage	Normalization of amygdala volumes in late childhood and adolescence; significantly larger right hippocampus in AD children; large volume reductions in right hippocampus of autistic individuals, compared to stable or slightly increased hippocampal volumes of healthy controls
Gori et al., 2015	3–5	70–113	21 m	3–5	74–123	20 m	1.5 T; 1.1 mm	GM, WM, CSF	VBM; SPM; Freesurfer	Altered GM in different brain regions for autistic and control brains, resulting in a classification accuracy of up to 80% between the 2 groups

Additional abbreviations: f, females; m, males; mo, month; Rf, reference; t1, t2, time periods; y, year; ANOVA, analysis of variances; ANCOVA, analysis of covariances; DD, developmental delay; HC, head circumference; MERM, mixed-effects regression models; TD, typical development; T, MRI magnetic field strength (tesla); MANOVA, multivariate analysis of variances; MANCOVA, multivariate analysis of covariances; TBV, total brain volume; ANALYZE, AREA, BAMM, BET, BrainImage, Caret, FreeSurfer, MEASURE, SEGMENT, SPM99, SPSS, VBA, WEKA, BRAINS, BRAINS2, data processing packages.

TABLE 3 | sMRI-based studying of the ASD at adolescence.

Rf	Autistic group			Control group			sMRI	Brain regions	Data analysis	Findings
	Age. y	IQ	Size	Age. y	IQ	Size				
Walter et al., 2004	13–18	FSIQ: 80–122	16 m	14–17	FSIQ: 81–118	16 m	1.5 T; 1.6 mm	TBV; GM, WM volumes	VBV; ANCOVA; <i>t</i> -test; SPM2	Increased GM volume in right fusiform gyrus, right temporal occipital region, and left frontal pole; decreased GM volume in right thalamus
Chung et al., 2004	11–21	–	16 m	14–20	–	12 m	3 T; 1.2 mm	WM density	VBV; GLM; SPM99+ GMM for segmentation	Lesser WM concentration in genu, rostrum, and splenium (also in CC due to hypoplasia, rather than atrophy)
Lotspeich et al., 2004	LFA: 10–14, HFA: 10–16, ASP: 10–15	LFA: 36–56, HFA: 86–124, ASP: 84–124	LFA: 13 m, HFA: 18 m, ASP: 21 m	10–15	101–125	21 m	1.5 T; 1.5 mm	CGM	RBV; ANOVA; BrainImage5.X (semi-automated segmentation)	HFA and LFA: Increased CGM w.r.t. controls (for ASP: intermediate between HFA and controls, yet insignificant)
Kwon et al., 2004	HFA: 11–17, ASP: 11–16	–	HFA: 9 m, ASP: 11 m	11–17	–	13 m	3 T; 1.5 mm	GM density	VBV; <i>t</i> -test; SPM99	HFA and ASP: decreased GM density in right inferior temporal gyrus, entorhinal cortex, and right rostral tip of fusiform gyrus
Walter et al., 2005	13–17	FSIQ: 78–123	15 m	14–17	FSIQ: 81–118	16 m	1.5 T; 1.6 mm	GM and WM volumes, TBV	VBV; ANCOVA; SPM2	Decreased WM volume in CC, left middle temporal, right middle frontal, and left superior frontal gyri
Hazlett et al., 2006	15–24	52–136	23 m	18–26	91–113	15 m	1.5 T; 1.5 mm	CGM and CWM volumes	RBV; RMML + BRAINS2 for tissue classification	Increased total cerebral and GM volume in AD brains with disproportionately increased left-sided GM volume; enlarged volumes of frontal and temporal, but not parietal or occipital lobes
Bonilha et al., 2008	8–16	–	12 m	8–18	–	16 m	2 T; 1 mm	GM, WM of cortical lobes, cerebellum, and claustrum	VBV; <i>t</i> -test + SPM5 for tissue segmentation	Increased GM volume in medial and dorsolateral frontal areas; lateral and medial parts of temporal lobes, and cerebellum and claustrum of parietal lobes; decreased WM volume in frontal, parietal, temporal, and occipital lobes
Hua et al., 2013	10–14 t1, 13–17 t2	FSIQ: 75–121	13 m	10–15 t1, 13–18 t2	FSIQ: 105–131	7 m	1.5 T; 1.2 mm	WM, frontal, parietal, temporal, and occipital lobes	RBV; longitudinal; BSE; Brainsuite	Decelerated WM growth in frontal, temporal, parietal, and occipital lobes; abnormally accelerated GM expansion in putamen and anterior cingulate cortex

(Continued)

TABLE 3 | Continued

Rf	Autistic group			Control group			sMRI	Brain regions	Data analysis	Findings
	Age, y	IQ	Size	Age, y	IQ	Size				
Wallace et al., 2015	15–20 t1, 17–22 t2	FSIQ: 104–130	17 m	16–19 t1, 18–22 t2	FSIQ: 106–126	18 m	3 T; 1.2 mm	Cortex	Area measurements; longitudinal; LS GLM; FreeSurfer5.1	Accelerated cortical thinning in AD brains w.r.t. controls in two areas of the left hemisphere: the posterior portion of ventral temporal cortex and superior parietal cortex (only in t2 in late adolescents and young adults)

Additional abbreviations: f, females; m, males; Rf, reference; t1, t2, time periods; w.r.t., with respect to;  
T, MRI magnetic field strength (tesla); y, year; CGM, cortical GM; CWM, cortical WM; GLM, general linear model;  
ANOVA, analysis of variances; ANCOVA, analysis of covariances; CC, corpus callosum;  
GMM, Gaussian mixture model; LS, least squares; RIMM, repeated measures mixed model;  
BrainImage, BRAINS2, Brainsuite, BSE, FreeSurfer, SPM – data processing packages.

brain tissues, the MD is recommended for the CSF-related disease studies Narr et al. (2009).

The **fractional anisotropy**, described first in Koay et al. (2006), is the most popular rotationally invariant (i.e., orientation-independent) measure of how isotropic is the voxel- or region-wise diffusion. The FA of a physically realizable diffusion with non-negative eigenvalues ranges from 0 to 1 in the opposite extreme complete isotropic and linear anisotropic cases, respectively. For example, the WM appears whiter due to its higher FA. The reduced FA values usually indicate changes in myelination or degraded axonal structures of the WM Lerner et al. (2014).

The **relative anisotropy** is similar to the FA and takes the range between 0 (the complete isotropy) to  $\sqrt{2}$  (the complete, i.e., linear anisotropy). The RA is also defined as the ratio of anisotropic and isotropic parts of the diffusion Le Bihan et al. (2001).

The **axial**, or **parallel diffusivity**,  $\lambda_{\parallel}$ , measures the diffusion along the principal axis (parallel to axons), whereas the **radial**, or **perpendicular diffusivity**,  $\lambda_{\perp}$ , averages the diffusion along the two minor axes to measure the degree of restriction due to membranes and other effects.

These two measurements are closely connected to the WM pathology Alexander et al. (2007) and have been used to observe developmental and pathological fiber alterations, e.g., to study dysmyelinating disorders Song et al. (2005).

Main fiber trajectories are extracted from the DTI and visualized using 2D color-coded **fiber orientation maps**. These maps provide unique information, which cannot be obtained with other MRI techniques. In particular, the fiber orientations could classify and stratify specific WM tracts in a host of medical applications that need more anatomical details Alexander et al. (2007).

These 2D color-coded maps present the voxel-wise fiber orientations related to the WM tracts, but cannot reveal 3D WM trajectories and connection patterns Mori and Tournier (2013). The latter are obtained with the computer-aided 3D **WM fiber tractography**, recognizing and tracing WM tracts and their connections with other WM tracts or GM structures. The tractography is either *deterministic*, or *probabilistic* Basser et al. (2000); Nucifora et al. (2007), and constructs, respectively, only one trajectory for each start voxel, or the most probable, or minimum-energy path between two selected voxels or regions Mori and Tournier (2013).

The **deterministic** (or tract propagation) **fiber tractography** is built by extracting fiber orientation and propagating pathway until termination criteria are met Mori and Tournier (2013). Generally, the local voxel-wise fiber orientations are estimated directly from planar diffusion profiles. These estimates fail if the ellipsoid is isotropic or the diffusion profile is planar.

Image noise, patient movements, and other imaging artifacts cause uncertainty in the fiber orientations obtained by the deterministic fiber tractography. The **probabilistic fiber tractography** attempts to increase the confidence Basser and Jones (2002) by estimating probability distributions of all fiber orientations and selecting the most probable orientations. Tracing many different pathways with marginally altered

TABLE 4 | sMRI-based studying of the ASD at adulthood.

Rf	Autistic group			Control group			sMRI	Brain regions	Data analysis	Findings
	Age, y	IQ	Size	Age, y	IQ	Size				
Hardan et al., 2001b	12–32	FSIQ: 88–118	16 m	12–32	FSIQ: 87–115	19 m	1.5 T; 5 mm	Third and fourth lateral ventricles, intracranial and cerebral volumes	RBV; ANCOVA; IMAGE1.45	Larger mean cerebral and third ventricles volumes in AD subjects after adjusting for intracranial volume and thus increasing TBV
Hardan et al., 2001a	12–52	FSIQ: 85–115	22 m	13–52	FSIQ: 87–115	22 m	1.5 T; 5 mm	Cerebellum, vermis, brain stem	RBV; area measurements; ANCOVA; IMAGE	Larger total cerebellar volume and cerebellar hemispheres in AD group with and without TBV correction; no significant differences in vermis and brainstem volumes and areas between groups
McAlonan et al., 2002	22–42	79–111	19 m; 2 f	26–40	100–128	22 m; 2 f	1.5 T; 1.5 mm	GM and WM density in cerebellum	VBM; SPSS; SMapt toolkit	Decreased GM density in frontostriatal and cerebellar regions; widespread differences in WM
Hardan et al., 2003	9–45	FSIQ: 88–118	38 m; 2 f	10–44	FSIQ: 94–114	39 m; 2 f	1.5 T; 1.5 mm	TBV, caudate	RBV; NIH Image (semi-automated segmentation)	No volume differences of basal ganglia and no difference in caudate and putamen (all ages)
Tsatsanis et al., 2003	11–38	82–141	12 m	11–30	87–138	12 m	1.5 T; 1.2 mm	TBV, thalamus	RBV; ANOVA; ANALYZE + manual segmentation	Significantly smaller mean thalamic volume in AD brains; positive correlation between TBV and thalamus in control group, yet insignificant in AD group (i.e., the absent in autism increase in thalamic volume with increase in TBV suggesting underdeveloped connections between cortical and subcortical regions)
Hardan et al., 2004	19–37	FSIQ: 88–112	18 m	19–28	FSIQ: 99–115	19 m	1.5 T; 1.5 mm	Cerebral folding	SBM; BRAINS2	No changes in left frontal gyrification index; decreased cortical folding in AD adults w.r.t. AD children and adolescents
Rojas et al., 2004	21–39	74–120	13 m; 2 f	41–49	109–135	8 m; 9 f	1.5 T; 1.7 mm	TBV; amygdala; hippocampus	RBV; Statistica 5.3; IDL 5.3	Larger left hippocampus was in both parents of AD children and adults with AD, w.r.t. control subjects; significantly larger hippocampus in AD adults, than in parents of AD children; smaller left amygdala in AD adults w.r.t. other two groups; no TBV differences between all groups

(Continued)

TABLE 4 | Continued

Rf	Autistic group			Control group			sMRI	Brain regions	Data analysis	Findings
	Age, y	IQ	Size	Age, y	IQ	Size				
Hadjikhani et al., 2006	21–45	98–128	AD: 8 m, ASP: 4 m, NPDD: 2 m	22–40	105–131	14 m	1.5 T; 1.25 mm	Cortex	SBM	Decreased thickness in inferior frontal gyrus pars opercularis, inferior parietal lobule, superior temporal sulcus, precentral gyrus, postcentral gyrus, inferior occipital gyrus, prefrontal cortex, anterior cingulate, medial parietal cortex, supramarginal gyrus, and middle and inferior temporal cortex
Hardan et al., 2006a	8–45	75–135	38 m; 2 f	9–43	86–121	39 m; 2 f	1.5 T; 3 mm	Thalamus	RBV; NIH Image	No difference between two groups in RBV of right and left thalamic nuclei; no linear relationship between TBV and thalamic volume
Rojas et al., 2006	9–44	FSIQ: 60–133	24 m	8–44	FSIQ: 99–139	23 m	1.5 T; 1.7 mm	Regional GM volume	VBV; longitudinal; ANCOVA; SPM2	Increased GM volume in medial frontal gyri, left precentral gyrus, right postcentral gyrus, right fusiform gyrus, caudate nuclei, and left hippocampus; decreased GM volume in cerebellum
Haznedar et al., 2006	17–55	55–125	AD: 10, ASP: 7; 15 m; 2 f	20–56	88–136	15 m; 2 f	1.5 T; 1.2 mm	Thalamus	RBV; ANOVA; manual segmentation	Larger volumes of right caudate nucleus in AD brains
Hyde et al., 2010	14–33	FSIQ: 89–113	13 m	14–34	FSIQ: 95–119	15 m	3 T; 1.5 mm	Cortical thickness	SBM; GLM; CIVET	Increased thickness in frontal, temporal, occipital, cingulate, and parietal gyrus and fusiform gyri; decreased thickness in pre- and postcentral gyri and paracentral gyrus
Toal et al., 2010	AD: 18–49, ASP: 16–59	AD: 53–133, ASP: 78–141	AD: 21 m; 5 f, ASP: 35 m; 4 f	19–58	74–122	30 m	1.5 T; 1.5 mm	GM and WM volumes	VBV; ANCOVA; SPSS; SPM2	Decreased GM volume in medial temporal, fusiform, and cerebellar regions; decreased WM volume in brain stem portions of cerebellum
Elnakib et al., 2011	19	–	17 m	19	–	17 m	1.5 T; 1.25 mm	CC	Area measurements	Significant reduction in the CC length of AD subjects

Additional abbreviations: f, females; m, males; mo, month; Rf, reference; T, MRI magnetic field strength (tesla); CC, corpus callosum; TBV, total brain volume; y, year; w.r.t., with respect to; ANOVA, analysis of variances; ANCOVA, analysis of covariances; ANALYZE, BRAINS, CIVET, IDL, IMAGE, NIH Image, SMat, SPM, SPSS, Statistica, data processing packages.

orientations allows for measuring the connection probability and assessing fiber connectivity between different brain regions by a voxel-wise connectivity index Behrens et al. (2003). The main advantage of the probabilistic fiber tractography is its ability to stratify the entire WM tracts. However, its accuracy is limited and depends on the accuracy of the DT and estimated pathway probability distributions. Moreover, the probabilistic tractography cannot differentiate between ante- and retrograde along the fiber's path Basser and Jones (2002).

### 3.2. Studying ASD Impacts on Anatomical Structures with DTI

Recent molecular and functional ASD studies confirmed the vital importance of localizing atypical development and examining neural networks and connectivity of different brain areas Travers et al. (2012). At the molecular level, the postmortem studies of brains of children with ASD have shown more reduced and less compact minicolumns Casanova et al. (2002a,b, 2006). At the functional level, examining brain connectivity with the fMRI revealed how activities of various brain areas are organized. Most of the ASD patients have demonstrated reduced connectivity between the frontal and posterior brain parts during various cognitive tasks and in a resting state Schipul et al. (2011). Therefore, according to both molecular and functional studies, the brain connectivity and the underlying WM tracts might be impaired in these patients.

However, earlier studies had limited abilities to provide sufficient morphological information about these WM tracts and their development in a living human Travers et al. (2012). To overcome this drawback, multiple noninvasive DTI-based studies of both the macro- and microstructure (e.g., axons) of the brain WM tracts were conducted for the last decade to investigate the ASD Travers et al. (2012). In particular, the DTI facilitated examining microstructural properties of the WM circuitry and detecting abnormalities of the WM fiber tract integrity Wolff et al. (2012). Below, the most important current methods of studying the ASD with the DTI (in total, from 60 publications) are summarized by stratification into five categories: (i) the whole-brain voxel-based analysis (VBA); (ii) the analysis of tract-based spatial statistics (TBSS); (iii) the ROI analysis; (iv) tractography; and (v) the classification-based analysis. Since the DTI findings in the literature are mainly concerned with WM connectivity across multiple structures, classification here is not based on the structures, such as in Section 2. It is rather based on the methodology the WM connectivity and the fiber tracts through those structures are investigated with. These methods differ in how group differences are investigated by measuring DTI heterogeneity, e.g., the FA. The same four age stages, as in Section 2, i.e., infancy, childhood, adolescence, and adulthood, are considered separately for more in-depth presentation of the ASD findings.

#### 3.2.1. Whole-Brain VBA

The brain images across subjects are spatially co-aligned in order to ensure that each individual voxel has the same anatomic location in all the subjects. Then the voxel-wise statistics are used to find areas of significant difference between the ASD

and control patients. Due to its comprehensive examination, the whole-brain VBA overcomes problems of possible user bias in and insufficient prior knowledge for selecting the ROI to be analyzed. However, the VBA has drawbacks that are absent in the ROI analysis: high sensitivity to accuracy of aligning the images and low reliability of voxel-wise statistical decisions. In spite of these drawbacks, the VBA is still widely used due to its simplicity and ability to explore the whole brain.

##### 3.2.1.1. Childhood

Relationships between communication, social interaction, and repetitive behavioral impairments have been investigated in Cheung et al. (2009) by the VBA of FA data for each group of subjects. For the ASD group, the bilateral prefrontal and temporal regions had reduced FA values, as well as lower FA along the frontal striatio-temporal pathways or more posterior brain pathways were associated with communication and social reciprocity impairments or repetitive behaviors, respectively. In a multi-modality study Ke et al. (2009), the WM abnormalities were investigated in HFA Chinese children, and the VBA showed that the WM density decreases in the right frontal lobe, left parietal lobe and right anterior cingulate. In addition, the FA values were lower in the frontal lobe and left temporal lobe. Combining the VBA and RBV of the DTI has showed consistent WM abnormalities in the HFA patients. Children with ASD and their unaffected siblings have been compared with the control group in Barnea-Goraly et al. (2010). The ASD and sibling groups had the prevalent reduced FA and  $\lambda_{\parallel}$  values in the frontal, parietal, and temporal lobes, especially, in the regions related to social cognition. However, no significant relationships between the WM measurements in the ASD and sibling groups have been reported. To what extent disconnectivity of networks, which are important for social communication, relates to behavioral impairments in children with ASD was investigated in Poustka et al. (2012). The VBA indicated the decreased FA values in the uncinate fasciculus and right superior longitudinal fasciculus. The additional analysis revealed a negative correlation between the FA values of the affected fiber tracts and the ASD symptoms.

##### 3.2.1.2. Adolescence

An early study Barnea-Goraly et al. (2004) of the WM abnormalities performed the VBA on a small group of male HFA children and adolescents. It has found low FA values in various brain regions, mainly, in the WM adjacent to the ventromedial prefrontal cortices, in the anterior cingulate gyri, and in the temporoparietal junctions. A similar, but larger study Keller et al. (2007), has investigated the WM abnormalities in a large male HFA group aged from 10 to 35 years. The HFA subjects had lower FA values near the corpus callosum and in the right retrolenticular portion of the internal capsule. A new tissue-specific, smoothing-compensated (T-SPOON) VBA introduced in Lee et al. (2009) minimizes effects of partial volume averaging and image smoothing by applying a regional mask with the same smoothing parameters. Compared to the conventional VBA, results of the T-SPOON on a large group of the ASD subjects and corresponding controls were more consistent with the FA obtained by analyzing the corpus callosum



and temporal lobe ROIs. The VBA of the WM of a small group of HFA and matched controls in Noriuchi et al. (2010) has shown the reduced FA and  $\lambda_{\perp}$  in various ROIs in the brain, including the left dorsolateral prefrontal cortex, cingulum bundle, arcuate fasciculus, and superior longitudinal fasciculus. Social impairment scores correlated negatively with the FA of the left dorsolateral prefrontal cortex, suggesting that the WM in cortical regions is vital for the ASD patients development. The WM integrity of the major fiber tracts connecting the amygdala, fusiform face area, and superior temporal sulcus in the ASD subjects was explored in Jou et al. (2011b) by the FA-based VBA. The ASD subjects had reduced FA values in the investigated WM tracts, including inferior longitudinal fasciculus, inferior fronto-occipital fasciculus, superior longitudinal fasciculus, corpus callosum, and cingulum bundle. A multi-modality study Groen et al. (2011) used the T1 MRI to study the brain volumetrics and the DTI to investigate both the WM and GM integrity in a limited group of HFA adolescents. There were no significant volumetric GM or WM differences between the two groups.

### 3.2.1.3. Adulthood

The ASP adults, examined in Bloemen et al. (2010) for the WM integrity of the whole brain, have shown lower FA of 13 WM clusters in the internal capsule, frontal, temporal, parietal, and occipital lobes, as well as the cingulum and corpus callosum. Studying the WM abnormalities on a small group of young LFA men Pardini et al. (2012) indicated a positive correlation between the FA in the uncinate fasciculus and clinical improvement, precocity, and intervention duration.

### 3.2.2. Tract-Based Spatial Statistics (TBSS)

To overcome some shortcomings of the traditional VBA, the recent DTI-optimized analysis of TBSS Smith et al. (2006) uses a non-linear registration to a common target to co-align the subjects' FA maps. Following the alignment, a mean FA skeleton is built and thresholded to exclude areas of high inter-subject variability. Based on the corresponding FA values, each aligned subject's FA map is projected onto the skeleton to facilitate collecting standard voxel-wise FA statistics across all the subjects. Generally, such tract-based analysis is more accurate than the VBA, but requires a sophisticated data projection method for better results. It also does not handle partial volume effects, is sensitive to motion distortions, has high computational complexity, and may fail if the tracks change much at junctions or due to apparent pathologies.

#### 3.2.2.1. Childhood

The deterministic tractography and TBSS were combined in Kumar et al. (2010) to investigate the corpus callosum region, including the uncinate fasciculus, in young ASD children aged 5 years on average. The ASD manifests itself in lower FA, higher MD, larger number of streamlines and voxels, and longer streamlines. There were also ASD-related macrostructural changes in the uncinate fasciculus correlate with the popular symptomatic scores of the GARS (Gilliam autism rating scale). The TBSS, VOI, and tractography have been used also in Weinstein et al. (2011) to investigate the WM abnormalities of

very young ASD children in several clusters within the genu and body of the corpus callosum, left superior longitudinal fasciculus, and right and left cingulum. The FA increased in these regions as a consequence of the decreased radial diffusivity,  $\lambda_{\perp}$ . The tractography revealed that increased FA was concentrated in the mid-body of the corpus callosum and in the left cingulum.

To study the integrity of the thalamic radiation of older ASD children in Cheon et al. (2011), four DTI measurements, namely, FA, MD,  $\lambda_{\perp}$ , and  $\lambda_{\parallel}$ , were examined in the anterior thalamic radiation, superior thalamic radiation, posterior thalamic radiation, corpus callosum, uncinate fasciculus, and inferior longitudinal fasciculus by combining the whole brain VBA analysis with the TBSS and ROI analyses. Anticipated WM abnormalities in the thalamo-frontal connections in the ASD children are indicated by the reduced FA and  $\lambda_{\parallel}$  and Increased MD and  $\lambda_{\perp}$  across various brain regions. The TBSS, combined with a VBA were applied in Jou et al. (2011a) to a small group of older ASD and control children. The FA was reduced, especially, in the forceps minor, inferior fronto-occipital fasciculus, and superior longitudinal fasciculus. Regional distributions of differences between young ASD and control children were examined in Walker et al. (2012) using the TBSS and the whole-brain VBA. While the FA values were reduced in various brain regions, the increased MD was found only in the posterior ones. These small (1–2%) regional differences between both groups were accompanied by distinct regional differences in imaging artifacts. They also demonstrated vulnerability of the between-group differences to such artifacts, which may cause errors in biological inferences. The TBSS and deterministic tractography were also used in Billeci et al. (2012) to analyze young ASD children with and without mental retardation. The statistics have detected a widespread FA increase in major WM pathways, and the tractography showed increased FA and fiber length in the cingulum and corpus callosum. Moreover, the MD increase was correlated with expressive language functioning in the indirect segments of the right arcuate and left cingulum.

#### 3.2.2.2. Adolescence

Examining differences in the WM integrity between the HFA and control subjects and its association with pictorial reasoning under various linguistic levels in Sahyoun et al. (2010a) indicated that visuospatial reasoning performance relates to the FA of the peripheral parietal and superior precentral WM in the HFA subjects, but the superior longitudinal fasciculus, callosal, and frontal WM in the controls. The whole-brain VBA followed by analyzing the TBSS in Ameis et al. (2011) evaluated the WM in a group of ASD and control children and adolescents. The VBA has shown the increased MD and radial diffusivity ( $\lambda_{\perp}$ ) in the ASD children, but not the adolescents in the frontal WM, and the statistics analysis has revealed alterations in the right uncinate fasciculus. The right inferior longitudinal fasciculus in the ASD case may indicate a disrupted fronto-temporal-occipital circuit playing a significant role in social and emotional processing. The TBSS was analyzed in Shukla et al. (2011b) to examine short- and long-distance WM tracts in the frontal, parietal, and temporal

lobes of the ASD subjects and matched controls. The short-distance tracts had reduced FA in the ASD group, increased MD and  $\lambda_{\perp}$  in the frontal, temporal, and parietal lobes. The age and DTI measurements were correlated in the control, but not ASD group. As was suggested, these typical age-related correlations were absent due to altered maturation of the short-distance tracts in the ASD group.

The whole-brain VBA with TBSS in Shukla et al. (2011a) assessed the WM tracts in the ASD children and adolescents. The reduced FA and the higher MD and radial diffusivity have been found for the ASD subjects in the corpus callosum, anterior and posterior limbs of the internal capsule, inferior longitudinal fasciculus, inferior fronto-occipital fasciculus, superior longitudinal fasciculus, cingulum, anterior thalamic radiation, and corticospinal tract. Moreover, the age-dependent analysis has shown no maturational changes in the ASD subjects. The WM tracts of a relatively larger group of the adolescents were studied in Bode et al. (2011) by examining the TBSS after correcting the entire image, rather than a ROI, which is more typical. As was found in the ASD group, the FA has increased, specially in the right inferior fronto-occipital fasciculus and affected visual perception. It suggests an abnormal information flow between the insular salience processing areas and occipital visual areas of the ASD patients.

### 3.2.2.3. Adulthood

A recent fMRI and DTI study Kana et al. (2014) examined causal attribution in the ASD and confirmed the relationship for the temporo-parietal junction that exists in the theory of mind. The response to intentional causality showed lower activation of the temporo-parietal junction in the fMRI of the ASD adults, and the analysis of the tract-based spatial DTI statistics revealed reduced FA in the temporal lobe. The tract-based statistics were used also in a more recent investigation Perkins et al. (2014) of the WM integrity in a small group of the ASD adults and their matched controls. The ASD subjects showed significantly decreased FA and high radial diffusivity,  $\lambda_{\perp}$ , values in the left hemisphere, mainly, in the thalamic and fronto-parietal pathways. Moreover, the WM disturbance was higher in the left hemisphere.

### 3.2.3. ROI Analysis

These analyses depend on prior assumptions about certain brain regions that might be impaired in the ASD subjects. The regions are extracted manually, semi-automatically (using delineation protocols), or automatically. Manual extraction is time-consuming and suffers from user variability, whereas automatic and semi-automatic region segmentation are affected by registration errors, as in the VBA. The fact that the VOI are grouped in a predefined way is the main advantage of analyzing the ROI, as the total number of multiple comparisons is much smaller than in the VBA, statistical decisions become more accurate. However, the ROI analysis cannot infer conclusions about microstructural properties of the WM tracts. It is impractical for examining every brain region, especially for large groups, and has limited accuracy because of low resolution and relatively thick slices of the DTI.

#### 3.2.3.1. Infancy

Microstructural WM differentiation between the ASD and control groups of infants and very young children was examined in Bashat et al. (2007). The fact that the left hemisphere's frontal lobe of the ASD subjects had predominately increased FA and probability, as well as reduced displacement supports the previous findings indicating an abnormal brain overgrowth in very young children.

#### 3.2.3.2. Childhood

The reduced FA of various cerebral WM tracts, which was found in Brito et al. (2009), suggests the ASD correlates with reduced connectivity in the corpus callosum, internal capsule, and superior and middle cerebellar peduncles. The ROI analysis of the cerebellar outflow and inflow pathways in Sivaswamy et al. (2010) has shown the bilaterally decreased MD in the superior cerebellar peduncles, together with the asymmetric FA of the middle cerebellar peduncle and the inferior cerebellar peduncle in the ASD patients. The effect of self-injurious behavior on cortical development of the ASD children was studied in Duerden et al. (2014) by using both T1 MRI and DTI scans. According to the sMRI analysis, both the thickness of the right superior parietal lobule and bilateral primary somatosensory cortices and the volume of the left ventroposterior nucleus of the thalamus correlate with the self-injury scores. The atlas-based ROI analysis has revealed that children engaged in self-injury had significantly decreased FA and increased MD in the the left posterior limb of the internal capsule, as well as increased radial diffusivity,  $\lambda_{\perp}$ , in the bilateral posterior limbs of the internal capsule and corona radiate. Recently, an atlas-based ROI analysis Peterson et al. (2015) was used to investigate abnormalities in various left and right hemispheric WM regions of the HFA children. Their significantly increased MD of the outer-zone cortical left hemisphere WM suggested hypomyelination and increased short-range cortico-cortical connections caused by the early WM overgrowth.

#### 3.2.3.3. Adolescence

The entire corpus callosum and its subregions (genu, body and splenium) were explored for a large group of the HFA subjects and matched controls in Alexander et al. (2007) using the DTI (FA, MD,  $\lambda_{\perp}$ , and  $\lambda_{\parallel}$ ) and RBV. The low-IQ HFA subgroup differed by small corpus callosum volumes, increased MD, decreased FA, and increased  $\lambda_{\perp}$ . The decreased FA and increased MD and  $\lambda_{\perp}$  in the superior temporal gyrus and temporal stem in the HFA subjects of the same group have been reported in Lee et al. (2007). Analyzing the WM over the whole brain and in several ROIs in Shukla et al. (2010) has detected decreased FA and increased  $\lambda_{\perp}$  in both the whole brain and corpus callosum; increased MD for the whole brain and the anterior and posterior limbs of the internal capsule; decreased  $\lambda_{\parallel}$  in the corpus callosum body, and decreased FA in the middle cerebellar peduncle of the HFA subjects.

#### 3.2.3.4. Adulthood

The fMRI and DTI have been used in Thakkar et al. (2008) to determine whether the structure and function of the anterior



cingulate cortex relate to a repetitive behavior in the ASD. The ASD subjects showed an increased rostral anterior cingulate cortex activation to both correct and erroneous responses and had reduced FA in the WM underlying the anterior cingulate cortex. These results correlate also with ratings of the rigid, repetitive behavior. A multi-modality study Beacher et al. (2012) used the VBM and ROI analysis to estimate the GM and WM volumes from the sMRI and evaluate the main WM tracts in the DTI, respectively, for the ASP adults. The total WM volume, regional GM volume in the right parietal operculum, and FA in the body of the corpus callosum, cingulum, and cerebellum suggested a correlation between the diagnosis and subject's gender. These findings confirmed the importance of understanding the sex-specific brain differentiation in the ASD.

### 3.2.4. Tractography

Tractography reconstructs virtual 3D trajectories of the WM tracts to define the ROIs required for examining several such tracts simultaneously and characterizes macrostructural tract properties with additional DTI measurements. The deterministic tractography reconstructs the WM tracts and measures their lengths, densities, or volumes from a number of streamlines propagated between voxels with similar diffusion properties. But it provides no uncertainty of the reconstructed tracks due to noise or insufficient spatial resolution, whereas the probabilistic tractography not only estimates the fiber tracts, but also measures their uncertainty. However, branching and false-positive tracts affect the tractography accuracy in defining the ROIs, specifically at the ends of the reconstructed tracts. Also, the DTI tractography fails if the DT is inadequate to describe a region. For example, the FA is significantly lower for complex WM fiber crossings. To meet these challenges, new diffusion models, scanning paradigms, and analysis methods are constantly being developed.

#### 3.2.4.1. Infancy

Data from the IBIS (infant brain imaging study) group have been used for a recent longitudinal DTI analysis Wolff et al. (2012) of how the WM fiber tract is organized from 6 to 24 months in high-risk siblings' infants, who developed the ASD by 24 months. The FA and axial ( $\lambda_{\parallel}$ ) and radial ( $\lambda_{\perp}$ ) diffusivity measured for the DTI were investigated to characterize microstructural properties of the WM fiber tracts. The FA for the infants who developed the ASD differed significantly from those who did not develop it in 12 out of the 15 fiber tracts investigated, including the fornix, uncinate fasciculus, and inferior longitudinal fasciculus. For most of the investigated ASD infants, the FA of the developing fiber tracts was higher at 6 months, had no differences at 12 months, and decreased at 24 months of age. This study provided evidence for the altered brain growth of the WM pathways related to manifesting autistic symptoms for the first year of life, thus confirming the critical importance of the longitudinal studies in revealing the age-related brain and behavior changes underlying the neurodevelopmental disorders. The DTI tractography in Ellison et al. (2014) used the same IBIS group, but focused on determining whether specific oculomotor functioning and visual orienting patterns characterize 7-month-old infants diagnosed

with the ASD at 24 months and detecting neural associates of their behaviors. The measurements included an average saccadic reaction time in a visually guided saccade procedure and the radial diffusivity,  $\lambda_{\perp}$ , of corticospinal pathways and the splenium and genu of the corpus callosum fiber tracts. Strong association between the  $\lambda_{\perp}$  of the splenium of the corpus callosum and visual orienting latencies in low-risk infants has been found, but this correlation was missing in the infants having the ASD. These results confirm the potential of acquiring infant imaging groups in identifying early ASD markers, which is critical for early clinical intervention.

#### 3.2.4.2. Childhood

Whether the deterministic tractography of the DTI can detect the WM abnormalities in the frontal lobe and check for short range connectivity changes in the ASD children was investigated in Sundaram et al. (2008). The higher MD in the whole frontal lobe, as well as in long and short range association fibers in the ASD group have been reported. The FA was reduced in the ASD group for the short range, but not long range fibers, and the necessity of advanced DTI technology to re-examine the short range connectivity in ASD was indicated. The brain connectivity in the corpus callosum of the HFA patients was examined in Hong et al. (2011) by measuring both the DTI and T1 MRI. The corpus callosum volume and density extracted from the MRI were compared to the FA, MD, average fiber length, and fiber number obtained from the DTI by deterministic tractography. The decreased WM density in the anterior third of the corpus callosum, and the higher MD and lower fiber number in the anterior third transcallosal fiber tracts of the HFA subjects have been found. The frontal lobe association pathways in the ASD children were studied in Jeong et al. (2011) by analyzing the tract curvature, FA,  $\lambda_{\parallel}$ , and  $\lambda_{\perp}$ . This study suggested that higher curvatures and  $\lambda_{\perp}$  in the parietotemporal junction of accurate fasciculus, frontotemporal junction of uncinate fasciculus, and the midline of the genu of the corpus callosum could be caused by larger attenuation of the thinner axons in the frontal lobe tracts of the ASD children.

The lack of the nonverbal ASD studies was addressed in Wan et al. (2012) by employing the probabilistic tractography to find language-related WM tracts (arcuate fasciculus). A small group of five nonverbal ASD children demonstrated the reversed arcuate fasciculus asymmetry. To what extent the ASD language ability is associated with the DTI measurements (FA and MD) of the language-related WM tracts (superior longitudinal fasciculus) and non-language-related WM tracts (corticospinal tracts) was investigated in Nagae et al. (2012) with the deterministic tractography. The obtained results have revealed the higher MD in the left hemisphere temporal portion of the superior longitudinal fasciculus fiber tracts of the ASD children with language impairment, as well as a significant negative correlation between the MD and language ability scores. The fMRI and probabilistic tractography of the DTI in Lai et al. (2012) examined the functional and structural organization of neural systems overlapping for language and music in the ASD children. The ASD children have demonstrated decreased functional responses to speech stimulation in the left inferior frontal gyrus and

secondary auditory cortices in the left temporal lobe, as well as decreased FA of the left dorsal pathway and the decreased tensor norms in the ventral tract. All the findings indicated that speech and song processing functional systems are more responsive for the song than the speech of the ASD children.

Relations between the WM microstructure and developing the morphosyntax in a spoken narrative were examined in Mills et al. (2013) on a small group of the older HFA children and their matched controls. The HFA children showed abnormally increased MD in the right inferior longitudinal fasciculus. A positive correlation between the morphological accuracy and WM integrity in the right inferior longitudinal fasciculus was found within the HFA group. This study has shown that the HFA children rely on the ventral, rather than typical pathways in their daily use of real world language. Both the sMRI and probabilistic DTI tractography were used in Joseph et al. (2014) to investigate the GM and WM related to language ability in the young ASD children. Compared to the control group, the ASD children had decreased leftward asymmetry of volume and  $\lambda_{\perp}$  of the arcuate fasciculus, but no difference in the GM asymmetries.

### 3.2.4.3. Adolescence

Examining the arcuate fasciculus in a group of ASD and control adolescent subjects with the probabilistic tractography Knaus et al. (2010) showed no group differences in FA. But atypical language laterality was more predominant in the ASD, than the control group. Advantages of volumetric DTI segmentation over tractography (its higher robustness to imaging noise, better compatibility with statistical analysis, and no region-to-region analysis) were exemplified in Fletcher et al. (2010) on extracting the WM tracts to study the same arcuate fasciculus on a group of the adolescent HFA and control subjects. The ASD group had increased MD and  $\lambda_{\perp}$ , and decreased FA. The overlap between specific LI and ASD LI in a group of the adolescents and children has been studied in Verhoeven et al. (2012). The deterministic tractography was applied to extract the superior longitudinal fascicle, and no significant differences in the FA and MD have been revealed between the ASD LI participants and controls. However, the FA was significantly reduced in children with the specific LI compared to their controls. The diffusion tractography was used in Lo et al. (2011) to investigate three association fibers, such as the bilateral cingulum bundle, bilateral arcuate fasciculus, and bilateral uncinate fasciculus, as well as the callosal fiber tracts. High-resolution diffusion spectrum imaging (DSI) was applied to a small group of the HFA subjects and controls in order to assess generalized fractional anisotropy (FA) and asymmetry patterns in the targeted fiber tracts. The HFA adolescents showed no leftward asymmetry found in the controls, but had the significantly reduced generalized FA in the three callosal fibers. The deterministic tractography in Ameis et al. (2013) extracted the cingulum bundle from a larger group of children and adolescent HFA subjects and controls. Significant age group interaction for the FA and diffusivity (MD,  $\lambda_{\perp}$ , and  $\lambda_{\parallel}$ ), which is driven by reduced FA and increased diffusivity in the ASD groups, but not in the adolescent groups, has been revealed. The fMRI and DTI probabilistic tractography were used in Nair et al. (2013) to examine the integrity of thalamo-cortical

connectivity in children and adolescents with the ASD. Increased MD and  $\lambda_{\perp}$  in the thalamo-cortical connections, and decreased functional connectivity in the thalamo-cortical circuitry, as well as a negative correlation between the fronto-thalamic FA and the social and total autism diagnostic observation schedule (ADOS) scores were reported. The cingulum bundle of a group of the ASD and control adolescents and young adults was investigated in Ikuta et al. (2014). By applying the probabilistic tractography, the low FA of the bilateral anterior cingulum bundle and negative correlation between this FA and the behavior rating inventory of executive function (BRIEF) scores were also identified.

### 3.2.4.4. Adulthood

The deterministic tractography was used in Catani et al. (2008) to examine microstructural integrity of the intracerebellar pathways in the ASP adults. The study revealed reduced FA of the short intracerebellar fibers and right superior cerebellar output peduncle. It also showed negative correlation with the autism diagnostic interview (ADI) scores. The deterministic tractography in Conturo et al. (2008) reconstructed the WM tracts from the amygdala to the fusiform cortex, and the hippocampus to the fusiform cortex in the ASD and control adults. The ASD group has shown increased  $\lambda_{\perp}$  in the bilateral amygdala fusiform connections and left hemisphere hippocampus fusiform connections, as well as decreased  $\lambda_{\perp}$  in the right hippocampus-to-fusiform connections, being associated with the lower face recognition scores and performance IQ. The very first study Pugliese et al. (2009), which examined connections between socio-emotional structures in the adults with ASD using the deterministic tractography, reported an increased number of streamlines (tract volume) in the right cingulum bundle and inferior longitudinal fasciculus of the ASP adults in contrast to their reduced number of streamlines in the right uncinate fasciculus. Significant age-related differences between the autistic and control groups were found in the MD of the left uncinate fasciculus. The deterministic tractography was used also in Thomas et al. (2011) to extract the intra-hemispheric visual-association WM tracts for the HFA adults and detect their high numbers of streamlines in the intra-hemispheric fibers, mainly, in the left hemisphere, and a low number of streamlines in the minor forceps and the body of the corpus callosum. A multi-modality (sMRI and DTI) approach in Langen et al. (2012) has examined differences in the bulk striatum volume and fronto-striatal WM integrity and their relationship with repetitive behavior and inhibitory control of the ASD adults. Analyzing the MRI has shown a smaller WM volume, and the DTI tractography revealed reduced FA in the WM connecting putamen to the frontal cortical areas and increased MD of the WM tracts connecting the accumbens to the frontal cortex. The relationship between the inter-hemispheric connectivity and the brain overgrowth in the ASD adults has been tested in Lewis et al. (2013) with the probabilistic tractography. The estimated callosal fiber length measured the maximum brain size achieved during the development, and compared to the size and structure of the corpus callosum extracted from the T1-weighted MRI. In the ASD adults, the callosal fiber length correlated inversely

with the corpus callosum size and positively with the radial diffusivity,  $\lambda_{\perp}$ .

### 3.2.5. Classification-Based Analysis

Since the advent of their basic concept in the mid-1980s, computer-aided diagnostic (CAD) systems remain in great demand among neuroradiologists Arimura et al. (2009). Most of the present CAD systems perform data preprocessing, feature extraction, and classification. Initial efforts to use features extracted from DTI to classify and diagnose ASD are detailed below.

#### 3.2.5.1. Childhood

Different DT coefficients from many areas across the brain were used in Ingallhalikar et al. (2011) to distinguish autistic children from controls. A high-dimensional nonlinear SVM has learned an underlying ASD pattern of numerous atlas-based regional DTI features, e.g., FA and MD, extracted from the various brain ROIs. According to the leave-one-out (LOO) cross validation, 84% specificity and 74% sensitivity were achieved in separating the autistic patients from the control ones.

#### 3.2.5.2. Adolescence

Shape representations of the WM tracts extracted from the DTI were utilized in Adluru et al. (2009) to distinguish between the autistic and control patients. These fiber bundles were seeded in the splenium of the corpus callosum, and the classification features were built using 3D shape context Belongie et al. (2002). The LOO cross-validation has resulted in an accuracy of 75%; both the specificity and sensitivity of 71%, and an average AUC of 0.765 (the area under the receiver operating characteristic curve). The DTI features of the ROI from the WM of superior temporal gyrus and temporal stem brain regions, which were assumed to have an important role in language, emotion, and social cognition development, were used in Lange et al. (2010) to study a large group of the HFA subjects and their matched controls. The extracted features included the FA, MD,  $\lambda_{\perp}$ ,  $\lambda_{\parallel}$ , normalized DT skewness, and hemispheric asymmetry index. Using the selected aforementioned six WM measurements, the system was able to separate the ASD subjects from the controls with 92% accuracy; 94% sensitivity, and 90% specificity.

## 3.3. Summary

**Tables 5–8** summarize, in accordance with the life stage, basic current results of studying the ASD with the DTI.

## 4. DISCUSSION

The overviewed results of the widespread investigation of the sMRI and DTI modalities in ASD diagnostics outline promising directions of the future work.

### *Diagnosing ASD with sMRI*

Obviously, from the sMRI investigations completed to date, it is clear that the brain of an autistic child is growing abnormally through early childhood. However, a consistent pathology amongst the autistic children is yet to be identified, and few, if any, studies include patients below 2 years of age. Nonetheless,

early brain overgrowth does appear to be a consistent and repetitive ASD feature, but this feature is heterogeneous and not all autistic children have an enlarged cerebral volume. Moreover, due to a common misconception of gender bias in the ASD, most of the studies primarily or exclusively focused on males. Also, the statistical significance of the reported findings are hindered due to the small population of subjects considered.

Within the literature, the effects of age on various anatomical features such as, the dynamics of the amygdalae and cerebral volumes, tend to be contradictory. Furthermore, multiple cross-sectional studies examining brain stem size in ASD patients have shown inconsistent results, and no study to date specifically assesses how the brain stem develops with age. Also, studying the brain stem should become volumetric and focus on selecting proper planes of cut, because most of the current studies have transected the brain stem and provided only area measurements. As a result, additional longitudinal studies are needed before any conclusions can be drawn on the role of brainstem development in autism.

Deciphering the role of different brain regions and networks in autism may benefit significantly from using multimodality approaches, which combine various resting state, task-evoked, and structural MRI measurements and rely on advanced data acquisition and analysis.

The utilization of MRI-based methods to study brain development in larger populations will likely begin to address heterogeneity in ASD patients and identify distinct autism subtypes, each with a specific associated neuroanatomical phenotype. However, it is anticipated that the maximum scientific benefit will be achieved from conducting longitudinal studies in younger populations with additional characterization of the underlying genetic abnormalities, along with other potential biomarkers, driving the overgrowth and onset of autistic symptoms at a critical time in the developmental process. Hence, it is of great significance to establish more effective biomarkers in order to facilitate diagnostics in patients before their conventional ASD symptoms become evident.

Future studies that include more than two time points of MRI data would be particularly helpful in the construction and comparison of ASD and normal brain development patterns. Yet, another promising method for understanding the relationship between brain development and ASD is to statistically analyze local 3D shapes and surfaces of the primary components of the brain and correlate these results to the common behavioral scores, such as the social responsiveness scale (SBS). However, correlating the results will be challenging, since such scales were developed as screening tools to qualitatively describe ASD severity, rather than to quantify the health deficits.

### *Diagnosing ASD with DTI*

The VBA, applied mostly to small and predominantly adolescent groups, has shown decreased FA in the major WM tracts of patients with ASD. The usefulness of VBA of DTI remains in doubt because this method depends on the size of the smoothing kernel and hinders confident conclusions. The TBSS, optimizing the VBA of DTI and thus outperforming the traditional VBA, have been used in the majority of cases to examine the whole

TABLE 5 | DTI-based studying of the ASD at Infancy.

Rf	Autistic group			Control group			sMRI	Brain regions	Data analysis	Findings
	Age, mo	IQ	Size	Age, mo	IQ	Size				
Bashat et al., 2007	22–40	–	7	4–23	–	18	1.5 T; 4.5 mm; 6000 b; 6 GD	CC genu and splenium; left posterior limb of IC; left EC; left forceps minor; left CST	ROI; t-test	ASD: Increased FA in CC genu and splenium; left hemisphere posterior limb IC, and left hemisphere EC; decreased FA left hemisphere CST; increased WM probability, and decreased displacement distribution
Wolff et al., 2012	t1: 6–7, t2: 12–13, t3: 23–25	t1: 67–115, t2: 69–111, t3: 65–109	24 HR	t1: 6–7, t2: 12–13, t3: 24–26	t1: 86–118, t2: 86–116, t3: 81–117	64	3 T; 2 mm; 1000 b; 25 GD	CC genu, body, and splenium; fornix; inferior longitudinal fasciculus; uncinate fasciculus; anterior thalamic radiation; IC anterior and posterior limbs	DTI; ROI; RCLGCM; DTIprep; 3D Slicer; SAS 9.2	6-mo ASD: subjects: Increased FA in CC body, left hemisphere fornix, inferior longitudinal fasciculus, uncinate fasciculus, and posterior limb IC; 12-mo ASD subjects: no significant FA difference, except of decreased FA in left hemisphere anterior thalamic radiation; 24-mo ASD subjects: decreased FA in left hemisphere anterior limb IC and anterior thalamic radiation
Elison et al., 2014	7	–	16 HR	7	–	41 LR 40 HR	3 T; 2 mm; 1000 b; 25 GD	CC splenium and genu; left and right CSTs	DTI; ROI; MANOVA; FiberViewer	ASD: Correlated $\lambda_{\perp}$ in CC splenium and visual orienting latencies in LR infants; no correlation in HR infants

Additional abbreviations: b, b-value ( $s/mm^2$ ); f, females; m, males; mo, month;  
Rf, reference; T, MRI magnetic field strength (tesla); t1, t2, t3, time periods during longitudinal studies;  
CC, corpus callosum; CST, cortico-spinal tract; DT, deterministic tractography; EC, external capsule;  
GD, gradient directions; IC, internal capsule;  
MANOVA, multivariate analysis of variances; RCLGCM, random coefficient linear growth curve model;  
DTIprep, 3D Slicer, FiberViewer, SAS 9.2, data processing packages.

TABLE 6 | DTI-based studying of the ASD at childhood.

Work	Autistic group			Control group			sMRI	Brain regions	Data analysis	Findings
	Age, y	IQ	Size	Age, y	IQ	Size				
Sundaram et al., 2008	2–7	–	50 AD, ASP, NPDD	3–11	–	16	3 T; 3 mm; 1000 b; 6 GD	Frontal lobe's long-/short-range association fibers	DTI; ROI; MANCOVA; DTI studio	ASD: Increased MD in short/long-range fibers and decreased FA in short-range fibers; insignificant negative correlation between FA and GARS AQ (social isolation subscale)
Brito et al., 2009	8–12	–	8 AD	8–12	–	8	1.5 T; 5 mm; 1000 b; 12 GD	Frontopontine and corticospinal tracts; frontal subcortical WM	ROI; ANOVA; EpInfo	ASD: Decreased FA in the anterior CC, right CST, posterior limb of right and left ICs, left superior cerebellar peduncle, and right and left middle cerebellar peduncles
Cheung et al., 2009	7–12	78–122	13 AD	7–13	92–132	14	1.5 T; 5 mm; 1200 b; 25 GD	Left orbitofrontal cortex; precentral gyrus; bilateral frontal pole	VBA; GLM; Linear regression; SPM2; SPSS15.0	ASD: Decreased FA in prefrontal lobes, ventral and middle temporal lobe, and cerebellum; increased FA in superior longitudinal fasc and left occipital lobe; strongly correlated higher ADI-R scores and lower FA in prefrontal lobes and ventral temporal lobes; negatively correlated communication and social reciprocity impairments (ADI-A and ADI-B) throughout fronto-striato-temporal pathways and posterior CC
Ke et al. (2009)	6–11	82–120	12 HFA	7–12	82–118	10	1.5 T; 3 mm; 1000 b; 15 GD	Bilateral middle frontal gyrus; left inferior frontal gyrus; left superior temporal gyrus; right middle temporal gyrus; right frontal lobe	VBA; WM density; SPM5	ASD: Decreased WM density in right frontal lobe, left parietal lobe and right anterior cingulate; increased WM density in right frontal lobe, left parietal lobe and left cingulate gyrus; decreased FA in the frontal lobe and left temporal lobe; positively correlated CARS score and FA in right frontal lobe; no significant correlation between ADI-R scores and mean FA
Sivaswamy et al., 2010	2–9	–	27 AD, ASP, NPDD	2–9	–	16	3 T; 3 mm; 1000 b; 6 GD	Superior, middle, and inferior cerebellar peduncles tracts	ROI; ANCOVA; SPSS17.0	ASD: Increased MD of bilateral superior cerebellar peduncles; increased FA of right middle cerebellar peduncle; reversed FA asymmetry pattern in middle and inferior cerebellar peduncles

(Continued)



TABLE 6 | Continued

Work	Autistic group			Control group			sMRI	Brain regions	Data analysis	Findings
	Age, y	IQ	Size	Age, y	IQ	Size				
Kumar et al., 2010	2–9	–	32 AD, ASP, NPDD	2–9	–	16	3 T; 3 mm; 1000 b; 6 GD	Uncinate fasc.; inferior fronto-occipital fasc.; arcuate fasc.; CC; CST	TBSS; DT; ANOVA; DTI studio 2.40	ASD and DevI: Decreased FA in right uncinate fasc., right cingulum, and CC; increased MD in right arcuate fasc.; DevI: Decreased FA in bilateral fronto-occipital fasc
Barnea-Goraly et al., 2010	9–14	69–103	13 AD	8–12	107–123	11	1.5 T; 3 mm; 900 b; 6 GD	Medial prefrontal WM; frontal corona radiate; CC genu, anterior forceps, and body	VBA; FSL	ASD and siblings: Decreased FA and $\lambda_{  }$ in multiple regions across frontal, temporal, and parietal lobes; no significant differences in WM structure; ASD: No significant correlation between ADOS and ADI-R subscale scores and FA or $\lambda_{  }$
Weinstein et al., 2011	2–4	–	22 AD	2–5	–	32	1.5 T; 3 mm; 1000 b; 15 GD	CC genu and body; left superior longitudinal fasc.; right and left cingulum	TBSS; DT; MRI studio; FSL	ASD: Increased FA and decreased $\lambda_{\perp}$ in CC genu and body, left superior longitudinal fasc., and bilateral cingulum
Hong et al., 2011	7–11	84–126	18 HFA	8–12	86–136	16	1.5 T; 2 mm; 1000 b; 15 GD	CC anterior third, anterior and posterior midbody, isthmus; and splenium	DT; ROI; WM density and volume; FSL; SPSS13.0	ASD: Decreased WM density in CC anterior third; increased MD and decreased fiber number in anterior third transcallosal fiber tracts; no significant correlation between DTI indices and CARS
Ingallhalikar et al., 2011	8–13	–	45 HFA	8–13	–	30	3 T; 2 mm; 1000 b; 30 GD	Middle occipital gyrus left; inferior occipital WM right; superior temporal WM right fornix	Classification; ROI; non-linear SVM	84% specificity and 74% sensitivity by LOO CV based on FA in right occipital regions, left superior longitudinal fasc., EC; IC; MD in right occipital gyrus and right temporal WM; correlated SRS/SCQ autism scores and classification results

(Continued)

TABLE 6 | Continued

Work	Autistic group			Control group			sMRI	Brain regions	Data analysis	Findings
	Age, y	IQ	Size	Age, y	IQ	Size				
Cheon et al., 2011	9–13	100–124	17 ASP; NPDD	8–12	103–125	17	1.5 T; 3 mm; 900 b; 30 GD	Anterior thalamic radiation; superior thalamic radiation; inferior longitudinal fasc	TBSS; ROI; ANOVA; DTIStudio; FSL; SPSS 11.5	ASD: Decreased FA and increased MD in right anterior thalamic radiation, CC, and left uncinate fasc.; decreased FA in left anterior thalamic radiation, and right and left inferior longitudinal fasc.; increased $\lambda_{\perp}$ in right and left anterior thalamic radiation, CC, left uncinate fasc., and left inferior longitudinal fasc.; decreased $\lambda_{\parallel}$ in left inferior longitudinal fasc.; negatively correlated SRS and FA in right anterior thalamic radiations and right uncinate fasc
Jeong et al., 2011	3–7	–	32	4–8	–	14	3 T; 3 mm; 1000 b; 6 GD	Bilateral arcuate fasc.; bilateral uncinate fasc.; CC genu.	DTI; ROI; TBSS; FSL; SPM	ASD: Increased curvature and $\lambda_{\perp}$ and decreased FA in parietotemporal junction for arcuate fasc., frontotemporal junction for uncinate fasc., and midline of CC genu; positively correlated curvature and $\lambda_{\perp}$ in all ROIs; Controls and ASD: Negatively correlated curvature and FA in all ROIs; Controls: Positively correlated curvature and $\lambda_{\perp}$ only in CC genu
Jou et al., 2011a	7–15	–	15 AD	9–14	–	8	3 T; 2.5 mm; 30 GD	Inferior fronto-occipital fasc.; superior longitudinal fasc.; uncinate fasc.; cingulum.	TBSS; FSL; SPSS17.0	ASD: Decreased FA in numerous association, commissural, and projection tracts, especially, the forceps minor, fronto-occipital fasc., and superior longitudinal fasc.; no significant correlation between FA and SRS scores
Wan et al., 2012	6–8	–	5 LFA	9–14	–	5	3 T; 1.5 mm; 1000 b; 25 GD	Arcuate fasc	PTI; ROI; FSL	Nonverbal ASD: no usual leftward pattern of arcuate fasc. asymmetry (actually the reversed pattern for four out of the five nonverbal subjects)

(Continued)

TABLE 6 | Continued

Work	Autistic group			Control group			sMRI	Brain regions	Data analysis	Findings
	Age, y	IQ	Size	Age, y	IQ	Size				
Walker et al., 2012	3–7	–	39 AD	3–7	–	39 AD	1.5 T; 2.5 mm; 1100 b; 50 GD	Cerebellum; CC genu, body and splenium; CSTs; pons	TBSS; RESTORE	ASD: Decreased FA in various WM regions; increased MD in posterior brain regions Significant age group interaction, indicating differences in FA and MD developmental trends between the two groups
Nagae et al., 2012	7–18 ASD/–LI; 7–15 ASD/+LI	–	18 ASD/–LI; 17 ASD/+LI	7–18	–	25	3T; 2mm; 1000 b; 30 GD	Superior longitudinal fasc.; temporal lobe component of the superior longitudinal fasc.; CSTs	DT; GLM; HRL; DTIStudio; SPSS 19.0	ASD/–LI: Increased MD in CSTs ASD/+LI: Increased MD in left hemisphere superior longitudinal fasc fiber tracts and temporal portion of superior longitudinal fasc ASD/±LI: Significant negative correlation between left hemisphere superior longitudinal fasc MD and clinical language ability assessment
Poustka et al., 2012	8–12	97–125	18 AD	8–12	98–128	18	1.5 T; 2 mm; 1000 b; 6 GD	Fornix; superior longitudinal fasc.; uncinate fasc.; CC	VBA; DT; SPM5; NeuroQlab	ASD: Decreased FA in bilateral uncinate fasc and right superior longitudinal fasc.; negative correlation between FA of affected fiber tracts and autism communication and interaction scores (ADI-R and ADOS); no significant altered GM or WM concentration after correction for multiple comparisons
Lai et al., 2012	7–15	–	16 LFA	7–16	–	18	1.5 T; 5 mm; 1000 b; 25 GD	Aruate and inferior fronto-occipital fasc	PT; t-test FSL4.1	ASD: Decreased FA in left part of left dorsal pathway; significantly lower tensor norms for ventral tract
Billeci et al., 2012	4–8	47–93	22 AD, NPDD	3–8	90–108	10	1.5 T; 3 mm; 1000 b; 25 GD	CC; cingulum; arcuate fasc	TBSS; DT; ANCOVA; FSL; BET; FNIRT; eDTI; SPSS	ASD: Increased FA in major WM pathways, especially in CC, cingulum, arcuate fasc and IC; increased fiber length and FA in cingulum and CC, and increased MD in indirect segments of right arcuate and the cingulum; significant correlation between MD of arcuate fasc., CC, and cingulum and expressive language abilities

(Continued)



TABLE 6 | Continued

Work	Autistic group			Control group			sMRI	Brain regions	Data analysis	Findings
	Age. y	IQ	Size	Age. y	IQ	Size				
Mills et al., 2013	8–11	VIQ: 77–117	10 HFA	7–11	109–133	17	1.5 T; 2.5 mm; 1000 b; 51 GD	Superior longitudinal fasc.; temporal and partial subsections of superior longitudinal fasc.; inferior fronto-occipital fasc	DT; ROI; FreeSurfer; DTISudio	ASD: Increased MD and $\lambda_{\perp}$ in right inferior longitudinal fasc. Positive correlation between higher FA and lower MD and $\lambda_{\perp}$ in inferior longitudinal fasc produced more morphologically accurate language
Duerden et al., 2014	8–13	86–122	30 AD	8–13	100–128	30	1.5 T; 3 mm; 1000 b; 35 GD	Cingulum bundle; posterior limb of IC; corona radiata	ROI; TBSS; MANCOVA; Camino; FLIRT	ASD and self-injury subjects: Decreased FA and increased MD in left posterior limb of ICs. Positive correlation between self-injury and increased $\lambda_{\perp}$ in bilateral posterior limbs of IC and corona radiata.
Joseph et al., 2014	4–6	VIQ: 73–119	20 AD	8–11	VIQ: 102–132	20	3 T; 2 mm; 1000 b; 15 GD	Arcuate fasc	PT; ANOVA; FSL4.1.2	Decreased leftward/increased rightward asymmetry of pars opercularis correlated with higher language ability and bilaterally increased FA and decreased $\lambda_{\perp}$ of the arcuate fasc
Peterson et al., 2015	9–12	86–118	36 HFA	9–12	100–118	37	3 T; 2.2 mm; 800 b; 32 GD	Left and right hemispheric WM regions	ROI; ANCOVA; CATNAP; RESTORE; LDDMM	ASD: Increased MD throughout left hemisphere, particularly in outer-zone cortical WM Controls and ASD: Negative correlation between MD and age in left-hemisphere WM regions

Additional abbreviations: *b*, *b*-value ( $\text{s/mm}^2$ ); *f*, females; *fasc.*, fasciculus; *m*, males; *Rf*, reference; *T*, MRI magnetic field strength (tesla); *y*, year;  
ADI-R, autism diagnostic interview - revised; ADOS, autism diagnostic observation schedule;  
ANCOVA, analysis of covariances; ANOVA, analysis of variances;  
AQ, autistic quotient; CARS, childhood autism rating scale; CC, corpus callosum;  
CV, cross-validation; CST, cortico-spinal tract; DevI, developmentally impaired;  
DT, deterministic tractography; EC, external capsule; FWE, family-wise error;  
GARS, Gilliam autism rating scale; GD, gradient directions; GLM, general linear model;  
HRL, hierarchical regression model; IC, internal capsule;  
LDDMM, large deformation diffeomorphic metric mapping; LOO, leave-one-out;  $\pm$ LI, with/without LI;  
MANCOVA, multivariate analysis of covariances; MANOVA, multivariate analysis of variances;  
PT, probabilistic tractography;  
RCLGCM, random coefficient linear growth curve model;  
SCQ, social communication questionnaire; SLI, specific LI; SNR, signal-to-noise ratio;  
SPM, statistical parametric mapping; SPS, social responsiveness scale; SVM, support vector machine;  
TBSS, tract-based spatial statistics;  
3D Slicer, BET, CATNAP, DTIprep, DTI studio;  
eDTI, FiberViewer, FLIRT, FNIRT, FSL, MRI studio, NeuroQlab, RESTORE;  
SAS, SPM, SPSS, data processing packages.

TABLE 7 | DTI-based studying of the ASD at adolescence.

Work	Autistic group			Control group			sMRI	Brain regions	Data analysis	Findings
	Age, y	IQ	Size	Age, y	IQ	Size				
Barnea-Goraly et al., 2004	11–18	89–113	7 HFA	10–16	98–116	9	3 T; 5 mm; 900 b; 6 GD	Right motor and premotor areas; temporoparietal junction; superior and middle temporal gyrus.	VBA; t-test SPM99	ASD: Decreased FA in ventromedial prefrontal cortices, anterior cingulate gyri, temporoparietal junctions, superior temporal sulcus bilaterally, temporal lobes approaching amygdala bilaterally, occipitotemporal tracts, and CC
Keller et al., 2007	12–26	87–117	34 HFA	13–25	101–119	31	3 T; 3 mm; 850 b; 6 GD	Posterior/midbody/isthmus of CC; left and right anterior corona radiata near CC genu	VBA; REWMRA; SPM2	ASD: Decreased FA in areas within and near CC and in right retrolenticular IC portion Positively correlated group and linear age effect on FA resulted in posterior right IC limb
Alexander et al., 2007	9–24	95–121	43 AD, ASP, NPDD	10–22	101–125	34	3 T; 2 mm; 1000 b; 12 GD	CC genu, body and splenium	ROI; ANOVA; BCA; AIR; FSL	ASD subgroup: Decreased FA and increased MD and $\lambda_{\perp}$ in CC; significantly lower performance IQ than for either ASP+NPDD or controls; positively correlated $\lambda_{\perp}$ and processing speed during the performance IQ tests (ASD subjects with low FA and high MD seem to have the highest $\lambda_{\perp}$ and slowest processing speeds)
Lee et al., 2007	9–23	95–121	43 AD, NPDD	10–22	101–125	34	3 T; 2 mm; 1000 b; 12 GD	ASD: Superior temporal gyrus; temporal stem	ROI; ANCOVA; FSL; SPSS14.0	ASD: In all regions, significantly decreased FA and significantly increased both MD and $\lambda_{\perp}$ ; very little age-related FA changes Controls: Increased FA with age Controls+ASD: Decreased MD and $\lambda_{\perp}$ with age
Lee et al., 2009	9–23	94–121	43 HFA, NPDD	10–22	101–125	34	3 T; 2.5 mm; 1000 b; 12 GD	CC; bilateral superior temporal gyrus; anterior cingulum bundle	VBA; T-SPOON; ANCOVA; AIR; FSL; SPSS 14.0	ASD: T-SPOON VBA is more consistent with ROI measurements in CC and temporal lobe regions; T-SPOON VBA found unobserved before in Lee et al. (2007) and significant focal CC body regions during FA vs. processing speed test
Adluru et al., 2009	9–23	–	41 HFA	10–22	–	32	2 mm	WM tracts through CC splenium	Classification; VBA; FSL	ASD vs. controls classification by WM tracts shapes: 75.3% accuracy, 71.9% specificity, and 0.7645 AUC

(Continued)

TABLE 7 | Continued

Work	Autistic group			Control group			sMRI	Brain regions	Data analysis	Findings
	Age, y	IQ	Size	Age, y	IQ	Size				
Noriuchi et al., 2010	11–17	86–100	7 HFA, NPDD	10–16	106–126	7	3 T; 2 mm; 800 b; 32 GD	Anterior cingulate cortex; left dorsolateral prefrontal cortex; right temporal pole; amygdala, superior longitudinal fasc.; occipitofrontal fasc.; mid- and left anterior CC	VBA, MVR; SPM2; SPSS 17.0	ASD: Reduced FA and $\lambda_{  }$ in left dorsolateral prefrontal cortex, posterior superior temporal sulcus/temporo-parietal junction, right temporal pole, amygdala, superior longitudinal fasc. and occipitofrontal fasc.; negatively correlated FA of left dorsolateral prefrontal cortex and SRS scores
Lange et al., 2010	10–22	93–127	30 HFA	10–22	102–128	30	3 T; 2 mm; 1000 b; 12 GD	Superior temporal gyrus; temporal stem	Classification; ROI; QDA	ASD: Reversed hemispheric DT skewness asymmetry in superior temporal gyrus; increased DT skewness on right and decreased FA in left superior temporal stem; increased MD, $\lambda_{  }$ , and $\lambda_{\perp}$ in right temporal stem; positively correlated FA of left superior temporal gyrus and composite Vineland score; negatively correlated FA of right temporal stem and performance IQ/language functioning ASD vs. controls classification by six WM measurements: 92% accuracy, 94% sensitivity, and 90% specificity
Knaus et al., 2010	11–19	VIQ: 104	14 AD	11–19	VIQ: 119	20	3 T; 2 mm; 1000 b; 15 GD	Arcuate fasc	PT; ROI; ANOVA; FreeSurfer; FSL; BET	ASD vs. controls: More prevalent atypical language laterality; no significant group differences in FA, but subjects with more typical leftward lateralization had greater FA in arcuate fasc. across both groups
Fletcher et al., 2010	12–16	85–123	10 HFA	12–14	93–113	10	3 T; 2.5 mm; 1000 b; 12 GD	Arcuate fasc	ROI; LME models; ITK-SNAP	ASD: Increased MD and $\lambda_{\perp}$ in the left arcuate fasc.; less lateralized MD and FA

(Continued)

TABLE 7 | Continued

Work	Autistic group			Control group			sMRI	Brain regions	Data analysis	Findings
	Age. y	IQ	Size	Age. y	IQ	Size				
Sahyoun et al., 2010b	11–15	89–113	12 HFA	11–16	97–115	12	3 T; 2 mm; 700 b; 60 GD	Inferior parietal and frontal sulcus; medial temporal gyrus; superior temporal sulcus; fusiform gyrus	PT; ROI; FSL	ASD: Decreased FA in pathways between inferior frontal sulcus and fusiform gyrus and in both hemispheres; decreased FA in pathways between inferior frontal sulcus and medial temporal gyrus and in right hemisphere
Shukla et al., 2010	12–13	VIQ: 107–113	26 HFA	12–14	VIQ; 107–113	24	3 T; 5 mm; 2000 b; 15 GD	CC genu, body, and splenium; IC genu and anterior and posterior limbs; middle cerebellar peduncle	ROI; VBA; ANOVA; FSL; SPMS5; SPSS 16.0	Decreased FA and increased $\lambda_{\perp}$ for whole-brain WM and all three segments of CC and IC; increased MD for whole brain and for IC anterior and posterior limbs; decreased $\lambda_{\parallel}$ in CC body and decreased FA in middle cerebellar peduncle
Sahyoun et al., 2010a	11–15	89–113	9 HFA	11–16	97–115	12	3 T; 2 mm; 700 b; 60 GD	Forceps minor; bilateral superior longitudinal fasc. and arcuate fasc.; bilateral inferior fronto-occipital fasc.; right cerebellar WM; bilateral uncinate fasc	TBSS; ANOVA; FSL; BET; IRTK	Controls: Increased FA in WM tracts connecting with frontal lobe; bilaterally within forceps minor, in left inferior fronto-occipital fasc adjacent to middle and inferior frontal gyri, left superior longitudinal fasc., and right posterior ASD: Increased FA bilaterally within uncinate fasc. in temporal lobe and in right superior longitudinal fasc. peripherally near middle frontal gyrus Group differences in correlations between task performance and FA of different brain areas
Jou et al., 2011b	9–17	46–116	10 AD, ASP, NPDD	10–18	87–123	10	1.5 T; 4 mm; 1000 b; 6 GD	Anterior radiata and body of CC/cingulum; left superior longitudinal fasc./accurate fasc.; left inferior fronto-occipital fasc.; bilateral inferior longitudinal fasc	VBA; VOI; DT; BiImage Suite	ASD: Decreased FA in inferior longitudinal fasc./inferior fronto-occipital fasc., superior longitudinal fasc., and CC/cingulum

(Continued)

TABLE 7 | Continued

Work	Autistic group			Control group			sMRI	Brain regions	Data analysis	Findings
	Age, y	IQ	Size	Age, y	IQ	Size				
Amels et al., 2011	9–15	79–119	19 AD, NPDD	8–16	86–116	16	3 T; 3 mm; 1250; 12 GD	Bilateral uncinate fasc.; bilateral inferior fronto-occipital fasc.; forceps minor and major	TBSS; VBA; HRM; FSL 4.1; ANALYZE 9.0; SPSS 15.0	ASD: Increased MD and $\lambda_{\perp}$ in corticocortical and inter-hemispheric WM tracts, especially in children and within frontal lobe
Verhoeven et al., 2012	12–15	–	19 AD	9–11	12		3 T; 2.2 mm; 800 b; 45 GD	Superior longitudinal fasc	DT; ROI; GLM; ExploreDTI	No significant differences in FA and ADC between ASD-LI and control subjects; decreased FA in ASD-SLI subjects w.r.t. their controls
Shukla et al., 2011b	10–16	106–112	26 AD, ASP	10–16	VIQ: 105–111	24	3 T; 5 mm; 2000 b; 15 GD	Short and long distance WM tracts in frontal, parietal, and temporal lobes in both hemispheres	TBSS; ROI; ANOVA; FSL; FNIRT	ASD: Decreased FA and increased MD and $\lambda_{\perp}$ in short distance tracts in frontal lobe; increased MD and $\lambda_{\perp}$ in short distance tracts in temporal and parietal lobes Significant positive correlations between age and FA and negative correlations between age and MD and $\lambda_{\perp}$ in short-distance tracts in each lobe in controls, but only in frontal lobe of ASD subjects
Groen et al., 2011	12–16	80–116	17 HFA	14–17	96–114	25	1.5 T; 2.5 mm; 900 b; 30 GD	Superior longitudinal fasc./accurate fasc.; inferior longitudinal fasc.; left corona radiate	VBA; SPM5	ASD: Decreased FA in left and right superior and inferior longitudinal fasc. (but this effect is insignificant after adjusting for age and IQ); increased kurtosis of WM FA probability distribution; increased MD in all brain regions and shifted GM and WM MD probability distributions; no difference in GM or WM volume
Lo et al., 2011	14–16	101–116	15 HFA	14–16	101–121	15	3 T; 2.7 mm; 4000 b; 102 GD	Bilateral cingulum bundle; arcuate fasc.; uncinate fasc	DSI; ROI; ODF; MARINA; SPM5; SPSS 13.0	ASD: Decreased GFA in the three callosal fiber tracts Consistent leftward asymmetry in three pairs of association fibers in controls, but not in ASD subjects

(Continued)

TABLE 7 | Continued

Work	Autistic group			Control group			sMRI	Brain regions	Data analysis	Findings
	Age, y	IQ	Size	Age, y	IQ	Size				
Shukla et al., 2011a	12–13	106–112	26 AD, ASP	12–14	VIQ: 105–111	24	3 T; 2.7 mm; 2000 b; 15 GD	Inferior longitudinal fasc.; inferior fronto-occipital fasc.; superior longitudinal fasc./accurate fasc.; cingulum	TBSS; TLOBT	ASD: Decreased FA and increased MD in IC anterior and posterior limbs, CC, inferior and superior longitudinal fasc., inferior fronto-occipital fasc., CST, cingulum, and anterior thalamic radiation Age was positively correlated with FA in clusters of significant group differences and negatively correlated with MD and $\lambda_{\perp}$ in controls, but not in ASD
Bode et al., 2011	13–15	–	27 HFA	13–16	–	26	3 T; 3.5 mm; 1000 b; 40 GD	Optic radiation; right inferior fronto-occipital fasc	TBSS; BET; FNIRT	ASD: Increased FA and decreased $\lambda_{\perp}$ in the area containing clusters of optic radiation and right inferior fronto-occipital fasc.; no age-related correlations
Arns et al., 2013	9–16	–	19 HFA	8–16	–	16	3 T; 3 mm; 1250; 12 GD	Cingulum bundle	DT; Diffusion Toolkit; SPSS 20	ASD: Significant age-group interaction effects across FA, MD, $\lambda_{\perp}$ , and $\lambda_{\parallel}$ in cingulum bundle; increased MD, $\lambda_{\perp}$ , and $\lambda_{\parallel}$ and decreased FA in cingulum bundle of younger subjects
Nair et al., 2013	11–17	VIQ: 96–127	26	12–16	VIQ: 95–117	27	3 T; 2 mm; 1000 b; 61 GD	Thalamic connections with prefrontal, parietal-occipital, motor, somatosensory and temporal cortices	PT; FSL	ASD: Increased MD in tracts connecting thalamus with motor and somatosensory cortices bilaterally and with prefrontal ROI in right hemisphere; increased $\lambda_{\perp}$ in thalamic tracts for motor ROI bilaterally and somatosensory ROI in left and prefrontal ROI in right hemisphere, with a further marginal increase for somatosensory ROI in right hemisphere; negatively correlated FA and social and total ADOS scores in fronto-thalamic tracts and temporo-thalamic connections in left hemisphere ASD and controls: No FA or tract volume differences

(Continued)

TABLE 7 | Continued

Work	Autistic group			Control group			sMRI	Brain regions	Data analysis	Findings
	Age, y	IQ	Size	Age, y	IQ	Size				
Ikuta et al., 2014	15–21	77–117	21 AD, ASP	15–21	98–122	21	3 T; 2.5 mm; 1000 b; 31 GD	Cingulum bundle; anterior thalamic radiation	PT; ROI; ANCOVA; FSL; FLIRT	ASD: Decreased FA within cingulum bundle Significant group-age interaction, such that ASD subjects show no typical age-associated FA increases observed among controls; significant negative correlation between cingulum FA and total BRIEF score in ASD subjects, but not controls; negatively correlated cingulum FA and shifting subscale in ASD subjects, but not in controls; neither group effect, nor group-age interaction in anterior thalamic radiation FA; insignificantly correlated anterior thalamic radiation FA and BRIEF BRI scores

Additional abbreviations: b, b value unit (s/mm<sup>2</sup>); f, females; fasc., fasciculus; m, males; y, year;  
vs., versus; w.r.t., with respect to; REWMRA, Random-effects voxel-wise multiple regression analysis.  
ADC, apparent diffusion coefficient; ADOS, autism diagnostic observation schedule;  
AIR, automated image registration; ANCOVA, analysis of covariances; T, MRI magnetic field strength (tesla);  
ANOVA, analysis of variances; AUC, area under ROC curve;  
BCA, bivariate correlation analysis; BRIEF, behavior rating inventory of executive function;  
CC, corpus callosum; CST, cortico-spinal tract; DSI, diffusion spectrum imaging;  
DT, deterministic tractography; GD, gradient directions;  
GFA, generalized FA; GLM, general linear models; HRM, hierarchical regression model;  
IC, internal capsule; LME, linear mixed effect;  
MANOVA, multivariate analysis of variances;  
MVR, multivariate regression; ODF, orientation distribution function; PT, probabilistic tractography;  
QDA, quadratic discriminant analysis; ROC, receiver operating characteristic;  
SLI, specific LI; SPS, social responsiveness scale;  
TBSS, tract based spatial statistics; TLCBT, tract labeling cluster-based thresholding;  
3D Slicer, ANALYZE, BET, BioimageSuite, Diffusion Toolkit,  
DSI Studio, DTIprep, ExploreDTI, FiberViewer, FLIRT, FNIPT, FreeSurfer, FSL, IRTK, ITK-SNAP, MARINA, PSL,  
RESTORE, SAS, SPM, SPSS, T-SPOON, data processing packages.

TABLE 8 | DTI-based studying of the ASD at adulthood.

Work	Autistic group			Control group			sMRI	Brain regions	Data analysis	Findings
	Age, y	IQ	Size	Age, y	IQ	Size				
Catani et al., 2008	22–40	92–126	15 ASP	24–46	99–141	16	1.5 T; 2.5 mm	Inferior, middle, and superior cerebellar peduncles; intracerebellar fibers	DTI; ROI; RMA; SPSS	ASD: Decreased FA in short intracerebellar fibers and right superior cerebellar (output) peduncle; negatively correlated FA of left superior cerebellar peduncle and ADI-R social scores ASD and control groups: no MD differences
Conturo et al., 2008	23–29	102–106	17 HFA	23–29	99–141	17	1.5 T; 2.5 mm; 7 GD	Hippocampo- and amygdalo-fusiform pathways	ROI; DTI; JMP 7.0	ASD: Decreased $\lambda_{\perp}$ in right hippocampo-fusiform pathway; increased $\lambda_{\perp}$ and $\lambda_{\parallel}$ in left hippocampo-fusiform pathway and bilateral amygdalo-fusiform pathways; decreased across-fiber diffusivity related to poorer Benton face interpretation and performance IQ scores
Thakkar et al., 2008	19–41	VIQ: 112–136	12 ASP; NPDD	19–35	VIQ: 95–123	12	3 T; 2 mm; 700 b; 72 GD	Anterior cingulate cortex	ROI; FLIRT; FSL; TRegister2	ASD: Decreased FA in WM underlying rostra1 and dorsal anterior cingulate cortex bilaterally, dorsolateral prefrontal cortex, ventral prefrontal cortex, and intraparietal sulcus; increased FA in right insula; increased activation on correct trials and reduced FA in rostra1 anterior cingulate cortex WM, which is associated with higher ratings of repetitive ADI behavior
Pugliese et al., 2009	11–35	93–117	12 ASP	15–35	105–137	42	2.5 mm; 1300 b	Inferior longitudinal fasc.; inferior frontal occipital fasc.; uncinate fasc.; cingulum; fornix	DTI; ROI; GLM; Z-observation analysis; SPSS	No significant between-group differences in FA and MD ASD: Increased number of streamlines in right and left cingulum, and right and left inferior longitudinal fasc.; decreased number of streamlines in right uncinate fasc Significant age-related differences in MD and number of streamlines, but not FA within each group; significant age-related between-group MD differences in left uncinate fasc,

(Continued)



TABLE 8 | Continued

Work	Autistic group		Control group		sMRI	Brain regions	Data analysis	Findings
	Age, y	IQ	Size	Age, y	IQ	Size		
Bloemen et al., 2010	29–49	94–126	13 ASP	27–47	101–129	13	3 T; 2.5 mm; 1300 b; 64 GD	<p>inferior fronto-occipital fasc.; minor and major forceps; anterior and posterior corona radiata; bilateral anterior thalamic radiation</p> <p>VBA; ANCOVA; permutation-based testing; SPM2; SPSS 12.0; XBAM</p> <p>ASD: Reduced FA and increased <math>\lambda_{\perp}</math> over large brain areas; decreased MD in brain-stem cluster</p>
Beacher et al., 2012	22–42 m; 25–39 f	–	28 ASP	20–36 m; 24–40 f	–	30	1.5 T; 2.6 mm; 1000 b; 64 GD	<p>CC; cingulum bundle; CST; cerebellum</p> <p>ROI; ANOVA; Diffusion Toolkit</p> <p>Significant sex–diagnosis interactions in total WM volume, regional GM volume in right parietal operculum, and FA in body of CC, cingulum, and corona radiata</p> <p>Post-hoc comparisons: increased FA in male controls w.r.t. females, but no sex difference in ASD subjects</p>
Thomas et al., 2011	19–39	97–117	12 HFA	18–27	102–122	18	1.5 T; 3 mm; 850 b; 6 GD	<p>Inferior longitudinal and fronto-occipital fasc.; uncinate fasc.; 3 sub-portions of major inter-hemispheric fiber tract; CC</p> <p>DT; ROI; ANOVA; DTIstudio</p> <p>ASD: Increased WM volume of intra-hemispheric fibers, particularly, in left hemisphere, and decreased WM volume of minor forceps and CC body; negatively correlated minor forceps WM volume and ADI-R repetitive and stereotypical behavior scores; no group FA differences</p>
Langen et al., 2012	20–32	92–122	21 AD	22–34	96–124	22	3 T; 2.4 mm; 1300 b; 32 GD	<p>Fronto-striatal WM tracts</p> <p>DT; ROI; GLM; MANOVA; SROC; ExploreDTI; FLIRT; TrackVis; SPSS</p> <p>Decreased total brain WM volume and FA and increased MD of the tracts connecting putamen and accumbens to frontal cortical areas in ASD subjects</p> <p>ASD subjects had a go/nogo task No significant relationship between differences in FA and on ADI-R or ADOS scores in ASD subjects</p>

(Continued)

TABLE 8 | Continued

Work	Autistic group			Control group			sMRI	Brain regions	Data analysis	Findings
	Age, y	IQ	Size	Age, y	IQ	Size				
Pardini et al., 2012	21–23	47–61	22 LFA	–	–	–	3 T; 2 mm; 1000 b; 33 GD	uncinate fasciculus	VBA; FSL; SPM5; SPSS16	Independent from symptoms' severity and IQ at therapy onset and from subject's age at time of MRI scanning and significant correlation between clinical improvement and FA of two WM clusters in uncinate fasc.; independent of symptoms severity and IQ scores and significant correlation between increasing uncinate fasc. structural organization and clinical improvement; precocity, and intervention length; more significant clinical improvement and higher uncinate fasc. FA for highly therapy-adherent subjects w.r.t. moderately adherent ones
Lewis et al., 2013	22–42	68–108 VIQ	20 AD	22–42	–	22	3 T; 3 mm; 1400 b; 15 GD	CC	PT; ROI; RFTCS; CIVET	ASD: Negatively correlated CC fiber length, adjusted for intracranial volume, and CC size; positively correlated adjusted CC fiber length and $\lambda_{\perp}$
Kana et al., 2014	20–22	102–112	8 AD	21–23	110–114	13	3 T; 3 mm; 1000 b; 12 GD	Posterior CC midbody; corona radiata; WM underlying right middle/superior temporal lobe	TBSS; ANOVA; FSL	ASD: Decreased FA in WM underlying temporal lobe; decreased functional connectivity participants in ToM-related areas and ventral premotor areas; no relationship between DTI and fMRI results
Perkins et al., 2014	15–25	–	12 HFA, ASP	16–22	–	12	3 T; 2.5 mm; 1000 b; 25 GD	Superior longitudinal fascicles; accurate fasc.; cingulum bundle; CC genu, splenium, and body; IC anterior and posterior limb	TBSS; SA; GLM; FSL	ASD: Decreased FA and increased $\lambda_{\perp}$ in left hemisphere, predominantly thalamic and fronto-parietal pathways; significantly increased WM disturbance in left w.r.t. right hemisphere, according to symmetry analysis

Additional abbreviations: b, b value unit (s/mm<sup>2</sup>); f, females; fasc., fasciculus; m, males; y, year; T, MRI magnetic field strength (tesla); w.r.t., with respect to ADI-R, autism diagnostic interview – revised; ANCOVA, analysis of covariances; ANOVA, analysis of variances; CC, corpus callosum; CST, cortico-spinal tract; DT, deterministic tractography; GD, gradient directions; GLM, general linear models; IC, internal capsule; MANOVA, multivariate analysis of variances; PT, probabilistic tractography; RMA, repeated measures analysis; SROC, Spearman's rank-order correlation; ToM, theory of mind; CIVET, Diffusion Toolkit, DTIstudio, ExploreDTI, FiberViewer, FLIRT, FSL, JIMP7, RFTCS, RIVA, SPM, SPSS, Tregister2, TrackVis, XBAM, data processing packages.

brain in older children and adolescents. Most of the larger studies have reported reduced FA and increased diffusivity in the ASD groups. Also, the ROI-based DTI studies of the older population (older children, adolescents, and adults) vs. their controls confirm the finding of decreased FA in various brain areas including the anterior cingulate, the superior temporal gyrus, and the temporal stem WM. However, since the ROIs target only specific components of particular WM tracts, conclusions cannot be drawn on the entire WM tract or other infrequently examined tracts. Nonetheless, studying the DTI of older children, adolescents, and adults using the VBA, TBSS, and ROI methods suggest that the ASD-related microstructural WM alterations differ depending on the age of the individuals studied.

Mostly, the deterministic, rather than the advanced probabilistic tractography is employed to study the DTI, and the bulk of these studies have focused on the WM abnormalities in the uncinate fasciculus, the arcuate fasciculus, the cingulum bundle, the inferior longitudinal fasciculus, and the inferior fronto-occipital fasciculus. The abnormalities include lower FA and higher diffusivity (primarily, in children and adolescents) and altered macrostructure (mainly, in adults). The only ASD-related longitudinal DTI study to date Wolff et al. (2012) confirmed that at least during the first 2 years of life, a number of WM tracts seem to be affected by a dynamic process occurring in the brains of children who develop the ASD.

## REFERENCES

- Abell, F., Krams, M., Ashburner, J., Passingham, R., Friston, K., Frackowiak, R., et al. (1999). The neuroanatomy of autism: a voxel-based whole brain analysis of structural scans. *Neuroreport* 10, 1647–1651. doi: 10.1097/00001756-199906030-00005
- Adluru, N., Hinrichs, C., Chung, M. K., Lee, J.-E., Singh, V., Bigler, E. D., et al. (2009). “Classification in dti using shapes of white matter tracts,” in *Engineering in Medicine and Biology Society, 2009. EMBC 2009. Annual International Conference of the IEEE* (Minneapolis, MN: IEEE), 2719–2722. doi: 10.1109/iembs.2009.5333386
- Adolphs, R., Tranel, D., Damasio, H., and Damasio, A. (1994). Impaired recognition of emotion in facial expressions following bilateral damage to the human amygdala. *Nature* 372, 669–672. doi: 10.1038/372669a0
- Akshoomoff, N., Lord, C., Lincoln, A. J., Courchesne, R. Y., Carper, R. A., Townsend, J., et al. (2004). Outcome classification of preschool children with autism spectrum disorders using MRI brain measures. *J. Am. Acad. Child Adolesc. Psychiatry* 43, 349–357. doi: 10.1097/00004583-200403000-00018
- Alexander, A. L., Lee, J. E., Lazar, M., Boudos, R., DuBray, M. B., Oakes, T. R., et al. (2007). Diffusion tensor imaging of the corpus callosum in autism. *Neuroimage* 34, 61–73. doi: 10.1016/j.neuroimage.2006.08.032
- Ameis, S. H., Fan, J., Rockel, C., Soorya, L., Wang, A. T., and Anagnostou, E. (2013). Altered cingulum bundle microstructure in autism spectrum disorder. *Acta Neuropsychiatrica* 25, 275–282. doi: 10.1017/neu.2013.2
- Ameis, S. H., Fan, J., Rockel, C., Voineskos, A. N., Lobaugh, N. J., Soorya, L., et al. (2011). Impaired structural connectivity of socio-emotional circuits in autism spectrum disorders: a diffusion tensor imaging study. *PLoS ONE* 6:e28044. doi: 10.1371/journal.pone.0028044
- Arimura, H., Magome, T., Yamashita, Y., and Yamamoto, D. (2009a). Computer-aided diagnosis systems for brain diseases in magnetic resonance images. *Algorithms* 2, 925–952. doi: 10.3390/a2030925
- Aylward, E., Minshew, N., Goldstein, G., Honeycutt, N., Augustine, A., Yates, K., et al. (1999). MRI volumes of amygdala and hippocampus in non-mentally retarded autistic adolescents and adults. *Neurology* 53, 2145–2145. doi: 10.1212/WNL.53.9.2145
- Aylward, E. H., Minshew, N., Field, K., Sparks, B., and Singh, N. (2002). Effects of age on brain volume and head circumference in autism. *Neurology* 59, 175–183. doi: 10.1212/WNL.59.2.175
- Bachevalier, J. (1994). Medial temporal lobe structures and autism: a review of clinical and experimental findings. *Neuropsychologia* 32, 627–648. doi: 10.1016/0028-3932(94)90025-6
- Bailey, A., Luthert, P., Bolton, P., Le Couteur, A., Rutter, M., and Harding, B. (1993). Autism and megalencephaly. *Lancet* 341, 1225–1226. doi: 10.1016/0140-6736(93)91065-T
- Bailey, A., Luthert, P., Dean, A., Harding, B., Janota, I., Montgomery, M., et al. (1998). A clinicopathological study of autism. *Brain* 121, 889–905. doi: 10.1093/brain/121.5.889
- Barnea-Goraly, N., Frazier, T. W., Piacenza, L., Minshew, N. J., Keshavan, M. S., Reiss, A. L., et al. (2014). A preliminary longitudinal volumetric mri study of amygdala and hippocampal volumes in autism. *Progress Neuro-Psychopharmacol. Biol. Psychiatry* 48, 124–128. doi: 10.1016/j.pnpbp.2013.09.010
- Barnea-Goraly, N., Kwon, H., Menon, V., Eliez, S., Lotspeich, L., and Reiss, A. L. (2004). White matter structure in autism: preliminary evidence from diffusion tensor imaging. *Biol. Psychiatry* 55, 323–326. doi: 10.1016/j.biopsych.2003.10.022
- Barnea-Goraly, N., Lotspeich, L. J., and Reiss, A. L. (2010). Similar white matter aberrations in children with autism and their unaffected siblings: a diffusion tensor imaging study using tract-based spatial statistics. *Arch. Gen. Psychiatry* 67, 1052–1060. doi: 10.1001/archgenpsychiatry.2010.123
- Bashat, D. B., Kronfeld-Duenias, V., Zachor, D. A., Ekstein, P. M., Hendler, T., Tarrasch, R., et al. (2007). Accelerated maturation of white matter in young children with autism: a high b value DWI study. *Neuroimage* 37, 40–47. doi: 10.1016/j.neuroimage.2007.04.060

## General conclusions

Although a variety of MRI-based studies consisting of small groups of individuals, ranging widely in age, present diverse clinical ASD symptoms compared to controls, these studies have yielded valuable, yet varying results. Multi-site studies with large patient groups that comprehensively characterize the clinical, behavioral, and cognitive symptoms may be one of the most important strategies for increasing the probability for the discovery of new, effective biomarkers. Future studies of particular importance will track brain maturation from infancy to adulthood in individuals at high risk of developing ASD by using multi-modality macro-/microstructural and functional brain images. By studying a larger, non-gender biased population of patients, it is anticipated that the “false positive” rate of ASD diagnosis will decrease.

## AUTHOR CONTRIBUTIONS

MI: wrote the structural MRI survey part, and helped in DTI part. Reviewed the entire paper. RK: reviewed the paper, reshaped the outline and structure. MM: wrote the DTI part. AELT: reviewed the paper, helped collecting literature. MC: reviewed, emphasized the clinical aspect of the paper, edited the future directions section. GG: reviewed the engineering aspect of the paper, reshaped the paper, and extensively edited it. AELB: directed the paper, helped with the outline and the general structure.

- Basser, P. J., and Jones, D. K. (2002). Diffusion-tensor MRI: theory, experimental design and data analysis—a technical review. *NMR Biomed.* 15, 456–467. doi: 10.1002/nbm.783
- Basser, P. J., Mattiello, J., and LeBihan, D. (1994a). Estimation of the effective self-diffusion tensor from the NMR spin echo. *J. Magn. Reson. B* 103, 247–254. doi: 10.1006/jmrb.1994.1037
- Basser, P. J., Mattiello, J., and LeBihan, D. (1994b). MR diffusion tensor spectroscopy and imaging. *Biophys. J.* 66, 259–267. doi: 10.1016/S0006-3495(94)80775-1
- Basser, P. J., Pajevic, S., Pierpaoli, C., Duda, J., and Aldroubi, A. (2000). *In vivo* fiber tractography using DT-MRI data. *Magn. Reson. Med.* 44, 625–632. doi: 10.1002/1522-2594(200010)44:4<625::AID-MRM17>3.0.CO;2-O
- Bauman, M., and Kemper, T. L. (1985). Histoanatomic observations of the brain in early infantile autism. *Neurology* 35, 866–866. doi: 10.1212/WNL.35.6.866
- Bauman, M. L., and Kemper, T. L. (1994). Neuroanatomic observations of the brain in autism. *Neurobiol. Autism* 612, 119–145.
- Beacher, F., Minati, L., Baron-Cohen, S., Lombardo, M., Lai, M.-C., Gray, M., et al. (2012). Autism attenuates sex differences in brain structure: a combined voxel-based morphometry and diffusion tensor imaging study. *Am. J. Neuroradiol.* 33, 83–89. doi: 10.3174/ajnr.A2880
- Behrens, T., Woolrich, M., Jenkinson, M., Johansen-Berg, H., Nunes, R., Clare, S., et al. (2003). Characterization and propagation of uncertainty in diffusion-weighted MR imaging. *Magn. Reson. Med.* 50, 1077–1088. doi: 10.1002/mrm.10609
- Belongie, S., Malik, J., and Puzicha, J. (2002). Shape matching and object recognition using shape contexts. *IEEE Trans. Patt. Anal. Mach. Intell.* 24, 509–522. doi: 10.1109/34.993558
- Billeci, L., Calderoni, S., Tosetti, M., Catani, M., and Muratori, F. (2012). White matter connectivity in children with autism spectrum disorders: a tract-based spatial statistics study. *BMC Neurol.* 12:148. doi: 10.1186/1471-2377-12-148
- Blackmon, K. (2015). Structural MRI biomarkers of shared pathogenesis in autism spectrum disorder and epilepsy. *Epilepsy Behav.* 47, 172–182. doi: 10.1016/j.yebeh.2015.02.017
- Bloemen, O. J., Deeley, Q., Sundram, F., Daly, E. M., Barker, G. J., Jones, D. K., et al. (2010). White matter integrity in asperger syndrome: a preliminary diffusion tensor magnetic resonance imaging study in adults. *Autism Res.* 3, 203–213. doi: 10.1002/aur.146
- Boddaert, N., Chabane, N., Gervais, H., Good, C., Bourgeois, M., Plumet, M., et al. (2004). Superior temporal sulcus anatomical abnormalities in childhood autism: a voxel-based morphometry MRI study. *Neuroimage* 23, 364–369. doi: 10.1016/j.neuroimage.2004.06.016
- Bode, M. K., Mattila, M.-L., Kiviniemi, V., Rahko, J., Moilanen, I., Ebeling, H., et al. (2011). White matter in autism spectrum disorders—evidence of impaired fiber formation. *Acta Radiol.* 52, 1169–1174. doi: 10.1258/ar.2011.110197
- Bonilha, L., Cendes, F., Rorden, C., Eckert, M., Dalgalarondo, P., Li, L. M., et al. (2008). Gray and white matter imbalance—typical structural abnormality underlying classic autism? *Brain Dev.* 30, 396–401. doi: 10.1016/j.braindev.2007.11.006
- Brambilla, P., Hardan, A., di Nemi, S. U., Perez, J., Soares, J. C., and Barale, F. (2003). Brain anatomy and development in autism: review of structural MRI studies. *Brain Res. Bull.* 61, 557–569. doi: 10.1016/j.brainresbull.2003.06.001
- Brito, A. R., Vasconcelos, M. M., Domingues, R. C., da Cruz, H. Jr., Celso, L., Rodrigues, L. D. S., et al. (2009). Diffusion tensor imaging findings in school-aged autistic children. *J. Neuroimaging* 19, 337–343. doi: 10.1111/j.1552-6569.2009.00366.x
- Brun, C. C., Nicolson, R., Leporé, N., Chou, Y.-Y., Vidal, C. N., DeVito, T. J., et al. (2009). Mapping brain abnormalities in boys with autism. *Hum. Brain Mapp.* 30, 3887–3900. doi: 10.1002/hbm.20814
- Carper, R. A., and Courchesne, E. (2000). Inverse correlation between frontal lobe and cerebellum sizes in children with autism. *Brain* 123, 836–844. doi: 10.1093/brain/123.4.836
- Carper, R. A., Moses, P., Tighe, Z. D., and Courchesne, E. (2002). Cerebral lobes in autism: early hyperplasia and abnormal age effects. *Neuroimage* 16, 1038–1051. doi: 10.1006/nimg.2002.1099
- Casanova, M. F., Buxhoeveden, D. P., and Brown, C. (2002a). Clinical and macroscopic correlates of minicolumnar pathology in autism. *J. Child Neurol.* 17, 692–695. doi: 10.1177/088307380201700908
- Casanova, M. F., Buxhoeveden, D. P., Switala, A. E., and Roy, E. (2002b). Neuronal density and architecture (gray level index) in the brains of autistic patients. *J. Child Neurol.* 17, 515–521. doi: 10.1177/088307380201700708
- Casanova, M. F., van Kooten, I. A., Switala, A. E., van Engeland, H., Heinsen, H., Steinbusch, H. W., et al. (2006). Minicolumnar abnormalities in autism. *Acta Neuropathol.* 112, 287–303. doi: 10.1007/s00401-006-0085-5
- Catani, M., Jones, D. K., Daly, E., Embiricos, N., Deeley, Q., Pugliese, L., et al. (2008). Altered cerebellar feedback projections in asperger syndrome. *Neuroimage* 41, 1184–1191. doi: 10.1016/j.neuroimage.2008.03.041
- Chen, R., Jiao, Y., and Herskovits, E. H. (2011). Structural MRI in autism spectrum disorder. *Pediatr. Res.* 69, 63R–68R. doi: 10.1203/pdr.0b013e318212c2b3
- Cheon, K.-A., Kim, Y.-S., Oh, S.-H., Park, S.-Y., Yoon, H.-W., Herrington, J., et al. (2011). Involvement of the anterior thalamic radiation in boys with high functioning autism spectrum disorders: a diffusion tensor imaging study. *Brain Res.* 1417, 77–86. doi: 10.1016/j.brainres.2011.08.020
- Cheung, C., Chua, S., Cheung, V., Khong, P., Tai, K., Wong, T., et al. (2009). White matter fractional anisotropy differences and correlates of diagnostic symptoms in autism. *J. Child Psychol. Psychiatry* 50, 1102–1112. doi: 10.1111/j.1469-7610.2009.02086.x
- Chung, M. K., Dalton, K. M., Alexander, A. L., and Davidson, R. J. (2004). Less white matter concentration in autism: 2d voxel-based morphometry. *Neuroimage* 23, 242–251. doi: 10.1016/j.neuroimage.2004.04.037
- Ciesielski, K. T., Harris, R. J., Hart, B. L., and Pabst, H. F. (1997). Cerebellar hypoplasia and frontal lobe cognitive deficits in disorders of early childhood. *Neuropsychologia* 35, 643–655. doi: 10.1016/S0028-3932(96)00119-4
- Conti, E., Calderoni, S., Marchi, V., Muratori, F., Cioni, G., and Guzzetta, A. (2015). The first 1000 days of the autistic brain: a systematic review of diffusion imaging studies. *Front. Hum. Neurosci.* 9:159. doi: 10.3389/fnhum.2015.00159
- Conturo, T. E., Williams, D. L., Smith, C. D., Gultepe, E., Akbudak, E., and Minshew, N. J. (2008). Neuronal fiber pathway abnormalities in autism: an initial MRI diffusion tensor tracking study of hippocampo-fusiform and amygdalo-fusiform pathways. *J. Int. Neuropsychol. Soc.* 14, 933–946. doi: 10.1017/S1355617708081381
- Courchesne, E., Karns, C., Davis, H., Ziccardi, R., Carper, R., Tighe, Z., et al. (2001). Unusual brain growth patterns in early life in patients with autistic disorder an MRI study. *Neurology* 57, 245–254. doi: 10.1212/WNL.57.2.245
- Courchesne, E., Müller, R.-A., and Saitoh, O. (1999). Brain weight in autism: normal in the majority of cases, megalencephalic in rare cases. *Neurology* 52, 1057–1057. doi: 10.1212/WNL.52.5.1057
- Courchesne, E., Press, G., and Yeung-Courchesne, R. (1993). Parietal lobe abnormalities detected with MR in patients with infantile autism. *Am. J. Roentgenol.* 160, 387–393. doi: 10.2214/ajr.160.2.8424359
- Courchesne, E., Saitoh, O., Yeung-Courchesne, R., Press, G., Lincoln, A., Haas, R., et al. (1994a). Abnormality of cerebellar vermal lobules VI and VII in patients with infantile autism: identification of hypoplastic and hyperplastic subgroups with MR imaging. *Am. J. Roentgenol.* 162, 123–130. doi: 10.2214/ajr.162.1.8273650
- Courchesne, E., Townsend, J., and Saitoh, O. (1994b). The brain in infantile autism posterior fossa structures are abnormal. *Neurology* 44, 214. doi: 10.1212/WNL.44.2.214
- Courchesne, E., Yeung-Courchesne, R., Hesselink, J., and Jernigan, T. (1988). Hypoplasia of cerebellar vermal lobules VI and VII in autism. *N. Engl. J. Med.* 318, 1349–1354. doi: 10.1056/NEJM198805263182102
- Damasio, A. R., and Maurer, R. G. (1978). A neurological model for childhood autism. *Arch. Neurol.* 35, 777–786. doi: 10.1001/archneur.1978.00500360001001
- Dawson, G., Meltzoff, A. N., Osterling, J., and Rinaldi, J. (1998). Neuropsychological correlates of early symptoms of autism. *Child Dev.* 69, 1276–1285. doi: 10.2307/1132265
- Dierker, D. L., Feczko, E., Pruett, J. R. Jr., Petersen, S. E., Schlaggar, B. L., Constantino, J. N., et al. (2015). Analysis of cortical shape in children with simplex autism. *Cereb. Cortex* 25, 1042–1051. doi: 10.1093/cercor/bht294
- Dong, Q., Welsh, R. C., Chenevert, T. L., Carlos, R. C., Maly-Sundgren, P., Gomez-Hassan, D. M., et al. (2004). Clinical applications of diffusion tensor imaging. *J. Magn. Reson. Imaging* 19, 6–18. doi: 10.1002/jmri.10424
- Duerden, E. G., Card, D., Roberts, S. W., Mak-Fan, K. M., Chakravarty, M. M., Lerch, J. P., et al. (2014). Self-injurious behaviours are associated with

- alterations in the somatosensory system in children with autism spectrum disorder. *Brain Struct. Funct.* 219, 1251–1261. doi: 10.1007/s00429-013-0562-2
- Egaas, B., Courchesne, E., and Saitoh, O. (1995). Reduced size of corpus callosum in autism. *Arch. Neurol.* 52, 794–801. doi: 10.1001/archneur.1995.00540320070014
- Elia, M., Ferri, R., Musumeci, S. A., Panerai, S., Bottitta, M., and Scuderi, C. (2000). Clinical correlates of brain morphometric features of subjects with low-functioning autistic disorder. *J. Child Neurol.* 15, 504–508. doi: 10.1177/088307380001500802
- Elia, M., Manfre, L., Ferri, R., Musumeci, S., Panerai, S., Bottitta, M., et al. (1997). Brain morphometry and psychobehavioural measures in autistic low-functioning subjects. *Rivista Neuroradiologia* 10, 431–436. doi: 10.1177/197140099701000406
- Elison, J. T., Paterson, S. J., Wolff, J. J., Reznick, J. S., Sasson, N. J., Gu, H., et al. (2014). White matter microstructure and atypical visual orienting in 7-month-olds at risk for autism. *Am. J. Psychiatry* 170, 899–908. doi: 10.1176/appi.ajp.2012.12091150
- Elnakib, A., Casanova, M., Gimel'farb, G., Switala, A. E., and El-Baz, A. (2011). "Autism diagnostics by centerline-based shape analysis of the corpus callosum," in *Biomedical Imaging: From Nano to Macro, 2011 IEEE International Symposium on* (Chicago, IL: IEEE), 1843–1846. doi: 10.1109/isbi.2011.5872766
- Fletcher, P. T., Whitaker, R. T., Tao, R., DuBray, M. B., Froehlich, A., Ravichandran, C., et al. (2010). Microstructural connectivity of the arcuate fasciculus in adolescents with high-functioning autism. *Neuroimage* 51, 1117–1125. doi: 10.1016/j.neuroimage.2010.01.083
- Fombonne, E., Rogé, B., Claverie, J., Courty, S., and Fremolle, J. (1999). Microcephaly and macrocephaly in autism. *J. Autism Dev. Disord.* 29, 113–119. doi: 10.1023/A:1023036509476
- Frazier, T. W., Keshavan, M. S., Minshew, N. J., and Hardan, A. Y. (2012). A two-year longitudinal MRI study of the corpus callosum in autism. *J. Autism Dev. Disord.* 42, 2312–2322. doi: 10.1007/s10803-012-1478-z
- Gaffney, G. R., Kuperman, S., Tsai, L. Y., and Minchin, S. (1988). Morphological evidence for brainstem involvement in infantile autism. *Biol. Psychiatry* 24, 578–586. doi: 10.1016/0006-3223(88)90168-0
- Gaffney, G. R., Kuperman, S., Tsai, L. Y., and Minchin, S. (1989). Forebrain structure in infantile autism. *J. Am. Acad. Child Adolesc. Psychiatry* 28, 534–537. doi: 10.1097/00004583-198907000-00011
- Gaffney, G. R., Kuperman, S., Tsai, L. Y., Minchin, S., and Hassanein, K. M. (1987a). Midsagittal magnetic resonance imaging of autism. *Br. J. Psychiatry* 151, 831–833. doi: 10.1192/bjp.151.6.831
- Gaffney, G. R., Tsai, L. Y., Kuperman, S., and Minchin, S. (1987b). Cerebellar structure in autism. *Am. J. Dis. Child.* 141, 1330–1332. doi: 10.1001/archpedi.1987.04460120096044
- Garber, H. J., and Ritvo, E. R. (1992). Magnetic resonance imaging of the posterior fossa in autistic adults. *Am. J. Psychiatry* 149, 245–247.
- Garber, H. J., Ritvo, E. R., Chiu, L. C., Griswold, V. J., Kashanian, A., Freeman, B. J., et al. (1989). A magnetic resonance imaging study of autism: normal fourth ventricle size and absence of pathology. *Am. J. Psychiatry* 146, 532–534.
- George, M. S., Costa, D. C., Kouris, K., Ring, H. A., and Ell, P. J. (1992). Cerebral blood flow abnormalities in adults with infantile autism. *J. Nervous Ment. Dis.* 180, 413–417. doi: 10.1097/00005053-199207000-00002
- Giedd, J. N., Snell, J. W., Lange, N., Rajapakse, J. C., Casey, B., Kozuch, P. L., et al. (1996). Quantitative magnetic resonance imaging of human brain development: ages 4–18. *Cereb. Cortex* 6, 551–559. doi: 10.1093/cercor/6.4.551
- Gillberg, C. (1999). Neurodevelopmental processes and psychological functioning in autism. *Dev. Psychopathol.* 11, 567–587. doi: 10.1017/S0954579499002217
- Girgis, R. R., Minshew, N. J., Melhem, N. M., Nutche, J. J., Keshavan, M. S., and Hardan, A. Y. (2007). Volumetric alterations of the orbitofrontal cortex in autism. *Prog. Neuro-Psychopharmacol. Biol. Psychiatry* 31, 41–45. doi: 10.1016/j.pnpbp.2006.06.007
- Gori, I., Giuliano, A., Muratori, F., Saviozzi, I., Oliva, P., Tancredi, R., et al. (2015). Gray matter alterations in young children with autism spectrum disorders: comparing morphometry at the voxel and regional level. *J. Neuroimaging* 25, 866–874. doi: 10.1111/jon.12280
- Groen, W. B., Buitelaar, J. K., Van Der Gaag, R. J., and Zwiers, M. P. (2011). Pervasive microstructural abnormalities in autism: a DTI study. *J. Psychiatry Neurosci.* 36, 32. doi: 10.1503/jpn.090100
- Gropman, A., Gertz, B., Shattuck, K., Kahn, I., Seltzer, R., Krivitsky, L., et al. (2010). Diffusion tensor imaging detects areas of abnormal white matter microstructure in patients with partial ornithine transcarbamylase deficiency. *Am. J. Neuroradiol.* 31, 1719–1723. doi: 10.3174/ajnr.A2122
- Hadjikhani, N., Joseph, R. M., Snyder, J., and Tager-Flusberg, H. (2006). Anatomical differences in the mirror neuron system and social cognition network in autism. *Cereb. Cortex* 16, 1276–1282. doi: 10.1093/cercor/bhj069
- Hardan, A. Y., Girgis, R. R., Adams, J., Gilbert, A. R., Keshavan, M. S., and Minshew, N. J. (2006a). Abnormal brain size effect on the thalamus in autism. *Psychiatry Res.* 147, 145–151. doi: 10.1016/j.psychres.2005.12.009
- Hardan, A. Y., Jou, R. J., Keshavan, M. S., Varma, R., and Minshew, N. J. (2004). Increased frontal cortical folding in autism: a preliminary MRI study. *Psychiatry Res.* 131, 263–268. doi: 10.1016/j.psychres.2004.06.001
- Hardan, A. Y., Kilpatrick, M., Keshavan, M. S., and Minshew, N. J. (2003). Motor performance and anatomic magnetic resonance imaging (MRI) of the basal ganglia in autism. *J. Child Neurol.* 18, 317–324. doi: 10.1177/08830738030180050801
- Hardan, A. Y., Libove, R. A., Keshavan, M. S., Melhem, N. M., and Minshew, N. J. (2009). A preliminary longitudinal magnetic resonance imaging study of brain volume and cortical thickness in autism. *Biol. Psychiatry* 66, 320–326. doi: 10.1016/j.biopsych.2009.04.024
- Hardan, A. Y., Minshew, N. J., Harenski, K., and Keshavan, M. S. (2001a). Posterior fossa magnetic resonance imaging in autism. *J. Am. Acad. Child Adolesc. Psychiatry* 40, 666–672. doi: 10.1097/00004583-200106000-00011
- Hardan, A. Y., Minshew, N. J., Mallikarjunn, M., and Keshavan, M. S. (2001b). Brain volume in autism. *J. Child Neurol.* 16, 421–424. doi: 10.1177/088307380101600607
- Hardan, A. Y., Muddasani, S., Vemulapalli, M., Keshavan, M. S., and Minshew, N. J. (2006b). An MRI study of increased cortical thickness in autism. *Am. J. Psychiatry* 163, 1290–1292. doi: 10.1176/ajp.2006.163.7.1290
- Hashimoto, T., Murakawa, K., Miyazaki, M., Tayama, M., and Kuroda, Y. (1992). Magnetic resonance imaging of the brain structures in the posterior fossa in retarded autistic children. *Acta Paediatrica* 81, 1030–1034. doi: 10.1111/j.1651-2227.1992.tb12169.x
- Hashimoto, T., Tayama, M., Miyazaki, M., Murakawa, K., and Kuroda, Y. (1993). Brainstem and cerebellar vermis involvement in autistic children. *J. Child Neurol.* 8, 149–153. doi: 10.1177/088307389300800207
- Hashimoto, T., Tayama, M., Murakawa, K., Yoshimoto, T., Miyazaki, M., Harada, M., et al. (1995). Development of the brainstem and cerebellum in autistic patients. *J. Autism Dev. Disord.* 25, 1–18. doi: 10.1007/BF02178163
- Hazlett, H. C., Gu, H., McKinstry, R. C., Shaw, D. W., Botteron, K. N., Dager, S. R., et al. (2012). Brain volume findings in 6-month-old infants at high familial risk for autism. *Am. J. Psychiatry* 169, 601–608. doi: 10.1176/appi.ajp.2012.11091425
- Hazlett, H. C., Poe, M., Gerig, G., Smith, R. G., Provenzale, J., Ross, A., et al. (2005). Magnetic resonance imaging and head circumference study of brain size in autism: birth through age 2 years. *Arch. Gen. Psychiatry* 62, 1366–1376. doi: 10.1001/archpsyc.62.12.1366
- Hazlett, H. C., Poe, M. D., Gerig, G., Smith, R. G., and Piven, J. (2006). Cortical gray and white brain tissue volume in adolescents and adults with autism. *Biol. Psychiatry* 59, 1–6. doi: 10.1016/j.biopsych.2005.06.015
- Haznedar, M. M., Buchsbaum, M. S., Hazlett, E. A., LiCalzi, E. M., Cartwright, C., and Hollander, E. (2006). Volumetric analysis and three-dimensional glucose metabolic mapping of the striatum and thalamus in patients with autism spectrum disorders. *Am. J. Psychiatry* 163, 1252–1263. doi: 10.1176/ajp.2006.163.7.1252
- Herbert, M., Ziegler, D., Deutsch, C., Lange, N., Bakardjiev, A., et al. (2003). Dissociations of cerebral cortex, subcortical and cerebral white matter volumes in autistic boys. *Brain* 126, 1182–1192. doi: 10.1093/brain/awg110
- Holttum, J. R., Minshew, N. J., Sanders, R. S., and Phillips, N. E. (1992). Magnetic resonance imaging of the posterior fossa in autism. *Biol. Psychiatry* 32, 1091–1101. doi: 10.1016/0006-3223(92)90189-7
- Hong, S., Ke, X., Tang, T., Hang, Y., Chu, K., Huang, H., et al. (2011). Detecting abnormalities of corpus callosum connectivity in autism using magnetic resonance imaging and diffusion tensor tractography. *Psychiatry Res.* 194, 333–339. doi: 10.1016/j.psychres.2011.03.009
- Horwitz, B., Rumsey, J. M., Grady, C. L., and Rapoport, S. I. (1988). The cerebral metabolic landscape in autism: intercorrelations of regional glucose utilization. *Arch. Neurol.* 45, 749–755. doi: 10.1001/archneur.1988.00520310055018



- Hsu, M., Yeung-Courchesne, R., Courchesne, E., and Press, G. A. (1991). Absence of magnetic resonance imaging evidence of pontine abnormality in infantile autism. *Arch. Neurol.* 48, 1160–1163. doi: 10.1001/archneur.1991.00530230068024
- Hua, X., Thompson, P. M., Leow, A. D., Madsen, S. K., Caplan, R., Alger, J. R., et al. (2013). Brain growth rate abnormalities visualized in adolescents with autism. *Hum. Brain Mapp.* 34, 425–436. doi: 10.1002/hbm.21441
- Hyde, K. L., Samson, F., Evans, A. C., and Mottron, L. (2010). Neuroanatomical differences in brain areas implicated in perceptual and other core features of autism revealed by cortical thickness analysis and voxel-based morphometry. *Hum. Brain Mapp.* 31, 556–566. doi: 10.1002/hbm.20887
- Ikuta, T., Shafritz, K. M., Bregman, J., Peters, B. D., Gruner, P., Malhotra, A. K., et al. (2014). Abnormal cingulum bundle development in autism: a probabilistic tractography study. *Psychiatry Res.* 221, 63–68. doi: 10.1016/j.psychres.2013.08.002
- Ingalhalikar, M., Parker, D., Bloy, L., Roberts, T. P., and Verma, R. (2011). Diffusion based abnormality markers of pathology: toward learned diagnostic prediction of ASD. *Neuroimage* 57, 918–927. doi: 10.1016/j.neuroimage.2011.05.023
- Jeong, J.-W., Kumar, A., Sundaram, S. K., Chugani, H. T., and Chugani, D. C. (2011). Sharp curvature of frontal lobe white matter pathways in children with autism spectrum disorders: tract-based morphometry analysis. *Am. J. Neuroradiol.* 32, 1600–1606. doi: 10.3174/ajnr.A2557
- Jiao, Y., Chen, R., Ke, X., Chu, K., Lu, Z., and Herskovits, E. H. (2010). Predictive models of autism spectrum disorder based on brain regional cortical thickness. *Neuroimage* 50, 589–599. doi: 10.1016/j.neuroimage.2009.12.047
- Joseph, R. M., Fricker, Z., Fenoglio, A., Lindgren, K. A., Knaus, T. A., and Tager-Flusberg, H. (2014). Structural asymmetries of language-related gray and white matter and their relationship to language function in young children with ASD. *Brain Imaging Behav.* 8, 60–72. doi: 10.1007/s11682-013-9245-0
- Jou, R., Mateljevic, N., Kaiser, M., Sugrue, D., Volkmar, F., and Pelphrey, K. (2011a). Structural neural phenotype of autism: preliminary evidence from a diffusion tensor imaging study using tract-based spatial statistics. *Am. J. Neuroradiol.* 32, 1607–1613. doi: 10.3174/ajnr.A2558
- Jou, R. J., Frazier, T. W., Keshavan, M. S., Minshew, N. J., and Hardan, A. Y. (2013). A two-year longitudinal pilot MRI study of the brainstem in autism. *Behav. Brain Res.* 251, 163–167. doi: 10.1016/j.bbr.2013.04.021
- Jou, R. J., Jackowski, A. P., Papademetris, X., Rajeevan, N., Staib, L. H., and Volkmar, F. R. (2011b). Diffusion tensor imaging in autism spectrum disorders: preliminary evidence of abnormal neural connectivity. *Aust. New Zealand J. Psychiatry* 45, 153–162. doi: 10.3109/00048674.2010.534069
- Jou, R. J., Minshew, N. J., Melhem, N. M., Keshavan, M. S., and Hardan, A. Y. (2009). Brainstem volumetric alterations in children with autism. *Psychol. Med.* 39, 1347–1354. doi: 10.1017/S0033291708004376
- Kana, R. K., Libero, L. E., Hu, C. P., Deshpande, H. D., and Colburn, J. S. (2014). Functional brain networks and white matter underlying theory-of-mind in autism. *Soc. Cogn. Affect. Neurosci.* 9, 98–105. doi: 10.1093/scan/nss106
- Kaufmann, W. E., Cooper, K. L., Mostofsky, S. H., Capone, G. T., Kates, W. R., Newschaffer, C. J., et al. (2003). Specificity of cerebellar vermian abnormalities in autism: a quantitative magnetic resonance imaging study. *J. Child Neurol.* 18, 463–470. doi: 10.1177/08830738030180070501
- Ke, X., Tang, T., Hong, S., Hang, Y., Zou, B., Li, H., et al. (2009). White matter impairments in autism, evidence from voxel-based morphometry and diffusion tensor imaging. *Brain Res.* 1265, 171–177. doi: 10.1016/j.brainres.2009.02.013
- Keller, T. A., Kana, R. K., and Just, M. A. (2007). A developmental study of the structural integrity of white matter in autism. *Neuroreport* 18, 23–27. doi: 10.1097/01.wnr.0000239965.21685.99
- Kleiman, M. D., Neff, S., and Rosman, N. P. (1992). The brain in infantile autism are posterior fossa structures abnormal? *Neurology* 42, 753–753. doi: 10.1212/WNL.42.4.753
- Knaus, T. A., Silver, A. M., Kennedy, M., Lindgren, K. A., Dominick, K. C., Siegel, J., et al. (2010). Language laterality in autism spectrum disorder and typical controls: a functional, volumetric, and diffusion tensor MRI study. *Brain Lang.* 112, 113–120. doi: 10.1016/j.bandl.2009.11.005
- Koay, C. G., Chang, L.-C., Carew, J. D., Pierpaoli, C., and Basser, P. J. (2006). A unifying theoretical and algorithmic framework for least squares methods of estimation in diffusion tensor imaging. *J. Magn. Reson.* 182, 115–125. doi: 10.1016/j.jmr.2006.06.020
- Kumar, A., Sundaram, S. K., Sivaswamy, L., Behen, M. E., Makki, M. I., Ager, J., et al. (2010). Alterations in frontal lobe tracts and corpus callosum in young children with autism spectrum disorder. *Cereb. Cortex* 20, 2103–2113. doi: 10.1093/cercor/bhp278
- Kwon, H., Ow, A. W., Pedatella, K. E., Lotspeich, L. J., and Reiss, A. L. (2004). Voxel-based morphometry elucidates structural neuroanatomy of high-functioning autism and asperger syndrome. *Dev. Med. Child Neurol.* 46, 760–764. doi: 10.1111/j.1469-8749.2004.tb00996.x
- Lai, G., Pantazatos, S. P., Schneider, H., and Hirsch, J. (2012). Neural systems for speech and song in autism. *Brain* 135, 961–975. doi: 10.1093/brain/awr335
- Lainhart, J. E., Piven, J., Wzorek, M., Landa, R., Santangelo, S. L., Coon, H., et al. (1997). Macrocephaly in children and adults with autism. *J. Am. Acad. Child Adolesc. Psychiatry* 36, 282–290. doi: 10.1097/00004583-199702000-00019
- Lange, N., DuBray, M. B., Lee, J. E., Froimowitz, M. P., Froehlich, A., Adluru, N., et al. (2010). Atypical diffusion tensor hemispheric asymmetry in autism. *Autism Res.* 3, 350–358. doi: 10.1002/aur.162
- Langen, M., Leemans, A., Johnston, P., Ecker, C., Daly, E., Murphy, C. M., et al. (2012). Fronto-striatal circuitry and inhibitory control in autism: findings from diffusion tensor imaging tractography. *Cortex* 48, 183–193. doi: 10.1016/j.cortex.2011.05.018
- Le Bihan, D., Mangin, J.-F., Poupon, C., Clark, C. A., Pappata, S., Molko, N., et al. (2001). Diffusion tensor imaging: concepts and applications. *J. Magn. Reson. Imaging* 13, 534–546. doi: 10.1002/jmri.1076
- Lee, J. E., Bigler, E. D., Alexander, A. L., Lazar, M., DuBray, M. B., Chung, M. K., et al. (2007). Diffusion tensor imaging of white matter in the superior temporal gyrus and temporal stem in autism. *Neurosci. Lett.* 424, 127–132. doi: 10.1016/j.neulet.2007.07.042
- Lee, J. E., Chung, M. K., Lazar, M., DuBray, M. B., Kim, J., Bigler, E. D., et al. (2009). A study of diffusion tensor imaging by tissue-specific, smoothing-compensated voxel-based analysis. *Neuroimage* 44, 870–883. doi: 10.1016/j.neuroimage.2008.09.041
- Lerner, A., Mogensen, M. A., Kim, P. E., Shiroishi, M. S., Hwang, D. H., and Law, M. (2014). Clinical applications of diffusion tensor imaging. *World Neurosurg.* 82, 96–109. doi: 10.1016/j.wneu.2013.07.083
- Levitt, J. G., Blanton, R., Capetillo-Cunliffe, L., Guthrie, D., Toga, A., and McCracken, J. T. (1999). Cerebellar vermis lobules viiix in autism. *Prog. Neuro-Psychopharmacol. Biol. Psychiatry* 23, 625–633. doi: 10.1016/S0278-5846(99)00021-4
- Lewis, J. D., Theilmann, R. J., Fonov, V., Bellec, P., Lincoln, A., Evans, A. C., et al. (2013). Callosal fiber length and interhemispheric connectivity in adults with autism: brain overgrowth and underconnectivity. *Hum. Brain Mapp.* 34, 1685–1695. doi: 10.1002/hbm.22018
- Lo, Y.-C., Soong, W.-T., Gau, S. S.-F., Wu, Y.-Y., Lai, M.-C., Yeh, F.-C., et al. (2011). The loss of asymmetry and reduced interhemispheric connectivity in adolescents with autism: a study using diffusion spectrum imaging tractography. *Psychiatry Res.* 192, 60–66. doi: 10.1016/j.psychres.2010.09.008
- Lotspeich, L. J., Kwon, H., Schumann, C. M., Fryer, S. L., Goodlin-Jones, B. L., Buonocore, M. H., et al. (2004). Investigation of neuroanatomical differences between autism and aspergersyndrome. *Arch. Gen. Psychiatry* 61, 291–298. doi: 10.1001/archpsyc.61.3.291
- Manes, F., Piven, J., Vrancic, D., Nanclares, V., Plebst, C., and Starkstein, S. E. (1999). An MRI study of the corpus callosum and cerebellum in mentally retarded autistic individuals. *J. Neuropsychiatry Clin. Neurosci.* 11, 470–474. doi: 10.1176/jnp.11.4.470
- McAlonan, G. M., Cheung, V., Cheung, C., Suckling, J., Lam, G. Y., Tai, K., et al. (2005). Mapping the brain in autism. a voxel-based mri study of volumetric differences and intercorrelations in autism. *Brain* 128, 268–276. doi: 10.1093/brain/awh332
- McAlonan, G. M., Daly, E., Kumari, V., Critchley, H. D., van Amelsvoort, T., Suckling, J., et al. (2002). Brain anatomy and sensorimotor gating in aspergers syndrome. *Brain* 125, 1594–1606. doi: 10.1093/brain/awf150
- Mills, B. D., Lai, J., Brown, T. T., Erhart, M., Halgren, E., Reilly, J., et al. (2013). White matter microstructure correlates of narrative production in typically developing children and children with high functioning autism. *Neuropsychologia* 51, 1933–1941. doi: 10.1016/j.neuropsychologia.2013.06.012

- Minschew N. J., and Dombrowski, S. M. (1994). "In vivo neuroanatomy of autism: neuroimaging studies," in *The Neurobiology of Autism*, eds M. L. Bauman and T. L. Kemper (Baltimore, MD: The Johns Hopkins University Press), 66–85.
- Minschew, N. J., and Payton, J. B. (1988). New perspectives in autism, part I: the clinical spectrum of autism. *Curr. Prob. Pediatr.* 18, 567–610. doi: 10.1016/0045-9380(88)90021-7
- Mori, S., and Tournier, J.-D. (2013). *Introduction to Diffusion Tensor Imaging and Higher Order Models* (Oxford, UK: Academic Press).
- Munson, J., Dawson, G., Abbott, R., Faja, S., Webb, S. J., Friedman, S. D., et al. (2006). Amygdalar volume and behavioral development in autism. *Arch. Gen. Psychiatry* 63, 686–693. doi: 10.1001/archpsyc.63.6.686
- Murakami, J. W., Courchesne, E., Press, G. A., Yeung-Courchesne, R., and Hesselink, J. R. (1989). Reduced cerebellar hemisphere size and its relationship to vermal hypoplasia in autism. *Arch. Neurol.* 46, 689–694. doi: 10.1001/archneur.1989.00520420111032
- Nagae, L., Zarnow, D., Blaskey, L., Dell, J., Khan, S., Qasmieh, S., et al. (2012). Elevated mean diffusivity in the left hemisphere superior longitudinal fasciculus in autism spectrum disorders increases with more profound language impairment. *Am. J. Neuroradiol.* 33, 1720–1725. doi: 10.3174/ajnr.A3037
- Nair, A., Treiber, J. M., Shukla, D. K., Shih, P., and Müller, R.-A. (2013). Impaired thalamocortical connectivity in autism spectrum disorder: a study of functional and anatomical connectivity. *Brain* 136, 1942–1955. doi: 10.1093/brain/awt079
- Narr, K. L., Hageman, N., Woods, R. P., Hamilton, L. S., Clark, K., Phillips, O., et al. (2009). Mean diffusivity: a biomarker for csf-related disease and genetic liability effects in schizophrenia. *Psychiatry Res.* 171, 20–32. doi: 10.1016/j.psychres.2008.03.008
- NIMH (2015). *Autism Spectrum Disorder*. Bethesda, MD: Office of Science Policy.
- Nordahl, C. W., Dierker, D., Mostafavi, I., Schumann, C. M., Rivera, S. M., Amaral, D. G., et al. (2007). Cortical folding abnormalities in autism revealed by surface-based morphometry. *J. Neurosci.* 27, 11725–11735. doi: 10.1523/JNEUROSCI.0777-07.2007
- Nordahl, C. W., Scholz, R., Yang, X., Buonocore, M. H., Simon, T., Rogers, S., et al. (2012). Increased rate of amygdala growth in children aged 2 to 4 years with autism spectrum disorders: a longitudinal study. *Arch. Gen. Psychiatry* 69, 53–61. doi: 10.1001/archgenpsychiatry.2011.145
- Noriuchi, M., Kikuchi, Y., Yoshiura, T., Kira, R., Shigeto, H., Hara, T., et al. (2010). Altered white matter fractional anisotropy and social impairment in children with autism spectrum disorder. *Brain Res.* 1362, 141–149. doi: 10.1016/j.brainres.2010.09.051
- Nowell, M. A., Hackney, D. B., Muraki, A. S., and Coleman, M. (1990). Varied mr appearance of autism: fifty-three pediatric patients having the full autistic syndrome. *Magn. Reson. Imaging* 8, 811–816. doi: 10.1016/0730-725X(90)90018-W
- Nucifora, P. G., Verma, R., Lee, S.-K., and Melhem, E. R. (2007). Diffusion-tensor MR imaging and tractography: exploring brain microstructure and connectivity. *Radiology* 245, 367. doi: 10.1148/radiol.2452060445
- Palmen, S. J., and van Engeland, H. (2004). Review on structural neuroimaging findings in autism. *J. Neural Transm.* 111, 903–929. doi: 10.1007/s00702-003-0068-9
- Pardini, M., Elia, M., Garaci, F. G., Guida, S., Coniglione, F., Krueger, F., et al. (2012). Long-term cognitive and behavioral therapies, combined with augmentative communication, are related to uncinate fasciculus integrity in autism. *J. Autism Dev. Disord.* 42, 585–592. doi: 10.1007/s10803-011-1281-2
- Perkins, T. J., Stokes, M. A., McGillivray, J. A., Mussap, A. J., Cox, I. A., Maller, J. J., et al. (2014). Increased left hemisphere impairment in high-functioning autism: a tract based spatial statistics study. *Psychiatry Res.* 224, 119–123. doi: 10.1016/j.psychres.2014.08.003
- Peterson, D., Mahajan, R., Crocetti, D., Mejia, A., and Mostofsky, S. (2015). Left-hemispheric microstructural abnormalities in children with high-functioning autism spectrum disorder. *Autism Res.* 8, 61–72. doi: 10.1002/aur.1413
- Piven, J., Arndt, S., Bailey, J., and Andreasen, N. (1996). Regional brain enlargement in autism: a magnetic resonance imaging study. *J. Am. Acad. Child Adolesc. Psychiatry* 35, 530–536. doi: 10.1097/00004583-199604000-00020
- Piven, J., Arndt, S., Bailey, J., Haverkamp, S., Andreasen, N. C., and Palmer, P. (1995). An MRI study of brain size in autism. *Am. J. Psychiatry* 152, 1145–1149. doi: 10.1176/ajp.152.8.1145
- Piven, J., Bailey, J., Ranson, B. J., and Arndt, S. (1997). An MRI study of the corpus callosum in autism. *Am. J. Psychiatry* 154, 1051–1056. doi: 10.1176/ajp.154.8.1051
- Piven, J., Bailey, J., Ranson, B. J., and Arndt, S. (1998). No difference in hippocampus volume detected on magnetic resonance imaging in autistic individuals. *J. Autism Dev. Disord.* 28, 105–110. doi: 10.1023/A:1026084430649
- Piven, J., Nehme, E., Simon, J., Barta, P., Pearlson, G., and Folstein, S. E. (1992). Magnetic resonance imaging in autism: measurement of the cerebellum, pons, and fourth ventricle. *Biol. Psychiatry* 31, 491–504. doi: 10.1016/0006-3223(92)90260-7
- Poustka, L., Jennen-Steinmetz, C., Henze, R., Vomstein, K., Haffner, J., and Sieltjes, B. (2012). Fronto-temporal disconnectivity and symptom severity in children with autism spectrum disorder. *World J. Biol. Psychiatry* 13, 269–280. doi: 10.3109/15622975.2011.591824
- Pugliese, L., Catani, M., Ameis, S., Dell'Acqua, F., de Schotten, M. T., Murphy, C., et al. (2009). The anatomy of extended limbic pathways in asperger syndrome: a preliminary diffusion tensor imaging tractography study. *Neuroimage* 47, 427–434. doi: 10.1016/j.neuroimage.2009.05.014
- Rane, P., Cochran, D., Hodge, S. M., Haselgrove, C., Kennedy, D. N., and Frazier, J. A. (2015). Connectivity in autism: a review of mri connectivity studies. *Harvard Rev. Psychiatry* 23, 223–244. doi: 10.1097/HRP.0000000000000072
- Ritvo, E. R., and Garber, H. (1988). Cerebellar hypoplasia and autism. *New Engl. J. Med.* 319, 1152–1154. doi: 10.1056/NEJM198810273191709
- Rojas, D. C., Peterson, E., Winterrowd, E., Reite, M. L., Rogers, S. J., and Tregellas, J. R. (2006). Regional gray matter volumetric changes in autism associated with social and repetitive behavior symptoms. *BMC Psychiatry* 6:56. doi: 10.1186/1471-244X-6-56
- Rojas, D. C., Smith, J. A., Benkers, T. L., Camou, S. L., Reite, M. L., and Rogers, S. J. (2004). Hippocampus and amygdala volumes in parents of children with autistic disorder. *Am. J. Psychiatry* 161, 2038–2044. doi: 10.1176/appi.ajp.161.11.2038
- Sahyoun, C. P., Belliveau, J. W., and Mody, M. (2010a). White matter integrity and pictorial reasoning in high-functioning children with autism. *Brain Cogn.* 73, 180–188. doi: 10.1016/j.bandc.2010.05.002
- Sahyoun, C. P., Belliveau, J. W., Soulières, I., Schwartz, S., and Mody, M. (2010b). Neuroimaging of the functional and structural networks underlying visuospatial vs. linguistic reasoning in high-functioning autism. *Neuropsychologia* 48, 86–95. doi: 10.1016/j.neuropsychologia.2009.08.013
- Saitoh, O., Courchesne, E., Egaas, B., Lincoln, A., and Schreibman, L. (1995). Cross-sectional area of the posterior hippocampus in autistic patients with cerebellar and corpus callosum abnormalities. *Neurology* 45, 317–324. doi: 10.1212/WNL.45.2.317
- Saitoh, O., Karns, C. M., and Courchesne, E. (2001). Development of the hippocampal formation from 2 to 42 years. *Brain* 124, 1317–1324. doi: 10.1093/brain/124.7.1317
- Schaefer, G. B., Thompson, J. N., Bodensteiner, J. B., McConnell, J. M., Kimberling, W. J., Gay, C. T., et al. (1996). Hypoplasia of the cerebellar vermis in neurogenetic syndromes. *Ann. Neurol.* 39, 382–385. doi: 10.1002/ana.410390316
- Schipul, S. E., Keller, T. A., and Just, M. A. (2011). Inter-regional brain communication and its disturbance in autism. *Front. Syst. Neurosci.* 5:7. doi: 10.3389/fnsys.2011.00010
- Schumann, C. M., Bloss, C. S., Barnes, C. C., Wideman, G. M., Carper, R. A., Akshoomoff, N., et al. (2010). Longitudinal magnetic resonance imaging study of cortical development through early childhood in autism. *J. Neurosci.* 30, 4419–4427. doi: 10.1523/JNEUROSCI.5714-09.2010
- Schumann, C. M., Hamstra, J., Goodlin-Jones, B. L., Lotspeich, L. J., Kwon, H., Buonocore, M. H., et al. (2004). The amygdala is enlarged in children but not adolescents with autism; the hippocampus is enlarged at all ages. *J. Neurosci.* 24, 6392–6401. doi: 10.1523/JNEUROSCI.1297-04.2004
- Sears, L. L., Vest, C., Mohamed, S., Bailey, J., Ranson, B. J., and Piven, J. (1999). An MRI study of the basal ganglia in autism. *Prog. Neuro-Psychopharmacol. Biol. Psychiatry* 23, 613–624. doi: 10.1016/S0278-5846(99)00020-2
- Shen, M. D., Nordahl, C. W., Young, G. S., Wootton-Gorges, S. L., Lee, A., Liston, S. E., et al. (2013). Early brain enlargement and elevated extra-axial fluid in infants who develop autism spectrum disorder. *Brain* 136, 2825–2835. doi: 10.1093/brain/awt166

- Shukla, D. K., Keehn, B., Lincoln, A. J., and Müller, R.-A. (2010). White matter compromise of callosal and subcortical fiber tracts in children with autism spectrum disorder: a diffusion tensor imaging study. *J. Am. Acad. Child Adolesc. Psychiatry* 49, 1269–1278.e2. doi: 10.1016/j.jaac.2010.08.018
- Shukla, D. K., Keehn, B., and Müller, R.-A. (2011a). Tract-specific analyses of diffusion tensor imaging show widespread white matter compromise in autism spectrum disorder. *J. Child Psychol. Psychiatry* 52, 286–295. doi: 10.1111/j.1469-7610.2010.02342.x
- Shukla, D. K., Keehn, B., Smylie, D. M., and Müller, R.-A. (2011b). Microstructural abnormalities of short-distance white matter tracts in autism spectrum disorder. *Neuropsychologia* 49, 1378–1382. doi: 10.1016/j.neuropsychologia.2011.02.022
- Siegel, D. J., Minshew, N. J., and Goldstein, G. (1996). Wechsler iq profiles in diagnosis of high-functioning autism. *J. Autism Dev. Disord.* 26, 389–406. doi: 10.1007/BF02172825
- Sivaswamy, L., Kumar, A., Rajan, D., Behen, M., Muzik, O., Chugani, D., et al. (2010). A diffusion tensor imaging study of the cerebellar pathways in children with autism spectrum disorder. *J. Child Neurol.* 25, 1223–1231. doi: 10.1177/0883073809358765
- Smith, S. M., Jenkinson, M., Johansen-Berg, H., Rueckert, D., Nichols, T. E., Mackay, C. E., et al. (2006). Tract-based spatial statistics: voxelwise analysis of multi-subject diffusion data. *Neuroimage* 31, 1487–1505. doi: 10.1016/j.neuroimage.2006.02.024
- Song, S.-K., Yoshino, J., Le, T. Q., Lin, S.-J., Sun, S.-W., Cross, A. H., et al. (2005). Demyelination increases radial diffusivity in corpus callosum of mouse brain. *Neuroimage* 26, 132–140. doi: 10.1016/j.neuroimage.2005.01.028
- Sparks, B., Friedman, S., Shaw, D., Aylward, E., Echelard, D., Artru, A., et al. (2002). Brain structural abnormalities in young children with autism spectrum disorder. *Neurology* 59, 184–192. doi: 10.1212/WNL.59.2.184
- Stanfield, A. C., McIntosh, A. M., Spencer, M. D., Philip, R., Gaur, S., and Lawrie, S. M. (2008). Towards a neuroanatomy of autism: a systematic review and meta-analysis of structural magnetic resonance imaging studies. *Eur. Psychiatry* 23, 289–299. doi: 10.1016/j.eurpsy.2007.05.006
- Sundaram, S. K., Kumar, A., Makki, M. I., Behen, M. E., Chugani, H. T., and Chugani, D. C. (2008). Diffusion tensor imaging of frontal lobe in autism spectrum disorder. *Cereb. Cortex* 18, 2659–2665. doi: 10.1093/cercor/bhn031
- Thakkar, K. N., Polli, F. E., Joseph, R. M., Tuch, D. S., Hadjikhani, N., Barton, J. J., et al. (2008). Response monitoring, repetitive behaviour and anterior cingulate abnormalities in autism spectrum disorders (ASD). *Brain* 131, 2464–2478. doi: 10.1093/brain/awn099
- Thomas, C., Humphreys, K., Jung, K.-J., Minshew, N., and Behrmann, M. (2011). The anatomy of the callosal and visual-association pathways in high-functioning autism: a DTI tractography study. *Cortex* 47, 863–873. doi: 10.1016/j.cortex.2010.07.006
- Toal, F., Daly, E., Page, L., Deeley, Q., Hallahan, B., Bloemen, O., et al. (2010). Clinical and anatomical heterogeneity in autistic spectrum disorder: a structural MRI study. *Psychol. Med.* 40, 1171–1181. doi: 10.1017/S0033291709991541
- Townsend, J., Courchesne, E., Covington, J., Westerfield, M., Harris, N. S., Lyden, P., et al. (1999). Spatial attention deficits in patients with acquired or developmental cerebellar abnormality. *J. Neurosci.* 19, 5632–5643.
- Travers, B. G., Adluru, N., Ennis, C., Tromp, D. P., Destiche, D., Doran, S., et al. (2012). Diffusion tensor imaging in autism spectrum disorder: a review. *Autism Res.* 5, 289–313. doi: 10.1002/aur.1243
- Tsatsanis, K. D., Rourke, B. P., Klin, A., Volkmar, F. R., Cicchetti, D., and Schultz, R. T. (2003). Reduced thalamic volume in high-functioning individuals with autism. *Biol. Psychiatry* 53, 121–129. doi: 10.1016/S0006-3223(02)01530-5
- van Gelderen, P., de Vleschouwer, M. H., DesPres, D., Pekar, J., van Zijl, P., and Moonen, C. T. (1994). Water diffusion and acute stroke. *Magn. Reson. Med.* 31, 154–163. doi: 10.1002/mrm.1910310209
- Verhoeven, J. S., Rommel, N., Prodi, E., Leemans, A., Zink, I., Vandewalle, E., et al. (2012). Is there a common neuroanatomical substrate of language deficit between autism spectrum disorder and specific language impairment? *Cereb. Cortex* 22, 2263–2271. doi: 10.1093/cercor/bhr292
- Waiter, G. D., Williams, J. H., Murray, A. D., Gilchrist, A., and Perrett, D. I. (2005). Structural white matter deficits in high-functioning individuals with autistic spectrum disorder: a voxel-based investigation. *Neuroimage* 24, 455–461. doi: 10.1016/j.neuroimage.2004.08.049
- Waiter, G. D., Williams, J. H., Murray, A. D., Gilchrist, A., Perrett, D. I., and Whiten, A. (2004). A voxel-based investigation of brain structure in male adolescents with autistic spectrum disorder. *Neuroimage* 22, 619–625. doi: 10.1016/j.neuroimage.2004.02.029
- Walker, L., Gozzi, M., Lenroot, R., Thurm, A., Behseta, B., Swedo, S., et al. (2012). Diffusion tensor imaging in young children with autism: biological effects and potential confounds. *Biol. Psychiatry* 72, 1043–1051. doi: 10.1016/j.biopsych.2012.08.001
- Wallace, G. L., Eisenberg, I. W., Robustelli, B., Dankner, N., Kenworthy, L., Giedd, J. N., et al. (2015). Longitudinal cortical development during adolescence and young adulthood in autism spectrum disorder: increased cortical thinning but comparable surface area changes. *J. Am. Acad. Child Adolesc. Psychiatry* 54, 464–469. doi: 10.1016/j.jaac.2015.03.007
- Wan, C. Y., Marchina, S., Norton, A., and Schlaug, G. (2012). Atypical hemispheric asymmetry in the arcuate fasciculus of completely nonverbal children with autism. *Ann. N.Y. Acad. Sci.* 1252, 332–337. doi: 10.1111/j.1749-6632.2012.06446.x
- Weinstein, M., Ben-Sira, L., Levy, Y., Zachor, D. A., Itzhak, E. B., Artzi, M., et al. (2011). Abnormal white matter integrity in young children with autism. *Hum. Brain Mapp.* 32, 534–543. doi: 10.1002/hbm.21042
- Wolff, J. J., Gu, H., Gerig, G., Elison, J. T., Styner, M., Gouttard, S., et al. (2012). Differences in white matter fiber tract development present from 6 to 24 months in infants with autism. *Am. J. Psychiatry* 169, 589–600. doi: 10.1176/appi.ajp.2011.11091447
- Zeglam, A. M., Al-Ogab, M. F., and Al-Shafer, T. (2015). MRI or not to MRI! should brain MRI be a routine investigation in children with autistic spectrum disorders? *Acta Neurol. Belgica* 115, 351–354. doi: 10.1007/s13760-014-0384-x
- Zilbovicius, M., Garreau, B., Samson, Y., Remy, P., Barthelemy, C., Syrota, A., et al. (1995). Delayed maturation of the frontal cortex in childhood autism. *Am. J. Psychiatry* 152, 248–252. doi: 10.1176/ajp.152.2.248
- Zola-Morgan, S., Squire, L. R., Clower, R. P., and Alvarez-Royo, P. (1991). Independence of memory functions and emotional behavior: separate contributions of the hippocampal formation and the amygdala. *Hippocampus* 1, 207–220. doi: 10.1002/hipo.450010208

**Conflict of Interest Statement:** The authors declare that the research was conducted in the absence of any commercial or financial relationships that could be construed as a potential conflict of interest.

The reviewer and handling Editor declared their shared affiliation, and the handling Editor states that the process nevertheless met the standards of a fair and objective review.

Copyright © 2016 Ismail, Keynton, Mostapha, ElTanboly, Casanova, Gimel'farb and El-Baz. This is an open-access article distributed under the terms of the Creative Commons Attribution License (CC BY). The use, distribution or reproduction in other forums is permitted, provided the original author(s) or licensor are credited and that the original publication in this journal is cited, in accordance with accepted academic practice. No use, distribution or reproduction is permitted which does not comply with these terms.



# Feasibility of Subcutaneous ECG Leads for Synchronized Timing of a Counterpulsation Device

S. WARREN,<sup>1</sup> G. A. GIRIDHARAN,<sup>1</sup> R. D. DOWLING,<sup>3</sup> P. A. SPENCE,<sup>3</sup> L. TOMPKINS,<sup>3</sup> ERIC GRATZ,<sup>4</sup>  
L. C. SHERWOOD,<sup>5</sup> M. A. SOBIESKI,<sup>2</sup> C. R. BARTOLI,<sup>6</sup> M. S. SLAUGHTER,<sup>2</sup> ROBERT S. KEYNTON,<sup>1</sup>  
and S. C. KOENIG<sup>1,2</sup>

<sup>1</sup>Department of Bioengineering, Cardiovascular Innovation Institute, University of Louisville, Louisville, KY, USA;

<sup>2</sup>Department of Surgery, Division of Cardiothoracic Surgery, University of Louisville, Louisville, KY, USA; <sup>3</sup>SCR Inc, Louisville, KY, USA; <sup>4</sup>Abiomed Inc, Danvers, MA, USA; <sup>5</sup>Research Resources Facilities (RRF), University of Louisville, Louisville, KY, USA; and <sup>6</sup>University of Louisville School of Medicine, Louisville, KY, USA

(Received 30 August 2011; accepted 22 October 2011; published online 4 November 2011)

Associate Editor W. Robert Taylor oversaw the review of this article.

**Abstract**—A counterpulsation device (Symphony) that works synchronously with the native heart to provide partial circulatory support was developed to treat patients with advanced heart failure. Symphony is implanted in a ‘pace-maker pocket’ without entry into the chest, and requires timing with ECG for device filling and ejection. Surface leads are limited to short-term use due to signal distortion and lead management. Transvenous leads are a clinical standard for pacemakers and internal defibrillators, but increase the complexity of the implant procedure. In this study, the feasibility of using subcutaneous leads for synchronized timing of Symphony was investigated. ECG waveforms were simultaneously measured and recorded using epicardial (control) and subcutaneous (test) leads in a bovine model for 7-days ( $n = 6$ ) and 14-days ( $n = 2$ ) during daily activity and treadmill exercise. Landmark features and R-wave triggering detection rates for each lead configuration were calculated and compared. Lead placement, migration, durability, and infection were quantified using fluoroscopy and histopathological examination. There were 2,849 data epochs (30-s each) recorded at rest (133,627 analyzed beats) and 35 data epochs (20 min each) recorded during treadmill exercise (37,154 analyzed beats). The subcutaneous leads provided an accurate and reliable triggering signal during routine daily activity and treadmill exercise ( $99.1 \pm 0.4\%$  positive predictive value,  $96.8 \pm 1.5\%$  sensitivity). The subcutaneous leads were also easily placed with minimal lead migration ( $0.5 \pm 0.1$  cm), damage (no fractures or failures), or infection.

These findings demonstrate the feasibility of using subcutaneous leads for synchronized timing of mechanical circulatory support while offering the advantage of less invasive surgery and associated risk factors.

**Keywords**—Subcutaneous, Electrocardiogram, ECG leads, Heart failure, Mechanical circulatory support.

## BACKGROUND

Intra-aortic balloon pumps (IABP) are the most widely used mechanical circulatory support device (~160,000 patients per year) for patients with heart failure. The IABP, which operates on the counterpulsation principle, has high clinical acceptance but also has been limited to short-term support (generally less than 2 weeks) due to the risk of septicemia and limb ischemia. Counterpulsation has many important clinical benefits for the heart (lower ventricular workload and increased myocardial perfusion) and improves end-organ perfusion.<sup>21,23</sup> Thus, there is growing interest in the development of chronic partial circulatory support devices, for which early clinical findings have been encouraging.<sup>20</sup> There are several devices that provide chronic counterpulsation that have completed or are currently in clinical trials, including the C-Pulse (Sunshine Heart, Eden Prairie MN) and CardioPlus (LVAD Technologies, Detroit MI). However, these devices require a sternotomy or a thoracotomy for device placement. Symphony (SCR, Louisville KY) is a counterpulsation device that can be placed via a limited operative approach, thereby avoiding

Address correspondence to S. C. Koenig, Departments of Bioengineering and Surgery, Cardiovascular Innovation Institute, University of Louisville, 302 East Muhammad Ali Blvd, Room 408, Louisville, KY 40202, USA. Electronic mail: steven.koenig@louisville.edu

thoracotomy or sternotomy approaches typically associated with ventricular assist devices (LVAD).<sup>2</sup>

Symphony is a 30-mL stroke volume device with a polyurethane-lined pumping chamber that is designed to fit comfortably in a pacemaker-like pocket on the right side of a patient (Fig. 1).<sup>7,16</sup> A short interposition graft (10 mm Dacron) is sewn to the subclavian artery. A silicone-coated ePTFE graft is then anastomosed to the interposition graft and connected to the Symphony device. A pneumatic driveline exits the skin near the costal margin and connects the pump to an external driver. During systole, the driver evacuates air from the pumping chamber, thus removing blood from the circulation and reducing cardiac work. During diastole, the Symphony ejects the blood into the circulation providing diastolic augmentation to increase coronary and end-organ perfusion. The pneumatic driver weighs 2.2 kg and can be carried or worn on a patient's belt. Pre-clinical studies have shown equivalent or better hemodynamic and metabolic benefits with the Symphony device compared to a 40-mL IABP.<sup>1,11,17,19,20</sup> Partial circulatory support with counterpulsation using a device that can be placed without a major operation may allow for up-titration of medications, improved quality of life, and may promote myocardial recovery.

Symphony requires synchronized timing using the patient's ECG and R-wave detection to control filling and ejections cycles and maximize hemodynamic performance. Surface leads remain the standard for short-term patient monitoring and diagnosis, but are impractical for this application. Although new technologies are being developed for chronic surface ECG monitoring,<sup>19</sup> difficulties associated with the skin-electrode interface often result in poor contact, motion artifact, and patient wire management challenges that preclude the use of surface leads for long-term applications. Epicardial and endocardial leads provide

robust ECG waveforms without these limitations, and thus, are more suitable for long-term use with chronic counterpulsation devices (i.e. C-Pulse, CardioPlus). Currently, since these devices require a major open-chest operation (sternotomy or thoracotomy) implantation of epicardial leads do not increase the invasiveness of surgery. One of the advantages of the Symphony device is that it can be implanted with a minor surface procedure without need to enter the chest (i.e. pacemaker-like pocket). Therefore, a subcutaneous lead system that offers a long-term, robust ECG while requiring a minimally invasive implant procedure is desired for timing the Symphony chronic counterpulsation device. The objective of this study was to investigate the feasibility of using subcutaneous leads for R-wave detection to enable synchronized timing (filling and ejection cycles) of the Symphony device and wearable pneumatic driver to provide chronic counterpulsation therapy.

## METHODS

### *Experimental Design*

To demonstrate feasibility, the hypothesis that subcutaneous ECG leads provide equivalent QRS detection as clinical-standard epicardial leads was tested. The technique used for lead placement was also evaluated to determine if facile lead placement without lead migration could be consistently achieved. In a bovine model, ECG data were simultaneously measured and recorded with subcutaneous and clinically approved epicardial leads for 7-days ( $n = 4$ ) and 14-days ( $n = 2$ ) during normal daily activity and treadmill exercise. Recorded ECG waveforms were analyzed to quantify QRS detection rates (Matlab, The Mathworks, Natick, MA) with design specifications of



**FIGURE 1.** Symphony is implanted on the right side in a pacemaker-like pocket, anastomosed to the subclavian artery, and the pneumatic driveline exits through the skin (left). The pump fills during systole and empties during diastole through a valveless, silicone-coated ePTFE graft (center). The pump is pneumatically actuated by a small, lightweight driver (right).

90% (normal activity) and 80% (exercise) sensitivity and specificity. Fluoroscopy images (GE Innova 3100, Waukesha, WI) of leads during placement (implant) and post-euthanasia (just prior to explant) were recorded and analyzed using ImageJ (NIH, Bethesda, MD) to quantify lead migration. At necropsy, subcutaneous and epicardial leads were photographed and examined for any signs of fracture, damage, or infection.

### Lead Fabrication

Subcutaneous ECG leads were fabricated using commercially-available lead coupler kits (Data Systems International, St. Paul, MN), Tygon tubing (Fischer Scientific, Pittsburgh, PA), and electronic pin and socket connectors (Allied Electronics Inc., Ft. Worth, TX) (Fig. 2). The prototype leads were fabricated using a modified version of the technique described in the Data Systems International technical bulletin.<sup>11</sup> Seven centimeters of lead were exposed, looped around a clamp, and secured with a suture. Leads were sterilized using ethylene oxide.

### Lead Implantation Technique

Prior to this study, several operative approaches and devices to deliver the subcutaneous ECG leads were developed using human cadavers (Fresh Tissue Laboratory, University of Louisville), including tunneling tools, modified endoscopic clip appliers, and laparoscopic instruments. The selected method was to simply pull the lead to the desired position using a standard straight needle. A 2-0 nylon suture was passed through the loops of wire at the end of the subcutaneous leads and then through the eye of a four-inch needle. A standard needle holder was then used to control the needle tip. Working through the device implantation wound, the needle was advanced to the desired position on the

chest and then the needle and attached suture were passed through the skin. The needle and suture were removed leaving the ECG lead in place beneath the skin. This method does not require any additional incision(s) or special training and can be accomplished with standard surgical instruments. Screw-in epicardial leads were placed in the left ventricle under direct vision through a limited anterior thoracotomy.

Since Symphony is designed to be implanted on the right side and anastomosed to the right subclavian artery, the subcutaneous leads need to be placed over the right chest. Ideally, leads should not cross the sternum in order to avoid issues with any future cardiac procedures that require a sternotomy. Surface voltage maps of the thorax during ventricular depolarization (ECGSIM, Radboud University medical Center, Nijmegen, The Netherlands) demonstrate that vertical lead-pairs over the right chest offer the largest differential in measured voltage (Fig. 3, left). Three lead-pair configurations were placed ventral and dorsal across the right chest of a calf model 6–15 cm apart and within 25 cm of the heart in order to best mimic the human analog configuration (Fig. 3, right). Preliminary experiments in a bovine model demonstrated that this lead configuration produced high-quality signals. The human analogue of this configuration is a pair of leads placed 6–8 cm apart and parallel to the electrical axis of the heart. Similar subcutaneous configurations have been reported with implantable cardioverter-defibrillators using a parasternal electrode.<sup>1</sup>

### Animal Study

Animal studies were conducted at the University of Louisville, which is accredited by the Association for Assessment and Accreditation of Laboratory Animal Care (AAALAC) International, and were approved by the University of Louisville Institutional Animal Care and Use Committee (IACUC). Animals received care in accordance with the *Guide for the Care and Use of Laboratory Animals*, NRC, 1996, and the *United States Animal Welfare Regulations*.

Male, castrated, 80–100 kg Holstein and Jersey calves (Oak Hill Genetics, Ewing, IL,) were implanted with Symphony devices, subcutaneous and epicardial leads, and monitored for 7-days ( $n = 4$ ) and 14-days ( $n = 2$ ). Animals were allowed to acclimate and were quarantined for 14-days prior to the initiation of experimental procedures. During quarantine the animals received a physical examination, 2.5 mg/kg tula-thromycin SC (Pfizer Animal Health, New York, NY), 0.2 mg/kg moxidectin SC (Cydectin®, Boehringer Ingelheim Vetmedica, Inc., St. Joseph, MO), and 5 mg/kg ponazuril PO (Marquis®, Bayer Animal

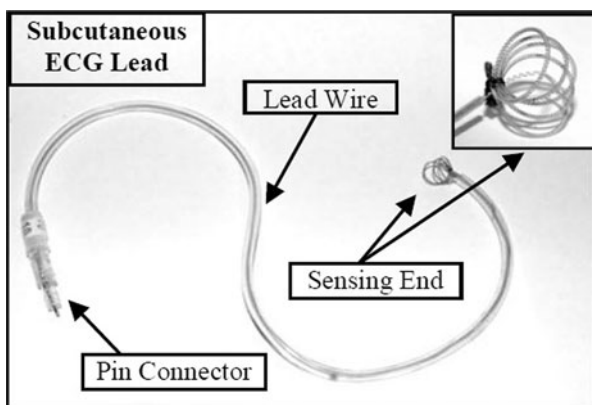


**FIGURE 2.** Subcutaneous ECG lead with extended sensing wire (far left). Enlarged view shows the coiled sensing wire.

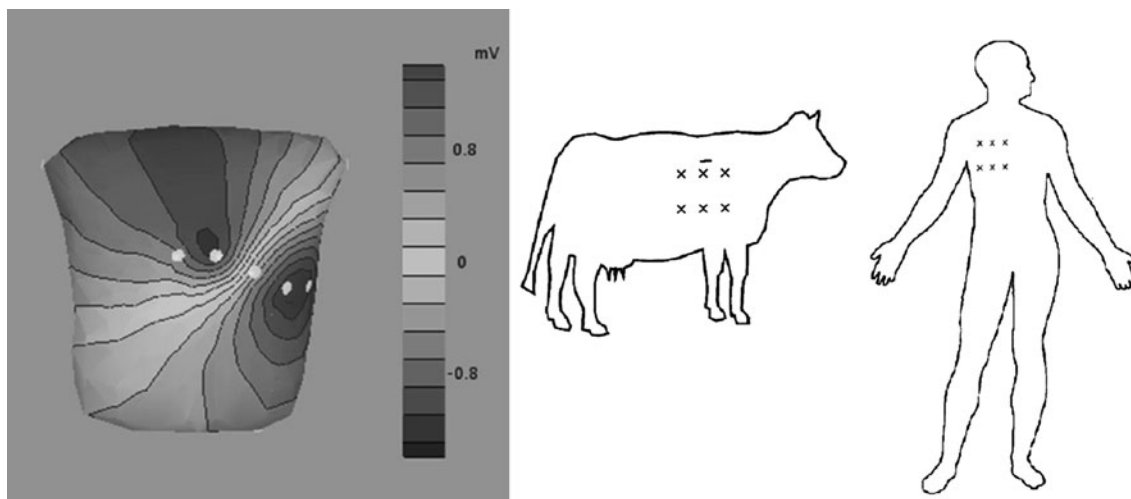


**FIGURE 3.** Measured surface voltages during ventricular depolarization show that the required voltage differential (0.8 mV) can be achieved with vertical lead pairs across the right chest (left). Placing subcutaneous leads in ventral position provides the greatest voltage differential. Analog lead configurations were tested in the bovine model to mimic potential human placement (right).

Health, Shawnee Mission, KS). CBC, serum biochemistries, and baseline coagulation and hemolysis panels were performed. One day prior to surgery 75 mg clopidogrel (Plavix<sup>®</sup>, Bristol-Myers Squibb, Bridgewater, NJ) was administered orally and pre-emptive analgesia was provided with the placement of a 50  $\mu$ g/h transdermal fentanyl patch (Duragesic<sup>®</sup>, Janssen Pharmaceuticals, Inc, Titusville, NJ) 12–18 h prior to surgery and was left in place for 72 h. Anesthesia was induced with 4 mg/kg ketamine (Ketaset<sup>®</sup>, Fort Dodge Animal Health, Fort Dodge, IA) and 0.4 mg/kg diazepam (Butler Schein Animal Health, Dublin, OH) administered simultaneously IV. Animals were then intubated and anesthesia was maintained with isoflurane (1–3%) in 100% oxygen and mechanical ventilation was initiated. Flunixin meglumine (2 mg/kg IV, Butler Schein Animal Health, Dublin, OH) was administered for additional analgesia, and 15 mg/kg cefazolin IV (Butler Schein Animal Health, Dublin, OH) was administered prior to surgery. Animals were then prepared for strict aseptic surgery on the right side and central lines were placed in the right external jugular vein and the right carotid artery. Physiologic fluids were administered throughout the procedure (Normosol-R<sup>®</sup>, 200 mL/h, Abbott Animal Health, Abbott Park, IL). Body temperature was supported with a warm water circulating blanket. Heart rate, respiratory rate, SpO<sub>2</sub>, body temperature, central venous pressure, arterial pressure and ECG were monitored continuously throughout the anesthetic and recovery periods.

Six leads were placed subcutaneously through a single incision over the right side of each animal ( $n = 6$  animals, total of 36 leads) in three ventral-dorsal pairs. The time to place all six subcutaneous leads was recorded to assess ease of implantation. The quality of

the ECG signal from each of the three pairs of vertical leads was measured and monitored. Surgical staples were placed at device implant as a landmark for lead placement. Subcutaneous ECG lead placement at time of Symphony device implant were digitally photographed and recorded in cardiac catheterization laboratory by fluoroscopy (GE Innova 3100, Waukesha, WI). Next, the animal was placed on its left side and the left neck and chest were prepared and draped. An incision was made over the fourth rib and carried down to the 4th intercostal space. Prior to the intercostal incision 30 mg succinyl choline (Butler Schein Animal Health, Dublin, OH) was administered IV. The chest was entered and a standard rib retractor was placed. The pericardium was identified and opened and two epicardial leads (CapSure EPI 5071, Medtronic, Minneapolis MN) were placed and connected to the Symphony driver. ECG signal quality was confirmed, leads were tunneled transcutaneously, and secured in position. A chest tube was placed and the chest was closed following the administration of 2 mg/kg bupivacaine IM (0.25% Sensorcaine<sup>®</sup> with epinephrine 1:200,000, APP Pharmaceuticals, Schaumburg IL) along the thoracotomy incision. Symphony was implanted in the left neck with anastomosis to the left carotid artery using previously described methods.<sup>17</sup> Following recovery from anesthesia the animals received 2 mg/kg flunixin meglumine IV, once daily for 3 days, 15 mg/kg cefazolin IV, BID for 7 days, 15 g Probios<sup>®</sup> (Bomac Vets Plus, Inc., Knapp WI) PO once daily for 7 days, 75 mg clopidogrel PO once daily, 200 mg atenolol (TEVA Pharmaceuticals, Sellersville PA) PO once daily, titrated in 25 mg increments to maintain a heart rate of 70–80 beats per minute, and 10 mg coumadin (Bristol-Myers Squibb Co., Princeton



NJ) titrated in 2.5 mg increments to maintain an INR of 2–2.5 times baseline. Intravenous heparin was administered to maintain an activated clotting time (ACT) of 200–250 s until the INR was within the target range. Treadmill testing for the 14-day experiments was initiated after the seventh postoperative day (to allow recovery) and repeated daily for 7 days. Calves were restricted to a walking speed of 30 meters/minute on a treadmill (Safe-T-Mill, Good Horsekeeping Inc, Ash Grove MO) and maintained at that rate for up to 20-min or until the animal showed signs of fatigue (as evaluated and advised by study veterinarian). Subcutaneous lead placement was digitally photographed immediately after euthanasia using fluoroscopy to quantify lead migration from implantation.

### Data Collection and Analysis

Following post-operative recovery, ECG data from the pair of epicardial and three pairs of subcutaneous leads were simultaneously measured and recorded with a GLP compliant data acquisition system.<sup>15</sup> Three pairs of subcutaneous leads were signal conditioned with a clinical-standard ECG amplifier (Gould Biotach 6600, Cleveland OH). The epicardial leads were signal conditioned by the Symphony pneumatic driver (iPulse, Abiomed, Danvers, MA). All signal conditioned ECG waveforms were sampled at 400 Hz (National Instruments, AT-MIO-16E-10, Austin, TX), filtered (60 Hz notch, Frequency Devices, Ottawa IL), and displayed real-time on a computer monitor using custom software<sup>4</sup> developed with LabVIEW (National Instruments, Austin TX). Specifically, thirty-second data epochs were recorded every hour for the duration of the study for all study animals. All recorded ECG waveforms were saved for post-processing and analysis. Image processing software (ImageJ, NIH, Bethesda, MD) was used to quantify subcutaneous lead migration by overlaying digital photographs collected at Symphony implant and prior to necropsy. The software scale was calibrated by to the known length of the implanted staples and lead migration was recorded as the change in distance of the sensing end between compared fluoroscopic images using the ImageJ measure tool. In addition, during necropsy all leads were surgically exposed, examined, and gross lead migration measured. Statistical analyses were performed in Minitab (State College, PA). An alpha of 0.05 was used for all statistical comparisons and in the calculation of confidence intervals.

### Calculation of QRS Detection Rates

The design criteria for ECG data analysis software included (1) use of a standard QRS detection strategy, (2) minimize noise and motion artifacts, (3) handle

large volumes of data, and (4) feasible for integration into the Symphony driver for real-time signal processing. Additionally, the analysis software has to allow for characterization of the subcutaneous signal by isolation of ECG landmarks. The selected algorithm was a modified version of the SQRS method described by Pino *et al.*<sup>24</sup> A Finite Impulse Response (FIR) bandpass filter ( $N = 80$ ) was implemented with a bandwidth of 1–50 Hz. This is in accordance with standard QRS detection filters, which often have bandpass filters with their upper limit in the range of 40–80 Hz for optimal detection<sup>8,27</sup> with lower limits in the range of 0.5–1 Hz to reject low-frequency baseline drift.<sup>6</sup> The implemented filter only causes a time delay of 100 ms, meaning that it can be realized in real-time driver software. An initial threshold and blanking period for QRS detection was also implemented, and after the third beat, the average of the past three thresholds and R–R intervals were used for determining the next threshold and blanking period. If an outlier was detected in the threshold or R–R interval, it was not included in the averaging calculations.

The recorded ECG waveforms from the subcutaneous and epicardial leads were post-processed and analyzed. If the QRS complex for epicardial (control) and subcutaneous (test) leads were detected within 150 ms of each other (in accordance with ANSI/AAMI EC 57) it was classified as a ‘true positive’ detection. If the QRS was detected with the subcutaneous lead pair but not the epicardial lead pair it was classified as a ‘false positive’. If the epicardial lead pair detected a QRS complex but the subcutaneous lead pair did not then it was classified as a ‘false negative’. The peak voltages of the P wave, QRS complex, and T wave were also measured and compared. The true positive (TP), false positive (FP), and false negative (FN) counts were used to calculate the positive predictive value (PPV) and sensitivity of each subcutaneous lead pair according to the following equations:

$$\text{Positive Predictive Value (PPV)} = \frac{TP}{TP + FP} \quad (1)$$

$$\text{Sensitivity} = \frac{TP}{TP + FN} \quad (2)$$

## RESULTS

### QRS Detection Rate

Subcutaneous and epicardial ECG (2,818 thirty-second data epochs) were recorded at rest and 24 data epochs (15–20 min each) were recorded during treadmill exercise for an aggregated total of 32 h of recorded data for all six animals (Fig. 4, left). QRS

detection with subcutaneous leads demonstrated a  $\geq 95\%$  sensitivity and  $\geq 95\%$  positive predictive value (PPV) in a bovine model during normal daily activities (Table 1). QRS detection with the subcutaneous leads demonstrated a  $\geq 90\%$  sensitivity and  $\geq 90\%$  positive predictive value during treadmill exercise (Fig. 4, right). These data also demonstrated that during exercise, noise and motion artifacts did not significantly distort the ECG waveform or impair the QRS detection rate with subcutaneous leads. None of the subcutaneous lead pairs showed a statistically significant difference in positive predictive value or sensitivity compared to the epicardial or other subcutaneous lead pair configurations ( $\alpha = .05$ ). The trigger (detection) rate was not significantly affected by QRS, T, or P voltage as determined by multivariate regression and best-subset analysis. The mean QRS voltage was  $818 \pm 99 \mu\text{V}$ , the mean T-wave voltage was  $371 \pm 55 \mu\text{V}$ , and the mean-P wave voltage  $256 \pm 48 \mu\text{V}$ . A summary of these results for each of the six animals is presented in Table 1.

#### *Lead Implant Time, Migration, and Durability*

Subcutaneous leads were accurately delivered and placed at distances up to 15 cm from the incision using the straight-needle method. The average time for

placement of a single lead was  $35 \pm 6$  s demonstrating simplicity and ease of lead implantation. The average placement time for 3 pairs of subcutaneous leads was  $9 \pm 2$  min. All leads (36/36) were within 1.4 cm of their initial placement with an average lead migration of  $0.5 \pm 0.1$  cm (Fig. 5). Surgical exposure at necropsy confirmed that none of the subcutaneous leads had significant migration within the subcutaneous space. Electrode position did not significantly increase lead migration, and average lead migration did not vary between animals ( $\alpha = 0.05$ ). There were no lead fractures, sensing wire damage, or permanent signal loss for all tested leads (36/36, 100% success rate). In all calves, no sign of lead infection was observed or identified at necropsy.

## DISCUSSION

Counterpulsation devices require precise timing with the native cardiac cycle to optimize afterload reduction during systole and augment myocardial and end-organ perfusion during diastole. Improper timing by 100–200 ms may diminish the benefits of counterpulsation therapy.<sup>10,25</sup> A longer timing error can produce adverse effects by increasing ventricular afterload during systole and diminishing coronary and

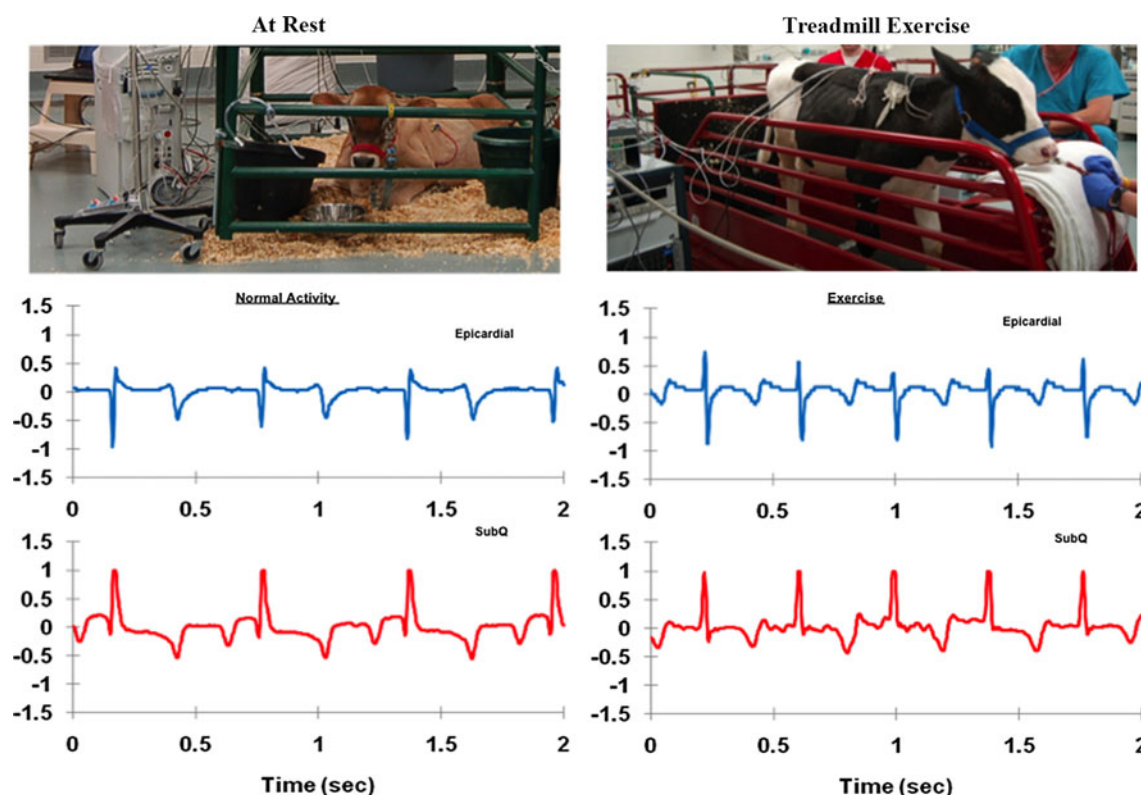


**FIGURE 4.** Sample of normalized ECG tracing measured with subcutaneous (bottom) and epicardial (top) leads during normal daily activity (left) and treadmill exercise (right) in a bovine model.

**TABLE 1. Positive predictive value (PPV), sensitivity, and peak voltages for the three subcutaneous lead pairs in 7-day ( $n = 4$ ) and 14-day ( $n = 2$ ) bovine experiments calculated from ECG recorded at rest and during treadmill exercise.**

N	SubQ pair	Epochs	PPV	Sensitivity	R wave (mV)	T wave (mV)	P wave (mV)
At rest data (30 s clips, 400 Hz)							
1	Pair 1	137	0.999 $\pm$ .001	0.996 $\pm$ .002	1.123	0.524	0.534
	Pair 2	125	0.971 $\pm$ .020	0.925 $\pm$ .021	0.964	0.597	0.405
	Pair 3	135	0.997 $\pm$ .002	0.972 $\pm$ .006	0.549	0.175	0.125
2	Pair 1	158	0.999 $\pm$ .001	0.998 $\pm$ .001	1.147	0.478	0.234
	Pair 2	157	0.998 $\pm$ .001	0.994 $\pm$ .003	0.845	0.337	0.169
	Pair 3	151	0.995 $\pm$ .002	0.987 $\pm$ .006	0.639	0.342	0.216
3	Pair 1	101	0.986 $\pm$ .012	0.962 $\pm$ .013	0.202	0.243	0.206
	Pair 2	158	0.995 $\pm$ .007	0.984 $\pm$ .008	0.691	0.207	0.147
	Pair 3	95	0.993 $\pm$ .012	0.992 $\pm$ .012	0.831	0.209	0.159
4	Pair 1	160	0.996 $\pm$ .002	0.992 $\pm$ .003	1.035	0.320	0.220
	Pair 2	83	0.994 $\pm$ .003	0.932 $\pm$ .009	0.828	0.334	0.239
	Pair 3	83	0.969 $\pm$ .014	0.890 $\pm$ .033	0.591	0.256	0.161
5	Pair 1	254	0.982 $\pm$ .012	0.969 $\pm$ .011	0.360	0.258	0.135
	Pair 2	263	0.999 $\pm$ .001	0.997 $\pm$ .001	0.880	0.237	0.157
	Pair 3	249	0.985 $\pm$ .005	0.968 $\pm$ .013	0.717	0.328	0.202
6	Pair 1	201	0.996 $\pm$ .004	0.986 $\pm$ .007	0.944	0.475	0.374
	Pair 2	153	0.991 $\pm$ .004	0.935 $\pm$ .016	0.953	0.458	0.341
	Pair 3	155	0.990 $\pm$ .005	0.950 $\pm$ .012	0.866	0.418	0.284
Treadmill data (10–20 min clips, 400 Hz)							
5	Pair 1	5	0.965 $\pm$ .076	0.972 $\pm$ .035	0.660	0.283	0.173
	Pair 2	4	0.992 $\pm$ .016	0.985 $\pm$ .021	1.045	0.424	0.259
	Pair 3	3	0.986 $\pm$ .064	0.922 $\pm$ .110	1.003	0.383	0.221
6	Pair 1	6	0.974 $\pm$ .012	0.919 $\pm$ .039	0.923	0.664	0.486
	Pair 2	3	0.969 $\pm$ .067	0.839 $\pm$ .290	0.778	0.452	0.278
	Pair 3	3	0.992 $\pm$ .023	0.960 $\pm$ .067	1.060	0.492	0.418

Note: When applicable, 95% confidence interval upper bound does not exceed 1.

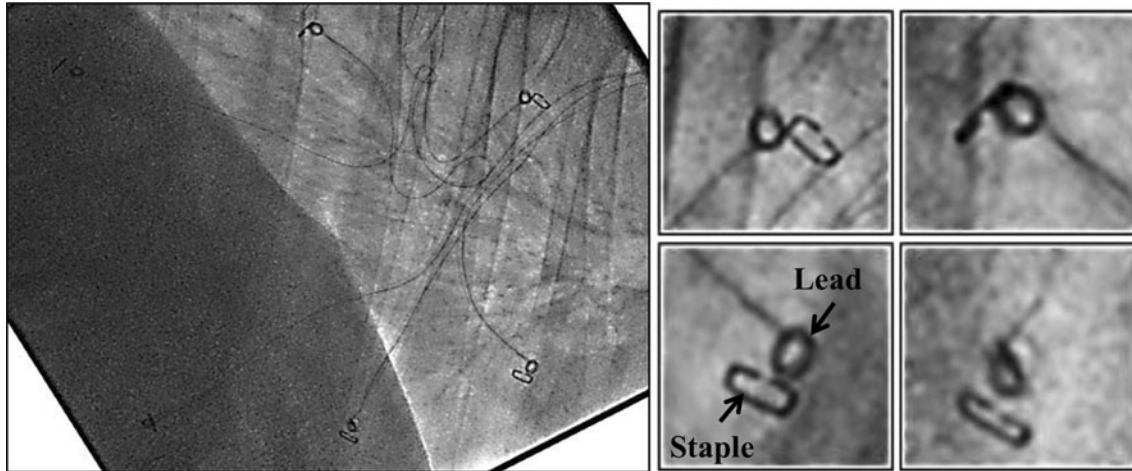


**FIGURE 5. Digital fluoroscopic image of subcutaneous leads in a bovine model recorded 14-days post-implant. Staples were placed on the skin at time of implant to mark placement of the subcutaneous leads (left). Overlaying images recorded at implant and explant revealed no significant lead migration (right) as quantified using ImageJ (NIH, Bethesda, MD) analysis software.**

end-organ flow during diastole. In this study, 150 ms was selected as a metric for evaluating sensitivity and specificity of Symphony timing (control algorithm), which is consistent with values reported in literature for IABP<sup>3,22</sup> and in accordance with ANSI/AAMI EC 57 standard. Unlike IABP, timing with the Symphony is a lot more forgiving. For example, the initiation and

period of diastolic filling with Symphony can be tuned to achieve optimal hemodynamic efficacy, but will not suffer from potentially catastrophic result(s) of sub-optimal timing that may occur with IABP support. Specifically, IABP requires rapid inflation and deflation at precise timing landmarks (i.e. diastolic notch and end-diastole). In contrast, Symphony can eject

over a longer period during diastole, fill over a longer period during systole, and these timing landmarks are not as critical as with IABP. Currently, short-term counterpulsation therapies, including IABP, use an ECG from surface leads and/or aortic pressure from fluid-filled domes or optical sensors for timing balloon inflation and deflation.

Surface ECG leads and arterial pressure are effective for short-term therapy because patients are typically bed-ridden. In ambulatory patients, surface ECG and pressure sensors are prone to respiratory and motion artifact, detachment, drift, sensor management complications including risk of thrombus, and a limited lifespan.<sup>26</sup> Transvenous right ventricular leads are routinely used in permanent pacemakers and defibrillation devices, and provide high-fidelity ECG signals. However, these leads would increase the complexity of Symphony implant procedure by requiring the use of fluoroscopy.<sup>14</sup> Postoperative complications, though uncommon, have been reported with transvenous leads and include lead dislodgment, lead fracture, subclavian vein thrombosis, sensing abnormalities, and lead infection.<sup>18,26</sup> Subcutaneous lead systems (a term broadly used to indicate lead positioning in the space external to the pericardium but below the dermis) have been developed for use in cardiac rhythm monitors.<sup>1,9,13</sup> Subcutaneous leads have long been theorized to be an adequate surrogate for surface signals<sup>12</sup> and QRS detection,<sup>5</sup> have been shown to be less susceptible to motion artifacts than surface leads,<sup>3</sup> and have recently been used in a subcutaneous implantable cardioverter-defibrillator.<sup>1</sup>

To overcome the limitations associated with surface and transvenous ventricular ECG leads, a subcutaneous ECG system was developed. The results of this study demonstrated that the prototype subcutaneous leads could be easily and rapidly implanted with standard surgical equipment and without increasing the complexity of the operation. Fluoroscopy confirmed that the leads did not migrate significantly over time, and there were no lead failures demonstrating the potential for use with a chronic device. In a prior investigation, ECG measurements with subcutaneous leads were at greater risk for motion and muscular artifact compared to epicardial leads during treadmill exercise in animals.<sup>18</sup> However, in our study, QRS detection with subcutaneous leads and standard signal processing was not impaired during normal daily activity or treadmill exercise as evidenced by positive predictive values >95% and sensitivity values >90% (mean  $93.3 \pm 5.6\%$ ) during Symphony support. The selected location of the subcutaneous leads provided excellent R wave and moderate T wave amplitudes, which minimized the number of false 'missed beats' and 'double triggering' events. The subcutaneous leads

provide greater signal amplitude than surface leads, though less signal amplitude than epicardial leads. However, ECG signal amplitudes were sufficient for highly reliable, real-time QRS detection with subcutaneous leads compared to epicardial leads.

The R-wave detection algorithm used in this study applies a simple adaptive-thresholding technique that is computationally inexpensive. While this is an accepted algorithm for QRS detection that is still often used in industry, other emerging techniques such as wavelet analysis may be considered to further improve detection rates. Despite the simplicity of the selected QRS detection algorithm, the PPV and sensitivity were greater than 95% at rest and 90% during exercise; suggesting that data from subcutaneous ECG leads would result in appropriate device performance. As noted, integrating advanced QRS detection strategies may further improve detection rates, PPV, and sensitivity.

Since the Symphony system is pneumatically-driven with an external, portable driver, we did not expect to see any electrical interface in the ECG waveform due to the Symphony controller. With the subcutaneous leads tunneled through the skin, we did not expect any lead movement, which was confirmed by fluoroscopy and at necropsy as evidenced by minimal sensor migration ( $0.5 \pm 0.1$  cm). Importantly, electrical interference or motion artifact in the ECG waveform was not observed in the bovine model during acute or chronic experiments with normal daily activity or treadmill exercise. We anticipate similar results clinically, but cannot confirm until clinical trials with subcutaneous leads are initiated.

### *Limitations*

The fabricated prototype leads require further development and are not considered suitable for human use. The ECG measurements with the epicardial leads were signal conditioned with FDA approved clinical driver (iPulse, Abiomed, Danvers, MA) while the subcutaneous leads were signal conditioned with a clinical-grade ECG amplifier (Gould, Cleveland OH). The study period of 14-days provided preliminary results to demonstrate feasibility, but is insufficient to quantify long-term lead migration (6 months–2 years), durability, and histological response. Chronic animals studies (i.e. 90-day study) with re-designed, clinical grade subcutaneous leads will be conducted in the near future.

### CONCLUSION

This study demonstrated the subcutaneous ECG leads provided results similar to epicardial leads for



triggering of a counterpulsation device (Symphony) as evidenced by equivalent QRS detection rates at rest (>95% positive predictive value and sensitivity) and exercise (>90% positive predictive value and sensitivity). We also demonstrated minimal lead migration, no lead fractures, no permanent signal loss, or lead infection while offering the advantages of a less invasive method of delivery. Further development of subcutaneous ECG leads for triggering of the Symphony device is warranted.

## ACKNOWLEDGMENTS

This study was funded by NIH SBIR phase I grant 1R43HL102981-01. Funding was provided to SCR (Louisville, KY) and the University of Louisville by NIH-SBIR phase II (R43HL102981) and Kentucky Science & Technology (KSTC-184-512-08-054) grants.

## DISCLOSURES

Landon Tompkins, Robert Dowling, MD and Paul Spence, MD are employees of SCR Inc (Louisville, KY) with commercial interests in the development of the Symphony system. Eric Gratz is an employee of Abiomed Inc (Danvers, MA) with commercial interests in the development of the Symphony system.

## REFERENCES

- <sup>1</sup>Bardy, G. H., *et al.* An entirely subcutaneous implantable cardioverter-defibrillator. *N. Engl. J. Med.* 363(1):36–44, 2010.
- <sup>2</sup>Bartoli, C. R., *et al.* A novel subcutaneous counterpulsation device: acute hemodynamic efficacy during pharmacologically induced hypertension, hypotension, and heart failure. *Artif. Organs.* 34(7):537–545, 2010.
- <sup>3</sup>Bellardine, B., *et al.* Is surface ECG a useful surrogate for subcutaneous ECG? *Pacing Clin. Electrophysiol.* 33(2):135–145, 2010.
- <sup>4</sup>Drew, G., and S. Koenig. Biomedical patient monitoring, data acquisition, and playback with LabVIEW. In: *Virtual Bio-Instrumentation: Biomedical, Clinical, and Healthcare Applications in LabVIEW*, edited by J. B. Olansen, and E. Rosow. Upper Saddle River, NJ: Prentice Hall, 2002, pp. 180–186.
- <sup>5</sup>Fotuhi, P., *et al.* R wave detection by subcutaneous ECG. possible use for analyzing R R variability. *Ann. Noninvas. Electrocardiol.* 6(1):18–23, 2001.
- <sup>6</sup>Frankel, R. A., *et al.* A filter to suppress ECG baseline wander and preserve ST-segment accuracy in a real-time environment. *J. Electrocardiol.* 24(4):315–323, 1991.
- <sup>7</sup>Giridharan, G. A., *et al.* Predicted hemodynamic benefits of counterpulsation therapy using a superficial surgical approach. *ASAIO J.* 52(1):39–46, 2006.
- <sup>8</sup>Gomes, J. A., *et al.* Optimal bandpass filters for time-domain analysis of the signal-averaged electrocardiogram. *Am. J. Cardiol.* 60(16):1290–1298, 1987.
- <sup>9</sup>Grace, A., *et al.* Evaluation of four distinct subcutaneous implantable defibrillator (S-ICD®) lead systems in humans. *Heart Rhythm* 3:S128–S129, 2006.
- <sup>10</sup>Hanlon-Pena, P. M., and S. J. Quaal. Intra-aortic balloon pump timing: review of evidence supporting current practice. *Am. J. Crit. Care* 20(4):323–333, 2011.
- <sup>11</sup>Hassler, C. ECG lead placement in quadrupeds. *Telemetry Times* (Technical Note, 8/3/94). Data Sciences Int, 1994.
- <sup>12</sup>Ho, C., and S. Kurtzman. Three perspectives of cardiac electrical activity. *Biomed. Sci. Instrum.* 37:325, 2001.
- <sup>13</sup>Iglesias, J. F., *et al.* The implantable loop recorder: a critical review. *Kardiovaskuläre Medizin* 12(3):85–93, 2009.
- <sup>14</sup>Kautzner, J., *et al.* Technical aspects of implantation of LV lead for cardiac resynchronization therapy in chronic heart failure. *Pacing Clin. Electrophysiol.* 27(6p1):783–790, 2004.
- <sup>15</sup>Koenig, S. C., *et al.* Integrated data acquisition system for medical device testing and physiology research in compliance with good laboratory practices. *Biomed. Instrum. Technol.* 38(3):229–240, 2004.
- <sup>16</sup>Koenig, S. C., *et al.* Development and early testing of a simple subcutaneous counterpulsation device. *ASAIO J.* 52(4):362, 2006.
- <sup>17</sup>Koenig, S. C., *et al.* Acute hemodynamic efficacy of a 32-ml subcutaneous counterpulsation device in a calf model of diminished cardiac function. *ASAIO J.* 54(6):578, 2008.
- <sup>18</sup>Lawton, J. S., *et al.* Sensing lead-related complications in patients with transvenous implantable cardioverter-defibrillators. *Am. J. Cardiol.* 78(6):647–651, 1996.
- <sup>19</sup>Lobodzinski, S. S., M. M. Laks, S. S. Lobodzinski, and M. M. Laks. Comfortable textile-based electrocardiogram systems for very long-term monitoring. *Cardiol. J.* 15(5):477, 2008.
- <sup>20</sup>Meyns, B., *et al.* Proof of concept: hemodynamic response to long-term partial ventricular support with the synergy pocket micro-pump. *J. Am. Coll. Cardiol.* 54(1):79–86, 2009.
- <sup>21</sup>Nanas, J. N., and S. D. Mouloupoulos. Counterpulsation: historical background, technical improvements, hemodynamic and metabolic effects. *Cardiology* 84(3):156–167, 1994.
- <sup>22</sup>Pantalos, G. M., S. C. Koenig, K. J. Gillars, G. S. Haugh, R. D. Dowling, and L. A. Gray. Intraaortic balloon pump timing discrepancies in adult patients. *Artif. Organs.* 35(9):857–866, 2011.
- <sup>23</sup>Papaioannou, T. G., and C. Stefanadis. Basic principles of the intraaortic balloon pump and mechanisms affecting its performance. *ASAIO J.* 51(3):296–300, 2005.
- <sup>24</sup>Pino, E., *et al.* Real-time ECG Algorithms for Ambulatory Patient Monitoring. 2005. American Medical Informatics Association.
- <sup>25</sup>Schreuder, J. J., *et al.* Beat-to-beat effects of intraaortic balloon pump timing on left ventricular performance in patients with low ejection fraction. *Ann. Thorac. Surg.* 79(3):872–880, 2005.
- <sup>26</sup>Schwartzman, D., *et al.* Postoperative lead-related complications in patients with nonthoracotomy defibrillation lead systems. *J. Am. Coll. Cardiol.* 26(3):776–786, 1995.
- <sup>27</sup>Thakor, N. V., J. G. Webster, and W. J. Tompkins. Estimation of QRS complex power spectra for design of a QRS filter. *IEEE Trans. Biomed. Eng.* (11):702–706, 1984.

# DETECTION OF WHITE MATTER ABNORMALITIES IN MR BRAIN IMAGES FOR DIAGNOSIS OF AUTISM IN CHILDREN

M. Ismail<sup>1</sup>, A. Soliman<sup>1</sup>, A. ElTanboly<sup>1,2</sup>, A. Switala<sup>1</sup>, M. Mahmoud<sup>1</sup>, F. Khalifa<sup>1</sup>, G. Gimel'farb<sup>3</sup>,  
M. F. Casanova<sup>4</sup>, R. Keynton<sup>1</sup>, and A. El-Baz<sup>1</sup>

<sup>1</sup>Bioengineering Department, University of Louisville, Louisville, KY, USA.

<sup>2</sup>Mathematics and Physical Engineering Department, Mansoura University, Egypt.

<sup>3</sup>Department of Computer Science, University of Auckland, Auckland 1142, New Zealand.

<sup>4</sup>Departments of Pediatrics and Biomedical Sciences, University of South Carolina, South Carolina, USA.

## ABSTRACT

This paper introduces a novel computer-aided diagnosis (CAD) system for the diagnosis of autism from magnetic resonance (MR) brain images of children. The proposed framework has two main components. First, cerebral white matter (CWM) is segmented from the brain volume using an adaptive shape model that is built from a set of co-aligned training images. A higher-order Markov Gibbs random field (MGRF) spatial interaction model is then integrated with an intensity model to account for data inhomogeneities. Secondly, CWM meshes are reconstructed and a curvature-based analysis is applied in order to differentiate between autistic and control brains. From the reconstructed CWM meshes, we estimated 3 shape features (curvedness, sharpness, and mean curvature) that could geometrically describe CWM folds. The statistical analysis conducted on 20 autistic and control brains using binomial regression on raw features as well as on their principal components reveals that the three curvature-based measures could be used as discriminatory features between autistic and control brains. Moreover, the accuracy of the diagnostic results using  $K$ -nearest neighbor (KNN) classifier is 95%. These results show the promise of the proposed technique as a supplement to current diagnostic instruments (e.g., Autism Diagnostic Interview, Revised (ADI-R)).

**Index Terms**— MGRF, CWM, Curvature, Sharpness

## 1. INTRODUCTION

Autism is a neurodevelopmental disorder that has an impact on both behavior and social cognition. It is acknowledged that early diagnosis allows for more effective interventions and better outcomes.

Structural MRI studies conducted for diagnostic screening of autism have used either volumetric or shape measurements of brain structures; however, to our knowledge, no surface analysis of subcortical structures has been conducted. As an example, studies of commissural tracts such as the corpus callosum have targeted its length and/or volume. Volumetric measurements of structures such as white matter (WM) and gray matter (GM) have also been addressed, with varying results [1, 2]. The main limitation of volumetric measurements is that they are age-sensitive and therefore in need of age correction coefficients. Shape measurements have also been addressed in the literature such as the implementation of sulcal depth maps to quantify the cortical folding [3] using spherical harmonics where morphological information was derived from the coefficients of a weighted SPHARM [4, 5]. Some shape studies have also conducted measurements on the corpus callosum (CC) [6, 7], where skeletal analysis was used to differentiate between autistic and control subjects. These studies have reported that the CC has smaller size in

the brains of autistic individuals. Skeletal analysis techniques limit the use of the surface and thus its classification rate is low. All the above-mentioned techniques have provided promising results, yet no surface analysis on the totality of the CWM has been conducted, or was applied to adult brains only without providing evidence that such changes could generalize to young age. We believe that surface analysis of deep brain parts, e.g. CWM, can lead to better biomarkers for autism diagnosis than those obtained from outer structures [8].

In order to develop a CAD system that is based on the shape analysis of CWM, it is crucial to have accurate segmentation that preserves its edges/surface [9]. Brain CWM segmentation has been widely addressed in the literature. Patenaude et al. [10], for example, exploited both active and shape appearance models within a Bayesian framework for brain segmentation. Wang et al. [11] used a random forest technique to integrate features from different modalities for infant brain segmentation along with probability maps of GM and CWM. Atlas-based segmentation was also used for CWM segmentation, such as the work employed by Ledig et al. [12], where global and stationary Markov random field (MRF) were incorporated with *a priori* defined model for labeling brain scans. Han et al. [13] applied an intensity re-normalization procedure to adjust the prior atlas intensity model to the input data. Morin et al. [14] applied an atlas-based segmentation framework using random walks, that combined registration and labeling propagation. shape priors was also addressed in [15], and applied on infant brains. Some approaches employ longitudinal scans at a late-time-point age, where the contrast is much better between different tissue types, from which probabilistic atlases are constructed to guide segmentation of neonatal images [16, 17]. Deformable models have also been used for brain labeling, such as [18], where a set of Wendlands radial basis functions (RBFs) represented the contour and was evolved by iterative updates of RBFs locations.

From the literature conducted above, some limitations can be observed. Most of the statistical methods depend only on predefined probability models that cannot fit all of the possible real data distributions. As to Atlas-based segmentation, it is mostly challenged by atlas selection along with heavy computation time. Also the accuracy of deformable models is based on the design of guiding forces and the initialization.

To overcome the aforementioned limitations, we propose a novel CAD system for the diagnosis of autism in children, with two main components of its pipeline. The brain volume is first segmented using an adaptive shape model that is combined with an intensity model and a higher-order MGRF model, which has the ability to capture the fine details of brain CWM regions. Curvature-based analysis is then applied to the extracted CWM to obtain discriminatory fea-

tures between neurotypicals and autistic subjects.

## 2. SEGMENTATION OF CWM FROM MR IMAGES

Let  $\mathbf{g} = \{g_{x,y,z} : (x,y,z) \in \mathbf{R}; g_{x,y,z} \in \mathbf{Q}\}$  and  $\mathbf{m} = \{m_{x,y,z} : (x,y,z) \in \mathbf{R}; m_{x,y,z} \in \mathbf{L}\}$  be a grayscale image taking values from  $\mathbf{Q}$ , i.e.,  $\mathbf{g} : \mathbf{R} \rightarrow \mathbf{Q}$ , and a region map taking values from  $\mathbf{L}$ , i.e.,  $\mathbf{m} : \mathbf{R} \rightarrow \mathbf{L}$ , respectively.  $\mathbf{R}$  denotes a finite 3D arithmetic lattice,  $\mathbf{Q}$  is a finite set of integer gray values, and  $\mathbf{L}$  is a set of region labels. An input brain image,  $\mathbf{g}$ , co-aligned to the training data base, and its map,  $\mathbf{m}$ , are described with a joint probability model:  $P(\mathbf{g}, \mathbf{m}) = P(\mathbf{g}|\mathbf{m})P(\mathbf{m})$ , which combines a conditional distribution of the images given the map  $P(\mathbf{g}|\mathbf{m})$ , and an unconditional probability distribution of maps  $P(\mathbf{m}) = P_{\text{sp}}(\mathbf{m})P_{\text{V}}(\mathbf{m})$ . Here,  $P_{\text{sp}}(\mathbf{m})$  denotes a weighted shape prior, and  $P_{\text{V}}(\mathbf{m})$  is a Gibbs probability distribution with potentials  $\mathbf{V}$ , which specifies a MGRF model of spatially homogeneous maps  $\mathbf{m}$ .

**First-Order Intensity Model,  $P(\mathbf{g}|\mathbf{m})$ :** The first-order visual appearance of each brain label is modeled by separating a mixed distribution of voxel intensities of the brain MRIs into individual components associated with the dominant modes of the mixture. The latter is approximated using the linear combinations of discrete Gaussians (LCDG) approach [19], which employs positive and negative Gaussian components.

**MGRF Model With Higher-order Cliques,  $P_{\text{V}}(\mathbf{m})$ :** The spatial interactions between the brain voxels are also taken into account using a higher-order MGRF spatial model, which adds the families of the triple and quad cliques to the pairwise cliques. The higher-order model has the ability to account for inhomogeneity of MR brain images, thus, reducing the noise effects and increasing the segmentation accuracy. Let  $\mathbf{C}_a$  denote a family of  $a$ -order cliques of an interaction graph with nodes in the 3D lattice sites  $p = (x,y,z)$  and edges connecting the interacting sites. The label interactions are modeled by a spatially homogeneous MGRF with up to fourth-order interactions over the nearest 26-neighborhoods of voxels:

$$P_{\text{V}}(\mathbf{m}) = \frac{1}{Z_{\text{V}}} \exp \left( \sum_{a=1}^A \sum_{\mathbf{c} \in \mathbf{C}_a} V_a(\mathbf{m}(x,y,z) : (x,y,z) \in \mathbf{c}) \right) \quad (1)$$

where  $A$  clique families describe the graph interactions,  $\mathbf{V} = [V_a : \{0, \dots, L\} \rightarrow (-\infty, \infty) : a = 1, \dots, A]$  is a collection of Gibbs potential functions  $V_a$  for the families  $\mathbf{C}_a$ , and the partition function  $Z_{\text{V}}$  normalizes the probabilities. An initial region map  $\mathbf{m}$  allows for analytically approximating the maximum likelihood estimates of the potentials and computing the voxel-wise probabilities of the region labels. The second-, third-, and forth-order potentials are given by Eqs. (2), (3), and (4), respectively:

$$V_a(m_{\mathbf{p}_1}, m_{\mathbf{p}_2}) = \begin{cases} V_{2:a:\text{eq}} & \text{if } m_{\mathbf{p}_1} = m_{\mathbf{p}_2} \\ -V_{2:a:\text{eq}} & \text{otherwise} \end{cases} \quad (2)$$

$$V_a(m_{\mathbf{p}_1}, m_{\mathbf{p}_2}, m_{\mathbf{p}_3}) = \begin{cases} V_{3:a:\text{eq}_3} & \text{if } m_{\mathbf{p}_1} = m_{\mathbf{p}_2} = m_{\mathbf{p}_3} \\ -V_{3:a:\text{eq}_3} & \text{otherwise} \end{cases} \quad (3)$$

$$V_a(m_{\mathbf{p}_1}, m_{\mathbf{p}_2}, m_{\mathbf{p}_3}, m_{\mathbf{p}_4}) = \begin{cases} V_{4:a:\text{eq}_4} & \text{if 4 equal labels} \\ V_{4:a:\text{eq}_3} & \text{if 3 equal labels} \\ -(V_{4:a:\text{eq}_3} + V_{4:a:\text{eq}_4}) & \text{otherwise} \end{cases} \quad (4)$$

where  $m_{\mathbf{p}_i}$  is the region map label at the voxel  $\mathbf{p}_i$ .

**Shape Model,  $P_{\text{sp}}(\mathbf{m})$ :** To enhance the segmentation accuracy, expected shapes of each brain label are constrained with an adaptive probabilistic shape prior. To create the shape database, a training set of images, collected for 15 subjects, are co-aligned by 3D affine transformations with 12 degrees of freedom in a way that maximizes their mutual information [20]. This set is then subdivided into 3 atlases based on the normalized cross correlation measure. This is done in order to improve the segmentation accuracy by integrating each atlas with both the intensity and spatial models, and finally applying the majority voting criterion to determine the structure of each voxel. For each input MR data to be segmented, the shape prior is constructed by an adaptive process guided by the visual appearance features of the input MRI data. The segmentation steps of our framework are summarized in Algorithm 1.

---

### Algorithm 1 Steps of the Proposed CAD System

---

- **MRI Preprocessing and Shape Database Construction**
    - A. Use the automated approach in [21] to remove the skull from the MR images.
    - B. Construct the shape database through co-alignment of the biased-corrected training brains (both grey scale and their ground truth).
    - C. Divide the database into 3 atlases (5 subjects each) using normalized-cross correlation (NCC).
  - **Brain Segmentation**
    - A. Align the test subject with the shape database to get the 3D affine matrix  $\mathbf{T}$ .
    - B. **For each Atlas:**
      1. Estimate the adaptive shape prior probability:
        - a. Use the matrix  $\mathbf{T}$  in Step A. to transform each voxel to the atlas domain.
        - b. Initialize a 3D window of size  $N_1 \times N_2 \times N_3$  and search inside it for voxels with corresponding grey level in all training sets with equalized intensities.
        - c. Increase the window size, if needed, and redo the search until a non-empty result is found. If maximum size is reached and no result is found, increase the grey level tolerance and get back to Step b.
        - d. Create probabilities based on the labels from the search results.
      2. Approximate  $P(\mathbf{g})$  using an LCDG with four dominant modes.
      3. Form region map  $\mathbf{m}$  using marginal estimated density and prior shape.
      4. Find the Gibbs potentials for the MGRF model from the initial map  $\mathbf{m}$ .
      5. Improve  $\mathbf{m}$  using the iterative conditional mode (ICM) algorithm [22].
    - C. Apply majority voting to fuse the segmentation results of the three atlases.
  - **Classification/Diagnosis**
    - A. Reconstruct CWM meshes using the marching cubes algorithm [23].
    - B. Compute  $\mathbf{H}$ ,  $\mathbf{C}$ , and  $\mathbf{S}$  measures, then apply  $K_n$  classifier and majority voting to classify the input subject.
-

### 3. ESTIMATION OF CWM SHAPE INDICES

The 3D brain CWM models are reconstructed from the segmentation results in Section 2 using the marching cubes algorithm [23]. Then three shape features (curvedness, sharpness, and mean curvature) are estimated to geometrically describe CWM. The mean curvature  $H = \frac{1}{2}(K1 + K2)$  [24] is an extrinsic measure that is the average of the maximum and minimum principal curvatures  $K1$  and  $K2$  respectively. Curvedness  $C = \sqrt{\{K1^2 + K2^2\}}/2$  is a measure of how much shape the neighborhood of a voxel includes [24]. It can distinguish the regions that are highly folded from others with less folding [25]. The sharpness  $S = (K1 - K2)^2$ , which is proportional to the Willmore integrand, is used to quantify the sharpness of folding. All measures are computed on the vertices of the constructed CWM meshes, Algorithm 1.

### 4. EXPERIMENTAL RESULTS AND CONCLUSIONS

The proposed framework was tested on 20 subjects (10 autistic, 10 control) obtained from the ABIDE database [26], aged 8-10 years. T1 weighted images were acquired using the MPRAGE pulse sequence with a voxel size of  $1 \times 1 \times 1 \text{ mm}^3$ .

As the segmentation step is important to the subsequent stage, we first validate the segmentation approach using ground truth for subjects, which was created by an MR expert. The performance of the proposed segmentation framework was evaluated using three metrics: (i) the Dice similarity coefficient (DSC) [27], (ii) the 95-percentile modified Hausdorff distance (MHD) [28], and (iii) the absolute brain volume difference (ABVD). Metrics were computed by comparing the ground truth segmentation to results from the proposed approach. The DSC, MHD, and ABVD for our segmentation of the CWM are  $94.7 \pm 1.53\%$ ,  $6.5 \pm 1.23 \text{ mm}$ , and  $3.17 \pm 1.73\%$ . Fig. 1 shows that the joint model combining the intensity, spatial, and shape information was a better performer than having only one or two of three models. The intensity information alone (Fig. 1(b)), or having it combined with the shape information, (Fig. 1(c)), failed to capture fine details. This is enhanced after using higher-order MGRF (Fig. 1(d)), where CWM edges are better retained.

The performance of the proposed segmentation approach is highlighted by comparing it against the software package (iBEAT) [11], that performs bias correction followed by brain segmentation. Segmentation accuracies for the iBEAT results are  $85.3 \pm 1.27\%$ ,  $8.27 \pm 1.63 \text{ mm}$ , and  $13.46 \pm 2.18\%$  for the DSC, MHD, and ABVD, respectively. These results emphasize the efficiency of the proposed approach that is required for the next phase of the proposed CAD system. In addition, the average time to segment a brain volume using the proposed approach is less than a minute, whereas it takes around 40 minutes using iBEAT. This is the only comparison conducted in this paper due to space limitations.

Following the segmentation of MR images, CWM meshes are reconstructed, then measures of  $H$ ,  $C$ , and  $S$  are calculated for mesh vertices. The obtained measures reveal that the CWM of an autistic brain mesh exhibits higher mean curvature and curvedness (more highly folded areas) than that of a control one. Also  $S$  values show that more sharply folded regions can be found in autism, Fig. 2. These findings are in line with the work in [8].

Statistical analysis of the  $H$ ,  $C$ ,  $S$  measures was performed using regression analysis. A control subject is first selected as a reference, then all curvature maps for the rest of the subjects were normalized with respect to it. The highest 1%, 5%, 10%, and 20% values of  $H$ ,  $C$ , and  $S$  for all subjects were selected, Fig. 2(c). The analysis showed that  $C$ , and  $S$  are significant discriminatory features between autistic and control meshes and  $H$  is extremely significant.

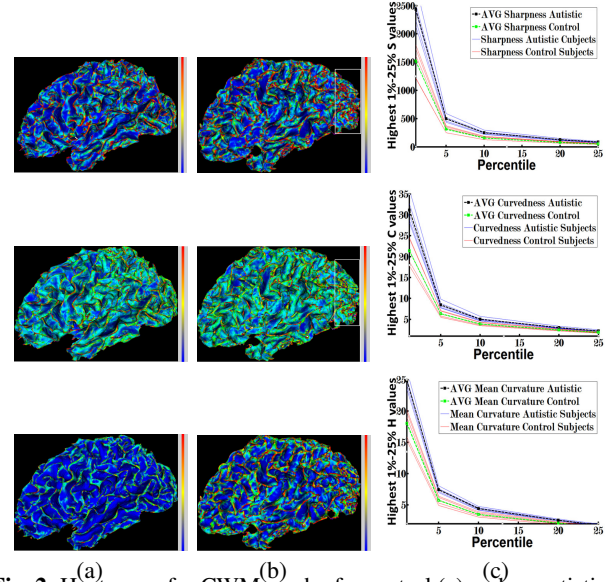


**Fig. 2.** Heat maps for CWM mesh of a control (a) and an autistic (b) subject showing  $S$  (first row),  $C$  (second row), and  $H$  (third row) measures. The  $S$  map shows more sharply folded areas in autism. The occipital CWM (bounded by boxes) shows higher  $S$  and  $C$  in autism. The  $H$  maps show that the autistic CWM meshes exhibit higher curvature. (c) Statistics for the 3 features on a sample of 5 autistic and 5 control subjects. **Visual results coincide with the statistical finding of having the  $H$  measure as an extremely significant feature for discrimination.** A color scale is provided (blue is for low measures values, and red is for high ones).

Binomial regression of group (autism or control) was performed on each raw measurement in turn, as well as on the principal components. The Akaike information criterion (AIC) took its lowest value of 15.95 for the regression on  $H_{1\%}$ . AIC took its largest value of 18.47 in the regression against  $K_{20\%}$ . This corresponds to a relative likelihood of 0.284, so the least informative single measurement is not significantly worse than the most informative.

Diagnostic classification was also conducted using the  $K$ -nearest neighbor (KNN) classifier and the leave-one-out approach. This was applied for each of the three features, followed by a majority voting criterion in order to fuse the classification results from the  $H$ ,  $C$ , and  $S$  measures and make the final decision. This approach successfully classified 9 autistic cases and identified all control ones.

In conclusion, this paper proposed an approach for autism diagnosis in subjects aged from 8-10 years old. It started with brain CWM segmentation, followed by curvature analysis. Results showed the higher curvature and sharpened folds the CWM exhibit in autism. Future work will target the surface analysis of lower age groups, such as the IBIS database (aged around 6 months and above). It will also target extracting curvature-based features on regions of interest that have been proved to associate with autism.

### 5. REFERENCES

- [1] M. K. Chung et al., "Less white matter concentration in autism: 2d voxel-based morphometry," *Neuroimage*, vol. 23, no. 1, pp. 242–251, 2004.
- [2] E. Courchesne et al., "Unusual brain growth patterns in early life in patients with autistic disorder an MRI study," *Neurology*, vol. 57, no. 2, pp. 245–254, 2001.



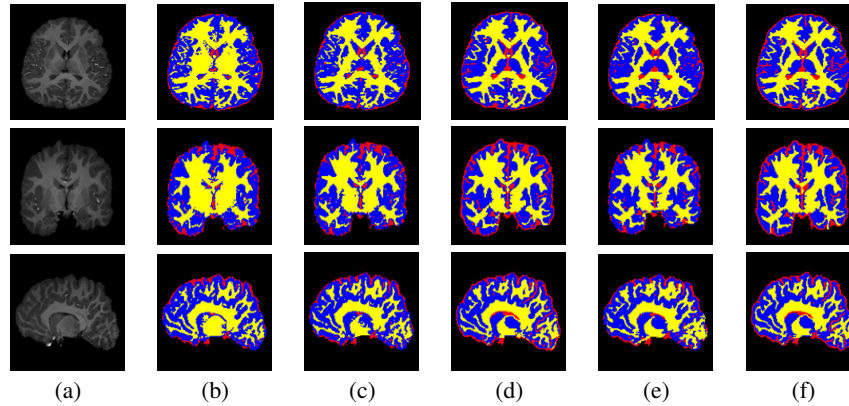


**Fig. 1.** Segmentation results projected onto axial, coronal, and sagittal planes: (a) original MRIs after skull stripping, and the segmentation using (b) intensity model alone; (c) intensity and shape models (d) intensity, shape, and higher-order MGRF models; and (e) the iBEAT method. Ground truth is shown in (f). CWM is in yellow, GM in blue, and cerebrospinal fluid (CSF) is in red for visualization purposes. All subjects are bias-corrected prior to segmentation using iBEAT or proposed method.

- [3] C. W. Nordahl et al., "Cortical folding abnormalities in autism revealed by surface-based morphometry," *J Neurosci*, vol. 27, no. 43, pp. 11725–11735, 2007.
- [4] M. K. Chung et al., "Tensor-based cortical surface morphometry via weighted spherical harmonic representation," *TMI*, vol. 27, no. 8, pp. 1143–1151, 2008.
- [5] G. Gerig et al., "Shape analysis of brain ventricles using spharm," in *Math Methods Biomed Image Anal*, 2001, pp. 171–178.
- [6] K. Gorgcowski et al., "Statistical shape analysis of multi-object complexes," in *CVPR*, 2007, pp. 1–8.
- [7] A. Elnakib et al., "Autism diagnostics by centerline-based shape analysis of the corpus callosum," in *ISBI*, 2011, pp. 1843–1846.
- [8] M.F. Casanova et al., "Reduced gyral window and corpus callosum size in autism: possible macroscopic correlates of a minicolumnopathy," *J Autism Dev Disord*, vol. 39, no. 5, pp. 751–764, 2009.
- [9] M.A. Balafar et al., "Review of brain MRI segmentation methods," *Artif Intell Rev*, vol. 33, no. 3, pp. 261–274, 2010.
- [10] B. Patenaude et al., "A bayesian model of shape and appearance for subcortical brain segmentation," *Neuroimage*, vol. 56, no. 3, pp. 907–922, 2011.
- [11] D. Yakang et al., "iBEAT: a toolbox for infant brain magnetic resonance image processing," *Neuroinformatics*, vol. 11, no. 2, pp. 211–225, 2013.
- [12] C. Ledig et al., "Multi-class brain segmentation using atlas propagation and EM-based refinement," in *ISBI. IEEE*, 2012, pp. 896–899.
- [13] X. Han et al., "Atlas renormalization for improved brain MR image segmentation across scanner platforms," *TMI*, vol. 26, no. 4, pp. 479–486, 2007.
- [14] J-P Morin et al., "Atlas-based segmentation of brain magnetic resonance imaging using random walks," in *(CVPRW). IEEE*, 2012, pp. 44–49.
- [15] M. Altaye et al., "Infant brain probability templates for mri segmentation and normalization," *Neuroimage*, vol. 43, no. 4, pp. 721–730, 2008.
- [16] L. Wang et al., "Longitudinally guided level sets for consistent tissue segmentation of neonates," *Hum brain mapp*, vol. 34, no. 4, pp. 956–972, 2013.
- [17] F. Shi et al., "Neonatal brain image segmentation in longitudinal mri studies," *Neuroimage*, vol. 49, no. 1, pp. 391–400, 2010.
- [18] J. Liu et al., "Accurate and robust extraction of brain regions using a deformable model based on radial basis functions," *J Neurosci Methods*, vol. 183, no. 2, pp. 255–266, 2009.
- [19] A. El-Baz et al., "Precise segmentation of 3-D magnetic resonance angiography," *IEEE Trans Biomed Eng*, vol. 59, no. 7, pp. 2019–2029, 2012.
- [20] P. A. Viola and W. M. Wells III, "Alignment by maximization of mutual information," *Int J Comput Vis*, vol. 24, no. 2, pp. 137–154, 1997.
- [21] A. Alansary et al., "An integrated geometrical and stochastic approach for accurate infant brain extraction," in *ICIP*, 2014, pp. 3542–3546.
- [22] J. Besag, "On the statistical analysis of dirty pictures," *J R Stat Soc Ser B*, vol. 48, no. 3, pp. 259–302, 1986.
- [23] W. E. Lorensen et al., "Marching cubes: A high resolution 3D surface construction algorithm," *ACM Siggraph Comput Graph*, vol. 21, no. 4, pp. 163–169, 1987.
- [24] J. Koenderink et al., "Surface shape and curvature scales," *Img Vis Comput*, vol. 10, no. 8, pp. 557–564, 1992.
- [25] R. Pienaar et al., "A methodology for analyzing curvature in the developing brain from preterm to adult," *IJIST*, vol. 18, no. 1, pp. 42–68, 2008.
- [26] A. Di Martino et al., "The autism brain imaging data exchange: towards a large-scale evaluation of the intrinsic brain architecture in autism," *Mol psychiatry*, vol. 19, no. 6, pp. 659–667, 2014.
- [27] L. R. Dice, "Measures of the amount of ecologic association between species," *Ecology*, vol. 26, no. 3, pp. 297–302, 1945.
- [28] G. Gerig et al., "Valmet: A new validation tool for assessing and improving 3D object segmentation," in *(MICCAI)*, 2001, pp. 516–523.

# A NOVEL AUTOMATIC SEGMENTATION OF HEALTHY AND DISEASED RETINAL LAYERS FROM OCT SCANS

A. ElTanboly<sup>1,2,\*</sup>, M. Ismail<sup>2,\*</sup>, A. Switala<sup>2</sup>, M. Mahmoud<sup>2</sup>, A. Soliman<sup>2</sup>, T. Neyer<sup>3</sup>, A. Palacio<sup>3</sup>,  
A. Hadayer<sup>3</sup>, M. El-Azab<sup>1</sup>, S. Schaal<sup>3</sup> and A. El-Baz<sup>2 †</sup>

<sup>1</sup>Mathematics and Physical Engineering Department, Mansoura University, Egypt.

<sup>2</sup>Bioengineering Department, University of Louisville, Louisville, KY, USA.

<sup>3</sup>Ophthalmology and Visual Sciences Department, School of Medicine,  
University of Louisville, Louisville, KY, USA.

## ABSTRACT

This paper introduces a novel framework for segmenting retinal layers from optical coherence tomography (OCT) images. In order to account for the noise and inhomogeneity of OCT scans, especially for diseased ones, the proposed framework is based on unique joint model that combines shape, intensity, and spatial information, and is able to segment 12 distinct retinal layers. First, the shape prior is built using a subset of co-aligned training OCT images. The alignment process is initialized using an innovative method that employs multi-resolution edge tracking which defines control points on the tracked retinal boundaries. The shape model is then adapted during the segmentation process using visual appearance characteristics that are described using pixel-wise image intensities and their spatial interaction features. In order to more accurately model the empirical grey level distribution of OCT images, a linear combination of discrete Gaussians (LCDG) is used that has positive and negative components. Also, in order to accurately account for noise, the model is integrated with a second-order Markov Gibbs random field (MGRF) spatial interaction model. The proposed approach was tested on 200 normal and diseased OCT scans (e.g. Age macular degeneration (AMD), diabetic retinopathy), having their ground truth delineated by retina specialists, then measured using the Dice similarity coefficient (DSC), agreement coefficient (AC1), and average deviation (AD) metrics. The accuracy achieved by the segmentation approach clearly demonstrates the promise it holds for robust segmentation of retinal layers which would aid in the early diagnosis of different retinal abnormalities.

**Index Terms**— OCT, shape prior, reflectivity, LCDG, MGRF.

## 1. INTRODUCTION

Optical coherence tomography (OCT) has become a powerful modality for the noninvasive diagnosis of various retinal abnormalities such as glaucoma, diabetic macular edema, and macular degeneration. Quantifying such diseases would require accurate automatic approaches. The goal of this paper is to develop an automated algorithm to segment 12 distinct layers in healthy and diseased subjects from OCT images, Fig. 1.

Segmenting intra-retinal layers from OCT images has been addressed in the literature. Bagci et al. [1] proposed an automated algorithm that extracted 7 retinal layers using a customized filter for edge

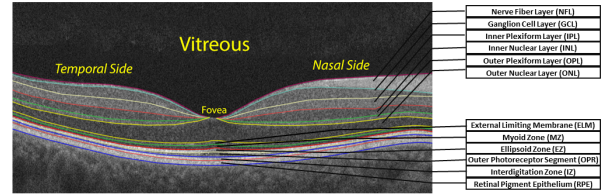


**Fig. 1.** A typical OCT scan of a normal subject showing the 12 distinct layers.

enhancement and a grey-level mapping technique that overcame uneven tissue reflectivity. More work is needed, however, to apply it to retinal abnormalities. Garvin et al. [2] proposed an automated approach for segmenting 3D macular OCT scans into 5 layers. The 6 surfaces were identified by finding a minimum cost closed set in a geometric graph constructed from regional information [3]. This work was later extended in [4] to segment 7 surfaces. The processing time and memory were extensive though. Mishra et al. [5] applied a two-step kernel-based optimization scheme to identify 7 retinal layers, but could not separate highly reflective image features. Another automated approach was proposed by Rossant et al. [6] to segment 8 layers using active contours,  $k$ -means, and random Markov fields. It also modeled the approximated parallelism between layers based on Kalman filter. The method performed well, but failed for blurred images. Kajić et al. [7] developed an approach to segment 8 layers using a large number of manually segmented images that were used as input to a statistical model. Supervised learning was performed by applying knowledge of the expected shapes of structures, their spatial relationships, and their textural appearances. Lu et al. [8] proposed an approach to segment OCT images into 5 layers. The detected blood vessels were used to divide the image into multiple vascular and nonvascular sections. The boundaries of the layers were finally detected after image filtering. Vermeer et al. [9] presented an automated method to segment 6 retinal layers using machine learning classifiers that were trained based on manually labeled subjects. Yaz et al. [10] presented a semi-automated approach to extract 9 layers from OCT images using Chan-Vese's energy-minimizing active contour without edges model along with shape priors. The proposed method, however, required user initialization and was never tested on human retinas nor on diseased cases. Lang et al. [11] segmented OCT images into 8 retinal layers using a random forest classifier that learned boundary pixels, yet modifications are needed to use it with pathologies. Kafieh et al. [12] used graph-based diffusion maps to segment the intraretinal layers in OCT scans from normal controls and glaucoma patients. Ehnes et al. [13] developed a graph-based algorithm for retinal segmentation which could segment up to 11 layers, yet worked only with high-contrast images.

\*\* indicates shared first authorship

<sup>†</sup>Corresponding author:- Tel:(502)-852-5092, Fax:(502)-852-6806, E-mail: aselba01@louisville.edu

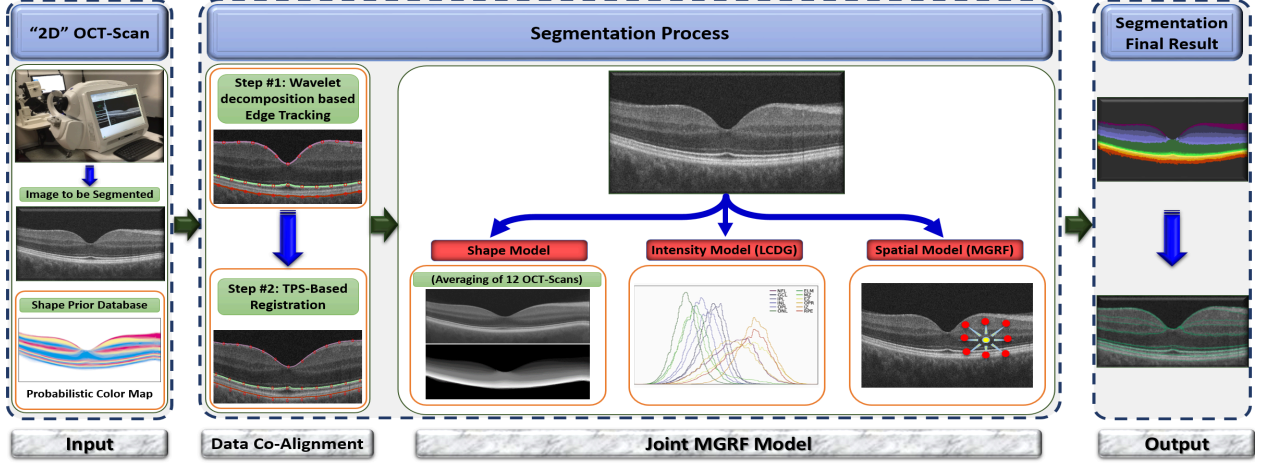


Fig. 2. Illustration of the basic steps of the proposed OCT segmentation framework.

The work in the literature suffers from many limitations that can be summarized as follows: i) most of the proposed approaches achieve good accuracy with OCT images having high signal to noise ratio (SNR), whereas fail with those of low SNR, ii) most of the proposed works in the literature have been tested on normal OCT images, yet not on diseased cases, and finally, iii) the majority of the previous work was able to segment up to six layers, while methods that segmented more layers, as [13], worked on high-contrast normal images. This would result in missed diagnosis of a certain abnormality if more than one layer were combined in the segmentation, e.g. cases of age macular degeneration (AMD) that need extracting RPE and interdigitation zone as 2 separate layers for better diagnosis [14].

To overcome the aforementioned limitations, we propose an innovative technique for segmenting OCT images that is generalized to work on normal cases as well as on diseased ones. The algorithm is based on a novel joint model that combines intensity, spatial, and shape information, Fig. 2. As demonstrated in the experimental results section, the proposed model performs well with low SNR images as well as images with different diseases. Moreover, the proposed model is able to segment 12 distinct layers. To the best of our knowledge, we are the first group to segment such number of layers on normal as well as diseased cases. This is crucial for the computer-aided diagnostic (CAD) system targeted by our research group that aims for early diagnosis as well as unbiased follow up of retinal diseases related to those layers.

## 2. METHODS

This paper proposes a novel framework, Fig. 2, that possesses the ability to accurately segment 12 distinct layers from OCT images. The proposed framework integrates shape, intensity, and spatial information and consists of three basic steps: (i) aligning the input subject to the constructed shape database, (ii) applying the joint model to the aligned image, and (iii) obtaining final segmentation. Mathematical details of the proposed joint model are detailed below.

Let  $\mathbf{g} = \{g(\mathbf{x}) : \mathbf{x} \in \mathbf{R}; g(\mathbf{x}) \in \mathbf{Q}\}$  and  $\mathbf{m} = \{l(\mathbf{x}) : \mathbf{x} \in \mathbf{R}; l(\mathbf{x}) \in \mathbf{L}\}$  be a grayscale image taking values from  $\mathbf{Q}$ , i.e.,  $\mathbf{g} : \mathbf{R} \rightarrow \mathbf{Q}$ , with the associated region map taking values from  $\mathbf{L}$ , i.e.,  $\mathbf{m} : \mathbf{R} \rightarrow \mathbf{L}$ , respectively.  $\mathbf{R}$  denotes a finite arithmetic lattice,  $\mathbf{Q}$  is a finite set of integer gray values, and  $\mathbf{L}$  is a set of region labels. An input OCT image,  $\mathbf{g}$ , co-aligned to the training database, and its map,  $\mathbf{m}$ , are described with a joint probability model:

$$P(\mathbf{g}, \mathbf{m}) = P(\mathbf{g}|\mathbf{m})P(\mathbf{m}) \quad (1)$$

which combines a conditional distribution of the images given the map  $P(\mathbf{g}|\mathbf{m})$ , and an unconditional probability distribution of maps  $P(\mathbf{m}) = P_{\text{sp}}(\mathbf{m})P_{\text{V}}(\mathbf{m})$ . Here,  $P_{\text{sp}}(\mathbf{m})$  denotes a weighted shape prior, and  $P_{\text{V}}(\mathbf{m})$  is a Gibbs probability distribution with potentials  $\mathbf{V}$ , that specifies a MGRF model of spatially homogeneous maps  $\mathbf{m}$ .

### 2.1. Adaptive Shape Model $P_{\text{sp}}(\mathbf{m})$

In order to account for the inhomogeneity of the OCT images, the shape information is incorporated in the segmentation process. The shape model is constructed using 12 OCT scans (6 men, 6 women). These 12 scans were selected to be representative and to capture the biological variability of the whole data set. ‘‘Ground truth’’ segmentations of these scans were delineated under supervision of retina specialists. Using one of the optimal scans as a reference (no tilt, centrally located fovea), the others were co-registered using a thin plate spline (TPS) [15, 16]. The shape prior is defined as:

$$P_{\text{sp}}(\mathbf{m}) = \prod_{\mathbf{y} \in \mathbf{R}} p_{\text{sp},\mathbf{y}}(l) \quad (2)$$

where  $P_{\text{sp}}(\mathbf{m})$  denotes the weighted shape prior,  $p_{\text{sp},\mathbf{y}}(l)$  is the pixel-wise probability for label  $l$ , and  $\mathbf{y}$  is the image pixel with gray level  $g$ . The same deformations were applied to their respective ground truth segmentations, which were then averaged to produce a probabilistic shape prior of the typical retina, i.e., each location  $x$  in the reference space is assigned a prior probability  $P(\mathbf{m})$  to lie within each of the 12 tissue classes.

In order to segment the input image, it must be first aligned to the shape database. In this paper, a new image alignment approach is proposed that integrates TPS with multi-resolution edge tracking method that identifies control points for initializing the alignment process. First, The ‘‘à trous’’ algorithm [17] was used to construct an undecimated wavelet decomposition of each scan. At a coarse enough level of detail, the retina takes on a three-banded appearance, with two hyperreflective bands separated by a hyporeflective band corresponding roughly to layers from ONL to MZ. Contours following the gradient maxima of this wavelet component provided initial estimates of the vitreous/NFL, MZ/EZ, and RPE/choroid boundaries, Fig. 3. The fourth gradient maximum could estimate the OPL/ONL boundary, but that is not sharp enough an edge to be of use. These ridges in gradient magnitude were followed through scale space to the third wavelet component, corresponding to a scale of approximately 15 micrometers for the OCT scans used in this study.



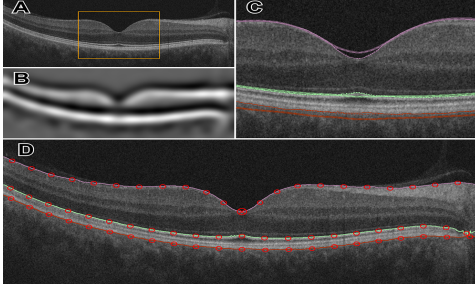


**Fig. 3.** Illustration of wavelet decomposition for an OCT image (A), highlighting the large scale structure of the retina in (B). Multiscale edges shown in (C) near the foveal peak, inside the bounded region of (A). At the finest level of detail, three boundaries are detected (D).

The foveal peak was identified as the point of closest approach of the vitreous/NFL and MZ/EZ contours. Control points were then located on these boundaries at the foveal peak and at uniform intervals nasally and temporally therefrom. Finally, the optimized TPS was employed in order to align the input image to the shape database using the control points identified.

## 2.2. First-Order Intensity Model $P(g|m)$

In order to make the segmentation process adaptive and not biased to only the shape information, we model the empirical gray level distribution of the OCT images. The first-order visual appearance of each label of the image is modeled by separating a mixed distribution of pixel intensities into individual components associated with the dominant modes of the mixture. The latter is approximated using the LCDG approach proposed in [18, 19, 20] which employs positive and negative Gaussian components that is based on a modified version of the classical Expectation Maximization (EM) algorithm. Let  $\Psi_\theta = (\Psi(q|\theta) : q \in \mathbf{Q})$  denote discrete Gaussian (DG) with parameters  $\theta = (\mu, \sigma)$ , integrating a continuous 1D Gaussian density with mean  $\mu$  and variance  $\sigma^2$  over successive gray level intervals. The LCDG with four dominant positive DGs and  $C_p \geq 4$  positive and  $C_n \geq 0$  negative subordinate DGs is:

$$P_{w,\Theta}(q|m) = \sum_{k=1}^{C_p} w_{p:k} \psi(q|\theta_{p:k}) - \sum_{k=1}^{C_n} w_{n:k} \psi(q|\theta_{n:k}) \quad (3)$$

where  $m$  takes one of the labels from 1 to 12, and all the weights  $w = [w_{p:k}, w_{n:k}]$  are non-negative and meet an obvious constraint  $\sum_{k=1}^{C_p} w_{p:k} - \sum_{k=1}^{C_n} w_{n:k} = 1$ . All LCDG parameters, including the DGs numbers, are estimated from the mixed empirical distribution to be modeled using the modified EM algorithm. For further details on the modified EM algorithm, please refer to [21, 22].

## 2.3. Second-Order MGRF model $P_V(m)$

In order to improve the spatial homogeneity of the segmentation, especially with diseased cases, the MGRF Potts model that accounts for spatial information was incorporated with the shape and intensity information [23]. This model is identified using the nearest pixels' 8-neighborhood  $\nu_s$  and analytical bi-valued Gibbs potentials [24, 25] as:

$$P(m) \propto \exp \left( \sum_{(x,y) \in \mathbf{R}} \sum_{(\xi,\zeta) \in \nu_s} \mathbf{V}(l_{x,y}, l_{x+\xi, y+\zeta}) \right) \quad (4)$$

where  $\mathbf{V}$  is the bi-value Gibbs potential, that depends on the equality of the nearest pair of labels:

$$\mathbf{V} = \begin{cases} V(\lambda, \lambda') = V_{eq} & \text{if } \lambda = \lambda' \\ V(\lambda, \lambda') = V_{ne} & \text{if } \lambda \neq \lambda' \end{cases} \quad (5)$$

Let  $f_{a,eq}(m)$  denote the relative frequency of the equal label pairs in the equivalent voxel pairs  $\{((x, y), (x + \xi, y + \zeta)) : (x, y), (x + \xi, y + \zeta) \in \mathbf{R}; (\xi, \zeta) \in \nu_s\}$ . The initial  $m$  results in approximate analytical maximum likelihood potentials estimates [24]:

$$V_{eq} = -V_{ne} \approx 2f_{eq}(m) - 1 \quad (6)$$

that allow for computing the pixel-wise probabilities  $p_{x,y}(l_{x,y} = \lambda)$  of each label  $\lambda \in \mathbf{L}$ . Fig. 2 shows the steps of the framework that integrate the three models used. Algorithm 1 also details the steps of the framework.

### Algorithm 1 Steps for the proposed segmentation approach

1. Load the atlas along with the test image.
2. Alignment of the test image with the atlas:
  - (a) Use the "a trous" algorithm to construct wavelet decomposition of the input image, and locate the vitreous/NFL, IPL/EL, and RPE/choroid boundaries.
  - (b) Identify the foveal peak using the 3 detected boundaries.
  - (c) Place fiducial points on each detected boundary, starting at the foveal peak and moving outward at equidistant intervals.
  - (d) Align the input image to the atlas using the control points identified.
3. Initial Segmentation:
  - (a) Initialize a 2D window of size  $N1 \times N2$  centered on each aligned pixel, and search within for the atlas pixel having intensity nearest the image pixel.
  - (b) Increase the window size, if needed, and redo the search until a non-empty result is found. If maximum size is reached and no result is found, increase the intensity tolerance and get back to previous step.
  - (c) Look up in the atlas the prior probability of the corresponding pixel belonging to each class.
4. Final Segmentation:
  - (a) Approximate the marginal intensity distribution  $P(g)$  of the OCT image using an LCDG with four dominant modes.
  - (b) Form an initial region map  $m$  using the marginal estimated density and prior shape of each label.
  - (c) Find the Gibbs potentials for the MGRF model (for pairwise and higher-order cliques) from the initial map  $m$ .
  - (d) Obtain the final segmentation using the joint model in Eq. 1.

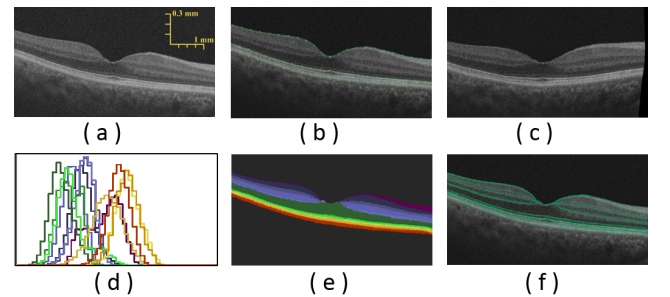


**Fig. 4.** Illustration of the segmentation steps: (a) an OCT image of a 65 year-old female, (b) edge tracking with wavelet decomposition, (c) co-alignment using TPS control points, (d) LCDG-modes for different layers, (e) segmentation after using the joint MGRF model, and (f) overlaid layers' edges on the original image.



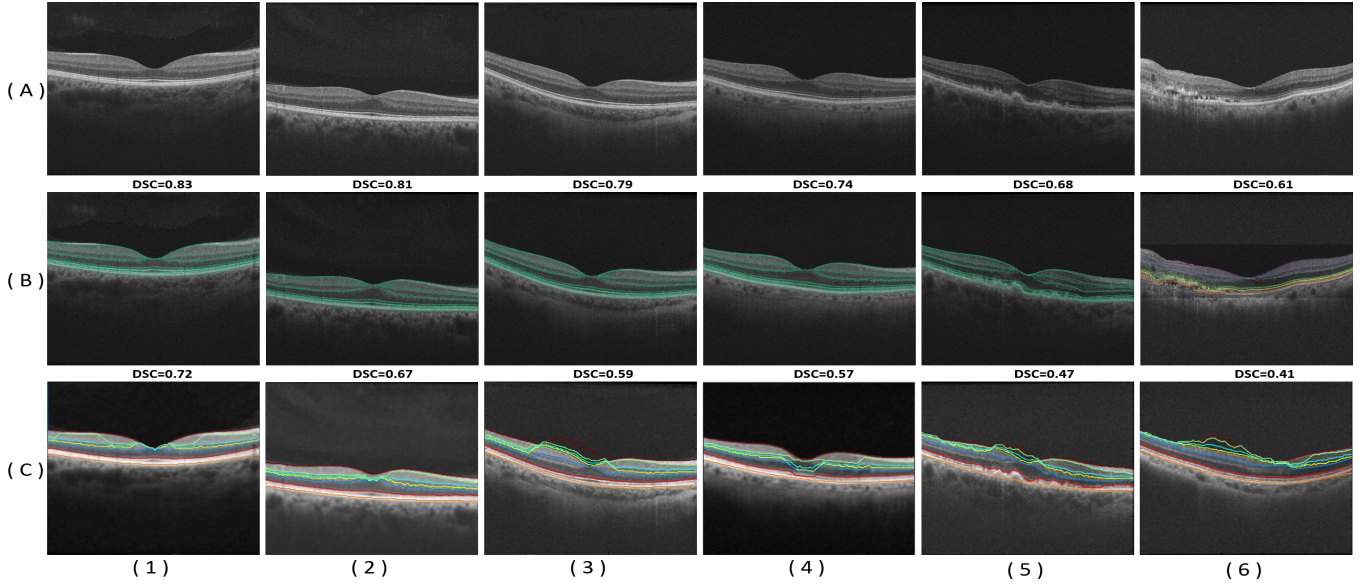


**Fig. 5.** Segmentation results for different OCT images in row (A) for normal (1-3), diabetic (4), and AMD (5-6) cases. Results of the proposed approach are displayed in row (B) and results of the approach [26] are displayed in row (C). The DC score is displayed above each result.

### 3. EXPERIMENTAL RESULTS

In order to test and validate the proposed segmentation method, spectral domain OCT scans (Zeiss Cirrus HD-OCT 5000) were prospectively collected from 200 subjects (165 normal, 35 diseased) aged 10–79 years. Subjects with high myopia ( $\leq -6.0$  diopters), and tilted OCT were excluded. The proposed segmentation approach was validated using ground truth for subjects, that was created by manual delineations of retina layers with the aid of retina specialists.

Step-by-step demonstration to show the ability of the proposed segmentation approach for a normal subject is shown in Fig. 4. First, the edges of the input OCT image (Fig. 4(a)) is tracked using wavelet decomposition method (Fig. 4(b)) and is followed by its co-alignment to the shape database using identified TPS control points (Fig. 4(c)). Initial segmentation result is first obtained using the shape model (Fig. 4(d)) then refined using the joint-MGRF model to obtain the final segmentation result (Fig. 4(e)). The proposed segmentation approach was tested on diseased cases as well. In many retinal diseases, such as age-related macular degeneration (AMD) and diabetic retinopathy, the anatomy of the layers is disrupted and the segmentation problem becomes more challenging. More segmentation results for normal and diseased subjects are demonstrated in Fig 5.

In addition to the visual results in Fig. 5, the robustness and accuracy of our approach are evaluated using both AC1 and DSC metrics, and the AD distance metric comparing our segmentation with the ground truth. Mean boundary error was 6.87 micrometers from ground truth, averaged across all 13 boundaries. The inner (vitreal) boundary of the retina was placed most accurately, with  $2.78\mu m$  mean error. The worst performance was on the outer (choroid) boundary, with  $11.6\mu m$ . Whereas, only the RPE/choroid boundary was reliably detected by the other approach [26].

Additionally, the advantage of the proposed segmentation technique is highlighted by comparing its performance against graph theory based approach proposed in [26]. Comparative segmentation results of our approach versus [26] for some selected data are shown in Fig. 5. Table 1 summarizes the quantitative comparison

of our segmentation method and the other method versus the ground truth, based on the three evaluation metrics for all subjects. Statistical analysis using paired *t*-test demonstrates a significant difference in terms of all three metrics of our method over [26], as confirmed by *p*-values  $< 0.05$  (see Table 1). This analysis clearly demonstrates the promise of the developed approach for the segmentation of the OCT scans.

**Table 1.** Comparative segmentation accuracy of the proposed segmentation technique and the proposed approach in [26] using the Dice coefficient (DSC), agreement coefficient (AC1), and the average deviation distance (AD) metrics. All values are represented as mean  $\pm$  standard deviation.

	Evaluation Metric		
	DSC	AC1, %	AD, $\mu m$
Our	$0.763 \pm 0.1598$	$73.2 \pm 4.46$	$6.87 \pm 2.78$
Other [26]	$0.41 \pm 0.263$	$2.25 \pm 9.7$	$15.1 \pm 8.6$
<i>p</i> -value	$< 0.0001$	$< 0.0001$	$< 0.00395$

### 4. CONCLUSIONS AND FUTURE WORK

In summary, this paper has proposed a novel framework for the segmentation of the 12 distinct retinal layers from OCT scans. Segmentation evaluation using a cohort of both normal and diseased subjects demonstrates the promises of our approach for accurate segmentation of OCT images, as documented using DSC, AC1, and AD metrics. This is due to the integration of an accurate co-alignment scheme with the adaptive shape prior and both first and second appearance into a joint MGRF model. Our future work will focus on using the proposed approach in a fully CAD system that has the ability to detect retinal abnormalities.

### 5. ACKNOWLEDGEMENT

This work was supported by the Coulter Translational Partnership Grant, University of Louisville (Schaal, El-Baz) 2015-2016.

## 6. REFERENCES

- [1] A. M. Bagci, M. Shahidi, R. Ansari, M. Blair, N. P. Blair, and R. Zelkha, "Thickness profiles of retinal layers by optical coherence tomography image segmentation," *Am. J. Ophthalmol.*, vol. 146, no. 5, pp. 679–687, 2008.
- [2] M. K. Garvin, M. D. Abramoff, R. Kardon, S. R. Russell, X. Wu, and M. Sonka, "Intraretinal layer segmentation of macular optical coherence tomography images using optimal 3-D graph search," *IEEE Trans. Med. Imag.*, vol. 27, no. 10, pp. 1495–1505, 2008.
- [3] P. A. Dufour, L. Ceklic, H. Abdillahi, S. Schröder, S. De Dzanet, U. Wolf-Schnurbusch, and J. Kowal, "Graph-based multi-surface segmentation of OCT data using trained hard and soft constraints," *IEEE Trans. Med. Imaging*, vol. 32, no. 3, pp. 531–543, 2013.
- [4] M. K. Garvin, M. D. Abramoff, X. Wu, S. R. Russell, T. L. Burns, and M. Sonka, "Automated 3-D intraretinal layer segmentation of macular spectral-domain optical coherence tomography images," *IEEE Trans. Med. Imag.*, vol. 28, no. 9, pp. 1436–1447, 2009.
- [5] A. Mishra, A. Wong, K. Bizheva, and D. A. Clausi, "Intraretinal layer segmentation in optical coherence tomography images," *Optics express*, vol. 17, no. 26, pp. 23 719–23 728, 2009.
- [6] F. Rossant, I. Ghorbel, I. Bloch, M. Paques, and S. Tick, "Automated segmentation of retinal layers in oct imaging and derived ophthalmic measures," in *Biomedical Imaging: From Nano to Macro, 2009. ISBI'09. IEEE International Symposium on*. IEEE, 2009, pp. 1370–1373.
- [7] V. Kajić, B. Považay, B. Hermann, B. Hofer, A. Marshall, P. L. Rosin, and W. Drexler, "Robust segmentation of intraretinal layers in the normal human fovea using a novel statistical model based on texture and shape analysis," *Opt. Express*, vol. 18, no. 14, pp. 14 730–14 744, 2010.
- [8] S. Lu, C.-I. Cheung, J. Liu, J. H. Lim, C. K.-S. Leung, and T. Y. Wong, "Automated layer segmentation of optical coherence tomography images," *Biomedical Engineering, IEEE Transactions on*, vol. 57, no. 10, pp. 2605–2608, 2010.
- [9] K. Vermeer, J. Van der Schoot, H. Lemij, and J. De Boer, "Automated segmentation by pixel classification of retinal layers in ophthalmic oct images," *Biomedical optics express*, vol. 2, no. 6, pp. 1743–1756, 2011.
- [10] A. Yazdanpanah, G. Hamarneh, B. R. Smith, and M. V. Sarunic, "Segmentation of intra-retinal layers from optical coherence tomography images using an active contour approach," *Medical Imaging, IEEE Transactions on*, vol. 30, no. 2, pp. 484–496, 2011.
- [11] A. Lang, A. Carass, M. Hauser, E. S. Sotirchos, P. A. Calabresi, H. S. Ying, and J. L. Prince, "Retinal layer segmentation of macular OCT images using boundary classification," *Biomed. Opt. Express*, vol. 4, no. 7, pp. 1133–1152, 2013.
- [12] R. Kafieh, H. Rabbani, M. D. Abramoff, and M. Sonka, "Intraretinal layer segmentation of 3D optical coherence tomography using coarse grained diffusion map," *Med. Image Anal.*, vol. 17, no. 8, pp. 907–928, 2013.
- [13] A. Ehnes, Y. Wenner, C. Friedburg, M. N. Preising, W. Bowl, W. Sekundo, E. Meyer zu Bexten, K. Stieger, and B. Lorenz, "Optical coherence tomography (oct) device independent intraretinal layer segmentation," *Transl. Vis. Sci. Technol.*, vol. 3, no. 1, 2014.
- [14] D. F. Kiernan, R. Zelkha, S. M. Hariprasad, J. I. Lim, M. P. Blair, and W. F. Mieler, "En face spectral-domain optical coherence tomography outer retinal analysis and relation to visual acuity," *Retina (Philadelphia, Pa.)*, vol. 32, no. 6, p. 1077, 2012.
- [15] J. Lim and M.-H. Yang, "A direct method for modeling non-rigid motion with thin plate spline," in *Computer Vision and Pattern Recognition, 2005. CVPR 2005. IEEE Computer Society Conference on*, vol. 1. IEEE, 2005, pp. 1196–1202.
- [16] Q. Yang *et al.*, "Automated layer segmentation of macular oct images using dual-scale gradient information," *Opt. Express*, vol. 18, no. 20, pp. 21 293–21 307, 2010.
- [17] E. Lega, H. Scholl, J.-M. Alimi, A. Bijaoui, and P. Bury, "A parallel algorithm for structure detection based on wavelet and segmentation analysis," *Parallel Comput.*, vol. 21, no. 2, pp. 265–285, 1995.
- [18] A. El-Baz, A. Elnakib, F. Khalifa, M. A. El-Ghar, P. McClure, A. Soliman, and G. Gimelfarb, "Precise segmentation of 3-d magnetic resonance angiography," *IEEE Trans. Biomed. Eng.*, vol. 59, no. 7, pp. 2019–2029, 2012.
- [19] M. Ismail, A. Soliman, A. ElTanboly, A. Switala, M. Mahmoud, F. Khalifa, G. Gimelfarb, M. Casanova, R. Keynton, and A. El-Baz, "Detection of white matter abnormalities in mr brain images for diagnosis of autism in children," *13th IEEE International Symposium on Biomedical Imaging (ISBI 2016)*, vol. 13, 2016.
- [20] R. An and X. Huang, "A compact c0 discontinuous galerkin method for kirchhoff plates," *Numerical Methods for Partial Differential Equations*, vol. 31, no. 4, pp. 1265–1287, 2015.
- [21] A. El-Baz and G. Gimelfarb, "Em based approximation of empirical distributions with linear combinations of discrete gaussians," in *Image Processing, 2007. ICIP 2007. IEEE International Conference on*, vol. 4. IEEE, 2007, pp. IV–373.
- [22] A. A. Farag, A. S. El-Baz, and G. Gimelfarb, "Precise segmentation of multimodal images," *Image Processing, IEEE Transactions on*, vol. 15, no. 4, pp. 952–968, 2006.
- [23] A. Alansary, M. Ismail, A. Soliman, F. Khalifa, M. Nitzken, A. Elnakib, M. Mostapha, A. Black, K. Stinebruner, and M. Casanova, "Infant brain extraction in t1-weighted mr images using bet and refinement using lcdg and mgrf models," *IEEE Journal of Biomedical and Health Informatics*, 2015.
- [24] A. S. El-Baz, *Novel stochastic models for medical image analysis*. ProQuest, 2006.
- [25] N. Liu, G. Gimelfarb, and P. Delmas, "High-order mgrf models for contrast/offset invariant texture retrieval," in *Proceedings of the 29th International Conference on Image and Vision Computing New Zealand*. ACM, 2014, pp. 96–101.
- [26] S. J. Chiu, X. T. Li, P. Nicholas, C. A. Toth, J. A. Izatt, and S. Farsiu, "Automatic segmentation of seven retinal layers in sdopt images congruent with expert manual segmentation," *Optics express*, vol. 18, no. 18, pp. 19 413–19 428, 2010.